NASA/TM-2003

SIMBIOS Project 2003 Annual Report

Giulietta S. Fargion, Science Applications International Corporation, Maryland
Charles R. McClain, Goddard Space Flight Center, Greenbelt, Maryland

National Aeronautics and
Space Administration

Goddard Space Flight Center
Greenbelt, Maryland 20771

December 2003

Preface

The purpose of this technical report is to provide current documentation of the the Sensor Intercomparison and Merger for Biological and Interdisciplinary Oceanic Studies (SIMBIOS) Project activities, NASA Research Announcement (NRA) research status, satellite data processing, data product validation, and field calibration. This documentation is necessary to ensure that critical information is related to the scientific community and NASA management. This critical information includes the technical difficulties and challenges of validating and combining ocean color data from an array of independent satellite systems to form consistent and accurate global bio-optical time series products. This technical report is not meant as a substitute for scientific literature. Instead, it will provide a ready and responsive vehicle for the multitude of technical reports issued by an operational project.

The SIMBIOS Science Team Principal Investigators (PIs) original contributions to this report are in chapters four and above. The purpose of these contributions is to describe the current research status of the SIMBIOS-NRA-99 funded research. The contributions are published as submitted, with the exception of minor edits to correct obvious grammatical or clerical errors.

Table of Contents

Chapter 1

An Overview of SIMBIOS Program Activities and Accomplishments

Giulietta S. Fargion
Science Applications International Corporation (SAIC), Beltsville, Maryland

Charles R. McClain
NASA Goddard Space Flight Center, Greenbelt, Maryland

1.1 INTRODUCTION

The SIMBIOS Program was conceived in 1994 as a result of a NASA management review of the agency's strategy for monitoring the bio-optical properties of the global ocean through space-based ocean color remote sensing. At that time, the NASA ocean color flight manifest included two data buy missions, the Sea-viewing Wide Field-of-view Sensor (SeaWiFS) and Earth Observing System (EOS) Color, and three sensors, two Moderate Resolution Imaging Spectroradiometers (MODIS) and the Multi-angle Imaging Spectro-Radiometer (MISR), scheduled for flight on the EOS-Terra and EOS-Aqua satellites. The review led to a decision that the international assemblage of ocean color satellite systems provided ample redundancy to assure continuous global coverage, with no need for the EOS Color mission. At the same time, it was noted that non-trivial technical difficulties attended the challenge (and opportunity) of combining ocean color data from this array of independent satellite systems to form consistent and accurate global bio-optical time series products. Thus, it was announced at the October 1994 EOS Interdisciplinary Working Group meeting that some of the resources budgeted for EOS Color should be redirected into an intercalibration and validation program (McClain *et al.*, 2002).

NASA Goddard Space Flight Center (GSFC) was directed to develop an intercalibration and validation program plan for submission to NASA Headquarters (HQ) by May 1995. This plan envisioned a Science Team funded by a NASA Research Announcement (NRA) (released in July 1996) and the SIMBIOS Project Office that was established at GSFC in January 1997. The initial SIMBIOS Program was scoped for five years (1997-2001) and included separate support for a science team and the Project Office. Dr. Mueller (San Diego State University) acted as an interim project manager at GSFC under a one-year assignment to assist in getting the project office organized and the science team contracts executed. During the second year of the SIMBIOS Project, Dr. McClain assumed project management for SeaWiFS and SIMBIOS, as both Dr. Cleave and Dr. Mueller stepped down in their roles as project managers of these two projects, respectively. In fall 1998, Dr. Fargion was hired as Deputy Project Manger to assist Dr. McClain.

In September 2000, Dr. McClain assumed new responsibilities in assisting HQ to develop a long-term program for global carbon cycle research. As a result, SeaWiFS and SIMBIOS Project Office were reorganized somewhat to allow Dr. McClain to focus on the carbon initiative. Dr. Feldman assumed management responsibilities for SeaWiFS and Dr. Fargion for SIMBIOS, respectively. Due to the success of the SIMBIOS Program combined with a strong collaboration with the US and international ocean communities, HQ release a second NRA (1999) and granted an extension of three years to the project. However, in 2002, NASA HQ decided to discontinue the program in its present form. The rationale centered on three considerations. The first was a desire by HQ to integrate the various ocean color calibration and validation activities of the SIMBIOS, SeaWiFS, and the MODIS programs under a common ocean color team which would also include investigators supported under the NASA Ocean Biogeochemistry program. While the three ocean color projects have separate management and funding structures, they have been coordinated and mutually supportive with little redundancy. The second consideration stems from initial problems with MODIS ocean data quality and accessibility which has made it imperative for NASA to focus its available resources on MODIS ocean calibration and validation.

The third consideration is the preparation for ocean color observations from the Visible-Infrared Radiometer Suite (VIRIS) on National Polar Orbiting Environmental Satellite System (NPOESS) Preparatory Project (NPP), which is scheduled to launch in 2006.

The SIMBIOS Project Office, co-located with the SeaWiFS Project Office, provides support and coordination for the SIMBIOS Program, such as administration, project documentation, and interagency and international coordination. It also incorporates aspects of post launch calibration and characterization, *in situ* data collection, protocol developments, round robins, algorithm development and evaluation, product merging, and data processing (Figure 1.1 and Table 1.1). All components illustrated in Figure 1.1 are tightly connected (and in some cases overlap) and were thoroughly developed and integrated by the Project during the operational years (1997-2003).

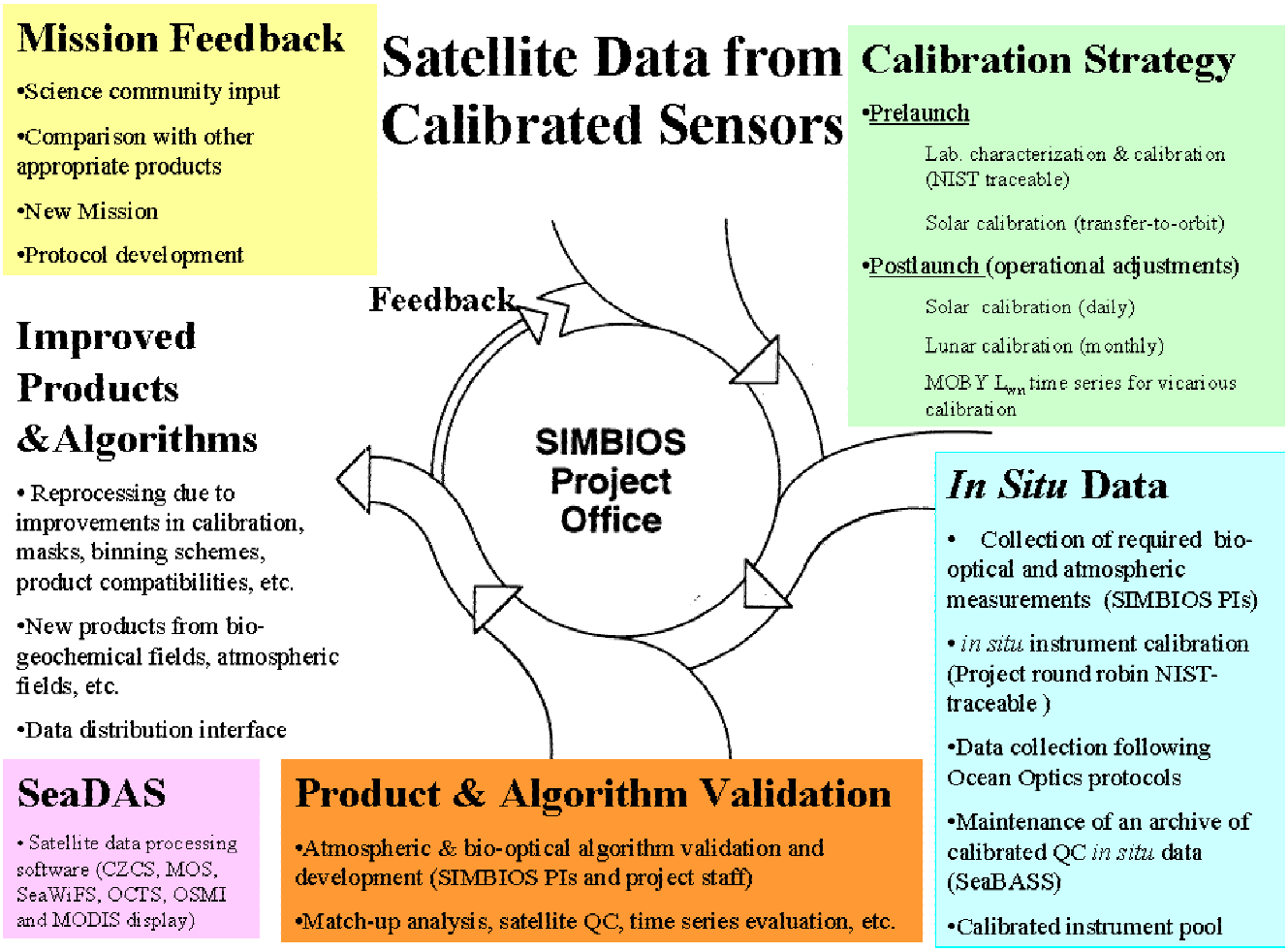

Figure 1.1: SIMBIOS Project activity areas

The specific proposed objectives of the SIMBIOS Program were: (1) to quantify the relative accuracy of measurements from the ocean color products from each mission, (2) to work with each project to improve the level of confidence and compatibility among these products, and (3) to develop methodologies for generating merged level-3 products. These objectives became operational. In particular, the intercomparison component performs many functions similar to those being performed by each individual mission (calibration, validation, quality control, algorithm development and data processing) but does so by integrating information from each project, augmenting activities where required, providing feedback to each project and the ocean color community, and coordinating with the international community. The program requirements were identified as:

- Field measurement and data processing protocol definition and development
- Global bio-optical and atmospheric *in situ* data collection
- Bio-optical and atmospheric database development (SeaBASS)
- Traceability of laboratory calibration sources to standards (round robin)
- Instrumented calibration sites (MOBY)
- Prelaunch sensor calibration and characterization protocols
- On-orbit calibration evaluation and methodology development
- Bio-optical and atmospheric correction algorithm development
- Product accuracy evaluation and methodology development
- Data merger algorithm development and data processing
- High volume data processing capabilities
- Technology evaluation and development (SQM)
- Multi satellite data processing software
- Systematic documentation (NASAtechnical memorandum and publications)

SIMBIOS has worked with several missions, such as SeaWiFS, Ocean Color and Temperature Scanner (OCTS), Polarization and Directionality of the Earth's Reflectances (POLDER), Modular Optoelectronic Scanner (MOS), Ocean Scanning Multispectral Imager (OSMI), MODIS (Terra and Aqua), Medium Resolution Imaging Specrometer (MERIS) and Global Imager (GLI). The Project staff ensured the development of internally consistent research products and time series from multiple satellite ocean color data sources; developed methodologies for cross-calibration of satellite ocean color sensors; developed methodologies for merging data from multiple ocean color missions; promoted cooperation between ocean color projects, and served as a prototype for future Earth observation programs. In order to better communicate with the community, the project held annual open science team meetings and workshops, participated as a member in several mission teams, documented all activities in NASA technical memorandum (TM) and hosted a web site organized to serve as the main information resource of Project activities, the Project Office, and the Science Team. The Project Office, in an effort to educate and promote the concept of an organized program of sensor cross-calibration and validation, has sent representatives to several international conferences. The objectives, and activities of SIMBIOS are discussed in more detail in a number of documents including the SIMBIOS Project Annual Reports (McClain and Fargion, 1998 & 1999; Fargion and McClain 2000, 2001 & 2002), the Ocean Optics Protocols TMs (Mueller & Fargion, 2003; Fargion *et al.*, 2001) and round robin reports (Riley and Bailey 1998; Meister *et al.*, 2002 & 2003; Van Heukelem *et al.* 2002) and others cited in this chapter.

Table 1.1: SIMBIOS Project Activities and Responsible Staff

- **Satellite Data Processing**
  Bryan Franz, Joel Gales, Sean Bailey and SeaWiFS staff
- **Satellite Characterization**
  Bob Barnes and Gerhard Meister
- **Data Merging**
  Ewa Kwiatkowska-Ainsworth and Bryan Franz
- **Support Services**
  Sean Bailey, Jeremy Werdell, Christophe Pietras and Kirk Knobelspiesse
- **Data Product Validation**
  Sean Bailey, Jeremy Werdell, Christophe Pietras and Kirk Knobelspiesse
- **Calibration Round Robin**
  Gerhard Meister and Bob Barnes

1.2 SIMBIOS SCIENCE TEAM

The SIMBIOS Science Team was selected through NRA's 1996 and 1999. NASA HQ manages the process of team selection, but the GSFC NASA Procurement Office handles the team contracts, work

statements and, if necessary, budget negotiations. The Project funds numerous US investigators and collaborates with several international investigators, space agencies [e.g., National Space Development Agency of Japan (NASDA), European Space Agency (ESA), Korea Aerospace Research Institute (KARI)] and international organizations [e.g., International Ocean Colour Coordinating Group (IOCCG), Joint Research Center (JRC)]. US investigators under contract provide *in situ* atmospheric and bio-optical data sets, and develop atmospheric correction and bio-optical algorithms and methodologies for data merger schemes. NASA Procurement requires formal evaluations for all contracts at the end of each contract year. These evaluations go into a database and are shared with the PI's institution or upper management. The locations of specific SIMBIOS team investigations are shown in Figures 1.2 and 1.3.

The international ocean color community's response to NRA-99 was overwhelming: a total of 75 PI's proposed collaborations with the Project. The twelve international proposals covered topics ranging from protocols, calibration-validation activities, atmospheric-biological algorithms, and data merging. The SIMBIOS Science Team meetings were held in August 1997 at Solomons Island (Maryland), in September 1998 at La Jolla (California), in September 1999 at Annapolis (Maryland), in January 2001 at GSFC (Maryland), and in January 2002 at Baltimore (Maryland). SIMBIOS Science meetings had large US and international contingents, including participants from space agencies and international organizations. During each year, the Project has hosted several US and international visiting scientists (e.g., Dr. Antoine, Dr. Deschamps, Dr. Frouin, Dr. Fukushima, Dr. Hagolle, Dr. Kopelevich, Dr. Miller, Dr. Nicolas, Dr. Souaidia, Dr. Subramaniam, Dr. Tanaka, Dr. Yamamoto and Dr. Zibordi), staying from 2 weeks to one year at GSFC.

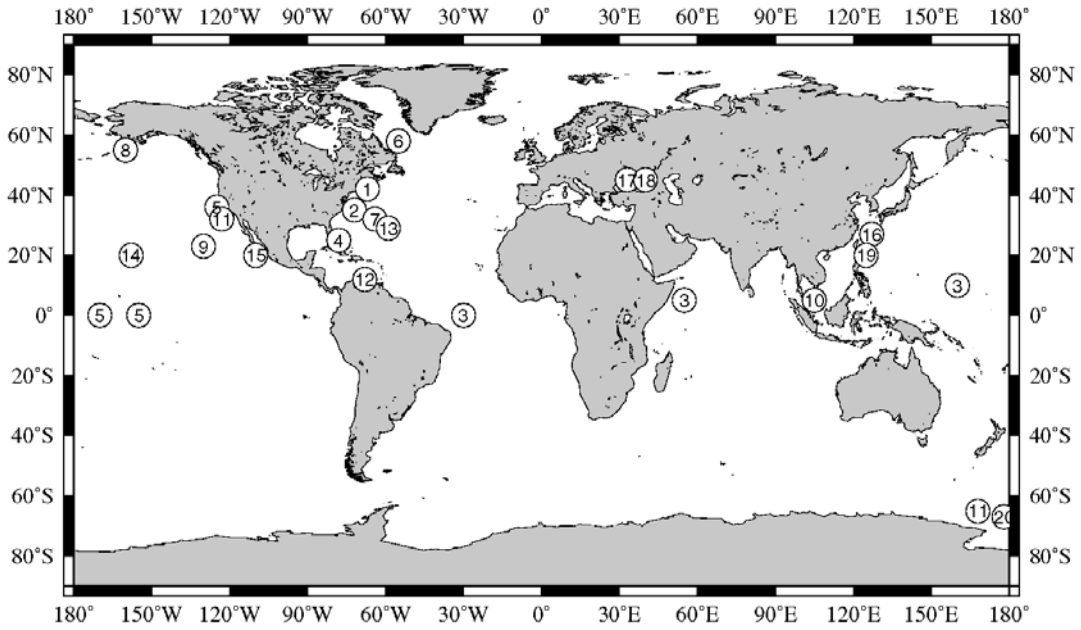

Figure 1.2: Global distribution of the NRA-96 selected SIMBIOS studies. United States (field): (1) Balch; (2) Brown/Brock; (3) Capone/Carpenter/Subramaniam and Miller; (4) Carder and Green; (5) Chavez; (6) Cota; (7) Dickey; (8) Eslinger; (9) Frouin; (10) Miller; (11) Mitchell and Green; (12) Müller-Karger; (13) Siegel; (14) Porter (15) Zaneveld and Mueller. United States (theoretical): Flatau; Siegel and Stamnes/Chen. International: He; Korotaev; Kopelevich; and Li.

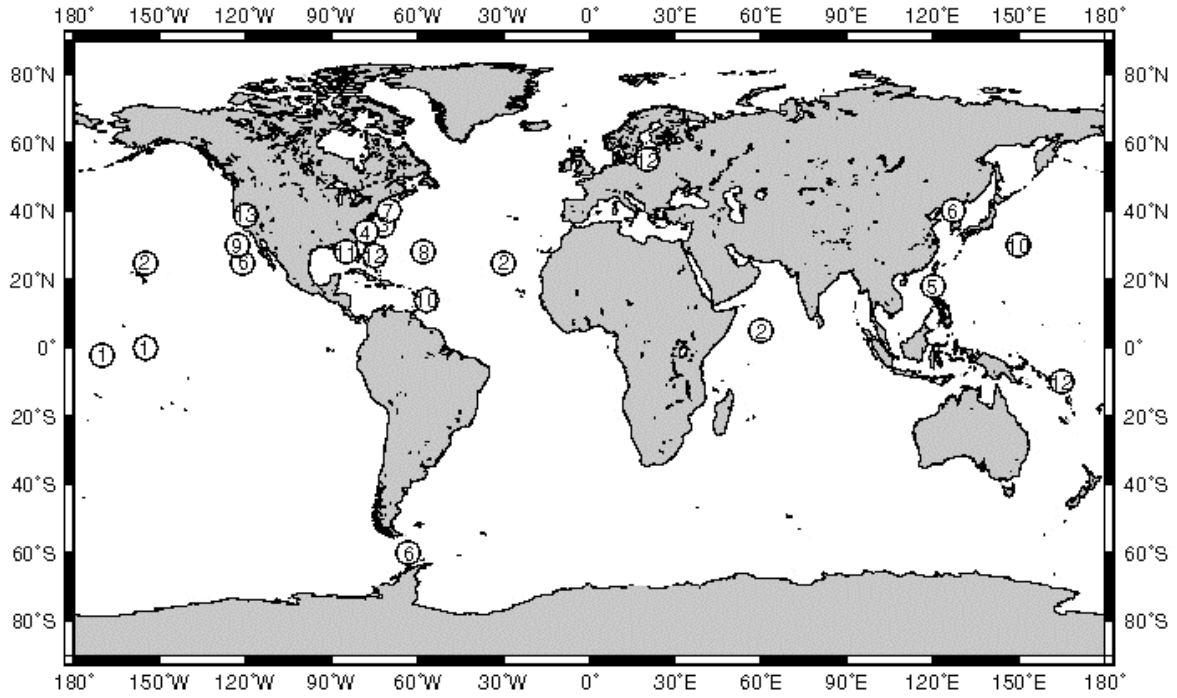

Figure 1.3: Global distribution of the NRA-99 selected SIMBIOS studies. United States (field): (1) Chavez; (2) Frouin; (3) Gao; (4) Harding; (5) Miller; (6) Mitchell; (7) Morrison; (8) Nelson; (9) Siegel; (10) Spinhirne; (11) Stumpf; (12) Subramaniam; (13) Zalewski. United States (theoretical): Gregg; Hooker; Maritorena; Mueller; Trees and Wang. International: Bohm; Zibordi; Fougnie; Deschamps; Antoine; Kopelevich; Ishizaka; Fukushima; Chen; Li & Lynch.

1.3 OCEAN COLOR SATELLITE DATA PROCESSING

Over the past several years, the SIMBIOS Project has been engaged in the characterization, validation, intercomparison, and cross-calibration of a host of space-borne ocean color sensors (Table 1.2 and Table 1.3). This work has included the characterization and calibration of OCTS and POLDER (Wang *et al.*, 2002), the cross-calibration and long-term intercomparison of MOS and SeaWiFS (Franz *et al.*, 2001; Wang anf Franz, 2000), the cross-calibration of OSMI to SeaWiF (Franz and Kim, 2001), and the intercomparison of MODIS/Terra (Fargion and McClain, 2003b) and MODIS/Aqua with SeaWiFS, as well as independent validation of MODIS (Terra & Aqua), SeaWiFS, OCTS, and POLDER using coincident *in situ* measurement archived in SeaWiFS Bio-optical Archive and Storage System (SeaBASS).

To facilitate the processing and intercomparison of ocean color products from multiple instruments, the SIMBIOS Project developed atmospheric correction code based on the SeaWiFS algorithm of Gordon and Wang (1994). The approach was to identify those few parts of the algorithm that were sensor or band-pass specific, and develop a software package that could process data from multiple ocean color sensors with minimal changes in the algorithms. The sensitivity of the atmospheric correction algorithm to differences in spectral bands was carefully assessed by Wang (1999), wherein he showed by simulation that these differences could be accurately accounted for through exact calculation of the Rayleigh reflectances and minor modifications to the diffuse transmittance calculation. The multi-sensor level-1 to level-2 code (MSL12) has been used to process data from MOS, OCTS, POLDER, OSMI, and SeaWiFS, with support

for MODIS currently underway. Due to its enhanced flexibility and maintainability, the software was adopted by the SeaWiFS Project for all standard production, calibration, and validation activities and is widely distributed and utilized by the international ocean color community through the SeaWiFS Data Analysis System (SeaDAS).

Table 1.2: Satellite data supported (1997-2003).

- MOS-SeaWiFS cross calibration and data merger with SeaWiFS
  - German Aerospace Research Establishment (DLR)
- MOS data acquisition at NASA Wallops Flight Facility
  - Indian Space Research Organization (ISRO)
- OCTS-POLDER cross calibration
  - National Space Development Agency of Japan (NASDA)
  - Centre National d'Etudes Spatiales (CNES), France
- OCTS global GAC reprocessing
  - NASDA
- OSMI-SeaWiFS cross calibration and data processing
  - Korean Aerospace Research Institute (KARI)
- SeaWiFS calibration and product validation
- MODIS (Terra & Aqua) product validation
- MODIS (Terra & Aqua) data merger with SeaWiFS (9km Chlorophyll product and diagnostic data set)
- MERIS calibration and product validation (MOBY)
  - European Space Agency (ESA)
- GLI characterization and field calibration cruise
  - NASDA

Table 1.3: Work done by sensor (1997-2003).

Satellite	Characterization	*in situ* matchups	L_w, & chlorophyll	MOBY	AOT
MOS	√	√			
OCTS	√	√			
POLDER	√	√			
SeaWiFS	√	√		√	√
OSMI	√	√		√	
GLI	√				
MODIS (Terra)	√	√		√	√
MODIS (Aqua)	√	√		√	√

The SIMBIOS Project, using MSL12, performed an independent vicarious calibration of the OCTS sensor, then reprocessed the entire global OCTS mission archive (Figure 1.4). This data was distributed through the Goddard DAAC, with processing and display support distributed through SeaDAS. This provided the ocean color community with a nearly complete, highly compatible ocean color time-series from September 1996 to the present day, including the first complete record of an El Niño/La Nina event. The SIMBIOS Project also developed and evaluated methods for cross-calibration of ocean color sensors, beginning with the MOS and SeaWiFS instruments. The MOS is a German ocean color sensor flying on the Indian Space Agency IRS-P3 satellite. Because the sensor has a small swath width of 192 km and only four ground stations capable of receiving the real time-only transmissions, there is limited opportunity for ground truth. In addition, the sensor is a push-broom CCD array with 384 independent detectors in each band, so calibration requires both a cross-scan, detector-relative calibration and an absolute calibration. As a prototype for future missions, the SIMBIOS Project developed a technique to vicariously calibrate MOS

using SeaWiFS (Wang and Franz, 2000). The method is analogous to that used by the SeaWiFS Project for vicarious calibration to MOBY, except that for MOS the Project used SeaWiFS observations rather than MOBY measurements as truth. A major advantage of this technique is that the Project was able to obtain a large number of matchups for each detector of each band, and thus derive both the absolute and detector-relative calibrations simultaneously. This vicarious cross-calibration, coupled with the instrument calibration performed by the MOS Project, has enabled the retrieval of oceanic optical properties which maintain good agreement with SeaWiFS, even after three years (Wang *et al.*, 2001).

The SIMBIOS Project performed a similar cross-calibration between SeaWiFS and OSMI (Franz and Kim, 2001). OSMI is a whisk-broom scanning CCD array with 96 detectors per band distributed along track. The detectors are divided into two independently amplified fields of 48-detectors each. Prior to cross-calibration, the calibrated level-1B radiances exhibited significant interdetector striping, banding between the detector fields, and absolute radiances that were below the predicted Rayleigh radiance in most bands. As such, it was not even possible to compute oceanic optical properties, as any atmospheric correction would fail. In this case, it was necessary to develop a calibration for the NIR channels as well as the visible bands. The NIR calibration was performed using the SeaWiFS retrieved aerosol optical thickness as truth, using a technique originally developed to calibrate SeaWiFS to in situ aerosol optical thickness measurements (Franz *et al.*, 2001). Once the NIR calibration was established, the calibration of the visible bands proceeded in a manner analogous to the MOS-to-SeaWiFS cross-calibration, with independent gains derived for each detector of each band. After this cross-calibration it was possible, for the first time, to process an OSMI scene and retrieve meaningful oceanic optical properties.

The final year of the SIMBIOS Project was largely dedicated to MODIS analyses. An extensive evaluation of the temporal trends in several standard ocean color products derived from SeaWiFS and MODIS/Terra was performed to determine the long-term relative stability between the two sensors and to develop an understanding of their similarities and differences. This time-series analysis investigated variations in the mean value of water-leaving radiance and chlorophyll products over the period from March 2000 through December 2002, for both global and regional geographic areas, between MODIS Collection #4 and SeaWiFS Reprocessing #4. The analysis was able to demonstrate the remarkable temporal stability of SeaWiFS, and assess the long-term stability of MODIS/Terra (see http://simbios.gsfc.nasa.gov/ simbios_modis.html; Fargion & MCClain, 2003b). This work on these various sensors has provided critical insight into the issues and limitations associated with the establishment of a long-term, multi-mission, climate data record for ocean color.

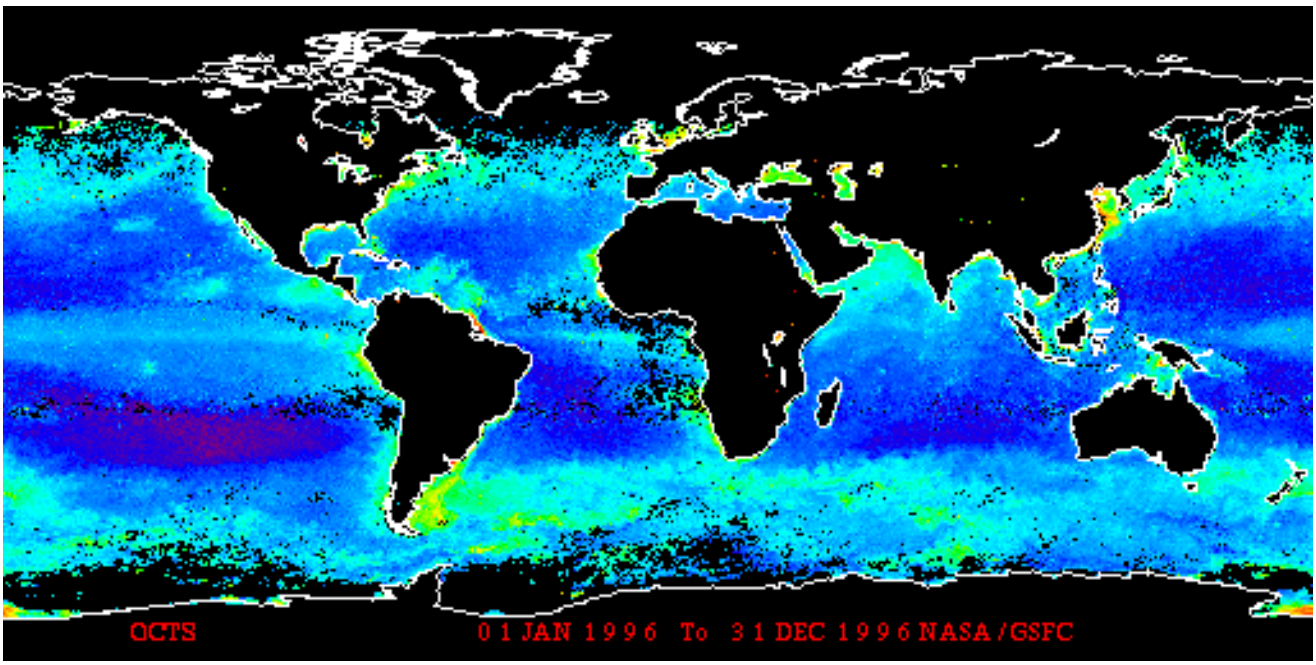

Figure 1.4: Retrospective satellite data processing reprocessing of OCTS GAC mission archive

1.4 DATA MERGER

The objective of ocean color data merger is to create a consistent series of systematic ocean color measurements from multi-instrument, multi-platform and multi-year observations based on accurate and uniform calibration and validation over the lifetime of the measurement. The most obvious benefit of data merger is improvement in spatial and temporal ocean color coverage. Data merger is the ultimate tool for the creation of ocean color climate data records. The major data merger effort undertaken by the SIMBIOS Project focused on integrating daily MODIS/Terra and SeaWiFS chlorophyll data sets. MODIS and SeaWiFS data were used to study methodologies to create a consistent series of long-term observations from sensors of different design, characterization, processing algorithms, and calibrations. Analyses of MODIS/Terra (Kilpatrick *et al.*, 2002; Fargion and McClain, 2003) daily oceans data in comparison with SeaWiFS were performed to facilitate the merger efforts (http://simbios.gsfc.nasa.gov/~ewa/SeaMODIS/seamodis-match.html). The analyses focused on assessing temporal trends in data discrepancies between MODIS and SeaWiFS and artifacts present in MODIS data caused by the difficulties in accurately characterizing this complex sensor for features such as polarization sensitivity. A time series of daily water-leaving radiance and chlorophyll products, evenly spread over the three years of joint MODIS/Terra and SeaWiFS coverage, was used to study MODIS trends in departure from SeaWiFS data and MODIS scan angle and latitudinal dependencies. Corresponding investigations were performed on a three-month time series of provisional MODIS/Aqua data and concurrent SeaWiFS coverage (http://simbios.gsfc.nasa.gov/~ewa/SeaMODISAqua/seamodis-aqua.html). The analyses provided vital information on MODIS data dependencies in relation to SeaWiFS ocean color records for the data merger activity. The information derived from MODIS/Terra and SeaWiFS comparisons was used to derive an ocean color sensor cross-calibration strategy where sensor artifacts, temporal, and spatial variabilities are not easily quantifiable and many dependencies are involved. Machine learning techniques were developed to cross-calibrate MODIS/Terra and SeaWiFS and produce a consistent ocean color baseline data set. The cross-calibration enabled the production of combined MODIS and SeaWiFS daily global chlorophyll coverages which were free from temporal trends, as well as MODIS scan angle and latitudinal dependencies (Kwiatkowska, 2003). An example of the cross-calibration result is shown in Figure 1.5.

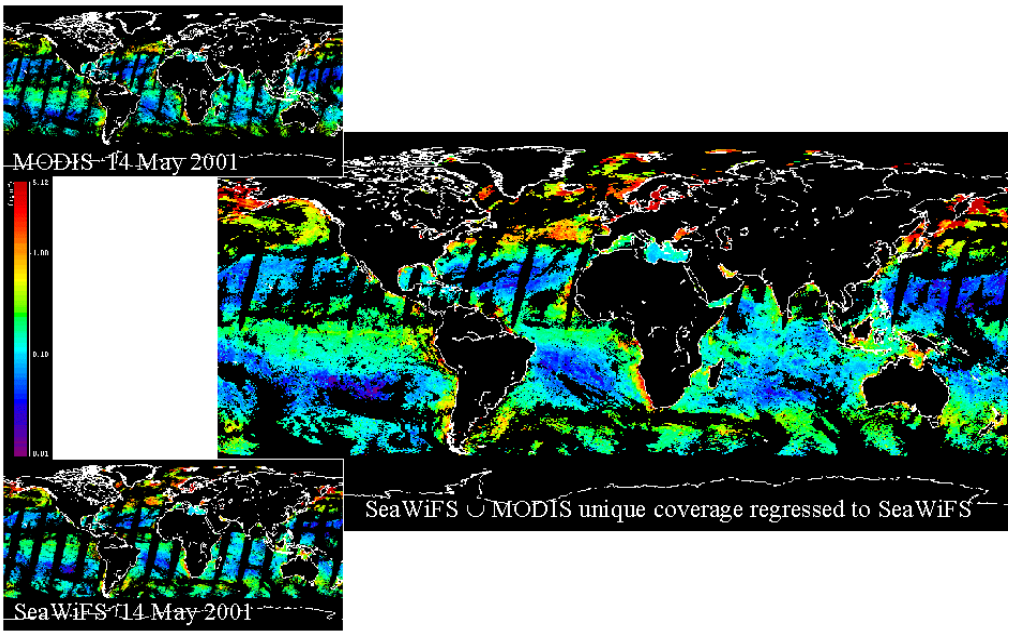

Figure 1.5: Result of machine learning cross-calibration of MODIS and SeaWiFS data. A merged, consistent daily chlorophyll map was produced using original SeaWiFS chlorophyll and MODIS data regressed to SeaWiFS baseline chlorophyll representation.

Statistical objective analysis was investigated to spatially and temporally interpolate MODIS/Terra (cross-calibrated with SeaWiFS) and SeaWiFS data onto daily global ocean color maps (Kwiatkoska and Fargion, 2002; Kwiatkoska 2001). The objective of the interpolation was to merge ocean color data sets using individual sensor chlorophyll accuracies and produce error bars for each data point. An addition to conventional statistical objective analysis was proposed to perform both space and time interpolation of ocean color data. Furthermore, the ensemble spatial and temporal correlation structure of the chlorophyll field was made dependent on the ocean spatial variability defined by local dynamical processes. An effort was made to merge ocean color data of different spatial resolutions to support data merger applications focused on local area coverage, such as on coastal zones. A wavelet transform multi-resolution analysis was applied to overlapping MOS and SeaWiFS scenes, where MOS data were at 0.5km resolution and SeaWiFS at 1.1km resolution (Kwiatkoska and Fargion, 2002a & b; Kwiatkoska 2001). The approach enabled enhancement of oceanic features in lower resolution imagery using higher resolution data.

In addition, the SIMBIOS Project developed an operational merged product at the level of observed radiances, water-leaving radiances, or derived products such as chlorophyll. As a demonstration of this technique, software and procedures were developed within the SIMBIOS Project to generate merged Level-3 products from SeaWiFS and MODIS. In coordination with MODIS/Terra oceans collection #4 reprocessing, the SIMBIOS Project began to receive daily Level-3 binned chlorophyll products, and to merge the MODIS products with SeaWiFS Level-3 chlorophyll products within the framework of the SeaWiFS Data Processing System (SDPS) (Figure 1.6). When the first daily binned chlorophyll products from MODIS/Aqua became available, these were immediately incorporated into the merging process as well.

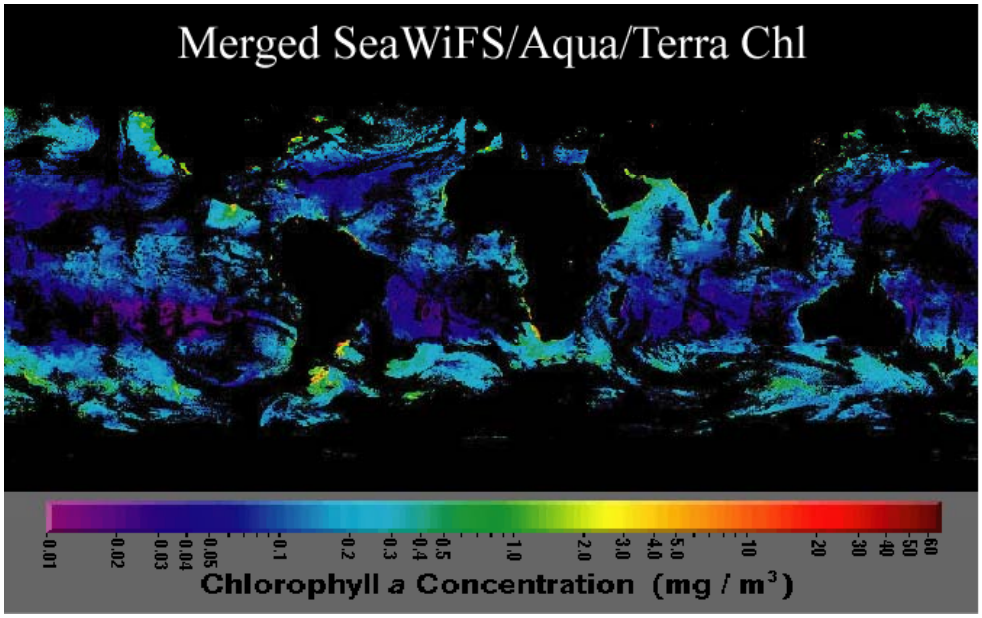

Figure 1.6: MODIS 4.6 km product converted to 9-km SeaWiFS format merged with standard SeaWiFS 9-km Level-3 chlor_a bin product, then mapped.

The SeaWiFS products used in the merging are standard 9-km resolution bin files composited over one-day periods. The MODIS products are standard Level-3 daily binned files at 4.6-km resolution. The specific ocean color parameters used are the chlor_a product of SeaWiFS, which is the chlorophyll concentration derived using the OC4V4 algorithm (O'Reilly, 2000), and the chlor_a_2 product of MODIS (Terra & Aqua), which is the chlorophyll concentration derived with the OC3M algorithm (O'Reilly, 2000). The MODIS product suite includes multiple chlorophyll products, but the chlor_a_2 product is considered to be the SeaWiFS-analog. Both the MODIS and SeaWiFS bin file formats use a sinusoidal distribution of equal area bin elements; however, the MODIS products are generated at a higher resolution

than SeaWiFS. The first step in the merging process is to convert the MODIS products to the 9-km resolution of SeaWiFS, to achieve a 1-to-1 mapping of the MODIS and SeaWiFS bins. The SIMBIOS Project developed two pieces of software to accomplish this task. The first, modbin2seabin, converts the MODIS format to a SeaWiFS-like format at the original MODIS bin resolution. This is just a slight reorganization of the Hierarchial Data Format (HDF) fields. The second program, reduce_bin_resolution, is essentially a modified version of the SeaWiFS time binning code, which performs spatial compositing of the input bins. For the MODIS files, reduce_bin_resolution effectively averages four 4.6-km bins into a single 9-km bin. The averaging is weighted by the square root of the number of observations within each 4.6-km bin, which is the same approach used for standard temporal compositing of MODIS and SeaWiFS (Campbell *et al.*, 1995).

Once the MODIS products have been converted to SeaWiFS-like format and resolution, the standard SeaWiFS temporal binning code, timebin, is employed to composite the files from both missions into daily, weekly, and monthly Level-3 bin products at 9-km resolution. Again, the time binner performs a weighted average, with weights computed as the square root of the number of observations within each input bin. These binned products are then mapped using the standard SeaWiFS mapping software, smigen, and the mapped files and browse images are distributed through the SeaWiFS Standard Mapped Image browser at http://seawifs.gsfc.nasa.gov/cgi/level3.pl?DAY=13Jul2002&PER=&TYP=modsea .

1.5 VALIDATION OF BIO-OPTICAL PROPERTIES

A standard set of measurement protocols is indispensable in developing consistency across the variety of international satellite ocean color missions either recently launched or scheduled for launch in the next few years. The SeaWiFS and SIMBIOS Projects allocated resources to describe and develop protocols or scientific approaches in accordance with the goals of the Projects (Mueller & Fargion, 2003; Fargion *et al.*, 2001). These efforts, described in NASA TMs, are intended to provide standards, which if followed carefully and documented appropriately, will ensure that any particular set of optical measurements will be acceptable for ocean color sensor validation and algorithm development. The protocols are guidelines and may be somewhat conservative. Continued development and refinement of these protocols help ensure coordination, collaboration, and communication between those involved. Furthermore, calibration round-robin intercomparison experiments are conducted by the Project (Riley and Bailey, 1998; Meister *et al.,* 2002 and 2003).

The SIMBIOS and SeaWiFS Projects maintained a local repository of *in situ* bio-optical data, known as SeaBASS, to support and sustain their regular scientific analyses (Hooker *et al.*, 1994; Werdell and Bailey, 2002; Werdell *et al.*, 2003). This system was originally populated with radiometric and phytoplankton pigment data used in the SeaWiFS Project's satellite validation and algorithm development activities. To facilitate the assembly of a global data set, SeaBASS was broadened to include oceanographic and atmospheric data sets collected by the SIMBIOS Project, which aided considerably in minimizing spatial and temporal biases in the data while maximizing acquisition rates. To develop consistency across multiple data contributors and institutions, the SIMBIOS Project also defined and documented a series of *in situ* sampling strategies and data requirements that ensure that any particular set of measurements are appropriate for algorithm development and ocean color sensor validation (McClain *et al.* 1992). The SeaBASS bio-optical data set includes measurements of apparent and inherent optical properties, phytoplankton pigment concentrations, and other related oceanographic and atmospheric data, such as water temperature, salinity, and aerosol optical thickness (AOT). Data were collected using a number of instrument packages from a variety of manufacturers, such as profilers and handheld instruments, on a variety of platforms, including ships and moorings. As of April 2003, SeaBASS included data collected by research groups at 44 institutions in 14 countries, encompassing over 1,150 individual field campaigns, including major international field experiments, such as the Asian Pacific Regional Aerosol Characterization Experiment (ACE-Asia) and the Indian Ocean Experiment (INDOEX) (Figure 1.7).

The full data set includes over 300,000 phytoplankton pigment concentrations, 13,500 continuous depth profiles, 15,000 spectrophotometric scans, and 15,000 discrete measurements of AOT. Participants of the SIMBIOS Program contributed just over 87% of these data. The SIMBIOS Project Office made use of a rigorous series of submission protocols and quality control metrics that range from file format verification to inspection of the geophysical data values (Fargion *et al.* 2001; Knobelspiesse *et al.*, 2003;

Mueller & Fargion, 2003). This ensures that observations fall within expected ranges and do not exhibit any obvious characteristics of measurement problems. A consistent methodology for validating satellite data retrievals was developed and applied to OCTS, MOS, POLDER, SeaWiFS and MODIS providing a means of objectively analyzing validation results across missions by minimizing the effect of processing differences on the overall results. Briefly, the validation analysis requires coincident measured *in situ* and satellite observations, quality controlled data sets (both satellite and *in situ*), derived from a well-defined, objective set of exclusion criteria (McClain *et al.*, 2000). An example of these validation results for SeaWiFS and MODIS (Terra) are presented in Figure 1.8.

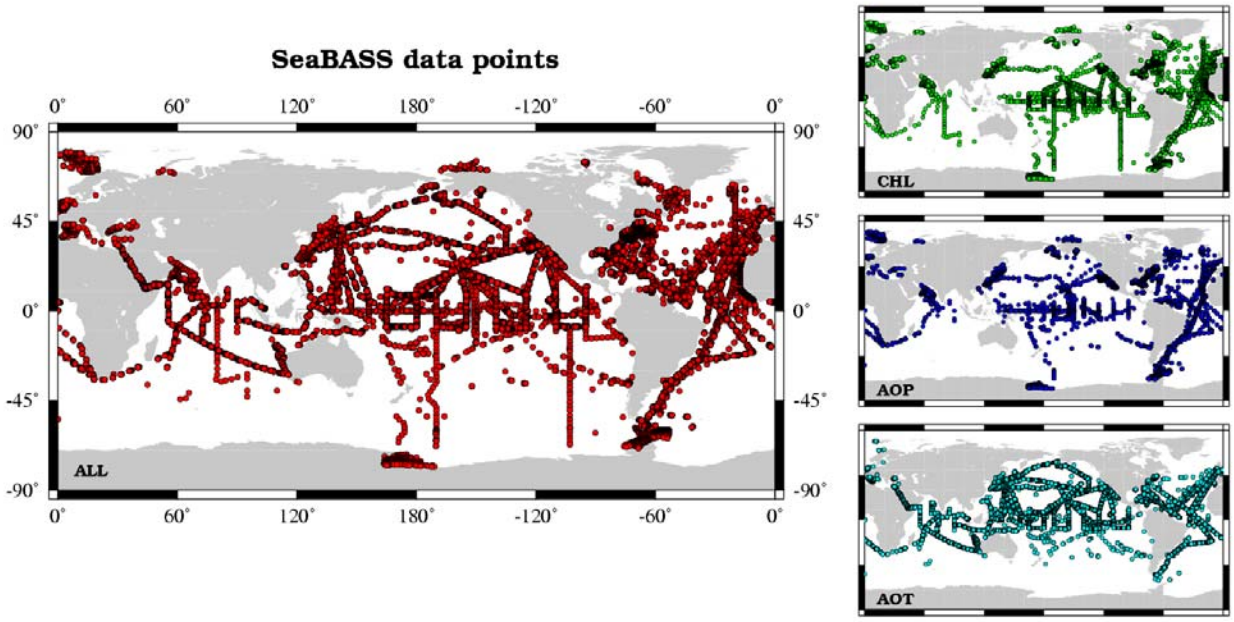

Figure 1.7: The global distribution of data included in the full SeaBASS bio-optical data set, as of April 2003. Clockwise from left: all archived data, chlorophyll a concentrations only (CHL), apparent optical properties only (AOP), and aerosol optical thickness only (AOT).

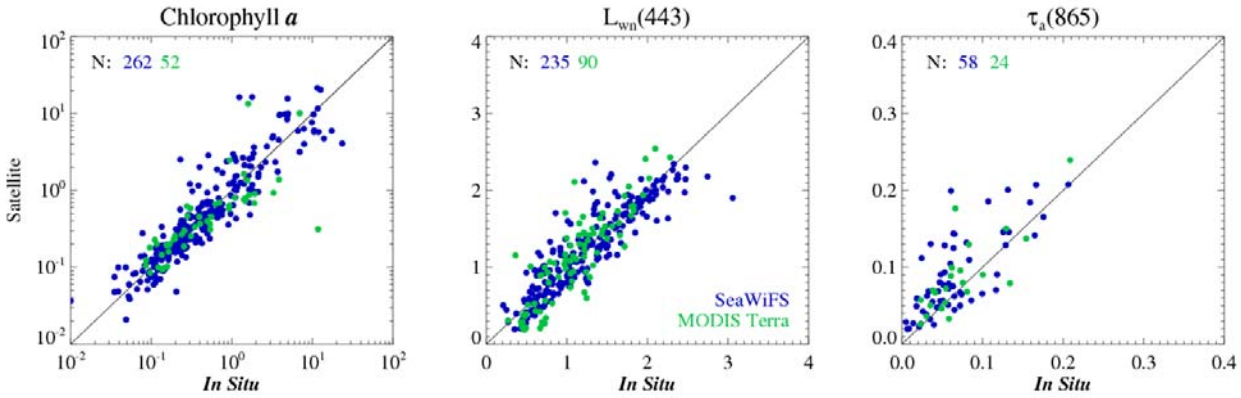

Figure 1.8: Scatter plots of coincident *in situ* and SeaWiFS (blue) and MODIS Terra (green) observations for chlorophyll *a*, water-leaving radiance (L_{wn}) at 443 nm, and aerosol optical thickness (τ) at 865 nm. The chlorophyll *a* data were transformed to account for their log-normal distribution. A one-to-one line has been included for clarity.

The SeaBASS World Wide Web site, located at http://seabass.gsfc.nasa.gov, provides a complete description of the system architecture, comprehensive documentation on policies and protocols, and direct access to the bio-optical data set and validation results. Briefly, the architecture consists of geophysical data and metadata recorded in digital ASCII text files, which reside on a dedicated server at NASA GSFC, and a relational database management system (RDBMS) used to catalog and distribute the data and files. Through the use of online search engines that interface with the RDBMS, the full bio-optical data set is queriable and available to authorized users via the Web (Figure 1.9). To protect the publication rights of contributors, access to data collected more recently than January 1, 2000 is limited to SIMBIOS Science Team members, NASA-funded researchers, and regular voluntary contributors, as defined by the SeaBASS access policy (Firestone and Hooker, 2001). The remainder of the data is fully available to the public and, additionally, has been released to the National Oceanic and Atmospheric Administration's (NOAA) National Oceanographic Data Center (NODC) for inclusion in their archive. As of September 2003, 45 research groups outside of the SIMBIOS and SeaWiFS Project Offices have been granted unrestricted access to SeaBASS. In 2002, these groups queried SeaBASS over 950 times and downloaded more than 60,000 data files from the bio-optical data set. During the same period, 146 research groups searched the public set 600 times and downloaded over 37,000 files.

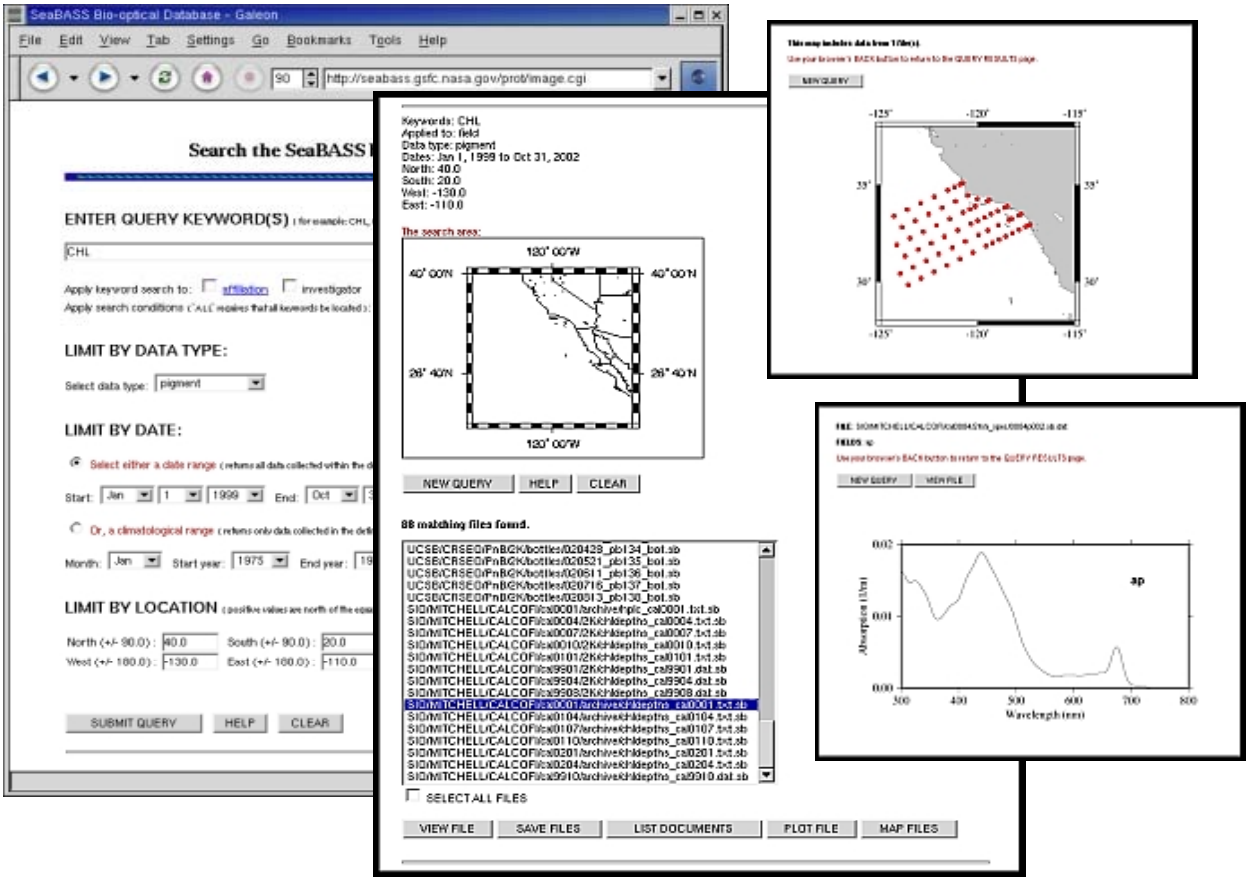

Figure 1.9: The full bio-optical data set is available online, using a variety of search engines and utilities.

1.6 SUPPORT SERVICES

In an effort to improve the quality and quantity of calibration and validation data sets, the SIMBIOS Project offered several support services to field investigators and the larger ocean color community. As of September 1, 2003, 397 cruises have been supported through services provided by the Project. These support services include: scheduling of on-board Local Area Coverage (LAC) recording for SeaWiFS; over

flight predictions for operational sensors; near real time SeaWiFS imagery for cruise locations; satellite data distribution and software support. The Project also provided optical instrumentation from a pool of investigator and project owned instruments; and round robin activities. Detailed information on the services is available on the SIMBIOS web site (http://simbios.gsfc.nasa.gov/).

Scheduling SeaWiFS On-board LAC Recording

Since much of the world's oceans are not covered by a SeaWiFS High Resolution Picture Transmission (HRPT) station, high-resolution data may have been recorded onboard the SeaWiFS sensor. As a service to the science community, the SIMBIOS Project, in conjunction with the SeaWiFS Project, scheduled SeaWiFS onboard LAC for cruises that occurred outside HRPT coverage. SeaWiFS has the ability to record a maximum of 10 minutes of high-resolution data per downlink. Typically, a 30-second interval was allotted for each LAC target, which corresponded to 180 scan lines or approximately 200 km along track at nadir.

Overflight Predictions for Operational Sensors

For calibration and validation purposes, *in situ* measurements should be made as close to the sensor over-flight time as possible. To aid investigators in determining when sampling should occur, the SIMBIOS Project offered over-flight predictions for all operational ocean color remote sensors. The sensors supported were SeaWiFS, MOS, Ocean Color Imager (OCI), OSMI, MERIS and MODIS (Terra & Aqua).

Near Real Time SeaWiFS & MODIS Imagery

In addition to providing predictions for satellite over-flight times, the SIMBIOS Project offered near real time imagery of the operational SeaWiFS products and MODIS (Terra & Aqua) to cruises at sea in JPEG and png format. These images may provide useful information in cruise planning both prior to and during oceanographic cruises. Level-1 images are available for SeaWiFS, and Level-2 products for SeaWiFS and MODIS. The SeaWiFS default specifications for the images provided include: available LAC, HRPT, and Global Area Coverage (GAC) (MODIS will be full resolution LAC equivalent); true color images from Level 1 bands 1, 5, and 6 (SeaWiFS only, no true color option available for MODIS); chlorophyll-a (chlor_a_2 algorithm for MODIS); image width 600 pixels; minimum percent valid chlorophyll pixels: 5%; same days as LAC coverage (SeaWiFS only). Images are also customized to best accommodate individual investigator needs.

Satellite Data Distribution

The OCTS is an optical radiometer which flew on the Japanese Advanced Earth Observing Satellite (ADEOS) from August 1996 to June 1997, collecting 10-months of global ocean color data. During the ADEOS mission lifetime, approximately 450 GB of real-time, 700m-resolution OCTS data were collected by the SeaWiFS project through NOAA ground stations at Wallops, Virginia and Fairbanks, Alaska. The archive consists of 337 scenes of the U. S. East Coast and 1,311 scenes over Alaska. These data were processed from raw telemetry through level-2 ocean color products using software developed by SIMBIOS and products distributed through a browse utility linked to the SIMBIOS Project's web site. Furthermore, the entire OCTS GAC data was reprocessed by the Project in 2001. This was a very productive collaboration with NASDA and Japanese scientists. OCTS-GAC data is available through the GSFC DAAC, the SIMBIOS Project and NASDA. Descriptions of the data processing stream, OCTS-specific modification to the algorithms, and statistical comparisons between OCTS and SeaWiFS can be found at: http://seawifs.gsfc.nasa.gov/SEAWIFS/RECAL/OCTS_Repro1/.

Since February 1999, the project has been operating a receiving station at NASA's Wallops Flight Facility (WFF) to acquire data from MOS onboard the Indian IRS-P3 spacecraft. When a pass is acquired at Wallops, the raw files are transferred to the SIMBIOS project at NASA's GSFC via an automated FTP process. The raw files are then converted to level-0 format through a software package provided by the Indian Space Research Organization (ISRO). The resulting level-0 files are made available to the German

Remote Sensing Data Centre (DLR-DFD) for archive and distribution. In addition, the SIMBIOS Project processes the data through level-1B using standard software provided by the German Institute for Space Sensor Technology (DLR-ISST) (Neumann *et al.*, 1995). All MOS data (1999-2003) processed by the SIMBIOS project is made available through the MOS browse system on the SIMBIOS web page.

In coordination with MODIS-Terra Collection 4 reprocessing, the Project initiated an operational process to collect and merge MODIS daily global chlorophyll products with SeaWiFS daily products. The merging scheme is a simple weighted averaging using standard SeaWiFS time-binning software. Presently a complete set of daily, weekly, and monthly merged chlorophyll products, including various perturbations such as MODIS-Terra with MODIS-Aqua, MODIS-Terra with SeaWiFS, MODIS-Aqua with SeaWiFS, and MODIS-Terra/MODIS-Aqua/SeaWiFS are made available at the SIMBIOS web page (http://seawifs.gsfc.nasa.gov/cgi/level3.pl?DAY=05Mar2000&PER=&TYP=tmsea). The merging process is fully automated and operational, with new products generated as soon as the MODIS data became available. The merged products can be displayed and manipulated with standard SeaWiFS software tools such as SeaDAS.

Diagnostic Data Set

During the first three SIMBIOS Science team meetings, it was recommended that a "diagnostic data set" be created for each ocean color sensor to aid in comparing data products and to allow rapid reprocessing of selected areas for calibration and algorithm evaluation. Two conditions for the selection of a diagnostic data set site were formulated. First, a reliable source of *in situ* data (bio-optical and/or atmospheric) for the site had to exist, and second, the principal investigator had to be willing to share the *in situ* data with the SIMBIOS project. Sites used as vicarious calibration sources were ranked with the highest priority. Time series sites were ranked as priority 2. All other sites were ranked as priority 3. Several sites were recommended, but did not meet one or both of the defined criteria. Several of the sites were modified, either at the request of an investigator, in order to reduce redundancy or improve coverage (by reducing the amount of land included in the extracted data). The list of sites as currently implemented is found in Table 1.4 and Figure 1.10 shows the MOBY diagnostic site.

By midyear 2001, the SIMBIOS project, in conjunction with the SeaWiFS project, had begun production of the L1A and L2 subsets of SeaWiFS LAC resolution data for the list of diagnostic data set sites. Prior to the start of the Collection 4 reprocessing of MODIS (Terra) data in March of 2002, the SIMBIOS project approached the MODIS Oceans Team with the request that MODIS produce a comparable set of extracted L1 and L2 data for inclusion in the diagnostic data set. The MODIS team agreed. However, as a consequence of the flow of data through MODAPS (the MODIS Adaptive Processing System), MODIS Oceans provides L1B and L2 extracts, rather than L1A as was the recommendation of the SIMBIOS Science Team and IOCCG Working Group. The diagnostic data set files produced by MODAPS are sent to the SIMBIOS project for post processing. In order to ensure that only useful data are included in the diagnostic data set, a threshold on the number of valid pixels within the region of interest was set. If this threshold (currently 25%) is not met, the files are excluded from further processing. If the threshold is met, a L2 (chlorophyll) browse image and two TAR files are created: one TAR file for the L2 granules and one for the L1B granules. Since the MODIS data are produced in five minute granules, the region of interest for a given site may cross the boundary between two granules. When this occurs, all L2 products from both granules are placed in the same TAR file, likewise for the L1B granules. The TAR files are then compressed using gzip compression.

The SIMBIOS and MODIS teams worked with the Goddard Distributed Active Archive Center (GDAAC) to make the diagnostic data set files for SeaWiFS and MODIS (Terra and Aqua) available through the GDAAC. All the necessary mechanisms for the transfer of the dataset to the GDAAC have been put in place, the most critical of which was the creation of six new Earth Science Data Type (ESDT) definitions, one for each L1 and L2 data type as well as for the SeaWiFS, MODIS-Terra and MODIS-Aqua data sources. Once the data are archived at the GDAAC, they are visible to both the GDAAC WHOM search engine and the EOSDIS EDG search engine. The diagnostic data set allows for the rapid processing and testing of atmospheric correction and geophysical product algorithms. The current list of sites cover a wide range of water types and aerosol conditions (see Table 1.4), which will aid algorithm assessments.

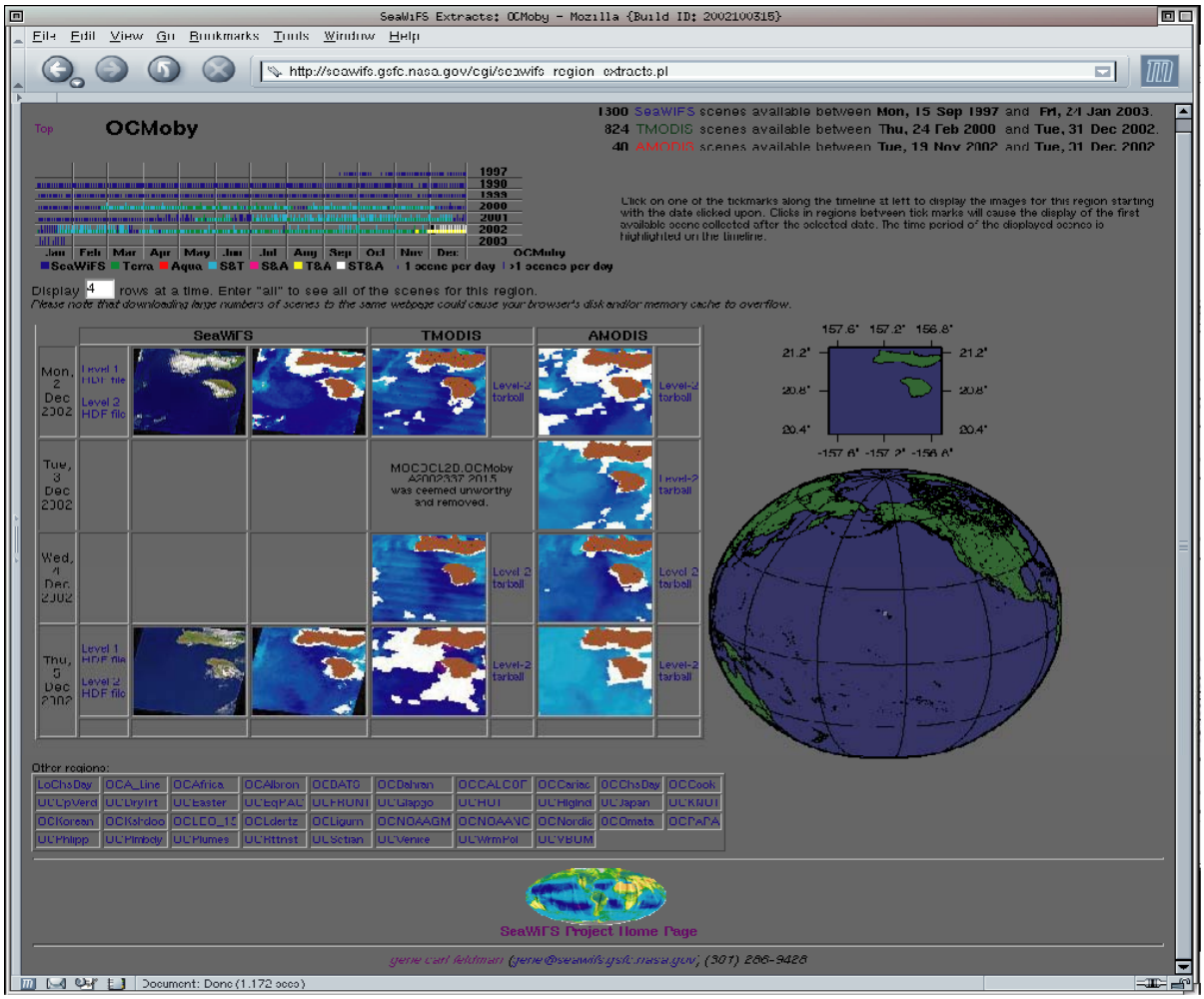

Figure 1.10: MOBY diagnostic site

SEADAS Software

The SeaDAS is a comprehensive software package for processing, displaying and analyzing all SeaWiFS data products (http://seadas.gsfc.nasa.gov). It was designed to serve a wide range of users, including individual scientists, SeaWiFS ground stations, and operational or commercial users. SeaDAS also provides level conversion processing designed to accurately replicate the operational data products (geophysical fields and data formats) generated by the SeaWiFS Project, when using the default input values. In addition, SeaDAS allows for flexibility in the algorithms applied, the map projections used, and other aspects of processing and analyses that enable users to customize their data products. Flexibility is further enhanced by providing executable programs, for those who only need the basic capabilities, and source code, for those who wish to insert alternative algorithms. The SeaDAS software package contains a full suite of interactive display and basic analysis tools. The SeaDAS tool kit includes many navigation, display, analysis, and output functions. Navigation functions include data registration, map projections, overlaying of coastlines, plotting of *in situ* data, and latitude/longitude point location. General display functions include data scaling, color bar definition, annotation, zooming, roaming, and color palette manipulation. General analysis functions include bathymetry generation, simple arithmetic functions, contour plots, profile plots, scatterplots, and histograms. Output functions allow output of either data or latitude/longitude values (ASCII, HDF, and binary flat files formats) or displayed images (PNG and PostScript formats). The SeaDAS group is co-located with the SeaWiFS and SIMBIOS Projects. SeaDAS was augmented by the SIMBIOS Project to include OCTS, MOS, OSMI, and soon, MODIS. The current SeaDAS user community includes approximately 500 research sites in 45 countries.

Table 1.4 Diagnostic site ID and location

Site ID	Location	North latitude	South latitude	West longitude	East longitude	Contact PI
OCAlbron	Alberon Gyre Eastern Med.	33.5N	32.5N	32.0 E	33.0E	
OCA Line	Japan East coast	42.0 N	41.0N	145.283E	146.283E	Tsuda
OCAfrica	Mauritanian Upwelling	21.5N	20N	18W	17W	Carder
OCBahrain	Bahrain, Persian Gulf	26.816 N	25.816N	50.0 E	51.0E	
OCBATS	BATS Bermuda	33.0N	31.0N	65.5W	63.5W	Nelson
OCCALCOF	CALCOFI, California Coast	34.5N	30.5N	124.0W	122.0W	Mitchell
OCCpVerd	Capo Verde, NW African Coast	17.217N	16.217N	23.433W	22.433W	Carder
OCCariac	Cariaco Basin, Venezuela	11.0N	10.0N	65.66W	64.16W	Mueller-Karger
OCChsBay	Chesapeake Bay	39.5N	36.8N	76.8W	75.6W	Harding
OCCook	Cook Island, Western South Pacific	19.5S	20.5S	163.5W	162.5W	
OCDryTrt	Dry Tortugas, Florida Keys	21.1N	24.1N	83.283W	82.283W	Voss
OCEaster	Easter Island, South Pacific Gyre	26S	28S	116W	114W	SIMBIOS Project
OCEqPAC	Eastern Equatorial Pacific	0.5N	0.5S	155.5W	154.5W	Chavez
OCFRONT	Long Island, New York	41.45N	40.45N	72.5W	71W	Morrison
OCGlapgo	Galapagos Islands	2.13N	1.87S	98.81W	88.81W	Feldman
OCHattrs	Cape Hatteras	37.5N	34.5N	76.5W	73.5W	Stumpf & Cota
OCHlglnd	Helgoland, North Sea	54.6N	53.6N	7.3E	8.3E	
OCHOT	HOT Station, Hawaii	23.25N	22.25N	158.5W	157.5W	Letelier
OCKshdoo	Kaashidoo, Maldives Islands	5.45N	4.45N	72.95E	73.95E	Holben & Frouin
OCKNOT	KNOT Station, NW Pacific	44.5N	43.5 N	154.5E	155.5E	Saitoch
OCKorean	Korean seawater Monitoring site, East China Sea	32.5N	31.5N	124.5E	125.5E	Kim
OCLeo 15	LEO 15 Station, New Jersey	40.1	38.5N	74.75W	73.5W	Arnone
OCLigurn	Ligurian Sea, Mediterranean	43.87 N	42.87 N	7.4 E	8.4 E	Antoine
OCLderz	Luderitz Upwelling, Namibian Coast	25.5S	26.5S	14E	15E	
OCMOBY	MOBY Buoy, Hawaii	21.3N	20.3N	157.75 W	156.7W	Clark & Trees
OCMontry	Monterey Bay,	37N	36.5N	122.75W	121.75W	Chavez

	California					
OCNOAAGM	Northern Gulf of Mexico	30N	29N	88W	87W	Arnone
OCNordic	Baltic Sea	55.5N	54.5N	18.8E	19.8E	
OCPAPA	Station PAPA, North Pacific	52 N	48 N	147 W	143 W	
OCPhlipp	Philippines	17.5 N	16.5 N	132.5 E	133.5 E	
OCPlumes	Plumes and Blooms region, Santa Barbara, CA	35.5 N	32.5 N	122 W	118 W	Siegel
OCPlymbdy	PlyMBoDY Mooring, English Channel	50.4 N	49.6 N	4.8 W	3.4 W	Aiken
OCRttnst	Rottnest Island, Western Australia	31.3 S	32.3 S	114.8 E	115.8 E	Lynch
OCSctian	Scotia Prince Ferry Route, Gulf of Maine	43.8N	42.8N	70.25W	65.75W	Balch
OCTahoe	Lake Tahoe	39.671N	38.671N	120.604W	119.604W	
OCVenice	Venice Tower (AAOT) Northern Adriatic	45.6N	44.8N	12.2E	13.4E	Zibordi
OCWrmPol	Warm Pool, Western Equatorial Pacific	0.5N	0.5S	164.5E	165.5E	
OCYBOM	YBOM replacement mooring, East China Sea	24.89N	23.89N	122.77E	123.77E	Ishizaka

Instrument Pool

Over the the years the Project has maintained and deployed a pool of sun photometers and above water radiometers intended to complement in-water optical measurements as well as the land-based Aerosol Robotic Network (AERONET) sun photometer network. The overall goal was to study aerosol optical properties and validate satellite retrievals of aerosol optical properties.

Three types of instruments composed the instrument pool (http://simbios.gsfc.nasa.gov/Sunphotometers/). The first type was a sun/sky photometer that measured the solar irradiance and the sky radiance. The second type was the shadow-band radiometer that measured the diffuse and total sky radiance. The third type was the Micropulse Lidar (MPL), which measured the vertical and horizontal distribution of aerosol backscatter, extinction and optical depth. The instruments were deployed by SIMBIOS or NASA principal investigators on cruises and the collected data was archived in SeaBASS. This instrument pool included fourteen Microtops II sun photometers (Morys *et al.*, 2001), one SIMBAD and two SIMBADA above water radiometers/sun photometers (Deschamps *et al.*, 2003), 2 PREDE sun photometers and one micro-pulse Lidar. The description, characteristics and advantages of each instrument have been reviewed in project protocols and project annual reports.

In addition to the instrument pool, the Project augmented the existing AERONET, which is dedicated to monitoring aerosol optical thickness (AOT) around the globe by supplying additional CIMELS. Most of the sun photometers used within the AERONET project (Holben *et al.*, 1998) are in continental zones, and SIMBIOS enhanced this network with island and coastal stations (Figure 1.11). SIMBIOS CIMEL sites included Lanai Hawaii (with backup in Honolulu, USA), Ascension Island, Bahrain, Papeete (Tahiti), Wallops Island (USA), Anmyon Island and Chinae (South Korea), Erdemli (Turkey), Horta (The Azores), Puerto Madryn (Argentina), Dahkla (Morocco) and Rottnest Island (Australia). This deployment activity ended in 2001 and all instrument are now managed by the AERONET group. SIMBIOS coastal stations have been used by the atmospheric community and their data have been used in several scientific papers.

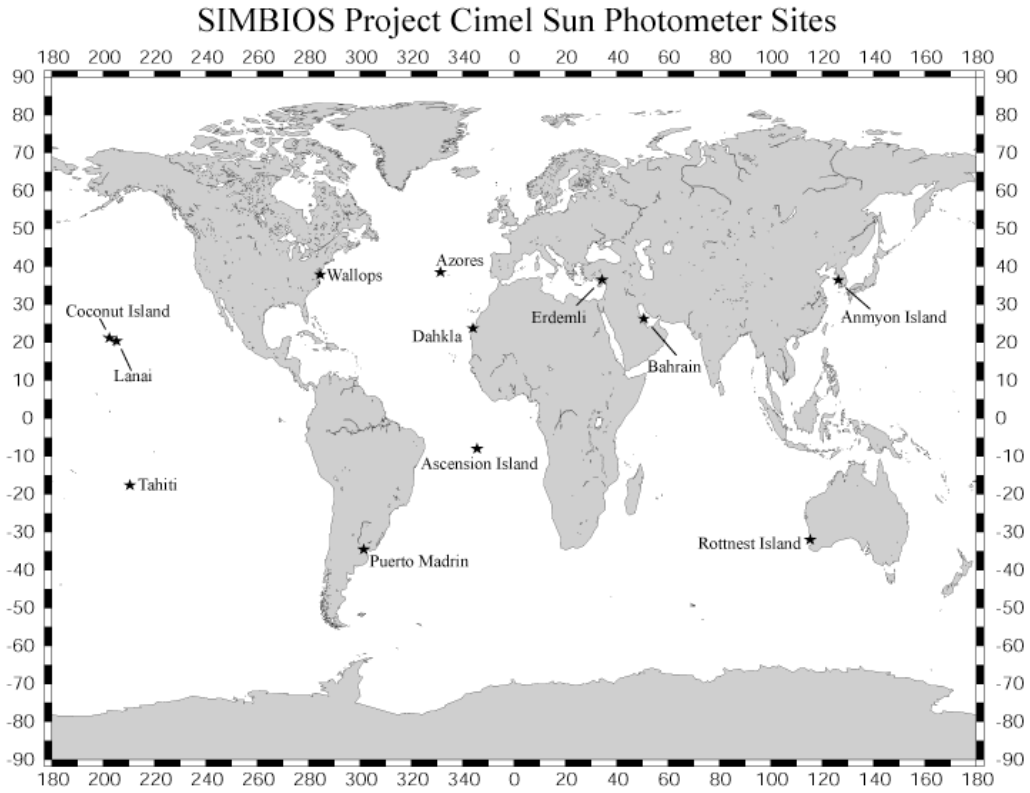

Figure 1.11: SIMBIOS CIMEL coastal and island sites.

SIMBIOS Project has taken a number of steps to ensure the consistency and quality of this atmospheric data set. Calibration was performed approximately every three months. Details on the operation, calibration and theoretical principles of sun photometry are posted at http://simbios.gsfc.nasa.gov/Sunphotometers /principle.html. To aid the organization and dissemination of collected data, the sun photometer instrument pool web site posts information about the deployment and data processing status of each instrument, along with calibration coefficient histories (Figure 1.12).

Several steps were taken to ensure data quality consistency from several instrument designs (Figure 1.13). The ACE-Asia cruise, on the R/V Ron Brown, was an ideal platform to validate SIMBIOS sun photometers. The R/V Ron Brown, which departed from Hawaii on March 15, 2001 and arrived in Yokosuka, Japan on April 19, 2001, encountered a variety of aerosol types, from maritime low optical thickness conditions to extremely high optical thickness due to Asian dust. Visual inspections of data time series suggest that despite differences in instrument design, calibration and deployment, AOT and Ångstrom exponent typically agree within uncertainties. Data from instruments whose bands (1) have similar (within 10nm) center wavelengths, and (2) have calculated uncertainty values were analyzed to find measurements taken within fifteen minutes of each other. These temporally similar measurements were plotted to assess trends or biases between the data. Nearly all AOT and Ångstrom exponent data fall within one uncertainty unit of the 1:1 line (data not shown). Generally speaking, at least 70% of all AOT data compare within one uncertainty unit of the value from another instrument, with the best agreement between the hand held instruments. With its high uncertainty values, the Angstrom exponent comparisons are even better, at 90% or more. Other problems, such as sun pointing for the Microtops II, were resolved by modifying the measurement protocols (Knobelspiesse *et al.*, 2003) and performing and uncertainty analysis for each instrument. Uncertainty values were computed and archived for each AOT and Ångstrom exponent measurement (Deschamps eta l.,2003; Russell *et al.*, 1993; Miller *et al.*, 2003). Computation of the Ångstrom exponent, which expresses the spectral character of the AOT values measured by sun

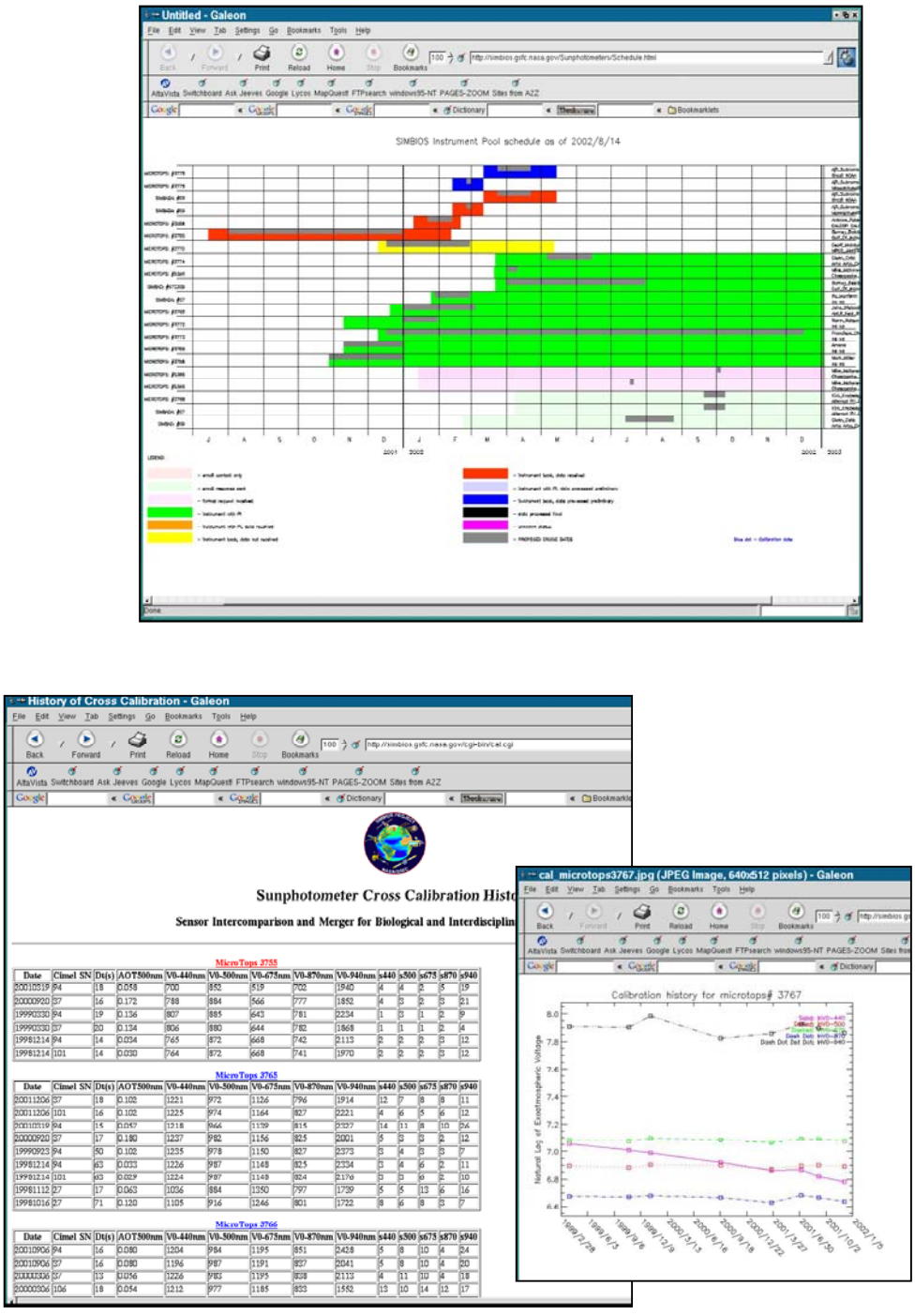

Figure 1.12: Instrument schedule for the pool deployment, calibration and data processing.

photometers, was standardized using multiple bands and a linear fitting routine to paired wavelength and natural logarithm of AOT values. The Ångstrom exponent is the negative slope of this fit. This Ångstrom exponent calculation method uses a recursive routine that makes an analytical computation of uncertainty impossible. To account for this, an Angstrom exponent calculation method was devised that incorporates the individual AOT uncertainties and the Chi-square error to determine and Ångstrom exponent

uncertainty. For several years the Project collected, processed and archived optical aerosol data from handheld sun photometers in marine locations. After standardizing the data processing of MicroTops and SIMBAD/A by using identical calibration methods, ancillary data and processing software, a statistical analysis was done (Knoblespiesse *et al.* 2003b). Statistical analyses reveals a dataset influenced by its temporal and geographical distribution, while the multi-modal histogram for AOT and Ångstrom exponent reveal varied aerosol populations (Knoblespiesse *et al.* 2003). This separation was validated by showing individual classes more likely to be log-normally (for AOTs) or normally (for Ångstrom exponents) distributed than the dataset as a whole. Properties of each class are represented in Figure 1.14. Results are also compared with the SeaWiFS atmospheric correction-aerosol models (Figure 1.15). The implications of this comparison are discussed in Knoblespiesse *et al* (2003b) and in Chapter 19 by M. Wang.

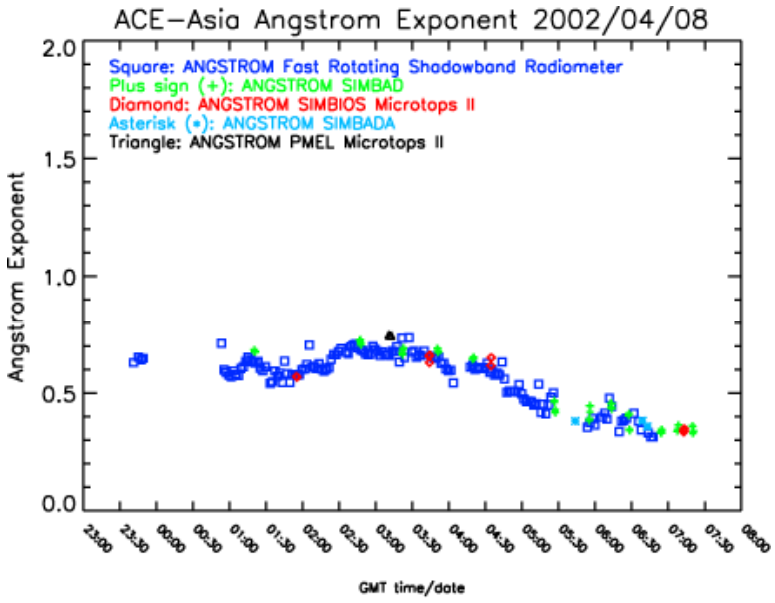

Figure 11.3: Validation of the SIMBIOS sun photometers on the ACE-Asia cruise.

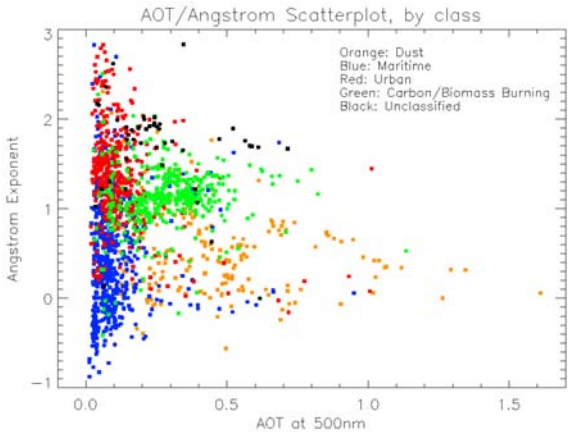

Figure 1.14: Location on an AOT/Angstrom Exponent scatter plot of each class. Data in blue represent class 1 type aerosols, encountered in 'maritime' conditions, while orange represents class 2 'dust', green shows class 3 aerosols and red represents class 4 aerosols encountered in 'urban' conditions. Data in black could not be classified.

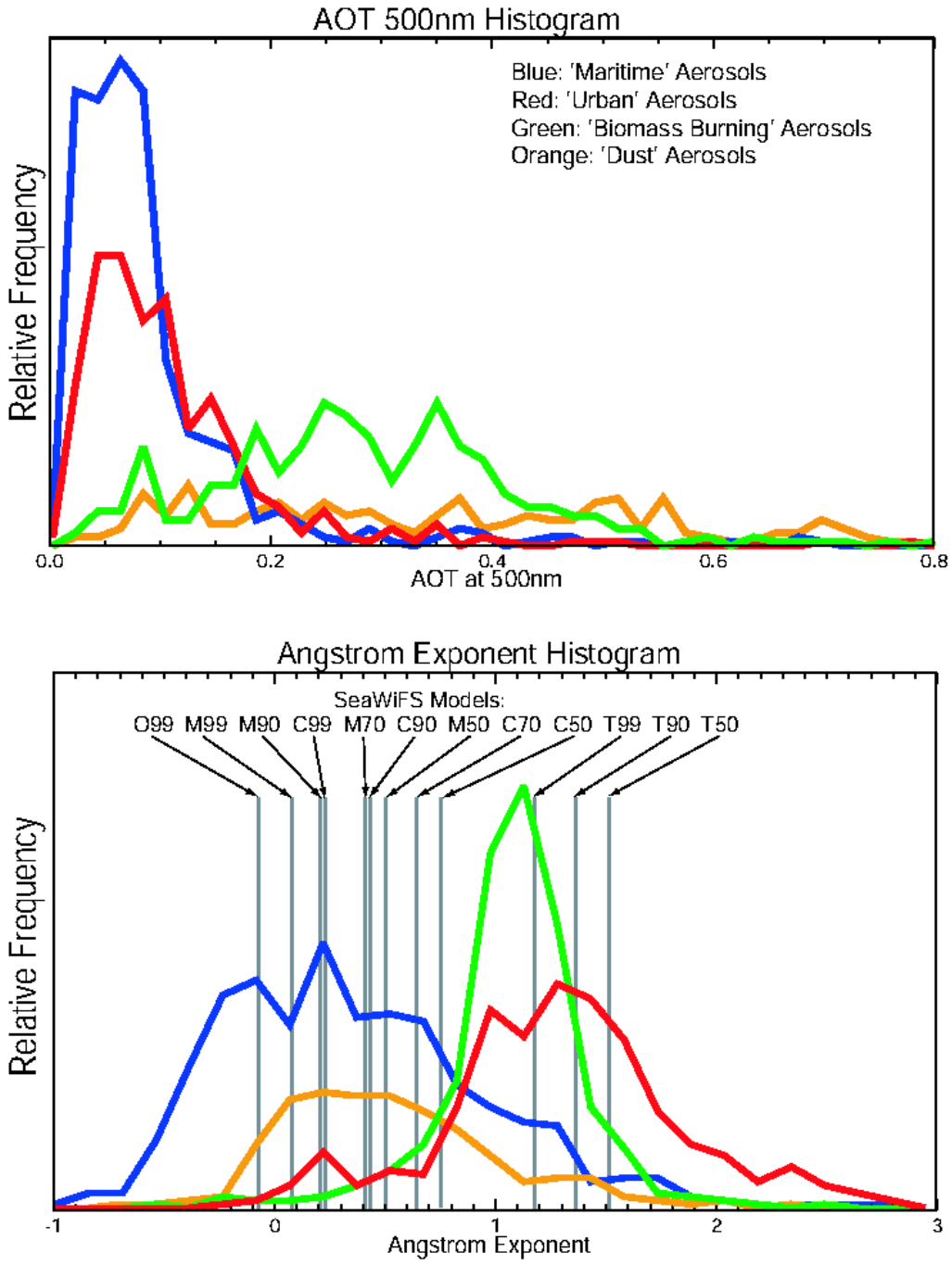

Figure 1.15: Histograms of AOT at 500nm and Angstrom Exponent for classified aerosol data. Class 1 is presented in blue, class 2 in orange, class 3 in green and class 4 in red. Bin sizes used in histogram computation were 0.02 for AOT at 500nm (A) and 0.1 for Angstrom Exponent (B). Vertical black bars on the Angstrom Exponent histogram show the equivalent Angstrom Exponents for SeaWiFS aerosol models (Gordon and Wang, 1994), (Shettle and Fenn, 1979).

1.7 CALIBRATION ROUND ROBIN

Two kinds of activities were performed by the Project to further ensure the adequate quality of *in situ* data. First, as mentioned, measurement protocols were developed, and their usage by the science community encouraged. Second, calibration round robin intercomparison experiments were conducted. The first SeaWiFS Transfer Radiometer (SXR) was built for the SeaWiFS Project to verify and compare measurements of spectral radiance at six discrete wavelengths in the visible and near infrared (Johnson *et al.*, 1998). The SXR is currently used to compare these sources to standards of spectral radiance maintained at the National Institute of Standards and Technology (NIST). The SIMBIOS Project had a second copy of the SeaWiFS Transfer Radiometer (SXR-II) built for use in the calibration round robin. This unit supplemented the first unit and was designed for easier travel. NASA personnel executed the first SIMBIOS-sponsored calibration round-robin experiment (the sixth SeaWiFS Intercalibration Round-Robin Experiment or SIRREX-6; previous round-robin had been sporsored by the SeaWiFS Project) from August 1997 to February 1998 (Riley and Bailey, 1998).

In SIRREX-6, four common field instruments (Satlantic in-water radiometers) were taken to nine separate laboratories and tested using the laboratories' standards and procedures. Two of the sensors were seven-channel radiance heads and two were seven-channel irradiance heads. The calibration and data reductions procedures used at each site followed the laboratories' normal procedures. The reference lamps normally used for the calibration of these types of instruments by the various laboratories were also used for this experiment. Project personnel processed the data to produce calibration parameters from the various laboratories for comparison. These tests showed an overall agreement at better than the +/-2% level. The SIRREX-6 was followed by the SIMBIOS Radiometric Intercomparison experiments (SIMRIC-I and II) in 2001 and 2002 (Fargion and McClain, 2003; Meister *et al.*, 2002; Meister *et al.* 2003). The purpose of these round-robins was to: 1) verify that all laboratories were on the same radiometric scale; 2) detect and correct problems at any individual laboratory in a timely fashion; 3) encourage the common use of calibration protocols; 4) identify areas where the calibration protocols need to be improved; and 5) document the calibration procedures specific to each laboratory. The participating laboratories included academic institutions, government agencies and instrument manufacturers that either directly or indirectly contributed to SeaBASS. They were, in alphabetical order: Biospherical Instruments Inc.; HOBI Labs Inc.; ICESS at the University of California, Santa Barbara; MOBY Project of Moss Landing Marine Laboratories; NASA Code 920.1, Goddard Space Flight Center; NASA Code 972, Wallops Flight Facility; Naval Research Laboratories, Washington; Satlantic Inc., Canada; Scripps Institute of Oceanography, University of California, San Diego; University of Miami; University of South Florida, St. Petersburg.

The SXR-II was calibrated on a yearly basis at NIST, in the Spectral Irradiance and Radiance Calibration with Uniform Sources (SIRCUS) facility. The radiometric stability of the SXR-II between NIST calibrations was monitored by the portable light sources the SeaWiFS Quality Monitors (SQM), the OCS-5002 from YES, Inc., and the SQM-II from Satlantic, Inc. The radiances produced by the laboratories for calibration were measured in the six SXR-II channels from 411 nm to 777 nm and compared to the radiances expected by the laboratories. Typically, the SXR-II measured radiances differed from the radiances expected by the laboratories by less than 2%. This level of agreement is satisfactory. In some cases, larger deviations were found and tracked to issues such as improper baffling, incorrect setup of the light sources, or deterioration of the main calibration bulb of the respective laboratory. Several issues were identified where the calibration protocols needed to be improved, especially the reflectance calibration of the reference plaques and the distance correction when using the irradiance standards at distances greater than 50 cm.

1.8 CONCLUDING REMARKS

Past and present satellite missions typically provide observations that are limited to the short-term, to specific processes of scientific interest or to test new technologies. Production of long-term products requires cross-calibrated measurements that have been merged in space and time measurements. The production of these products is usually beyond the scope of individual missions. SIMBIOS Program goals and tasks addressed the complexity of issues involved with how to produce a long-term calibrated data set across missions for use in climate research.

The specific objectives of the SIMBIOS Program were: (1) to quantify the relative accuracy of measurements from the ocean color products from each mission, (2) to work with each project to improve the level of confidence and compatibility among these products, and (3) to develop methodologies for generating merged level-3 products. Clearly, these objectives encompass both experimental and operational requirements. The Project has established links with all of currently operational missions (1997-2003) and has built up an operational project with the activities described in Figure 1.1. These activities build on the "*know how*" and experience of the SIMBIOS and SeaWiFS inhouse staff. One of the SIMBIOS Project's unique capabilities is to address the complexity of all the characterization and calibration processing steps as a "*start to finish"* process. This approach is a success story on how to tackle these issues while engaging the ocean color community. An open, peer review process within the Project staff and with the larger ocean color community on algorithm development, merging techniques and protocol development is the valid model for the operation of future missions.

The following specific conclusions may be drawn from the SIMBIOS experience: simple merging techniques (big bin or other averaging methods) applied on known biases result in degradation of merged data set and is not recommended; cross calibration and characterization in time and space with overlapping periods are essential steps before proceding with data set merging or producing long time series; neural network and semi-analytical merging algorithms can produce merged products with lower uncertainties while providing the desired improvements in daily coverage, and both methods require *a priori* knowledge of the uncertainty and charaterization over time of the merged missions; the funded global *in situ* bio-optical collection and SeaBASS data set have been invaluable resource for evaluating satellite products and data merging methodologies and it, or a similar data set, is required for further efforts.

The achievements were certainly due to the well thought out tasks (accurate characterization, calibration, establishment of traceability by national measurement institutions, validation, etc.) and operational configuration (Figure 1.1). Over the past several years, a set of key resources were developed:

- a comprehensive *in situ* bio-optical database;
- a program to evaluate different atmospheric correction algorithms;
- a program to link the calibrations of individual ocean color satellite instruments;
- a program (including cross-calibrations and measurement protocols) to develop a consistent *in situ* calibration and validation data set for the satellite measurements;
- a model for funded collection of *in situ* data, including rapid turn around;
- alternate algorithms to convert radiometric measurements to derived geophysical products;
- alternate methods to combine ocean color measurements from different sources into a single data set; and
- a strong documentation record.

The calibration and validation programs for individual missions (both domestic and international) had a wide range of approaches and methodologies, making international cooperation imperative to ensure high quality climate data. Calibration of long-term, high quality data, mission data overlap and consistent data sets are the basis of data stability. Natural signals are very small and impossible to detect with unstable and/or gappy data. Further data stability requires a system that should have the capability to reprocess large data sets as our understanding improves. Our hope is that the organizational structure, lessons learned, and knowledge achieved by SIMBIOS will benefit future ocean color programs. Finally, and perhaps most importantly, the SIMBIOS program demonstrated that international projects, agencies, and science teams could work effectively together in tangible ways (e.g., sharing data, processing code, algorithms, and product evaluations, and in collaborating on joint mission reprocessings) to improve the products each mission was generating and to generate a high quality time series of global observations.

REFERENCES

Baith, K., R. Lindsay, G. Fu, and C.R. McClain, 2001: SeaDAS: Data Analysis System Developed for Ocean Color Satellite Sensors. *Eos Trans. AGU*, **82**(18), 202.

Campbell, J. W., J. M. Blaisdell, and M. Darzi, 1995: Level-3 SeaWiFS Data Products: Spatial and Temporal Binning Algorithms, *NASA Technical Memorandum 104566*, Volume **32**, S.B. Hooker, E.R. Firestone, and J.G. Acker, Eds., NASA Goddard Space Flight Center, Greenbelt, Maryland.

Deschamps, P-Y, B. Fougnie, R. Frouin, P. Lecomte and C. Verwaerde, 2003: SIMBAD: A field radiometer for satellite ocean-color validation, *Applied Optics* (in press).

Dubovik, O., *et al.*, 2000: Accuracy Assessments Of Aerosol Optical Properties Retrieved From Aerosol Robotic Network (AERONET) Sun And Sky Radiance Measurements, *J. Geophys. Res*., **105**, D8, 9791-9806.

Fargion G.S. and C.R. McClain, 2001: SIMBIOS Project 2000 Annual Report, *NASA Tech. Memo. 2000-209976*, NASA GSFC, Greenbelt, Maryland, 164 pp., http://simbios.gsfc.nasa.gov/ye_reports.html.

Fargion, G. S. *et al.*, 2001: In situ Aerosol Optical Thickness Collected by the SIMBIOS Program (1997-2000): Protocols, and Data QC and Analysis, *NASA Tech. Memo. 2001-209982*, NASA GSFC, Greenbelt, Maryland, 103 pp., http://simbios.gsfc.nasa.gov/ye_reports.html.

Fargion G.S. and C.R. McClain, 2002: SIMBIOS Project 2001 Annual Report, *NASA Tech. Memo. 2002-210005*, NASA GSFC, Greenbelt, Maryland, 184 pp., http://simbios.gsfc.nasa.gov/ye_reports.html.

Fargion G.S. and C.R. McClain, 2003a: SIMBIOS Project 2002 Annual Report, *NASA Tech. Memo. 2003-211622*, NASA GSFC, Greenbelt, Maryland, 157 pp., http://simbios.gsfc.nasa.gov/ye_reports.html.

Fargion G.S. *et al.*, 2003b: MODIS, Validation, Data Merger and Other Activities Accomplished by the SIMBIOS Project: 2002-2003, NASA Tech. Memo., Goddard Space Flight Center, Greenbelt , Maryland, 1-80 (in press).

Firestone, E.R., and S.B. Hooker, 2001: Seawifs Postlaunch Technical Report Series Cumulative Index: Volumes 1-11, *NASA Tech. Memo. 2001-206892,* Vol. **12**, S.B. Hooker and E.R. Firestone, Eds., NASA GSFC, Greenbelt, Maryland, 24 pp.

Franz, B.A., *et al.*, 2001: A Three-Year Intercomparison of Oceanic Optical Properties from MOS and SeaWiFS*, Proc. AGU 2001,* Fall Meeting, San Francisco, California.

Franz, B.A., and Y. Kim, 2001: A Comparative Study and Intercalibration between OSMI and SeaWiFS, *Proc. AGU 2001,* Fall Meeting, San Francisco, California.

Franz, B.A., *et al.*, 2001: SeaWiFS Vicarious Calibration: An Alternative Approach Utilizing Simultaneous In situ Observations of Oceanic and Atmospheric Optical Properties, *NASA Tech. Memo.2001-209982*, 137 pp., 2001.

Gordon H.R. and M. Wang, 1994: Retrieval of Water-Leaving Radiance and Aerosol Optical Thickness Over the Oceans With Seawifs: A Preliminary Algorithm, *Appl. Opt.,* **33,** 443-452.

Holben B.N., T.F. Eck, I. Slutsker, *et al.*, 1998: AERONET - A federated instrument network and data archive for aerosol characterization", *Remote Sens. Environ.,* **66**, 1-16, 1998.

Hooker, S.B. *et al.*, 1994: The SeaWiFS Bio-Optical Archive And Storage System (SeaBASS), Part 1*, NASA Tech. Memo. 104566,* Vol. **20**, S.B. Hooker and E.R. Firestone, Eds., NASA GSFC, Greenbelt, Maryland, 37 pp..

Johnson B.C., Fowler J.B., Cromer C.L., 1998: The SeaWiFS Transfer Radiometer (SXR), *NASA Tech. Memo. 1998-206892*, Vol. **1**, NASA GSFC, Greenbelt, Md., 58 pp.

Kilpatrick, K., *et al.*, 2002: Time Series of Calibrated Ocean Products from NASA's Moderate Resolution Scanning Spectrometer (MODIS), *Proceedings of the Ocean Sciences Meeting*, Honolulu, Hawaii.

Knobelspiesse, K.D., C. Pietras and G.S. Fargion, 2003: Sun-Pointing Error Correction for Sea Deployment of the Microtops II Handheld Sun Photometer, *J. Atmos. Ocean. Tech*., Vol. **20**, No. 5, 767-771.

Knobelspiesse, K.D., C. Pietras, G.S. Fargion, M. Wang, R. Frouin, M.A. Miller, A. Subramaniam and W.M. Balch, 2003b: Maritime aerosol optical properties measured by handheld sun photometers. Submitted to Remote Sensing of Environment

Kwiatkowska, E.J., 2003: Application of Machine Learning Towards the Creation of a Consistent and Calibrated Global Chlorophyll-a Concentration Baseline Data Set, *IEEE Trans. on Geoscience and Remote Sensing*, (accepted).

Kwiatkowska E.J. and G.S. Fargion, 2002: Merger of Ocean Color Information from Multiple Satellite Missions under the NASA SIMBIOS Project Office, *Proc. of the Fifth International Conference on Information Fusion*, Annapolis, Maryland, **1**, 291-298.

Kwiatkowska E.J. and G.S. Fargion, 2002: Merger of Ocean Color Data from Multiple Satellite Missions within the SIMBIOS Project", *Proc. of SPIE Symposium,* Hangzhou, China.

Kwiatkowska-Ainsworth, E.J, 2001: Merger of Ocean Color Information of Different Spatial Resolution: SeaWiFS and MOS", *EOS Trans. American Geophysical Union*, Vol. **82**, no. 47, 675.

McClain, C. R., W. E. Esaias, W. Barnes, B. Guenther, D. Endres, S. B. Hooker, B. G. Mitchell and R. Barnes, 1992: SeaWiFS Calibration and Validation Plan, *NASA Tech. Memo. 104566,* Vol. **3**, S. B. Hooker and E. R. Firestone (eds.), NASA Goddard Space Flight Center, Greenbelt, Maryland, 41 pp.,.

McClain, C.R., *et al.*, 2002: The Proposal for the NASA SIMBIOS Program, 1995, *NASA Tech. Memo. 2002-210008*, NASA GSFC, Greenbelt, Maryland, 54 pp., http://simbios.gsfc.nasa.gov/ye_reports.html.

McClain C.R. and G.S. Fargion, 1999: SIMBIOS Project 1998 Annual Report, *NASA Tech. Memo. 1999-208645*, NASAGSFC, Greenbelt, Maryland, 105 pp., http://simbios.gsfc.nasa.gov/ye_reports.html.

McClain C.R. and G.S. Fargion, 1999: SIMBIOS Project 1999 Annual Report, *NASA Tech. Memo. 1999-209486*, NASA GSFC, Greenbelt, Maryland, 128 pp., http://simbios.gsfc.nasa.gov/ye_reports.html.

McClain C.R., R.A. Barnes *et al.*, 2000: SeaWiFS Postlaunch Calibration and Validation Analyses, Part 2, *NASA Tech*., *Memo. 2000-206892*, Vol **10**, S.B. Hooker and E.R. Firstone, Eds., NASA GSFC, Greenbelt, Maryland, 57pp.

Meister G. *et al.*, 2002: The First SIMBIOS Radiometric Intercomparison (SIMRIC-1), April-September 2001*, NASA Tech. Memo. 2002-210006*, GSFC, Greenbelt, Maryland, 60 pp., http://simbios.gsfc.nasa.gov/ye_reports.html.

Meister G. *et al.*, 2003: Comparison of Spectral Radiance Calibrations at Oceanographic and Atmospheric Research Laboratories", *Metrologia*, Vol. **40**, 93-96.

Miller, M.A., M.J. Bartholomew, and R.M. Reynolds, 2003: The Accuracy of Marine Shadow-band Sun Photometer Measurements of Aerosol Optical Thickness and Angstrom Exponent", *J. Atmos. Ocean Tech* (in press).

Morys, M., F. M. Mims III *et al.*, 2001: Design, Calibration, And Performance Of MICROTOPS II Handheld Ozone Monitor And Sun Photometer, *J. Geophys. Res*., **106**, 14, 573-14,582.

Mueller J.M. and G. S. Fargion, 2003: Ocean Optics Protocols for Satellite Ocean Color Sensor Validation, Revision 4, Part I, *NASA Tech. Memo. 2003-210004/Rev 4/Vol.I*, NASA Goddard Space Flight Center, Greenbelt, Maryland, 1-50 pp. http://simbios.gsfc.nasa.gov/ye_reports.html.

Mueller J.M. and G. S. Fargion, 2003: Ocean Optics Protocols for Satellite Ocean Color Sensor Validation, Revision 4, Part II, *NASA Tech. Memo. 2003-210004/Rev 4/Vol. II,* NASA Goddard Space Flight Center, Greenbelt, Maryland, 1-56 pp. http://simbios.gsfc.nasa.gov/ye_reports.html.

Mueller J.M. and G. S. Fargion, 2003: Ocean Optics Protocols for Satellite Ocean Color Sensor Validation, Revision 4, Part III, *NASA Tech. Memo. 2003-210004/Rev 4./Vol.III*, NASA Goddard Space Flight Center, Greenbelt, Maryland, 1-78 pp. http://simbios.gsfc.nasa.gov/ye_reports.html.

Mueller J.M. and G. S. Fargion, 2003: Ocean Optics Protocols for Satellite Ocean Color Sensor Validation, Revision 4, Part V, *NASA Tech. Memo. 2003-210004/Rev 4/Vol.V*, NASA Goddard Space Flight Center, Greenbelt, Maryland, 1-25 pp. http://simbios.gsfc.nasa.gov/ye_reports.html.

Mueller J.M. and G. S. Fargion, 2003: Ocean Optics Protocols for Satellite Ocean Color Sensor Validation, Revision 4, Part VI, *NASA Tech. Memo. 2003-210004/Rev 4./Vol. VI*, NASA Goddard Space Flight, Grenbelt, Maryland, 1-148 pp., http://simbios.gsfc.nasa.gov/ye_reports.html.

Neumann, A., T. Walzel *et al.*, 1995: MOS-IRS Data Processing, Software and Data Products (Preliminary Documentation), DLR Institute for Space Sensor Technology, DLR Institute for Space Sensor Technology.

Riley T. and S. Bailey, 1998: The Sixth Seawifs/SIMBIOS Intercalibration Round-Robin Experiment (SIRREX-6), *NASA Tech. Memo. 1998-206878*, NASA GSFC, Greenblet, Maryland, 26 pp.

Russell, P.B., J.M. Livingston *et al*., 1993: Pinatubo and Pre-Pinatubo Optical-Depth Spectra: Mauna Loa Measurements, Comparisons, Inferred Particle Side Distributions, Radiative Effects, and Relationships to Lidar Data, *J. Geophys. Res*., **98**, D12, 22, 969-22,985.

Van Heukelem L. C.S. Thomas and P.M. Glibert, 2002: Sources of Variability in Chlorophyll Analysis by Fluorometry and High-Performance Liquid Chromatography in a SIMBIOS Inter-Calibration Exercise, *NASA Tech. Memo. 2002-211606*, NASAGSFC, Greenbelt, Maryland, 51 pp., http://simbios.gsfc.nasa.gov/ye_reports.html.

Wang, M., 1999: A Sensitivity Study of the SeaWiFS Atmospheric Correction Algorithm: Effects of Spectral Band Variations", *Remote Sens.Environ*., **67**, 348-359.

Wang, M. and B.A. Franz, "Comparing The Ocean Color Measurements Between MOS and SeaWiFS: A vicarious intercalibration approach for MOS"*, IEEE Trans. Geosci. Remote Sensing,* **38***,* 184-197*,* 2000.

Wang, M., *et al.*, 2002: Ocean Color Optical Property Data Derived from OCTS and POLDER: A Comparison Study, *Appl. Optics, Vol.* **41**, No 6, 974-990.

Werdell, P.J. and S.W. Bailey, 2002: The SeaWiFS Bio-optical Archive and Storage System (SeaBASS): Current architecture and implementation, *NASA Tech. Memo. 2002-211617*, G.S. Fargion and C.R. McClain, Eds., NASA GSFC, Greenbelt, Maryland, 45 pp.

Werdell, P.J, S.W. Bailey, G.S. Fargion *et al.*, 2003: Unique Data Repository Facilitates Ocean Color Satellite*, EOS,* Vol. **84**, N. 38, 387 and 377.

This Research was Supported by the SIMBIOS Project Office

Publications

Barnes, R., R. E. Eplee, and F. S. Patt, 1998: SeaWiFS Measurements of the Moon. EurOpt Series, Sensors, Systems, and Next-Generation Satellites II, *SPIE,* **3498**, 311-324.

Barnes, R. A., D. K. Clark, W. E. Esaias, G. S. Fargion, G. C. Feldman, and C. R. McClain, 2003: Development of a consistent multi-sensor global ocean color time series, *Int. J. Remote Sens.*, Issue 20 of Vol. 24, 2047-4067.

Fargion, G. S., C. R. McClain, H. Fukushima, J. M. Nicolas, and R. A. Barnes, 1999: Ocean color instrument intercomparisons and cross-calibrations by the SIMBIOS Project. *SPIE, **3870-68**,* 397-403.

Fargion, G. S., C. R. McClain, and R. A. Barnes, 2000: Ocean color instrument intercomparisons and cross-calibrations by the SIMBIOS Project (1999-2000). *SPIE,* **4135***,* 411-420.

Fargion G. S. and C. R. McClain, 2000: Three Year of Ocean Color Instrument Intercomparisons and Cross-Calibrations by the SIMBIOS Project, Remote Sensing of the Ocean and sea Ice 2000, SPIE vol. 4172, 44-55.

Fargion G.S. *et al.*, 2003: SIMBIOS PROGRAM in Support of OCEAN COLOR Mission: 1997-2003, *SPIE Conference*, 3-8 August, San Diego, SPIE # 5155-7 (in press).

Gregg, W. W., M. E. Conkright, J. E. O'Reilly, F. S. Patt, M. Wang, J. Yoder, and N. Casey-McCabe, 2002: NOAA-NASA Coastal Zone Color Scanner reanalysis effort, *Appl. Opt.*, **41**, 1615-1628.

Gross-Colzy L., R. J. Frouin, C. M. Pietras, G. S. Fargion, 2002: Nonsupervised classification of aerosol models for ocean color remote sensing Ocean Remote Sensing and Applications, Editors: R. J. Frouin, Y. Yuan, H. Kawamura, Proceedings of SPIE Vol. 4892, [4892-14].

Holben B.N., D. Tanre, A. Smirnov, T.F. Eck, I. Slutsker, N. Abuhassan, W.W. Newcomb, J. Schafer, B. Chatenet, F. Lavenue, Y.F. Kaufman, J. Van de Castle, A. Setzer, B. Markham, D. Clark, R. Frouin, R.Halthore, N.A. Karnelli, N.T. O'Neill, C. Pietras, R. Pinker, K. Voss, G. Zibordi, 2001, An emerging ground-based aerosol climatology: Aerosol Optical Depth from AERONET*, J. Geophys. Res*., **106**, 12 067-12 097.

Ichoku C., R. Levy, Y. J. Kaufman, L. A. Remer, R. Li, V. J. Martins, B. N. Holben , N.K. Abuhassan, I. Slutsker, T.F. Eck, C. Pietras, 2002: Analysis of the performance characteristics of the five-channel Microtops II Sunphotometer for measuring aerosol optical thickness and precipitable water vapor, *J. Geophys. Res*, Vol. **107**, D13, 10.1029

Johnson B. C., S. Brown, K.Lykke, C. Gibson, G. S. Fargion *et al.*, 2003: Comparison of Crygenic Radiometry and Thermal Radiometry Calibrations at NIST Using Multichannel Filter Radiometers, *Metrologia*, **40**, S70-S77.

Knoblelspiesse K., C. Pietras and G.S. Fargion, 2003: Error Correction for Sea Deployment of Microtops II Hand Held Sun Photometer, *Journal of Atmospheric & Oceanic Tech*., Vol. **20**, 767-771

Knobelspiesse, K.D., C. Pietras, G.S. Fargion, M. Wang, R. Frouin, M.A. Miller, A. Subramaniam and W.M. Balch, 2003b: Maritime aerosol optical properties measured by handheld sun photometers. Submitted to Remote Sensing of Environment

Kwiatkowska E. J. and G. S. Fargion, 2002: Merger of Ocean Color Information from Multiple Satellite Missions under the NASA SIMBIOS Project Office. *Proceedings of the Fifth International Conference on Information Fusion*, Annapolis, MD, USA, **1**, 291-298.

Kwiatkowska E. J. and G. S. Fargion, 2002: Merger of Ocean Color Data from Multiple Satellite Missions within the SIMBIOS Project. *Proceedings of SPIE Symposium – Remote Sensing of the Atmosphere, Ocean, Environment, and Space*, Oct., Hangzhou, China, Ocean Remote Sensing and Applications, **4892**, 168-182.

Kwiatkowska, 2003: Application of Machine Learning Techniques Toward the Creation of Consistent and Calibrated Global Chlorophyll Concentration Baseline Dataset Using Remotely Sensed Ocean Color Data, IEEE Trans. Geocience and Remote Sensing, vol. **41**, no. 12, (in press)

Legrand M., C. Pietras, G. Brogniez, M. Haeffelin, N.K. Abuhassan, and M. Sicard, 2000, A High-Accuracy Multiwavelength Radiometer for In Situ Measurements in the Thermal Infrared. Part I: Characterization of the instrument, *J. Atmos. Ocean. Technol*., Vol. **17**, 1203-1214.

Meister G., P. Abel, R. Barnes, J. Cooper, C.Davis, M.Godin, G. S. Fargion et al, 2003: Comparison of Spectral Radiance Calibrations at Oceanographic and Atmospheric Research Laboratories, *Metrologia*, **40**, S93-S96

Mueller, J., C. McClain, R. Caffrey, and G. Feldman, 1998: The NASA SIMBIOS Program, *Backscatter.*

Porter J.N., M. Miller, C. Pietras, C. Motell, 2001, Ship-Based Sun Photometer Measurements Using Microtops Sun Photometers, *J. Atmos. Ocean. Technol*., Vol. **18**, 765-774.

Smirnov, A., B.N.Holben, O.Dubovik, D.L.Westphal, A.K.Goroch, C.R.McClain, T.F.Eck, and I.Slutsker, C. Pietras, 2002: Atmospheric aerosol optical properties in the Persian Gulf region, *J. Atmos. Sci*., **59**, 620-634.

Smirnov, A., B.N.Holben, Y.J. Kaufman, O.Dubovik, T.F.Eck, and I.Slutsker, C. Pietras, R.N. Halthore, 2002: Optical properties of Atmospheric aerosol in the Maritime Environments, *J. Atnos. Sci*., **59**, 501-523.

Tanaka, T. and M. Wang, Solution of radiative transfer in anisotropic plane-parallel atmosphere, *J. Quant. Spectr. Rad. Trans.* (In press).

Wang, M., 1999: Atmospheric correction of ocean color sensors: Computing atmospheric diffuse transmittance, *Appl. Opt.* , **38**, 451-455.

Wang, M. and B. A. Franz, 2000: Comparing the ocean color measurements between MOS and SeaWiFS: A vicarious intercalibration approach for MOS, *IEEE Trans. Geosci. Remote Sensing*, **38**, 184-197.

Wang, M., S. Bailey, and C. R. McClain, 2000: SeaWiFS Provides Unique Global Aerosol Optical Property Data, *EOS*, Vol. **81**, 197.

Wang, M., A. Isaacman, B. Franz, and C. R. McClain, 2002: Ocean Color Optical Property Data Derived from OCTS and POLDER: A Comparison Study, *Appl. Optics, Vol.* **41**, No 6, 974-990.

Wang, M. and H. R. Gordon, 2002: Calibration of ocean color scanners: How much error is acceptable in the near-infrared, *Remote Sens. Environ*., **82**, 497-504.

Werdell J., S. Bailey, G.S.Fargion *et al.*, 2003: Unique Data Repository Facilates Ocean Color Satellite Validation, *EOS*, Vol **84**, n.38, 377 & 387.

Zhao T. X-P., I. Laslo, B. Holben, C. Pietras, and K. Voss, 2003: Validation of two-channel VIRS retrievals of aerosol optical thickness over ocean and quantitative evaluation of the impact from potential subpixel cloud contamination and surface, *J. Geophys. Res*, **108**(D3), 4106.

Zhao, T. X.-P., I. Laszlo, O. Dubovik, B. N. Holben, J. Sapper, D. Tanré, and C. Pietras, 2003: A study of the effect of non-spherical dust particles on the AVHRR aerosol optical thickness retrievals, *Geophys. Res. Lett*., **30**(6), 1317.

NASA Techical Memorandum

McClain, C.R. and G.S. Fargion, 1999: SIMBIOS Project 1998 Annual Report, *NASA Tech. Memo. 1999-208645*, NASA Goddard Space Flight Center, Greenbelt, Maryland, 105 pp.

McClain, C.R. and G.S. Fargion, 1999: SIMBIOS Project 1999 Annual Report*, NASA Tech. Memo. 1999-209486*, NASA Goddard Space Flight Center, Greenbelt, Maryland, 128 pp.

McClain, C. R., W. Esaias, G. Feldman, R. Frouin, W. Gregg, and S. Hooker, 2002: The Proposal for the NASA Sensor Intercalibration and Merger for Biological and Interdisciplinary Oceanic Studies (SIMBIOS) Program, 1995, *NASA/TM-2002-210008*, NASA Goddard Space Flight Center, Greenbelt, Maryland, 63 pp.

Fargion, G.S. and J.L. Mueller 2000: Ocean Optics Protocols for Satellite Ocean Color Sensor Validation, Revision 2, *NASA Tech. Memo. 2000-209966*, NASA Goddard Space Flight Center, Greenbelt, Maryland, 183 pp.

Fargion G.S. and R.C. McClain, 2001: SIMBIOS Project 2000 Annual Report, *NASA Tech. Memo. 2001-209976*, NASA Goddard Space Flight Center, Greenbelt, Maryland, 1-164 pp.

Fargion G.S., R. Barnes and R.C. McClain, 2001: In situ AOT collected by the SIMBIOS Program (1997-2000): protocols, and data QC and analysis, *NASA Tech. Memo. 2001-209982*, NASA Goddard Space Flight Center, Greenbelt, Maryland, 1-103 pp.

Fargion G.S. and R.C. McClain, 2002: SIMBIOS Project 2001 Annual Report, *NASA Tech. Memo. 2002-210005*, NASA Goddard Space Flight Center, Greenbelt, Maryland, 1-184 pp.

Fargion G.S. and R.C. McClain: 2003: SIMBIOS Project 2002 Annual Report, *NASA Tech. Memo. 2003-210005*, NASA Goddard Space Flight Center, Greenbelt, Maryland, 1-184 pp.

Meister, G., and others, 2002: The First SIMBIOS Radiometric Intercomparison (SIMRIC-1), April-September 2001, *NASA/TM2002-210006*, NASA Goddard Space Flight Center, Greenbelt, Maryland, 60 pp.

Meister G. *et al.*, 2003: The Second SIMBIOS Radiometric Intercomparison (SIMRIC-2), March-November 2002*, NASA Tech. Memo. 2003-01930,* GSFC, Greenbelt, Maryland, 1-71 pp.

Mueller J.M. and G. S. Fargion, 2002: Ocean Optics Protocols for Satellite Ocean Color Sensor Validation, Revision 3, Part I, *NASA Tech. Memo. 2002-210004*, NASA Goddard Space Flight Center, Greenbelt, Maryland, 1-137 pp.

Mueller J.M. and G. S. Fargion, 2002: Ocean Optics Protocols for Satellite Ocean Color Sensor Validation, Revision 3, Part II, *NASA Tech. Memo. 2002-210004*, NASA Goddard Space Flight Center, Greenbelt, Maryland, 138-308 pp.

Mueller J.M. and G. S. Fargion, 2003: Ocean Optics Protocols for Satellite Ocean Color Sensor Validation, Revision 4, Part I, *NASA Tech. Memo. 2003-210004/Rev 4/Vol.I*, NASA Goddard Space Flight Center, Greenbelt, Maryland, 1-50 pp.

Mueller J.M. and G. S. Fargion, 2003: Ocean Optics Protocols for Satellite Ocean Color Sensor Validation, Revision 4, Part II, *NASA Tech. Memo. 2003-210004/Rev 4/Vol. II,* NASA Goddard Space Flight Center, Greenbelt, Maryland, 1-56 pp.

Mueller J.M. and G. S. Fargion, 2003: Ocean Optics Protocols for Satellite Ocean Color Sensor Validation, Revision 4, Part III, *NASA Tech. Memo. 2003-210004/Rev 4./Vol.III*, NASA Goddard Space Flight Center, Greenbelt, Maryland, 1-78 pp.

Mueller J.M. and G. S. Fargion, 2003:Ocean Optics Protocols for Satellite Ocean Color Sensor Validation, Revision 4, Part V, *NASA Tech. Memo. 2003-210004/Rev 4/Vol.V*, NASA Goddard Space Flight Center, Greenbelt, Maryland, 1-25 pp.

Mueller J.M. and G. S. Fargion, 2003: Ocean Optics Protocols for Satellite Ocean Color Sensor Validation, Revision 4, Part VI, *NASA Tech. Memo. 2003-210004/Rev 4./Vol. VI*, NASA Goddard Space Flight, Greenbelt, Maryland, 1-148 pp.

Van Heukelem, L., C. S. Thomas, and P. M. Glibert, 2002: Sources of Variability in Chlorophyll Analyseis by Fluorometry and High-Performance Liquid Chromatography in a SIMBIOS Inter-Calibration Exercise, G. S. Fargion and C. R. McClain (eds*.), NASA Tech. Memo. 2002-211606*, Goddard Space Flight Center, Greenbelt, Maryland, 50 pp.

Werdell, P. J., and S. W. Bailey, 2002: The SeaWiFS Bio-Optical Archive and Storage System (SeaBASS): Current Architecture and Implementation, G. S. Fargion and C. R. McClain (eds.), *NASA Tech. Memo 2002-211617*, Goddard Space Flight Center, Greenbelt, Maryland, 45 pp.

Presentations

Bailey, S. W., J. Werdell and C. R. McClain, 2001: Validation of Satellite-Derived Ocean Color: Theory and Practice, *EOS. Trans. AGU, **82**(47)*, Fall Meet., Suppl., Abstract OS52A-0520, 2001.

Bailey S. W., P. J. Werdell, C. McClain and G. Fargion, 2000: Validation of SeaWiFS-derived Chlorophyll: Comparisons at Several Spatial and Temporal Scales, Venice 2000, Italy

Bailey S., C. Pietras, K. Knobelspiesse, G. Fargion, and C. McClain, SeaWiFS Aerosol Product Compared to Coastal and Island In situ Measurements, Eos Trans. AGU, 83(19), Spring Meet. Suppl., Abstract A51B-08, **2002**.

Barnes R., D. Clark, W. Esaias, G. S. Fargion, G. Feldman, C. R. McClain, 2001: Requirements for a self-consistent multi-sensor global ocean color time series" *Proceedings of the International Workshop on Geo-Spatial Knowledge Processing for Natural Resource Management*, Varese, Italy, 28-29 June 2001, 13-18.

Bartholomew M. J., M. Miller, G.S. Fargion, S. Bayley and R. Reynolds, 2001: Comparison of Satellite Estimates of Aerosol Optical Thic ness and Cloud Cover with Shipboard Measurements, Eos Trans. AGU, 82(47), Fall Meet. Suppl., Abstract OS51E-11.

Fargion, G. S., C. R. McClain, H. Fukushima, J. M. Nicolas, and R. A. Barnes, 1999: Ocean color instrument intercomparisons and cross-calibrations by the SIMBIOS Project. EOS/SPIE Symposium on Remote Sensing, Florence, Italy.

Fargion, G.S., 1999: An Overview of SIMBIOS Project. International Symposoium on Ocean color Remote Sensing and Carbon Flux by CERES and JUWOC, Chiba, Japan.

Fargion G. S., C. R. McClain and Robert A. Barnes, 2000: Ocean Color Instrument Intercomparisons and Cross-Calibrations by the SIMBIOS Project, Earth Observing System V, SPIE, San Diego.

Fargion G. S. and C. R. McClain, 2000: Three Years of Ocean Color Instrument Intercomparisons and Cross-Calibrations by the SIMBIOS Project (1997-2000), Conference on Remote Sensing of the Ocean and Sea Ice VI, Barcelona.

Fargion G.S. *et al.*, 2003: SIMBIOS PROGRAM in Support of Ocean Color Mission: 1997-2003", *SPIE Conference*, 3-8 August, San Diego.

Franz, B. A., 1998: A Simple Destriping Algorithm for MOS Images. Proc. of the 2nd International Workshop on MOS-IRS and Ocean Color, Berlin.

Franz, B. A., 1999: Status of the MOS Ground Station at NASA/Wallops. Proc. of the 3rd International Workshop on MOS-IRS and Ocean Color, Berlin.

Franz, B. A., 1999: An Overview of SeaWiFS Mission. International Symposoium on Ocean color Remote Sensing and Carbon Flux by CERES and JUWOC, Chiba, Japan.

Franz B. A. and J. M. Gales, 2001: A Long Term Intercomparison of MOS and SeaWiFS, 4th Berlin Workshop on Remote Sensing "5Years of MOS-IRS", 9-16.

Gales J., B. Franz and M. Wang, 2001: A Three Year Intercomparison of Oceanic Optical Properties from MOS and SeaWiFS, EOS. Trans. AGU, 82(47), Fall Meet., Suppl., Abstract OS52A-0513, 2001

Gross, L, R. Frouin, C. Pietras, K.D. Knobelspiesse and G.S. Fargion, 2002: Non-supervised Classification of Ground-based Radiometer Retrievals in Order to Assess the Natural Distribution of Aerosol Volume Size Distributions and Refractive Indexes, Spring 2002 American Geophysical Union Meeting, Washington, DC.

Gross L., R. Frouin, C. Pietras and G.S. Fargion, 2002: Non-Supervised Classification of aerosol Mixtures for ocean Color Remote Sensing, *Proceedings of the "Remote Sensing of the Atmosphere, Ocean, Environment and Space Proc. of SPIE Symposium*, Hangzhou, China.

Kilpatrick, K., E. Kearns, E.J. Kwiatkowska-Ainsworth, and R.L. Evans, 2002: Time Series of Calibrated Ocean Products from NASA's Moderate Resolution Scanning Spectrometer (MODIS), Proceedings of the Ocean Sciences Meeting, Honolulu, Hawaii.

Kim Y. , S. Yoo, Byung-Ju Sohn , G. S.Fargion *et al.*, 2001: The OSMI Post-launch Calibration", Eos Trans. AGU, 82(47), Fall Meet. Suppl., Abstract OS42D-08.

Knobelspiesse K., C. Pietras and G.S. Fargion, 2001: MicroTops II Hand-held Sun Photometers Sun Pointing Error Correction for Sea Deployment, *EOS. Trans. AGU,* **82***(47)*, Fall Meet., Suppl., Abstract OS52A-0532, 2001.

Knobelspiesse, K.D., C. Pietras, M. Miller, M. Reynolds, R. Frouin, P. Quinn, P-Y. Deschamps, J. Werdell, and G.S. Fargion, 2002: Comparison of In Situ Aerosol Data from the ACE-Asia 2002 Experiment, Spring 2002 American Geophysical Union Meeting, Washington, DC.

Kwiatwska-Ainsworth, 2001; Merger of Ocean Color Information of Different Spatial Resolution: SeaWiFs and MOS,*EOS. Trans. AGU,* **82***(47)*, Fall Meet., Suppl., Abstract OS52A-0514, 2001.

Kwiatkowska E. and G.S. Fargion, 2002: Merger of Ocean Color Data from Multiple Satellite Missions within the SIMBIOS Project, Proceedings of SPIE's Symposium on Remote Sensing of the Atmosphere, Ocean, Environment, and Space, Hangzhou, China.

Kwiatkowska E. and G.S. Fargion, 2002: Merger of Ocean Color Information from Multiple Satellite Missions under the NASA SIMBIOS Project Office, Proceedings of the Fifth International Conference on Information Fusion, Annapolis, Maryland, 291-298.

Kwiatkowska-Ainsworth, E. 2001: Merger of Ocean Color Information of Different Spatial Resolution: SeaWiFS and MOS, *Eos Trans. American Geophysical Union*, vol. **82**, no. 47, F675 (OS52A-0514).

Isaacman, A., B. A. Franz, and R. E. Eplee, Jr., 1999: An Investigation of Time Variability in-water-Leaving Radiances Retrieved from the Ocean Color Measurements, ALPS 99 Conference, Méribel, France.

McClain R. C., G.S. Fargion and G. Feldman, 2001: Overview of Ocean Color Calibration and Validation Efforts, Eos Trans. AGU, 82(47), Fall Meet. Suppl., Abstract OS42D-01.

Meister, G., G.S. Fargion and C.R. McClain, 2002: Monitoring the Radiometric Stability of the SeaWiFS Transfer Radiometer II, Spring 2002 American Geophysical Union Meeting, Washington, DC.

Meister G., P. Abel , J. Cooper, C. Davis, R. Frouin, D. Goebel, M. Godin, D. Korwan, S. McLean, R. Maffione, D. Menzies, A. Poteau, J. Robertson, G. S. Fargion and C. R. McClain, 2001: Results from a Round-Robin-Comparison of Radiance Calibrations at Oceanographic and Atmospheric Research Laboratories, Eos Trans. AGU, 82(47), Fall Meet. Suppl., Abstract OS52A-0534 .

Morrison R., H. Sosik, S. Gallager and G.S.Fargion, 2001: Time Series Measurements and Algorithm Dev lopment at the FRONT Site on the New England Continental Shelf, Eos Trans. AGU, 82(47), Fall Meet. Suppl., Abstract OS52A-0525

Pietras C.M., Ainsworth E., Bailey S., Hsu C., Wang M., Fargion G., McClain C., Abuhassan N., and Holben B., 2000: Aerosol Properties from Field Measurements Using Hand-Held and Automatic Sun Photometers, AGU Spring Meeting Washington D.C. May 30-June 3.

Pietras C., E. Ainsworth, S.W. Bailey *et al.*, 2000: Initial Results of Validation of Satellyte Sensor Derived Aerosol Optical Thickness Against In Situ Atmospheric Observations Collected by the SIMBIOS Project, to be presented at the Eighth International Symposium Physical Measurements and Signatures in Remote Sensing, Aussois, France, January 8-12, 2001.

Pietras C., Frouin R., Nakajima T., Yamano M., Knobelspiesse K., Werdell J., Meister G., Fargion G., and McClain C., 2001: Aerosol Properties Derived from the PREDE POM-01 Mark II Sun Photometer, *EOS. Trans. AGU,* **82***(47)*, Fall Meet., Suppl., Abstract OS52A-0531, 2001.

Pietras, C, K.D. Knobelspiesse, S. Bailey, J. Werdell, R. Frouin, M. Miller, G.S. Fargion and C.R. McClain, 2001: SeaWiFS Aerosol Product Compared to In Situ Measurements Over Open Oceans, Spring 2002 American Geophysical Union Meeting, Washington, DC.

Smirnov A., B. Holben, R. Frouin, G.S. Fargion *et al.*, 2001: Maritime Aerosol Optical Model Based on the Aerosol Robotic Network (AERONET)Measurements, Eos Trans. AGU, 82(47), Fall Meet. Suppl., Abstract OS51E-12.

Souaidia N., C. Pietras, S. Brown, K. Lykke, G. Fargion, B. C. Johnson, R. Frouin, P.Y. Deschamps, 2002: Radiometer laser and lamp based radiometric calibrations; comparison with the Langley technique and implications on remote sensing, EOS Trans. AGU, 83(47), Fall Meet. Suppl., Abstract A52A-0098, **2002**

Vermeulen A., Devaux C., Tanre D., Herman M., Holben B., Blarel L., Chatenet B., and Pietras C., 2001: AERONET Polarization Measurements, AGU Fall Meeting San Francisco. December 10-14.

Wang, M. and B. A. Franz, 1998: A Vicarious Intercalibration between MOS and SeaWiFS, Proc. 2nd International Workshop on MOS-IRS and Ocean Colour, Berlin, Germany, 95-102.

Wang, M., 1998: A validation of the SeaWiFS O2 A-band absorption correction, Proc. the 4th Pacific Ocean Remote Sensing Conference, Qingdao, China, 32-36, 1998.

Wang, M., 1998: Applying the SeaWiFS atmospheric correction algorithm to MOS, Proc. the 4th Pacific Ocean Remote Sensing Conference, Qingdao, China, 88-91,

Wang, M., S. Bailey, C. R. McClain, C. Pietras and J. T. Riley, 1999: Remote Sensing of the Aerosol Optical Thickness from SeaWiFS in Comparison with In situ Measurements. ALPS 99 Conference, Méribel, France.

Wang, M., A. Isaacman, B. A. Franz, and C. R. McClain, 2001: A comparison study of the ocean color data derived from OCTS and POLDER," The AGU Fall Meeting, San Francisco, California, December 10-14.

Werdell P. J., S. W. Bailey and G.S. Fargion, 2001: The Architecture and Utility of SeaBASS: the SeaWiFS Bio-Optical Archive and storage System, *EOS. Trans. AGU,* 82*(47)*, Fall Meet., Suppl., Abstract OS52A-0533, 2001.

Chapter 2

SIMBIOS: Science Team and Contracts

Giulietta S. Fargion
Science Applications International Corporation (SAIC), Beltsville, Maryland

2.1 SCIENCE TEAM

The SIMBIOS Science Team was selected through two NASA Research Announcements (NRA), in 1996 and 1999. NASA HQ managed the process of team selection, while the Goddard Space Flight Center (GSFC) NASA Procurement Office handled the team contracts, work statements and, if necessary, budget negotiations. The Project funded numerous US investigators and collaborated with several international investigators, space agencies (e.g., NASDA, CNES, KARI, etc.) and international organizations (e.g., IOCCG, JRC). US investigators were under contract to provide *in situ* atmospheric and bio-optical data sets, as well as develop algorithms and methodologies for data merger schemes. NASA GSFC Procurement requires formal evaluations for all contracts at the end of each contract year. These evaluations go into a database and are shared with the PI's institution or upper management. Chapters 3 to 19 contain the individual PI's contributions and describe the funded research topics, field study activities, and results of concluded research. These chapters are reproduced as submitted with minimal editing by the Project Office.

2.2 CONTRACT OVERVIEW

The third-year of the SIMBIOS NRA-99 contracts ended on November 30, 2003. The Project Office followed the same procedure used in 1999 before compiling the final evaluations. The four categories to be evaluated are suggested in the "Evaluation of Performance" from the Federal Acquisition Regulation (FAR) 42.15 and NASA FAR Supplement (NSF) 1842.15 or NASA form 1680 used by GSFC. Under the "quality" category the following are considered:

- data quality and completeness;
- ancillary information provided on the data (metadata);
- the data's usefulness in relation to SIMBIOS goals, i.e., calibration, validation, and algorithm development; and
- quality of technical reports.

The "time" category is a mixed bag, but is viewed with respect to data and documentation (monthly and year-end reports, and special topic publications) and delivery times. Under the "other" category is considered:

- scientific publications and scientific achievements;
- science team collaboration and involvement; and
- other significant events occurring during the contract period evaluated.

As a result of the formal final evaluation with the SIMBIOS PIs, all investigators were evaluated as very good or excellent. The GSFC Procurement Office implemented and executed one no cost exstension option. Further details on the research status and progress reports can be found on our web site at http://simbios.gsfc.nasa.gov/status.html.

Chapter 3

Adaptation of a Hyperspectral Atmospheric Correction Algorithm for Multi-spectral Ocean Color Data in Coastal Waters

Bo-Cai Gao, Marcos J. Montes, and Curtiss O. Davis

Remote Sensing Division, Naval Research Laboratory, Washington, D.C.

3.1 INTRODUCTION

This SIMBIOS contract supports several activities over its three-year time-span. These include certain computational aspects of atmospheric correction, including the modification of our hyperspectral atmospheric correction algorithm Tafkaa for various multi-spectral instruments, such as SeaWiFS, MODIS, and GLI. Additionally, since absorbing aerosols are becoming common in many coastal areas, we are making the model calculations to incorporate various absorbing aerosol models into tables used by our Tafkaa atmospheric correction algorithm. Finally, we have developed the algorithms to use MODIS data to characterize thin cirrus effects on aerosol retrieval.

3.2 RESEARCH ACTIVITIES

One of our accomplishments this year included further modifications of our hyperspectral atmospheric correction algorithm (Gao et al. 2000; Montes et al. 2001) suggested at the 2002 year-end review, as well as others that allow us flexibility in examining the results of different aerosol corrections applied to different scenes.

One of the inputs for Tafkaa is the wind speed. This is used to aid in correcting for the specular reflections from the ocean surface. Previously we had the ability to only read one wind speed value for the whole scene; this does not make much sense for typical MODIS and SeaWiFS scenes that span a reasonably large surface area. Tafkaa can now read an input data plane that has the wind speed, and it can use that information for each pixel. This does not tend to slow Tafkaa too much, although it does require more memory since the complete lookup tables for each wind speed need to be held in memory. Similar modifications were made for ozone amount, so Tafkaa may be run either for a single ozone value for the whole scene, or with an ozone input array provided.

Other modifications to Tafkaa include the ability to exclude certain classes of aerosol from consideration, the ability to force Tafkaa to use a certain aerosol model and optical depth, and the ability to solve only for aerosol optical depth when given a fixed aerosol model. Tafkaa now has the ability to ignore masked data, which makes it faster in areas where the clouds and land have been masked. Finally, an absorbing urban aerosol has been added to the lookup tables, which is useful in many areas, including off the east coast of both North America and Asia.

These modifications are on top of the previously reported modifications from the first two years of our report: making a fast, portable (the source code has been compiled on multiple architecture/OS/compiler platforms), modular version of Takfaa using the geometry on a pixel-to-pixel basis.

We participated in the field observations of Asian Dust events over the Monterey Bay in April 2003, along with many other researchers in the ADAM (Asian Dust Above Monterey) collaboration. We obtained some imagery with the PHILLS; unfortunately, it was not on the best days (in terms of the presence of Asian dust), and so we were not able to fly above, in, and below the dust layers, as was originally planned. Our collaborators did sample the Asian dust, where the layers were located, etc., and we anticipate being able to use the results of their research in the future to characterize the Asian dust that crosses the Pacific. This will allow us to build some aerosol lookup tables for similar events.

We are still in the process of calculating the Asian dust aerosol models, a project which has run behind schedule. We are in the process of writing papers about our research results. Of particular interest are the scenes at the time of the 2001 Leo-15 experiment.

3.3 RESEARCH RESULTS

During the first year of the SIMBIOS program we analyzed scenes from April, 2000, when AVIRIS flew under MODIS and SeaWiFS over the MOBY site (see Figures 3.1 & 3.2). We developed software to navigate the AVIRIS scene, and additional processing software to transfer the AVIRIS radiance measurements to space. We found that near 0.47 micron, the observed reflectance (corrected to the top of the atmosphere) for AVIRIS is 9% greater than that measured by MODIS; at 0.747 micron the difference is about 8%, with the MODIS values being greater than those of AVIRIS. Comparisons of water-leaving reflectance showed that MOBY agrees quite well with MODIS, but not with AVIRIS. This was, however, based on a single underflight, and the results needs to be revisited as all the instruments have different calibrations now than in the past.

The modifications to the base multi-spectral version of Tafkaa have continued. The modifications allow Tafkaa to execute more quickly, as well as increasing the types of aerosols available. As these modifications have occurred in the base version, it takes little more than recompiling the source code in order to propagate the modifications to the executables for the sensor-specific versions of Tafkaa.

We have processed several scenes from MODIS and SeaWiFS data with the pixel-to-pixel versions of the atmospheric correction code. For MODIS scenes, our algorithm and Gordon's algorithm return very similar results over areas of the open ocean. Our algorithm makes use of both the ocean channels of MODIS, as well as the land channels. Use of the land channels allows us to perform atmospheric corrections in certain turbid areas where the normal algorithms fail – for example, in areas with enough sediment so that there is measurable signal at 0.75 micron (see Figure 3.3). MODIS land channels also give us flexibility in presenting spectra when the ocean-color channels saturate, as can happen in certain circumstances as in some turbid waters as well as in some regions with coccolithophores (see Figures 3.4 & 3.5). For SeaWiFS scenes, our results tend to differ. First, the SeaWiFS correction uses the 0.765 mm band, a band that encompasses the O2 A-band absorption feature. Because of the presence of the strong absorption feature, it is difficult (impossible?) for our algorithm to use this band as the basis of atmospheric correction. Likewise, maps of the 0.665 mm band show that coastal ocean color features are still visible in that band, making it impossible to use that band for atmospheric correction.

Other areas of research include B.-C. Gao's collaborations to study methods of discriminating the effects of cirrus clouds and aerosols at longer wavelengths (Gao et al., 2002) and algorithms for masking sediment laden waters where it is necessary to use longer wavelengths to achieve any atmospheric correction (Li et al., 2003).

Products

We have shared previous versions of our algorithms with groups at GSFC and NRL-Stennis. Current source code, executables, look-up tables, and user guides for the atmospheric correction algorithms will be provided to the SIMBIOS office.

3.4 CONCLUSIONS

We have made progress in modifying our atmospheric correction algorithm to be used with multi-spectral data from MODIS and SeaWiFS. Our algorithm takes advantage of MODIS' long wavelength and land bands to provide atmospheric correction over brighter ocean scenes including sediments and coccolithophore blooms. These algorithms now use the complete geometry of each pixel, incorporate new aerosols, and allow for ozone and wind speed to vary on a pixel-by-pixel basis. Our results are promising, especially over turbid areas. We are in the process of refining our algorithms and are involved in testing with both groups working with the SIMBIOS program at GSFC and NRL-Stennis.

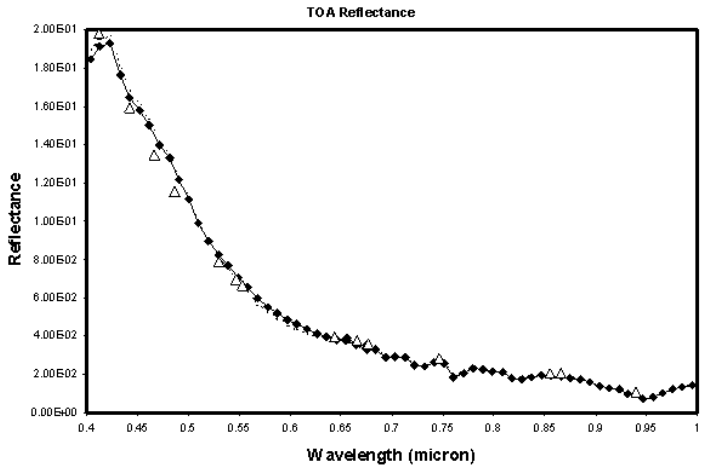

Figure 3.1: Top of the atmosphere reflectance observed near the MOBY site by AVIRIS (dashed line) and MODIS (open triangles). Note that while the radiance measurements are generally in good agreement, the AVIRIS radiance near 0.4 micron is significantly less than radiance observed by MODIS. The AVIRIS radiance at 0.747 micron is also about 10% less than that measured MODIS. The solid line with solid diamonds is the observed atmospheric reflectance before being transferred to the top of the atmosphere.

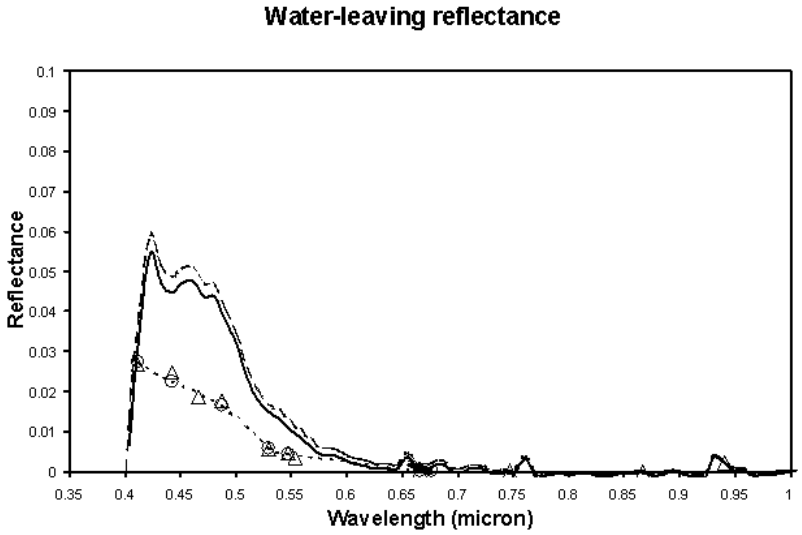

Figure 3.2: Derived water-leaving reflectance spectra from AVIRIS and MODIS (open triangles), compared to MOBY (open circles, small dashes) measurements. The solid line is AVIRIS corrected using the two MODIS bands near 0.75 micron and 0.865 micron to determine the atmospheric correction. The long-dashed line is the atmospheric correction derived using four window channels longer than 1 micron.

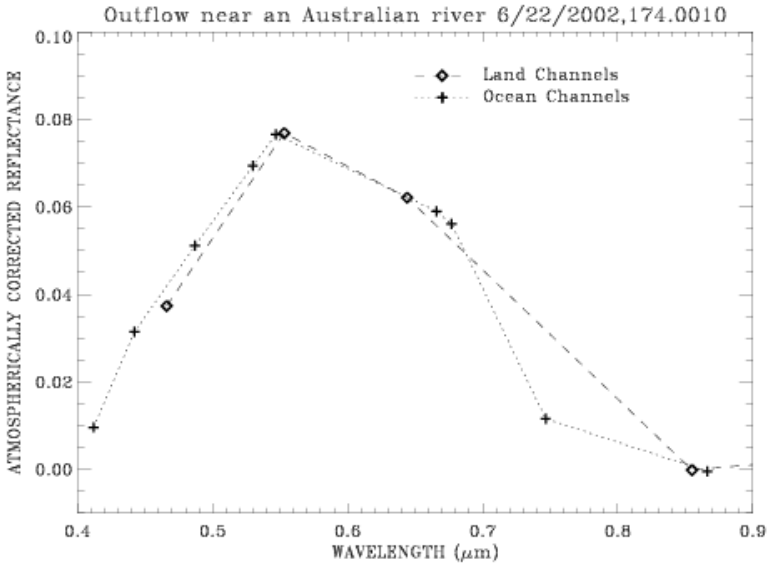

Figure 3.3: Atmospherically corrected reflectance from a MODIS image off the coast of Eastern Australia. The long dashes connect the sets of land channels (open diamonds), and the short dashes connect sets of ocean channels (plusses). These results were derived using some of the land channels and the pixel-to-pixel version of Tafkaa to determine an atmospheric correction. Note, in particular, that our results yield significant water leaving radiance at 0.75 micron. Water leaving reflectance cannot be retrieved for pixels like this one using Gordon's algorithm.

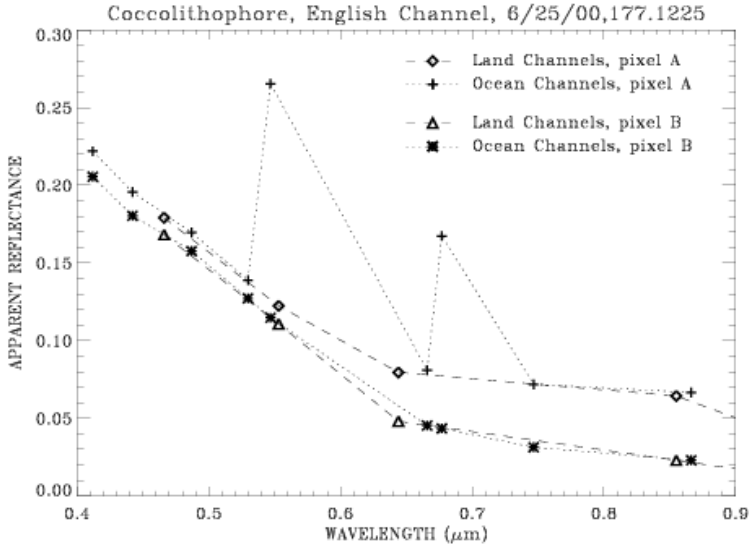

Figure 3.4: The at-sensor apparent reflectance from a MODIS image of the English Channel, 2000 June 25, comparing results from land and ocean channels from two different pixels in a coccolithophore bloom. The long dashes connect the land channels, and the short dashes connect ocean channels. The open diamonds (land channels) and plusses (ocean channels) are from pixel A, which is clearly saturated in the fifth and seventh ocean channels from the left. Spectra from nearby unsaturated pixel B are shown with open triangles (land channels) and asterisks (ocean channels).

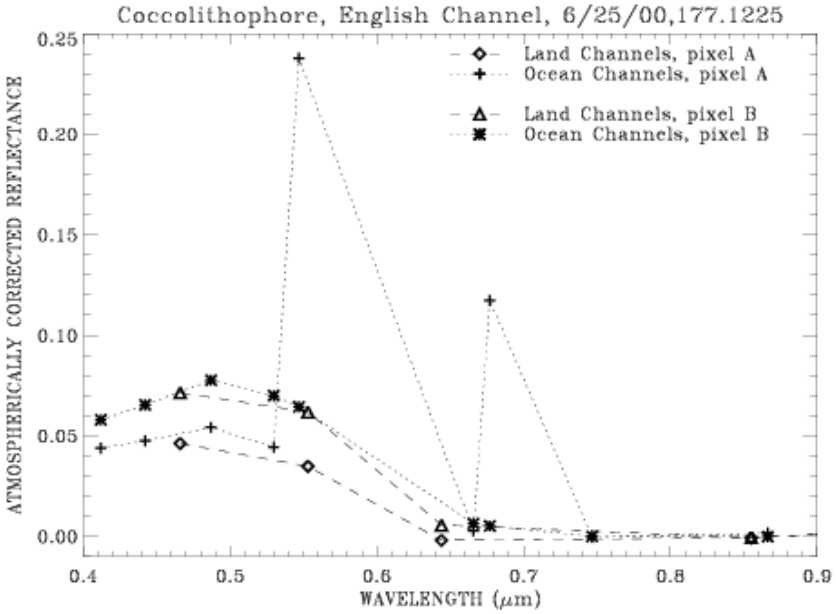

Figure 3.5: Atmospherically corrected reflectance from the same locations as in Figure 4. The symbols are the same as in Figure 4. Note the quite reasonable agreement between the atmospherically corrected land channels and ocean channels except for the two saturated channels.

REFERENCES

Gao, B.-C., M.J. Montes, Z. Ahmad, and C.O. Davis, 2000. Atmospheric correction algorithm for hyperspectral remote sensing of ocean color from space. Appl Opt., 39(6), 887-896.

Montes, M.J., B.-C. Gao, and C.O. Davis. 2001: A new algorithm for atmospheric correction of hyperspectral remote sensing data. SPIE, 4383, 23-30.

This Research was Supported by
the NASA Interagency Agreement S-44797-X

Publications

Gao, B.-C., Y. J. Kaufman, D. Tanre, and R.-R. Li, 2002: Distinguishing tropospheric aerosols from thin cirrus clouds for improved aerosol retrievals using the ratio of the 1.38 micron and 1.24 micron channels, *Geophysical Research Letters*, **29**, 1890, 2002.

Li, R.-R., Y. J. Kaufman, B.-C. Gao, and C. O. Davis, Remote sensing of suspended sediments and shallow coastal waters, *IEEE Trans. Geosci. Remote Sensing***, 41**, 559-566, 2003.

Presentations

Montes, M. J., B.-C. Gao, and C. O. Davis 2003: Tafkaa atmospheric correction of hyperspectral and multispectral data, a talk presented 2003 Aug. 6 by M. J. Montes at SPIE's 48th Annual Meeting in San Diego, CA.

Montes, M. J., C. O. Davis, and B.-C. Gao 2003, Hyperspectral Imaging and Atmospheric Correction, a lecture presented 2003 July 9 by M. J. Montes to the "Spatio-Temporal Statistical Analysis of Multi-

platform Optical Ocean Observations" class at the University of Maine's Darling Marine Center, Walpole, Maine.

Montes, M. J., C. O. Davis, B.-C. Gao, and M. Moline 2003: Analysis of AVIRIS Data from Leo-15 and Other sites using Tafkaa atmospheric correction , a talk presented 2003 Feb. 27 by M. J. Montes at the 2003 AVIRIS Earth Science and Applications Workshop in Pasadena, CA.

Gao, B.-C., M. J. Montes, and C. O. Davis, 2003: Adaptation of a Hyperspectral Atmospheric Correction Algorithm for Multi-Spectral Ocean Color Data in Coastal Waters, a poster at the Feb. 2003 MODIS workshop in New Hampshire.

Davis, C.O., B.-C. Gao, M.J. Montes, G. Feldman, B. Franz, F. Patt, and R. Stumpf, 2001: Atmospheric Correction of Ocean Color Data at the MOBY site in Hawaiian Waters. Presented at the Tenth JPL AVIRIS Science and Applications Workshop, Pasadena.

Chapter 4

Bio-Optical Measurements in Upwelling Ecosystems in Support of SIMBIOS

Francisco P. Chavez, Peter G. Strutton, Victor S. Kuwahara, Kevin L. Mahoney, and Eric Drake
Monterey Bay Aquarium Research Institute, Moss Landing, California

4.1 INTRODUCTION

The upwelling region of the equatorial Pacific Ocean, which spans one quarter of the earth's circumference, strongly impacts global biogeochemistry. This upwelling system has significant implications for global CO_2 fluxes (Tans *et al*., 1990; Takahashi *et al.*, 1997; Feely *et al.*, 1999), as well as primary and secondary production (Chavez and Barber, 1987; Chavez and Toggweiler, 1995; Chavez *et al*., 1996; Dugdale and Wilkerson, 1998; Chavez *et al*., 1999; Strutton and Chavez, 2000). In addition, the region represents a vast oceanic (case 1) region over which validation data for SeaWiFS are needed. This project consists of an optical mooring program and cruise-based measurements focused on measuring biological and chemical variability in the equatorial Pacific and obtaining validation data for SeaWiFS. Since 1996, the MBARI equatorial Pacific program has demonstrated ability to:

1. obtain high quality, near real time measurements of ocean color from moored platforms in the equatorial Pacific.
2. process and quality control these data into files of the required format for the SeaBASS database.
3. obtain robust ship-based optical profiles and pigment concentration measurements, also for submission to SeaBASS.
4. process and interpret the time series, satellite and ship-based data in order to quantify the biogeochemical processes occurring in the equatorial Pacific on time scales of days to years (Chavez *et al*., 1998; Chavez *et al*., 1999; Strutton & Chavez, 2000; Strutton *et al*., 2001, Ryan *et al*., 2002).

4.2 RESEARCH ACTIVITIES

Moorings

The arrangement of the moored MBARI bio-optical and chemical instruments positioned at 0°, 155°W and 2°S, 170°W has previously been described (Chavez *et al.* 1998, Chavez *et al.* 1999, McClain and Fargion 1999). The moorings are two of ~70 which form the Tropical Atmosphere Ocean (TAO) array. From these locations, daily local 10 am and noon (approximate time of MODIS and SeaWiFS overpasses, respectively) bio-optical and chemical data are transmitted via service ARGOS in near real time to MBARI, and then presented on the internet at: http://bog.shore.mbari.org/~bog/oasis.html.

Higher frequency, publication-quality data (15-minute intervals) are also recovered at approximately six month intervals, and sent to the SeaBASS database after thorough quality control. Derived products, such as water leaving radiance (L_w), and remote sensing reflectance (Rrs) are incorporated into these data files for validation efforts. In previous years, L_w has been determined through three different methods (McLain and Fargion, 1999b), but L_w is now computed only as follows. The diffuse attenuation coefficient (K_λ) throughout the upper 20m of the water column is calculated using Ed_{3m+} and Ed_{20m-}. Then, using this K_λ, Lu_{20m} is extrapolated back to just below the surface (Lu_{0m-}) and multiplied by 0.544 (a scaling factor that considers the transmission of light across the air-sea interface) to obtain Lu_{0m+}. Of the three methods previously used, this has been shown to be the most reliable, primarily because the 3m+ and 20m-

instruments are less susceptible to fouling. With the addition of a 10 m hyperspectral radiometer, the efficacy of this method can now be assessed.

During 2003 our data processing, quality control and data provision capabilities have improved. The following quality control procedures are currently employed:

1. Measured surface-incident irradiance (E_s) can not be greater than 1.15 times modeled, clear-sky E_s (Frouin, 1989).
2. K_λ must be greater than that of pure water (Morel, 1988).
3. OC4V4 chlorophyll is computed for the Rrs ratios of 412/555, 443/555, 490/555, and 510/555 and the coefficient of variance is determined for each wavelength combination. Coefficients of variance greater than 0.4 are not acceptable.
4. Time series of all parameters at all wavelengths for all individual instrument deployments are plotted together as one long time series to identify discontinuities between deployments, due to problems such as vandalism, fouling and calibration issues. Normalizing specific wavelengths against others is also used to identify discontinuities.

With the buoy design and data collection methods now verified in the field, we are making significant advancements to the quantity and quality of optical data collected during this funding period. In October 2002, HOBILabs HR3 hyperspectral radiometers were deployed at 10m on both equatorial Pacific moorings (0° 155°W and 2°S 170°W) to supplement the discrete wavelengths measured at 20 m. These configuration changes yielded data of significantly higher quality for almost the same cost as the existing discrete-wavelength instruments. These instruments were retrieved in June 2003 (new HR3 units were subsequently deployed after recovery) providing hyperspectral data consisting of:

- downwelling irradiance above the surface (3m)
- downwelling irradiance and upwelling radiance at 10m depth.

The Hydrorad data are available in programmable bin sizes (highest resolution 0.37nm), over the range ~300 to 850nm, but for deployment in the equatorial Pacific we have binned the data to ~2nm resolution. We also successfully recovered and deployed HOBILabs Hydroscat 2 (HS2) instruments fitted with new copper anti-fouling shutters. The HS2 measures backscatter and fluorescence at two wavelengths (490 and 676 nm). With the deployment of these new instruments, particularly the hyperspectral radiometers, we have been able to submit optical data beyond our initial deliverables as stated in the SIMBIOS grant, and can better support recent and forthcoming ocean color missions such as MODIS and GLI and the development of ocean color algorithms that will go beyond chlorophyll.

Optical profiling measurements

On mooring maintenance cruises, optical profiles of the euphotic zone are performed daily, when possible, close to local noon using a Satlantic SeaWiFS Profiling Multispectral Radiometer (SPMR). Profile data are processed using Satlantic's ProSoft software, and a suite of derived products, including diffuse attenuation coefficients, water leaving radiances (L_{wn}) and light penetration depths are obtained. Products of interest (mostly L_{wn}) are provided to NASA post-cruise, and the profile data are archived at MBARI along with existing optical profiles from almost every oceanic region.

In situ measurements

Table 4.1 recaps the cruises embarked on by MBARI this fiscal year in support of SIMBIOS. The cruise-based measurements consist primarily of fluorometric chlorophyll (Chavez *et al.* 1995) & nutrient profiles (8 depths, 0-200m) obtained at CTD stations between 8°N and 8°S across the Pacific from 95°W to 165°E. Latitude-depth sections of shipboard data can now be viewed at:http://www.mbari.org/~ryjo/tropac/sections

On mooring maintenance cruises (the 155°W and 170°W meridional transects), HPLC samples are collected and productivity (^{14}C, ^{15}N) measurements are also performed. These data are stored at MBARI and the pigment data supplied to the SeaBASS database for algorithm development. Figure 4.1 shows a

regression comparison, with good agreement between shipboard measurements and HPLC analysis of chlorophyll *a*. The HPLC analysis was conducted by the Center for Hydor-Optics and Remote Sensing (CHORS).

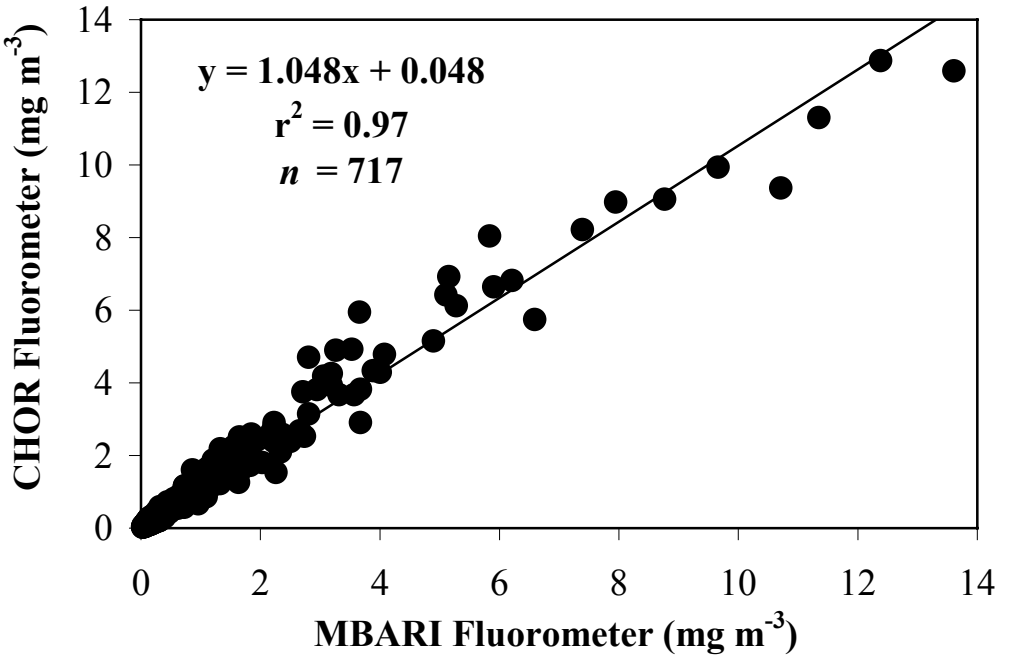

Figure 4.1: Regression model comparing *in situ* Chlorophyll *a* determined by a Turner fluorometer at sea versus chlorophyll determined by HPLC at the Center of Hydro-Optics and Remote Sensing (CHORS). Samples were collected from both the equatorial Pacific and Monterey Bay.

4.3 RESULTS

Biogeochemical cycles

Several publications describing ecosystem variability in the equatorial Pacific have been produced under MBARI's SIMBIOS funding. Chavez *et al.* (1998) used mooring data from 0°, 155°W to describe the biological-physical coupling observed in the central equatorial Pacific during the start of the 1997-98 El Niño. Chavez *et al*. (1999) combined the physical, biological and chemical data from moorings, ships and SeaWiFS to provide a complete picture of the ecosystem's reaction to the intense physical forcings that occurred during the 1997-98 El Niño. Strutton and Chavez (2000) summarized the *in situ* cruise measurements spanning the period from November 1996 to December 1998, and used these data to describe the perturbations to chlorophyll, nutrients and productivity during the same time period. Strutton *et al*. (2001) used time series from smaller Satlantic bio-optical packages and SeaWiFS imagery to detail the extreme anomalies in chlorophyll related to the passage of tropical instability waves (TIWs) during the latter half of 1998 and 1999. These data not only documented the magnitude of the observed chlorophyll variability, but also shed light on the mechanisms possibly responsible for the concentration of chlorophyll in connection with TIWs. Ryan *et al*. (2002) thoroughly described and explained the intense and widespread blooms that dominated the equatorial Pacific during the 1998 La Niña.

Chavez *et al*. (2000) documented the design, and demonstrated the effectiveness of a shutter mechanism that prevents bio-fouling of the *in situ* radiometers on the moorings. Kuwahara *et al*. (2003) contributed to the 4th revision of the Ocean Optics Protocols series with a chapter titled, "Radiometric and Bio-optical Measurements from Moored and Drifting Buoys: Measurement and Data Analysis Protocols".

Other manuscripts currently in press/preparation include a chapter in Seuront and Strutton (Eds): 'Handbook of scaling methods in aquatic ecology: Measurements, analysis, simulation' (CRC Press, publication October 2003), a manuscript describing the biological component of the equatorial Pacific heat budget (Strutton and Chavez, in press), and a paper that analyzes the time series of optical data collected at the mooring location (Kuwahara *et al*.)

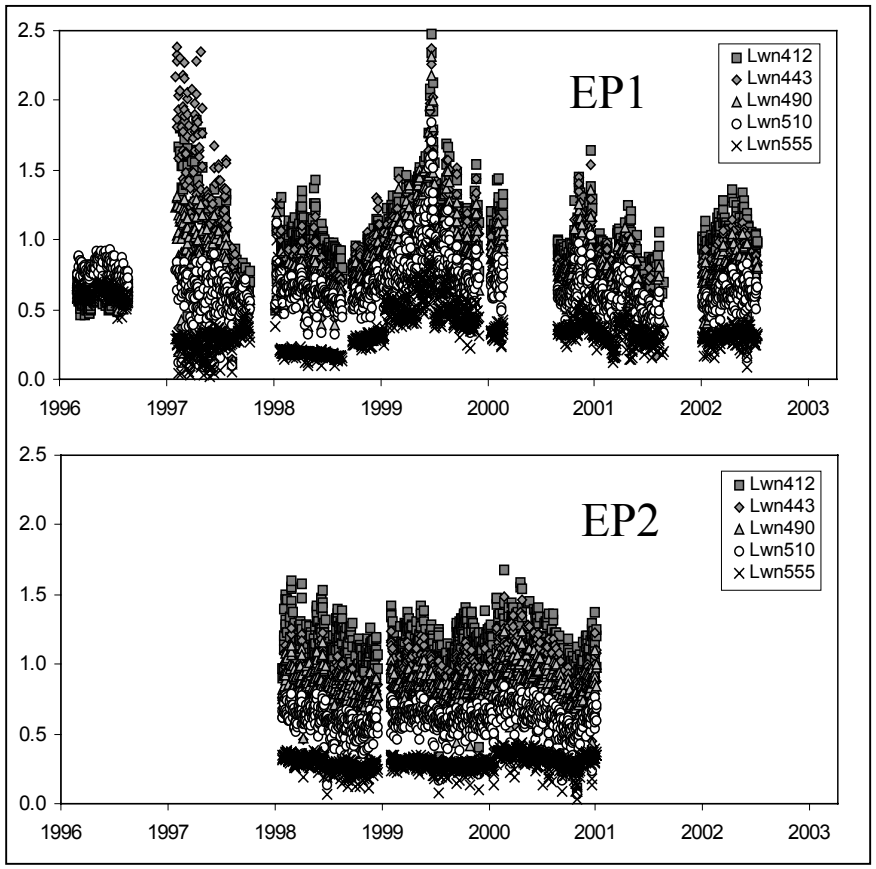

Figure 4.2: The time series (December 11,1996 – June 18, 2003) of normalized water-leaving radiance, L_{wn} [$\mu W\ cm^{-2}\ nm^{-1}\ sr^{-1}$], derived from the L_u and K_d data obtained from MBARI optical instruments on the TAO moorings at 0° 155°W (EP1) and 2°S 170°W (EP2). The data have been subject to quality control as described in the methods.

SeaWiFS Calibration/Validation

At the present time, we are concentrating on refining our data analysis and quality control protocols of the full mooring records (1996-2003) for both moorings in combination with the newly reprocessed SeaWiFS data. Analysis and improvements to quality control methods continue on the reprocessed data. These data have been uploaded to SeaBASS. Figure 4.2 shows our most recent update of the time series of L_{wn}. Note: L_{wn} collected from the upwelling region is more variable than data collected from EP2, which is less susceptible to upwelling.

McClain and Fargion (1999b) showed matchup data derived from optical profiles of the SPMR in the equatorial Pacific. The mooring data collected at EP1 (excluding the anomalous El Nino year) indicated good agreement between the satellite- and profile-derived water-leaving radiance values (Figure 4.3). Similarly, Figure 4.4 compares the surface chlorophyll values obtained from SPMR casts with the extracted chlorophyll samples obtained at the same location.

In addition to our deliverables, the mooring data collected at EP1 during 2002 yielded hyperspectral E_d data (Figure 4.5) and backscattering data, namely $b_b(490)$ and $b_b(676)$ (Figure 4.6).

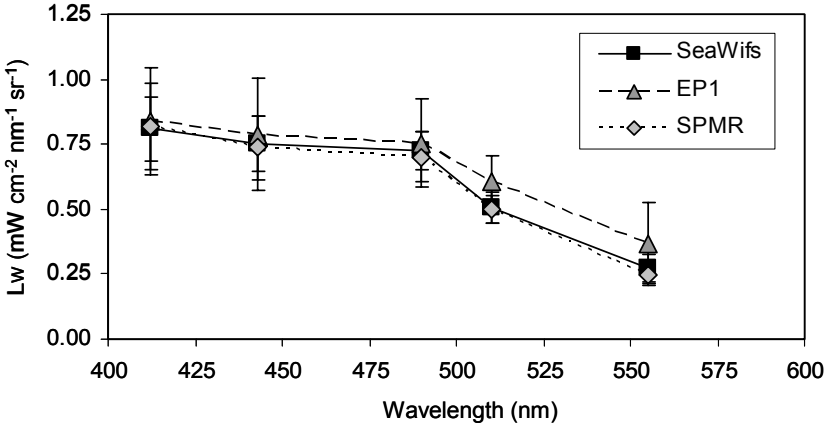

Figure 4.3: Water leaving radiance matchups between SeaWiFS, EP1 (0, 155W) optical mooring, and SPMR profiles (where available) from June 1998 to Oct 2001. Anomalous data collected during the 1997 – 1998 El Nino period were not included. The number of matching points between SeaWiFS and the optical mooring at 412, 443, 490, 510, and 555 nm were, n = 245, 238, 236, 208 and 210, respectively. For SPMR profiles conducted at the mooring location, n = 10.

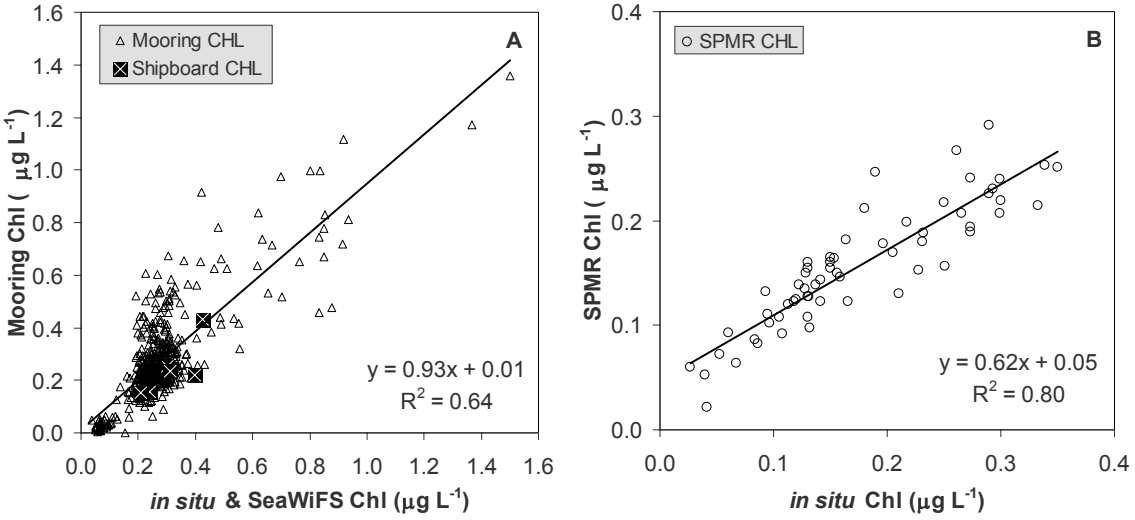

Figure 4.4: (A) Comparison of SeaWiFS and shipboard *in situ* chlorophyll with mooring-derived chlorophyll for the MBARI instruments at 0° 155°W (EP1). Mooring-derived chlorophyll was calculated using an algorithm by Morel (1988). Regression analysis for SeaWiFS vs. Mooring Chl is also shown. (B) Comparison of chlorophyll from shipboard water samples with chlorophyll calculated from SPMR casts. SPMR chlorophyll is calculated using OC4V4 algorithm by O'Reilly (2001) applied to normalized water-leaving radiance from the SPMR. All data have been subject to quality control.

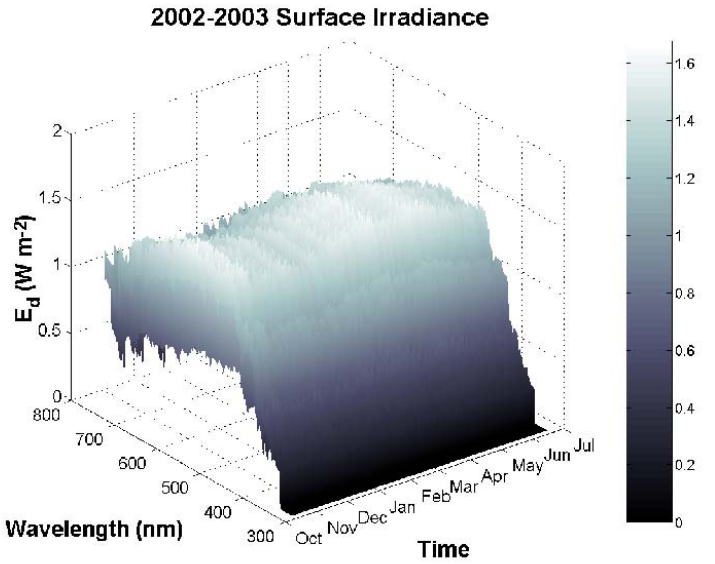

Figure 4.5: Time series of hyperspectral downwelling irradiance at EP1. Data of this kind could be used in further algorithm development or as validation data for future ocean color missions.

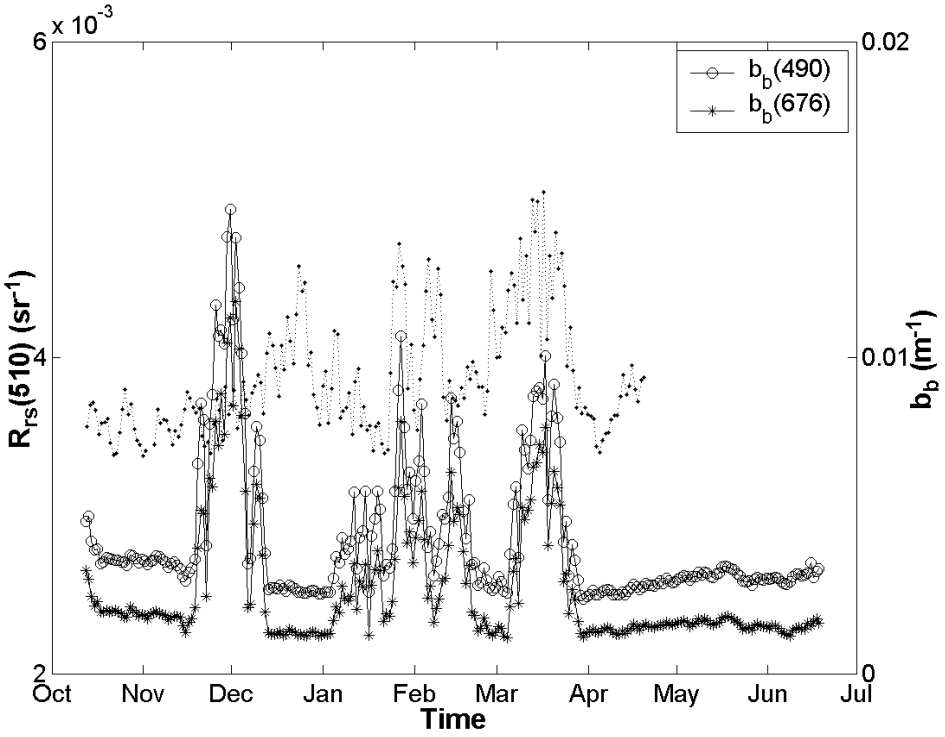

Figure 4.6: In situ backscatter data between October 2002 and June 2003, measured with a HOBI Labs, Inc. HS-2 illustrates the variability in particle density at EP1. At times this variability can also be seen in the R_{rs} data (dotted line, $R_{rs}(510)$ shown as an example) derived from mooring data.

4.4 CONCLUSIONS

Aside from setbacks related to vandalism (mainly tower and instrument controller theft), the two major mooring installations at 0°, 155°W and 2°S, 170°W are operating relatively well. The deployment of hyperspectral and backscatter instruments at both moorings is demonstrating significant potential and will better support validation efforts for ocean color missions.

This year alone we have preformed ~30 SPMR profiles, analyzed more than 2500 shipboard chlorophyll measurements, processed over 500 nutrient samples, processed 200 a* samples and collected close to 1000 HPLC samples. The program of cruise-based measurements as described above will continue on eight equatorial Pacific cruises during 2003-2004, with scheduled SeaWiFS LAC where applicable.

Table 4.1: Summary of cruises (in 2003) during which *in situ* data have been obtained by MBARI in support of SIMBIOS. All cruises were undertaken aboard the NOAA ship *Ka'imimoana*, with the exception of GP6-02-RB aboard the *Ronald H. Brown*. Meridional transects indicate the lines occupied by the ship. Along each line, CTD stations were performed approximately every degree of latitude from 8°N to 8°S, and every 0.5° between 3°N and 3°S. Measurements consisted of chlorophyll (Chl) plus nitrate, nitrite, phosphate and silicate (Nutrients) at 8 depths between 0 and 200m. On selected cruises, primary production (PP) and new production (NP) measurements were also made using ^{14}C and ^{15}N incubation techniques, respectively. Daily optical profiles were obtained using the Satlantic SeaWiFS Profiling Multispectral Radiometer (SPMR) where indicated.

Cruise ID	Dates	Meridional transects	Measurements
GP2-03-KA	24-Mar-03 to 28-Apr-03	95W and 110W	Chl, Nutrients, a*
GP3-03-KA	05-Jun-03 to 11-Jul-03	155W and 170W	Chl, NP, PP, Nutrients, SPMR, a*, HPLC
GP4-03-KA	13-Jul-03 to 11-Aug-03	165E and 180W	Chl, Nutrients, a*
GP5-03-KA	21-Aug-03 to 27-Sep-03	125W and 140W	Chl, Nutrients, a*
GP6-03-RB	11-Oct-03 to 12-Nov-03	95W and 110W	Chl, Nutrients, a*
GP7-03-KA	16-Oct-03 to 14-Nov-03	155W and 170W	Chl, NP, PP, Nutrients, SPMR, a*, HPLC
GP8-03-KA	16-Nov-03 to 14-Dec-03	165E and 180W	Chl, Nutrients, a*

REFERENCES

Chavez, F.P., and Barber, R.T., 1987: An estimate of new production in the equatorial Pacific, *Deep-Sea Research*, **34**, 1229-1243.

Chavez, F.P., Buck, K.R.., Bidigare, R.R., Karl, D.M., Hebel, D., Latasa, M., Campbell, L. and Newton, J., 1995: On the chlorophyll a retention properties of glass-fiber GF/F filters. *Limnology and Oceanography*, ***40*****,** 428-433.

Chavez, F.P. and Toggweiler, J.R., 1995: Physical estimates of global new production: the upwelling contribution, in *Upwelling in the Ocean: Modern Processes and Ancient Records* C. P. Summerhayes, K. C. Emeis, M. V. Angel, R. L. Smith, B. Zeitzschel, Eds., J. Wiley & Sons, Chichester, pp. 313-320.

Chavez, F.P., Buck, K.R., Service, S.K., Newton, J. and Barber, R.T., 1996: Phytoplankton variability in the central and eastern tropical Pacific. *Deep-Sea Research*, **43***(4-6)*, 835-870.

Chavez, F.P., Strutton, P.G., and McPhaden, M.J., 1998: Biological-physical coupling in the central equatorial Pacific during the onset of the 1997-98 El Niño. *Geophysical Research Letters*, **25**(19), 3543-3546.

Chavez, F.P., Strutton, P.G., Friederich, G.E., Feely, R.A., Feldman, G., Foley, D. and McPhaden, M.J., 1999: Biological and chemical response of the equatorial Pacific Ocean to the 1997-98 El Niño. *Science*, **286**, 2126-2131.

Chavez, F.P., Wright, D., Herlien, R., Kelley, M., Shane, F. and Strutton, P.G., 2000: A device for protecting moored spectroradiometers from bio-fouling. *Journal of Oceanic and Atmospheric Technology*, **17,** 215-219.

Dugdale, R.C. and Wilkerson, F.P., 1998: Silicate regulation of new production in the equatorial Pacific upwelling, *Nature*, **391**, 270-273.

Feely, R.A., Wanninkhof, R., Takahashi, T. and Tans, P., 1999: Influence of El Niño on the equatorial Pacific contribution to atmospheric CO_2 accumulation. *Nature*, **398**, 597-601.

Frouin, R., Ligner, D.W., and Gautier, C., 1989: A simple analytical formula to compute clear sky total and photosynthetically available solar irradiance at the ocean surface. *Journal of Geophysical Research*, **94**, 9731-9742.

Kuwahara, V. S., Strutton, P.G., Dickey, T.D., Abbott, M.R., Letelier, R.M., Lewis, M.R., McLean, S., Chavez, F.P., Barnard, A., R. Morrison, J.R., Subramaniam, A., Manov, D., Zheng, X. and Mueller, J.L., 2003: Radiometric and Bio-optical Measurements from Moored and Drifting Buoys: Measurement and Data Analysis Protocols. *NASA Tech. Memo,* Eds. J.L. Muller and G.S. Fargion, NASA Goddard Space Flight Center, Goddard, Maryland, Volume VI.

McClain C.R. and Fargion, G.S., 1999a: SIMBIOS Project 1998 Annual Report. *NASA Tech. Memo. 1999-208645*, NASA Goddard Space Flight Center, Greenbelt, Maryland, 105pp.

McClain C.R. and Fargion, G.S., 1999b: SIMBIOS Project 1999 Annual Report. *NASA Tech. Memo. 1999-209486*, NASA Goddard Space Flight Center, Greenbelt, Maryland, 137pp.

Morel, A., 1988: Optical modeling of the upper ocean in relation to its biogenous matter content (Case I waters). *Journal of Geophysical Research*, *93*, 10749-10768.

O'Reilly, J. E., Maritorena, S., O'Brien, M.C., Siegel, D.A., Toole, D., Menzies, D., Smith, R.C., Mueller, J.L., Mitchell, B.G., Kahru, M., Chavez, F.P., Strutton, P.G., Cota, G.F., Hooker, S.B., McClain, C.R., Carder, K.L., Muller-Karger, F., Harding, L., Magnuson, A., Phinney, D., Moore, G.F., Aiken, J., Arrigo, K.R., Letelier, R.M. and M. Culver, 2001: SeaWiFS Postlaunch Calibration and Validation Analyses, Part 3, SeaWiFS Postlaunch Technical Report Series, Volume **11**, *NASA Tech. Memo. 2000-206892*, S.B. Hooker and E.R. Firestone, Eds., NASA Goddard Space Flight Center, Greenbelt, Maryland.

Strutton, P.G and Chavez, F.P. Radiant heating in the equatorial Pacific: Spatial and Temporal variability. *Journal of Climate*, in press.

Ryan, J.P., Polito, P.S., Strutton, P.G. and Chavez, F.P. Anomalous phytoplankton blooms in the equatorial Pacific. *Progress in Oceanography*, **55**, 263-285.

Strutton, P.G., Ryan, J.P. and Chavez, F.P., 2001: Enhanced chlorophyll associated with tropical instability waves in the equatorial Pacific. *Geophysical Research Letters,* **28**(10), 2005-2008.

Strutton, P.G. and Chavez, F.P., 2000: Primary productivity in the equatorial Pacific during the 1997-98 El Niño. *Journal of Geophyiscal Research,* **105**(C11), 26,089-26,101.

Strutton, P.G. and Chavez, F.P., 2003: Scales of biological-physical coupling in the equatorial Pacific. In *Handbook of scaling methods in aquatic ecology: Measurement, analysis simulation*, Seuront, L. and Strutton, P.G. (Eds) CRC Press, Boca Raton, FL.

Tans, P.P., Fung, I.Y., Takahashi, T., 1990: Observational constraints on the global atmospheric CO_2 budget, *Science***, 247**, 1431-1438.

Takahashi, T, Feely, R.A., Weiss, R.F., Wanninkhof, R., Chipman, D.W., Sutherland, S.C. and Takahashi, T., 1997: Carbon dioxide and climate change. *Proceedings of the National Academy of Sciences*, **94**, 8314-8319.

This Research was Supported by
the NASA Contract # 00193

Publications

Chavez, F.P., Strutton, P.G., Friederich, G.E., Feely, R.A., Feldman, G.C., Foley, D.G. and McPhaden, M.J., 1999. Biological and chemical response of the equatorial Pacific Ocean to the 1997-98 El Niño. *Science*. **286**: 2126-2131.

Chavez, F.P., Strutton, P. G. & McPhaden, M. J., 1998. Biological-physical coupling in the equatorial Pacific during the onset of the 1997-98 El Niño. *Geophysical Research Letters*. **25**(19): 3543-3546.

Chavez, F.P., Wright, D., Herlien, R., Kelley, M., Shane, F. and Strutton, P.G., 2000. A device for protecting moored spectroradiometers from bio-fouling. *Journal of Oceanic and Atmospheric Technology*. **17**: 215-219.

Cosca, C.E., Feely, R.A., Boutin, J., Etcheto, J., McPhaden, M.J., Chavez, F.P. and Strutton, P.G., 2003. Seasonal and interannual CO_2 fluxes for the central and eastern equatorial Pacific Ocean as determined by fCO_2-SST relationships. *Journal of Geophysical Research,* **108**(C8), doi: 10.1029/ 2000JC000677.

Frouin, R., Franz, B., Wang, M., Werdell, P.J., Bishop J.K.B., Chavez, F., and Gower, J.F. Algorithm to estimate photosynthetically available radiation at the ocean surface from SeaWiFS data, in preparation.

Johnson, K.S. and Coletti, L.J., 2002. In situ ultraviolet spectrophotometry for high resolution and long-term monitoring of nitrate, bromide and bisulfide in the ocean. *Deep-Sea Research I*, **49**, 1291–1305.

Ryan, J.P., Polito, P.S., Strutton, P.G. and Chavez, F.P., 2002. Anomalous phytoplankton blooms in the equatorial Pacific. *Progress in Oceanography*, **55**, 263-285.

Sabine, C.L., Feely, R.A., Johnson, G.C., Strutton, P.G., Lamb, M.F. and McTaggart, K.E. Carbon chemistry of the water column during the GasEx-2001 experiment. *Journal of Geophysical Research*, submitted.

Schwarz, J.N., Gege, P., Kowalczuk, P., Kaczmarek, S., Carder, K.L., Muller-Karger, F., Varela,R., Chavez, F.P., Clark, D.K., Cota, G.F., Cunningham, A., McKee, D., Kishino, M., Mitchell, B.G., Phinney, D.A., Raine, R., Trees, C.C., Zaneveld, J.R.V., Pegau, S. Two models for Gelbstoff absorption. *Oceanologia*, in revision.

Strutton, P.G. and Chavez, F.P., 2000. Primary productivity in the equatorial Pacific during the 1997-98 El Niño. *Journal of Geophyiscal Research*, **105**(C11), 26,089-26,101.

Strutton, P.G., Ryan, J.P. and Chavez, F.P., 2001. Enhanced chlorophyll associated with tropical instability waves in the equatorial Pacific. *Geophysical Research Letters*, **28**(10), 2005-2008.

Strutton, P.G. and Chavez, F.P., 2003. Scales of biological-physical coupling in the equatorial Pacific, in *Handbook of scaling methods in aquatic ecology: Measurment, analysis, simulation.*, Seuront, L. and Strutton, P.G., Eds, CRC Press, Boca Raton, FL.

Strutton, P.G and Chavez, F.P. Radiant heating in the equatorial Pacific: Observed variability and potential for real-time calculation. *Journal of Climate*, in press.

Strutton, P.G., Chavez, F.P., Dugdale, R.C. and Hogue, V. Primary productivity and its impact on the carbon budget of the upper ocean during GasEx-2001. *Journal of Geophysical Research*, accepted pending revision.

NASA Technical Memorandum

Kuwahara, V.S., Strutton, P.G., Subramaniam, A., Dickey, T.D., Abbot, M.R., Letelier, R., Lewis, M.R., McLean, S., Barnard, A., Ru Morrison, J. and Chavez, F.P. Radiometric and Bio-optical Measurements from Moored and Drifting Buoys: Measurement and Data Analysis Protocols, Chapter VI-3, Ocean Optics Protocols for Satellite Ocean Color Sensor Validation, Volume 4, in press.

O'Reilly, J. E., Maritorena, S., O'Brien, M.C., Siegel, D.A., Toole, D., Menzies, D., Smith, R.C., Mueller, J.L., Mitchell, B.G., Kahru, M., Chavez, F.P., Strutton, P.G., Cota, G.F., Hooker, S.B., McClain, C.R., Carder, K.L., Muller-Karger, F., Harding, L., Magnuson, A., Phinney, D., Moore, G.F., Aiken, J., Arrigo, K.R., Letelier, R.M. and Culver, M. SeaWiFS Postlaunch Calibration and Validation Analyses, Part 3, SeaWiFS Postlaunch Technical Report Series, Volume 11, *NASA Tech. Memo. 2000-206892*, S.B. Hooker and E.R. Firestone, Eds., NASA Goddard Space Flight Center, Greenbelt, Maryland, 2001.

Presentations

Chavez, F.P., Feldman, G.C., McPhaden, M.J., Foley, D.G. and Strutton, P.G., 1998: Remote Sensing of the Equatorial Pacific during 1997-98. *AGU* Fall Meeting, San Francisco, CA, December, Invited

Friederich, G.E., Chavez, F.P., Strutton, P.G. and Walz, P., 1998: Bio-optical and Carbon Dioxide Time Series From Moorings in the Equatorial Pacific During 1997-1998. *AGU* Fall Meeting, San Francisco, CA.

Friederich, G E Walz, P M Strutton, P G Burczynski, M G Chavez, F P Seasurface pCO2 Time Series from Moorings in Equatorial and Coastal Upwelling Systems. *AGU* Ocean Sciences meeting, San Antonio, TX.

Kuwahara, V.K., Strutton, P.G., Penta, B., Drake, E., and Chavez, F.P., 2001: Bio-optics from Moorings: Satellite Validation and Ecosystem Dynamics. *AGU* Fall Meeting, San Francisco, CA, December.

Strutton, P.G., Poster presentation, *AGU*, Fall Meeting, San Francisco, December 2002.

Strutton, P.G., Poster presentation and session chair, *Ocean Optics XVI* meeting, Santa Fe, November 2002.

Strutton, P.G., Oral presentation, American Geophysical Union / American Society of Limnology and Oceanography, *Ocean Sciences Meeting*, Honolulu, February 2002.

Strutton, P.G., Chavez, F.P., Drake, E., Kuwahara, V.K, Friederich, G. and Ryan, J., 2001: Merging Data from Ships, Satellites and Moorings to Understand Biological-Physical Coupling in the Equatorial Pacific. *AGU* Fall Meeting, San Francisco, CA, December 2001.

Strutton, P.G., Chavez, F.P., Foley, D.G., Sclining, B.M. and McPhaden, M.J., 1999: Remote Sensing of Biological-Physical Coupling in the Equatorial Pacific. *ASLO* Ocean Sciences Meeting, Santa Fe, NM.

Strutton, P.G., Chavez, F.P. and McPhaden, M.J., 1998: In situ measurements of primary productivity in the equatorial Pacific during the 1997-98 El Niño. *AGU* Fall Meeting, San Francisco, CA.

Strutton, P.G., Chavez, F.P. and McPhaden, M.J., 1998: Primary productivity in the equatorial Pacific during the onset of the 1997-98 El Nino. *AGU/ASLO* Ocean Sciences Meeting, San Diego, CA.

Strutton, P.G., Ryan, J.P., Polito, P. and Chavez, F.P., 2000: High Chlorophyll in the Equatorial Pacific During 1998 Associated With Tropical Instability Wave Fronts. *AGU* Ocean Sciences meeting, San Antonio, TX

Strutton, P.G., Chavez, F.P. and McPhaden, M.J., 1998: Biological-physical coupling in the central equatorial Pacific during the 1997-98 El Niño, *Ocean Optics XIV*, Kailua-Kona, HI

Chapter 5

Satellite Ocean-Color Validation Using Ships of Opportunity

Robert Frouin, David L. Cutchin, Lydwine Gross-Colzy and Antoine Poteau
Scripps Institution of Oceanography, University of California San Diego, La Jolla

Pierre-Yves Deschamps
Laboratoire d'Optique Atmosphérique, Université des Sciences et Technologie de Lille, France

5.1 INTRODUCTION

The investigation's main objective is to collect from platforms of opportunity (merchant ships, research vessels) concomitant normalized water-leaving radiance and aerosol optical thickness data over the world's oceans. A global, long-term data set of these variables is needed to verify whether satellite retrievals of normalized water-leaving radiance are within acceptable error limits and, eventually, to adjust atmospheric correction schemes.

To achieve this objective, volunteer officers, technicians, and scientists onboard the selected ships collect data from portable SIMBAD and Advanced SIMBAD (SIMBADA) radiometers. These instruments are specifically designed for evaluation of satellite-derived ocean color. They measure radiance in spectral bands typical of ocean-color sensors. The SIMBAD version measures in 5 spectral bands centered at 443, 490, 560, 670, and 870 nm, and the Advanced SIMBAD version in 11 spectral bands centered at 350, 380, 412, 443, 490, 510, 565, 620, 670, 750, and 870 nm. Aerosol optical thickness is obtained by viewing the sun disk like a classic sun photometer. Normalized water-leaving radiance, or marine reflectance, is obtained by viewing the ocean surface through a vertical polarizer in a specific geometry (nadir angle of 45^o and relative azimuth angle of 135^o) to minimize direct sun glint and reflected sky radiation. The SIMBAD and SIMBADA data, after proper quality control and processing, are delivered to the SIMBIOS project office for inclusion in the SeaBASS archive. They complement data collected in a similar way by the Laboratoire d'Optique Atmosphérique of the University of Lille, France.

The SIMBAD and SIMBADA data are used to check the radiometric calibration of satellite ocean-color sensors after launch and to evaluate derived ocean-color variables (i.e., normalized water-leaving radiance, aerosol optical thickness, and aerosol type). Analysis of the SIMBAD and SIMBADA data provides information on the accuracy of satellite retrievals of normalized water-leaving radiance, an understanding of the discrepancies between satellite and in situ data, and algorithms that reduce the discrepancies, contributing to more accurate and consistent global ocean color data sets.

5.2 RESEARCH ACTIVITIES

Since November 2002, SIMBAD measurements were made during 7 research cruises of opportunity, bringing to 69 the number of campaigns with SIMBAD measurements realized during the period October 1996-Otober 2003. These 7 cruises, as well as ongoing and planned cruises, are listed in Table 1 with name of cruise, SIMBAD and SIMBADA instrument(s) used, region of measurements, name of operator, and dates of measurements. The data were collected In the Pacific Ocean, off the West Coast of the United States and Baja California, Mexico (CalCOFI and IMECOCAL cruises), between Peru and New Zealand (P500304), and between Australia and Papeete (BEAGLE2003, Leg1). The location of the measurements from the first 5 cruises, which have been processed, is displayed in Figure 5.1. The processed data (a total of 606 complete data sets) have been transferred to the SeaBASS archive.

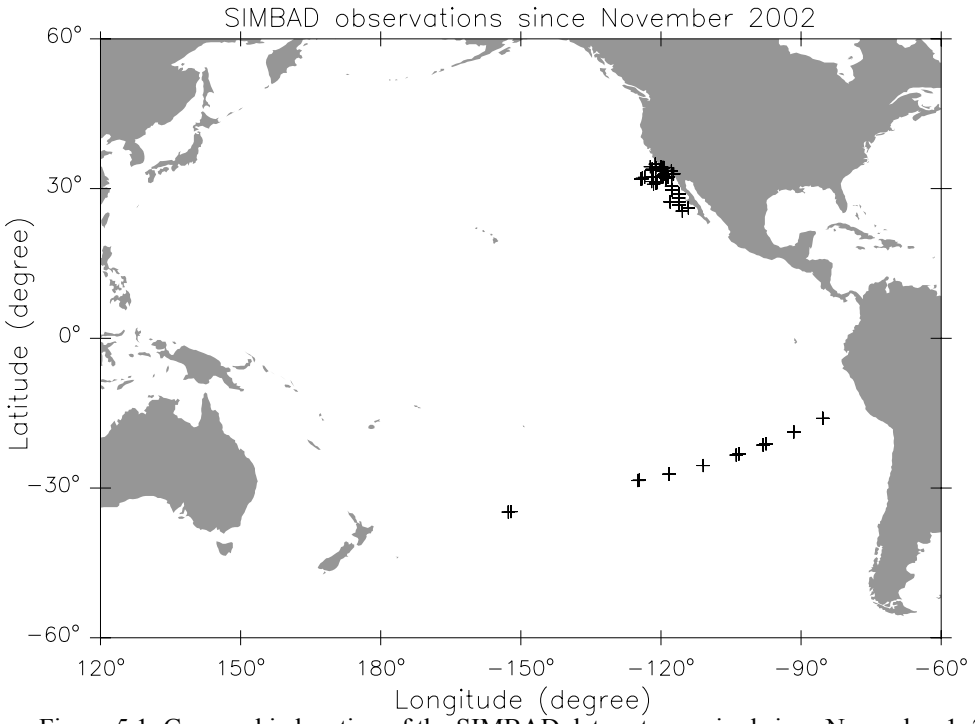

Figure 5.1: Geographic location of the SIMBAD data sets acquired since November 1, 2002.

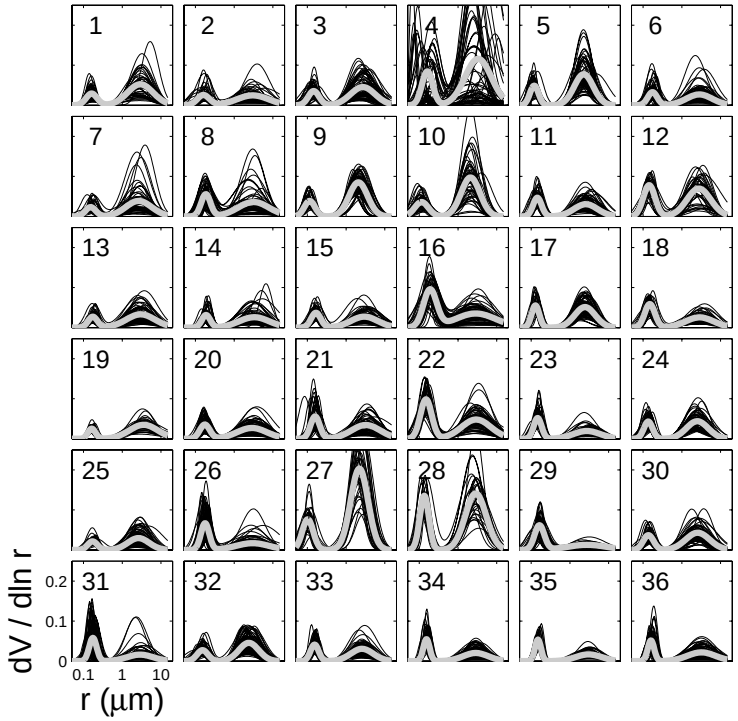

Figure 5.2: The calibrated 36 PRSOM neurons: Volume size distribution dV/dLnr. In each plot, the data gathered by the corresponding neuron is plotted in black, while their referent vector is plotted in gray.

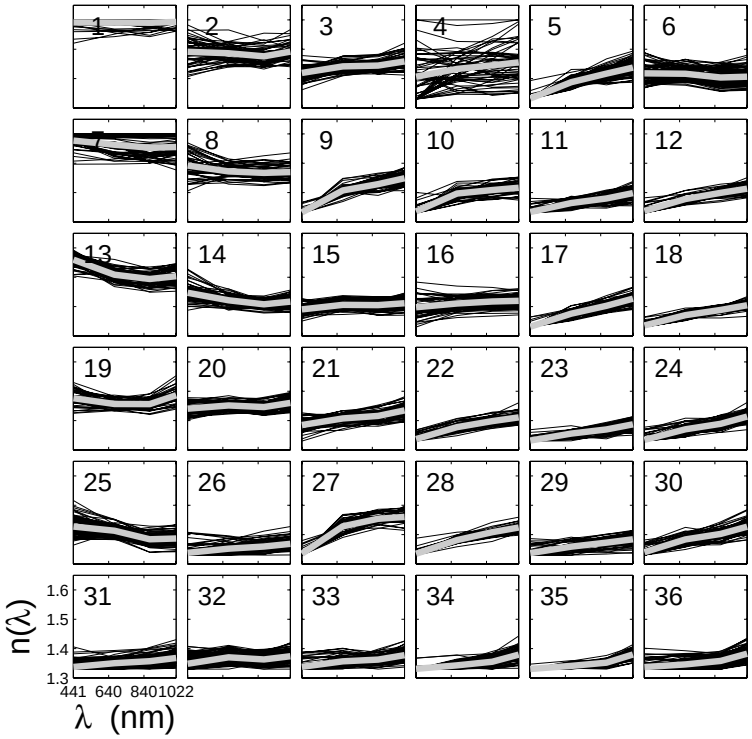

Figure 5.3: Same as Figure 5.2, but real part n of the refractive index

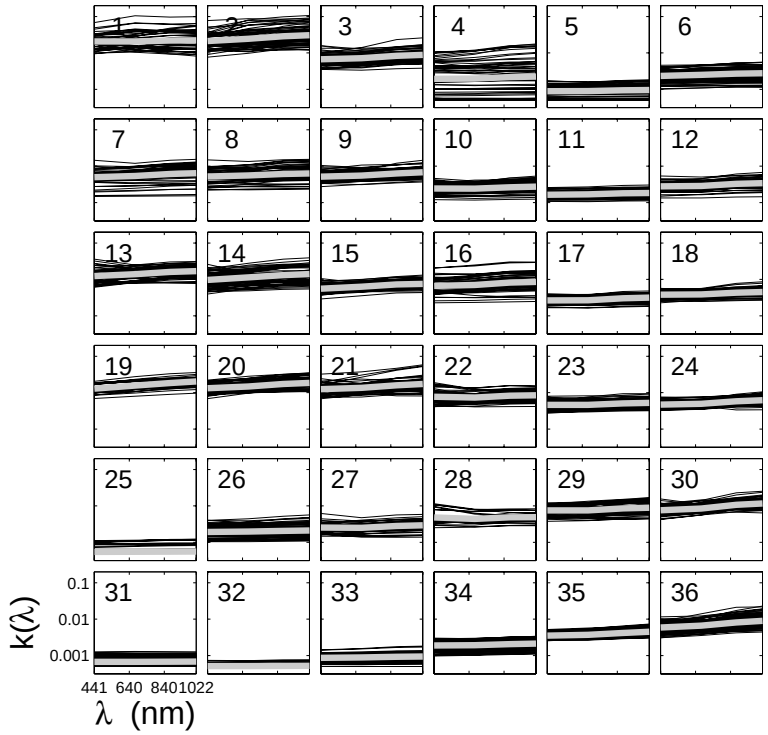

Figure 5.4: Same as Figure 5.2, but imaginary part k of the refractive index, plotted on a logarithmic scale.

Table 5.1. SIMBAD cruises during November 2002 –October 2003.

- IMECOCAL 0210/11,Ensenada-San Carlos, B/O Francisco de Ulloa, Simbad08, Jushiro Cepeda, 16 Oct - 06 Nov 02
- IMECOCAL 0301/02, Baja California, B/O Francisco de Ulloa, Simbad08, Jushiro Cepeda, 08 Feb - 15 Feb 03
- CalCOFI0304, Southern California Bight, R/V Roger Revelle , Simbad03, Haili Wang, 03 Apr - 27 Apr 03
- IMECOCAL 0304/05, Baja California, B/O Francisco de Ulloa, Simbad06, Jushiro Cepeda, 08 Apr - 22 Apr 03
- P500304, Southern Pacific, M/V Nacre, Simbad 07 David Cutchin, 24 Apr - 5 May 03
- IMECOCAL 0307, Baja California, B/O Francisco de Ulloa, Simbad08, Martin de la Cruz, 01 Jul - 22 Jul 03
- BEAGLE2003, Leg1, Western Pacific, R/V Mirai, Simbad 03/07, SimbadA01, Brian Irvin, 03 Aug - 06 Sep 03
- BEAGLE2003, Leg2, Eastern Pacific, R/V Mirai, Simbad 03/07, SimbadA01, Gadiel Alarcon, 09 Sep - 16 Oct 03
- IMECOCAL 0310, Baja California, B/O Francisco de Ulloa, Simbad08, Martin de la Cruz, 10 Oct - 31 Oct 03
- BEAGLE2003, Leg3, Valparaiso-Santos, R/V Mirai, Simbad 03/07, SimbadA01, Vivian Lutz, 19 Oct - 02 Nov 03
- OAS1003, Western South Atlantic, R/V Aldebaran, Simbad06, SimbadA02, Denise Vizziano, 26 Oct – 04 Nov 03

The history of SIMBAD calibration coefficients and the accuracy of the view angles measured by the radiometers have been analyzed. This effort started during the first year of the investigation, but was continued the second and third years with additional data. Trends in the calibration coefficients and biases in the view angles were removed, and all the SIMBAD data acquired since October 1996 have been re-processed or processed with adjusted calibration coefficients. Several aspects of satellite ocean-color remote sensing have been examined. They include the selection of aerosol models for atmospheric correction, the SeaWiFS performance in varied oceanic regions, a new algorithm to retrieve marine reflectance and chlorophyll-a concentration based on principal component analysis of atmospheric effects, and the SeaWiFS radiometric calibration in the near infrared. An inversion scheme was also developed to retrieve aerosol scale height from POLDER and MERIS data. The main results and findings are summarized in the next section (see also, below, the list of publications since 2002).

5.3. RESEARCH RESULTS

Aerosol mixtures for ocean color remote sensing

A Probabilistic Self-Organizing Map (PRSOM) has been applied to AERONET retrievals of aerosol size distribution and refractive index at island and coastal sites (Figures 5.2, 5.3, and 5.4). The PRSOM suggests that there are two strong (likely) situations: weakly absorbing mixtures on the one hand, and absorbing dust or urban soot aerosols on the other hand. Intermediate situations are possible, but not probable. The weakly absorbing mixtures (Figure 5.5) are very different from the classical (Shettle and Fenn, 1979) aerosol models (Figures 5.6 and 5.7). If we assume that AERONET provides representative conditions for ocean color remote sensing, two important results have to be emphasized. First, the classical models allow one to process low values of the Angström exponent α (670), but these conditions may not be the most encountered, even in the open ocean. Second, the PRSOM mixtures indicate a different association between Angström exponent and single scatttering albedo. As expected, it is not possible to separate absorbing from weakly absorbing mixtures from a given (observed) ε (χ, 670, 865) (Figures 5.8 and 5.9). However, within one of the two types of situations, the PRSOM neurons can be clearly identified using a directional sampling of the ε parameter (case of POLDER & MISR). Figure 5.9 summarizes the directional behavior of ε using a principal component analysis. Three principal components restore 99% of the information The principal components of the weakly absorbing mixtures have the same range of variability as those of the absorbing mixtures (Figure 5.9b).

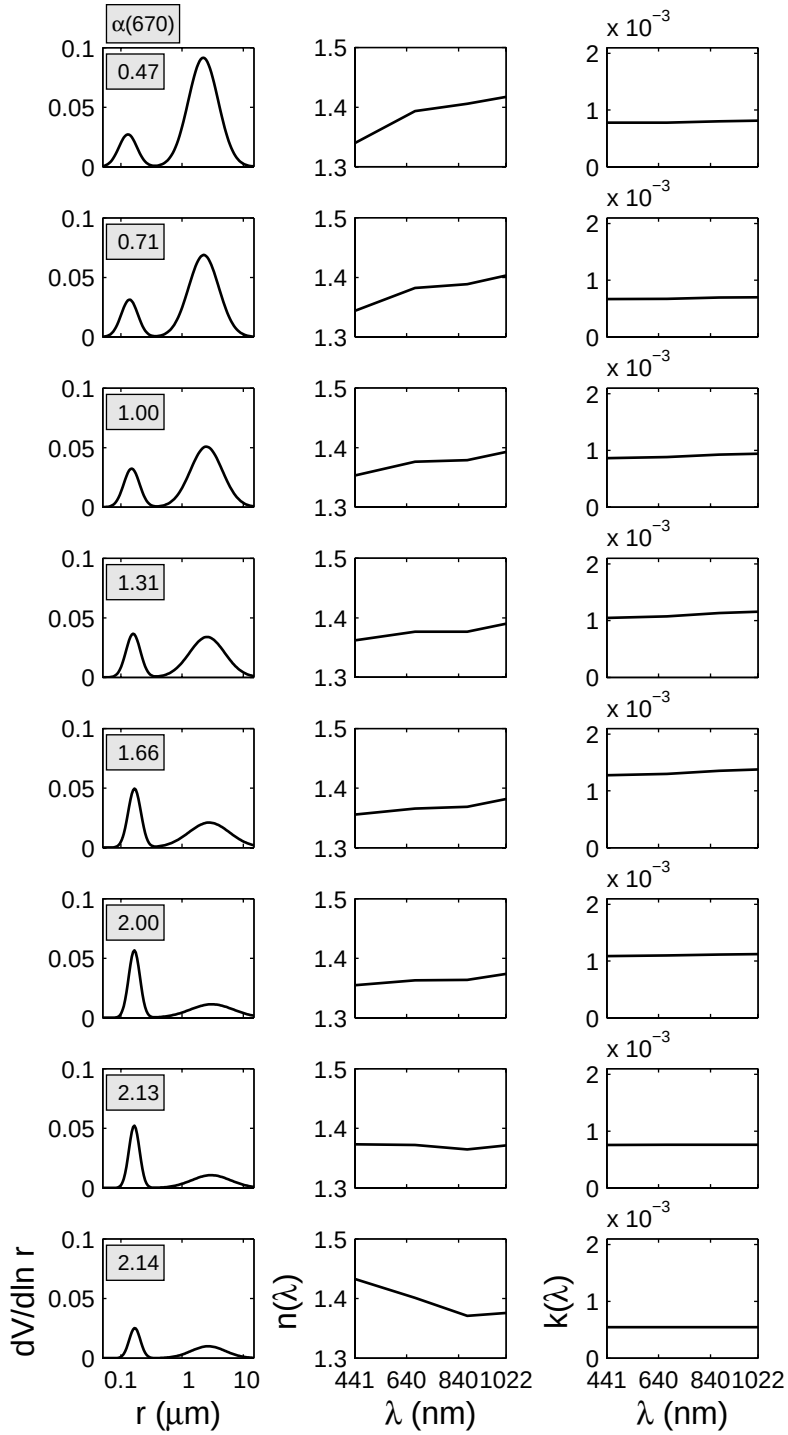

Figure 5.5: Gravity centers of the eight bins dividing the "open ocean" ensemble. First column is dV/dLnr, second column is n, and third column is k. In each plot of dV/dLnr, the corresponding Angström exponent, α(670) is indicated in a framed box.

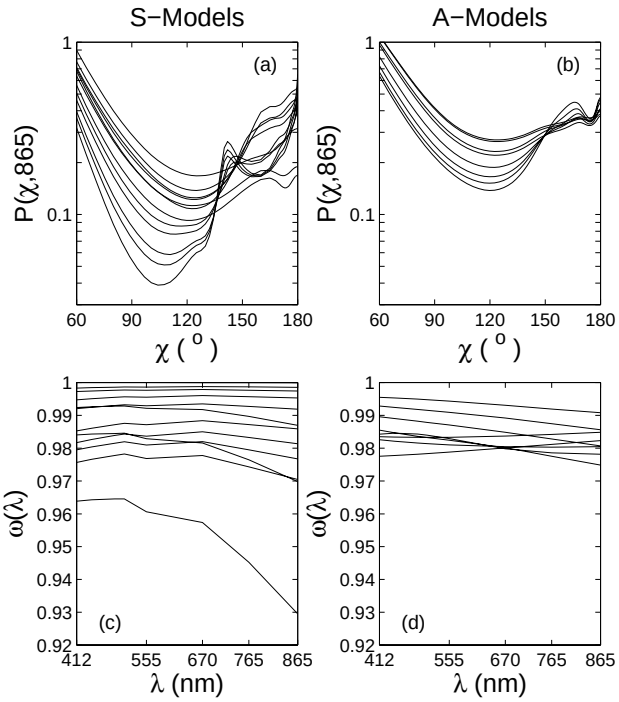

Figure 5.6: Phase function and single scattering albedo of the Standard (S-) models, (a) and (c), and of the AERONET (A-) models, (b) and (d).

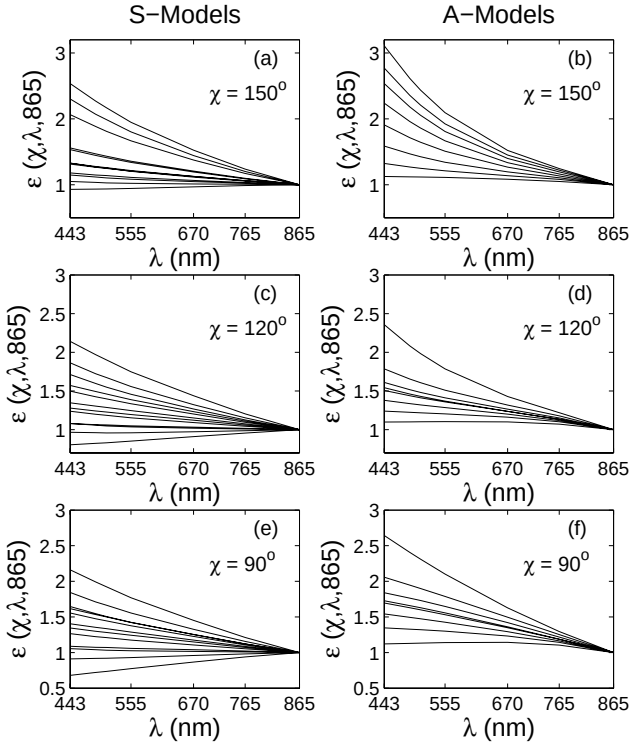

Figure 5.7: Spectral behavior of ε for the two sets of aerosol models and three scattering angles, χ.

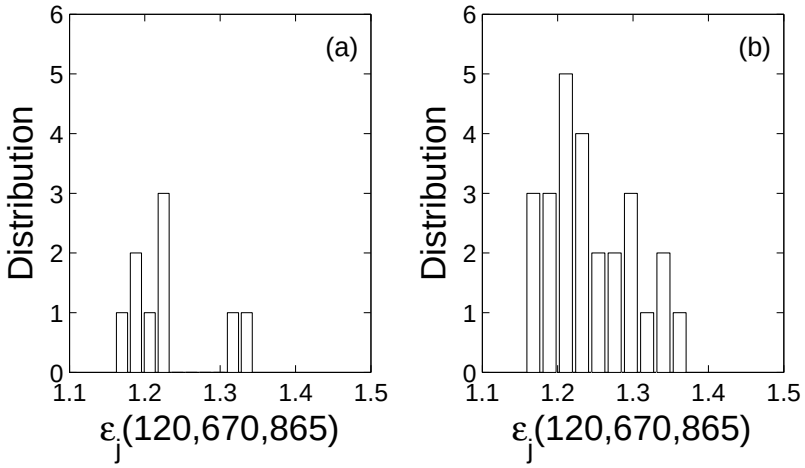

Figure 5.8: Histogram of e(c = 120, 670, 865) for the weakly absorbing neurons (a) and the absorbing neurons (b).

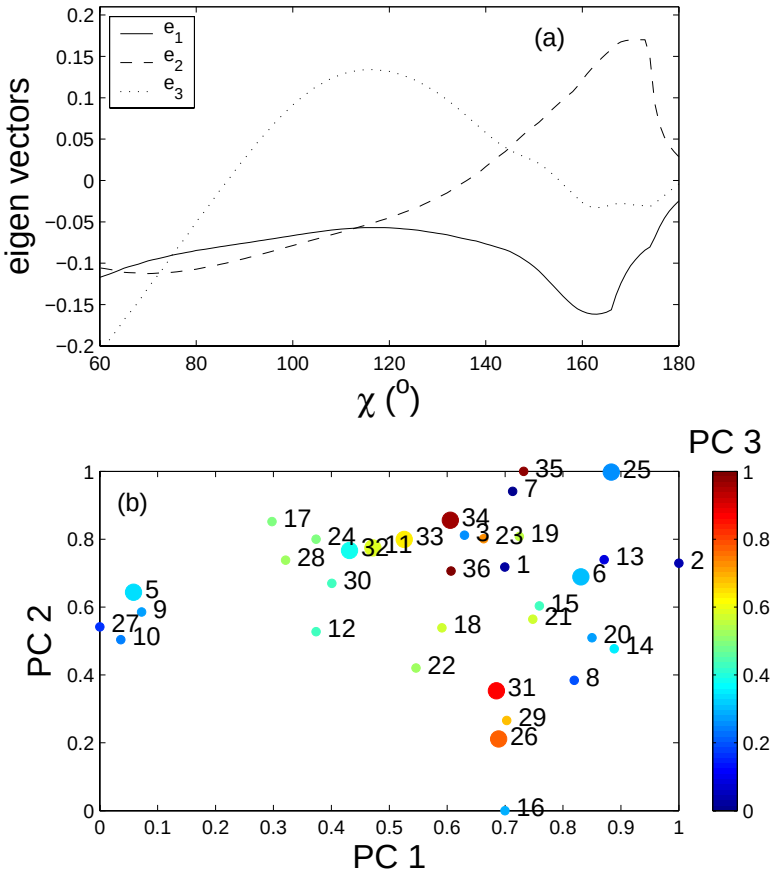

Figure 5.9: The results of a principal component analysis performed on the PRSOM neurons. (a) The first, second, anf third eigen vectors of the ε(χ, 670, 865) covariance matrix, for c ranging from 60 to 180°. (b) Three-dimensional plot of the first three principal components (PC) of the PRSOM neurons (encoded between 0 and 1 for commodity). The third PC (PC3) is displayed using a color scale. Small circles denote absorbing neurons and large circles weakly absorbing neurons. The neuron number is indicated in the vicinity of its coordinates.

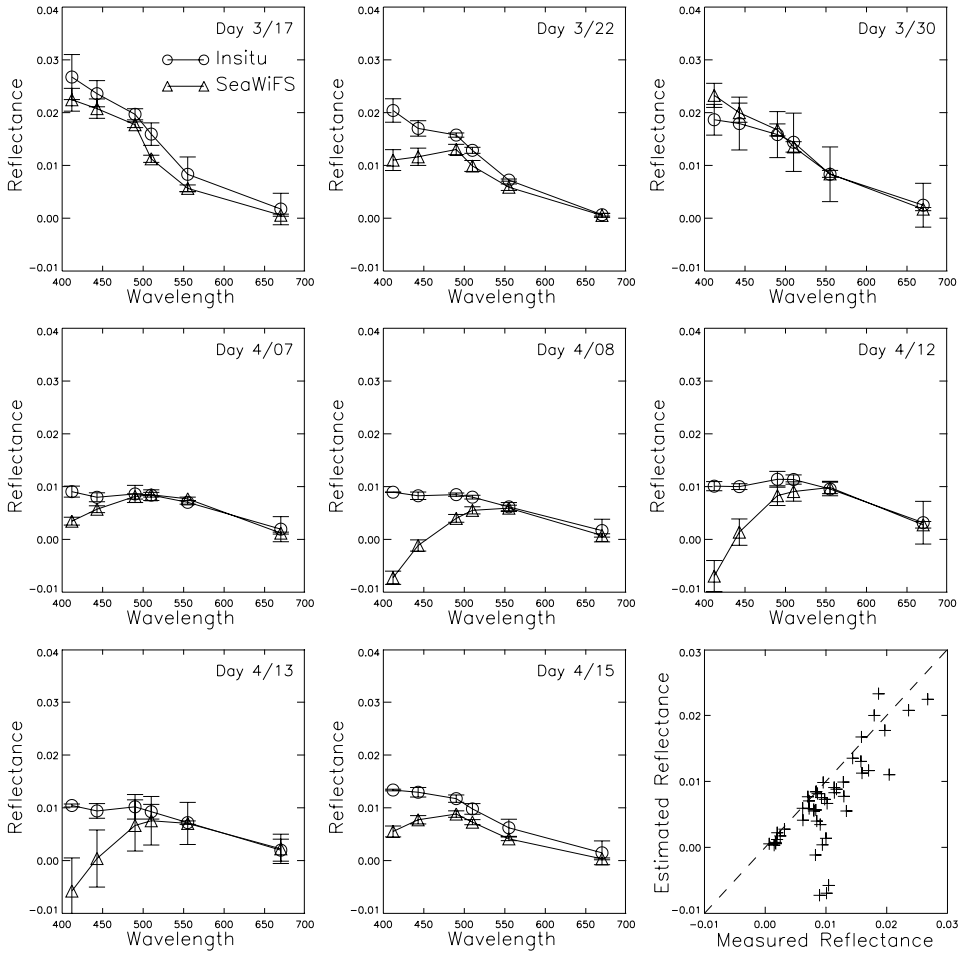

Figure 5.10: SeaWiFS-derived and measured marine reflectance at match-up stations during ACE-Asia. Marine reflectance from SeaWiFS is generally underestimated, especially in the blue.

Thus the two types of mixtures cannot be distinguished. However, within the absorbing mixtures, the dust neurons are easily separated from the urban/soot neurons. In an operational situation, the sampling of the χ space may vary from a pixel to another, but a scalar product between the measured ε and the eigen vectors (displayed in Figure 5.9a) can still be computed, even over a restricted χ range. A simple study made for a POLDER orbit shows that the PRSOM weakly absorbing mixtures can be always separated by computation of their principal components, which may be used in an ocean color processing line. Details about the study can be found in Gross *et al*., (2003) and Gross-Colzy and Frouin (2003).

Evaluation of SeaWiFS-derived marine reflectance and chlorophyll concentration

Marine reflectance, chlorophyll-a concentration, and particulate back-scattering coefficient derived from SeaWiFS imagery have been evaluated in various oceanic regions and atmospheric environments. These include East Asian Seas (Li *et al.*, 2003), the Black Sea and the Eastern Mediterranean Sea (Sancak *et al.*, 2003), and various bio-provinces of the Atlantic Ocean (Frouin *et al.*, 2003).

Figures 5.10 and 5.11 display retrieved and measured marine reflectance and aerosol optical thickness, respectively, at match-up stations during ACE-Asia (R/V Brown cruise). The SeaWiFS marine reflectance is generally lower than the measurements, especially in the blue. The SeaWiFS aerosol optical thickness at 865 nm is larger than the measurements, but its spectral dependence is smaller. Despite the discrepancies, retrieved and measured chlorophyll-a concentrations are in fairly good agreement, with a correlation coefficient squared of 0.78 and a rms difference of 62%. The lower marine reflectance in the blue may be

attributed to absorbing aerosols, not only dust, but also sub-micron particles (soot from diesel fuel and coal consumption), as suggested by Li *et al.* (2003).

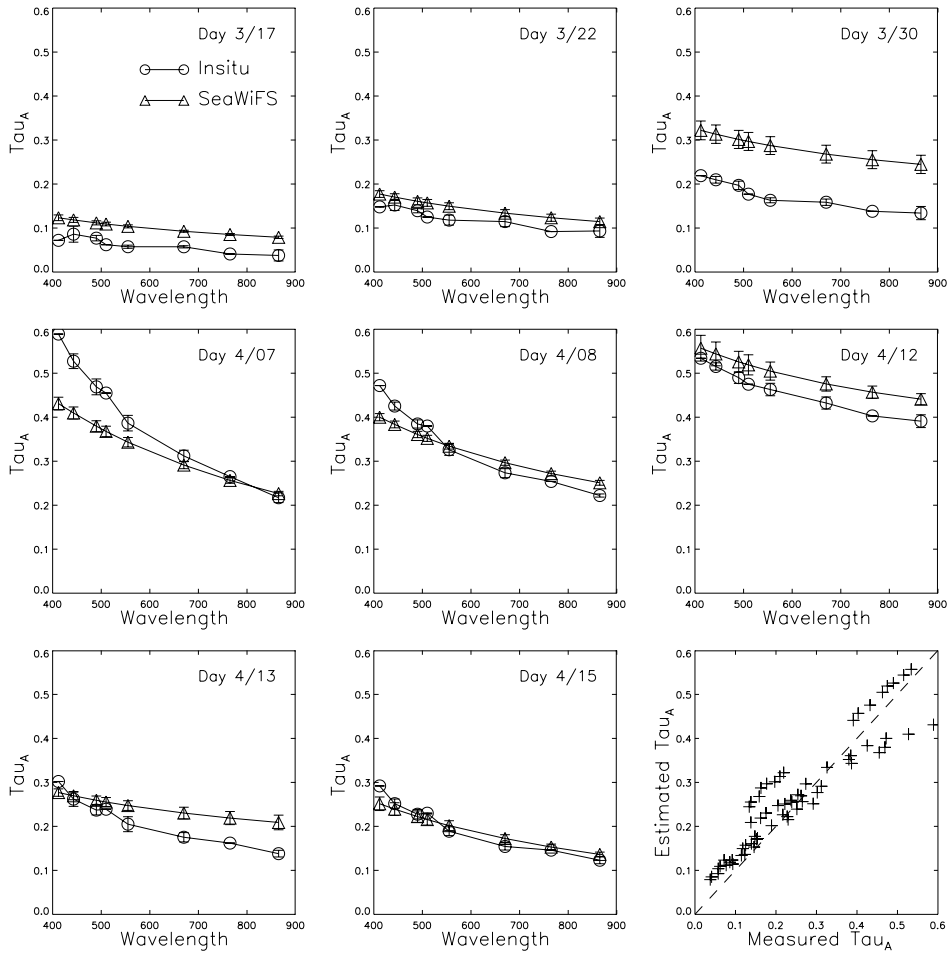

Figure 5.11: SeaWiFS-derived and measured aerosol optical thickness at match-up stations during ACE-Asia. Optical thickness from SeaWiFS is often larger at 865 nm, but its spectral dependence is smaller.

Along Atlantic transects in October-November 2001 and March-April 2002 (R/V Ioffe cruise), SeaWiFS and HPLC chlorophyll-a concentrations agree qualitatively, but there is overestimation by the SeaWiFS algorithm in the oligotrophic waters of both transects (Frouin *et al.*, 2003). Changes in the absolute values and in the form of the spectral absorption of the particulate matter are observed in the waters of different productivity sampled (Fig. 5.12), and such features are important in the development of regional bio-optical algorithms. A general resemblance is noted between particulate back-scattering and chlorophyll distributions. This is not surprising, because back-scattering coefficient depends on particulate matter in seawater that can originate from phytoplankton as a primary source. But the particulate back-scattering distributions (Fig. 5.13) also bear a similarity to the aerosol optical thickness distributions in the central Atlantic (Fig. 5.14), where high values due to transport of Saharan dust occur.

The performance of the OC2 and OC4 algorithms to estimate chlorophyll-a concentrations has also been tested in two contrasted bio-optical environments, the Black Sea and the Mediterranean Sea (Sancak *et al.*, 2003). The in situ bio-optical measurements were made during October 1999 at 25 stations (R/V Bilim cruise). Comparisons of the in situ measurements with the concurrent SeaWiFS retrievals indicate that the OC2 and OC4 algorithms are not working satisfactorily in both seas. Case 2 waters dominate the Black Sea and the failure of the algorithms is expected. On the other hand, failure of the algorithms in the Case 1 waters of the Mediterranean Sea may be due to their specific optical properties. Modifying the OC4 algorithm to include SeaWiFS information at 412 nm yields a better performance in the Mediterranean Sea

without degrading performance in the Black Sea. Combining a local algorithm adapted to oligotrophic waters of the Mediterranean Sea and OC4 provides the best results overall.

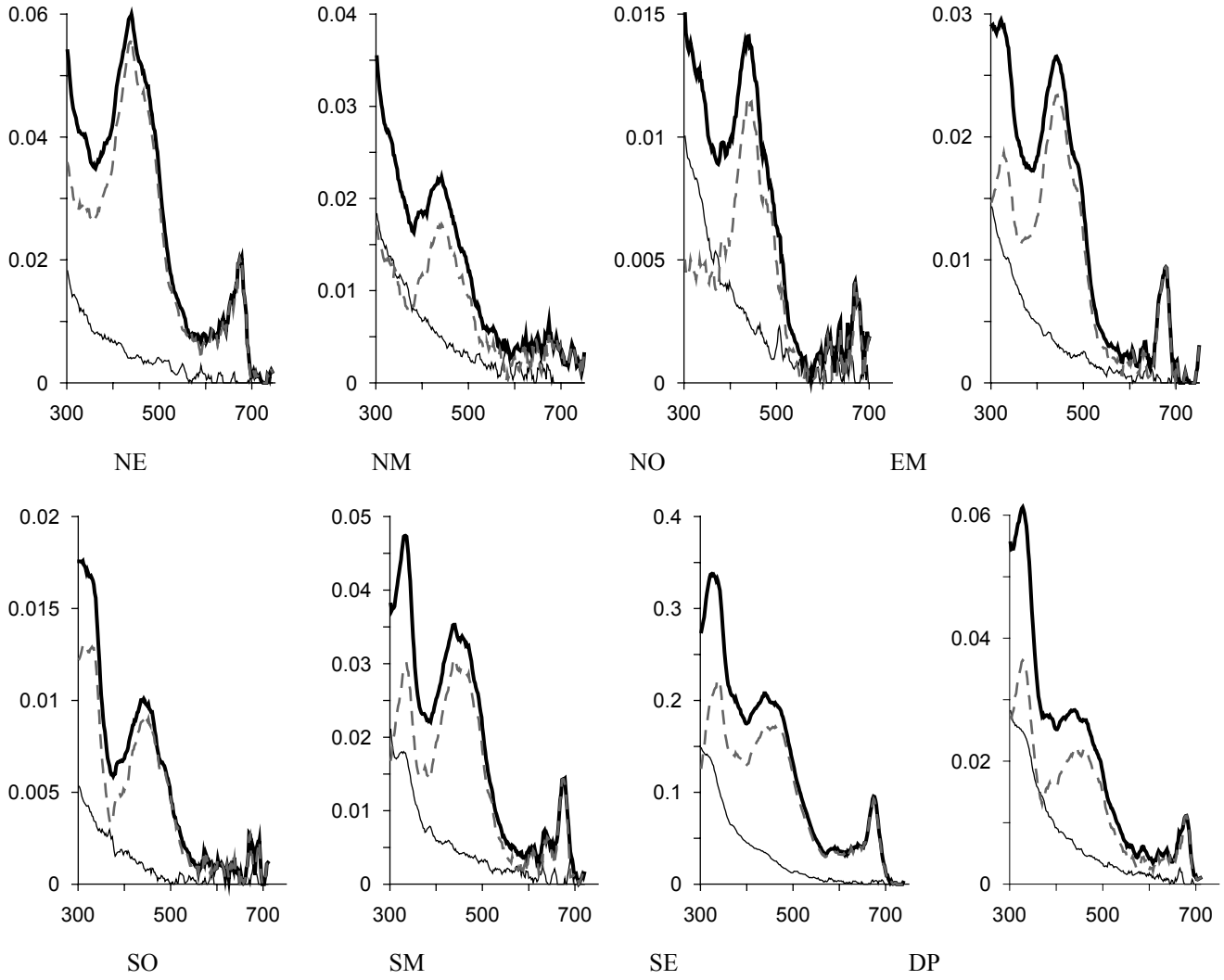

Figure 5.12: Spectra of the absorption coefficients of the particulate matter (thick line), phytoplankton pigment (dash), and detritus (thin line) in different waters in October-November 2001: NE - North eutrophic (Chl=0.77 mg·m^{-3}); NM- North mesotrophic (Chl=0.17 mg·m^{-3}); NO - North oligotrophic (Chl=0.11 mg·m^{-3}); EM - Equatorial mesotrophic (Chl=0.32 mg·m^{-3}); SO - South oligotrophic (Chl=0.07 mg·m^{-3}); SM - South mesotrophic (Chl=0.38 mg·m^{-3}); SE - South eutrophic (Chl=4.9 mg·m^{-3}); DP - Drake Passage (Chl=0.40 mg·m^{-3}).

Atmospheric correction of ocean color via principal component analysis

A methodology has been proposed to retrieve marine reflectance and chlorophyll-a concentration from space by decomposing the satellite reflectance, Rp, into principal components (Gross-Colzy and Frouin, 2003). The components sensitive to the ocean signal (Table 5.2, Fig. 5.15) are combined to retrieve the principal components of marine reflectance, Rw, allowing reconstruction of marine reflectance and estimation of chlorophyll-a concentration. Multi-layered perceptrons are used to approximate the functions relating the useful principal components of satellite reflectance to the principal components of marine reflectance (Fig. 5.16). The algorithm is developed and evaluated using non-noisy and noisy synthetic data sets created for a wide range of angular and geophysical conditions. In the absence of noise on satellite

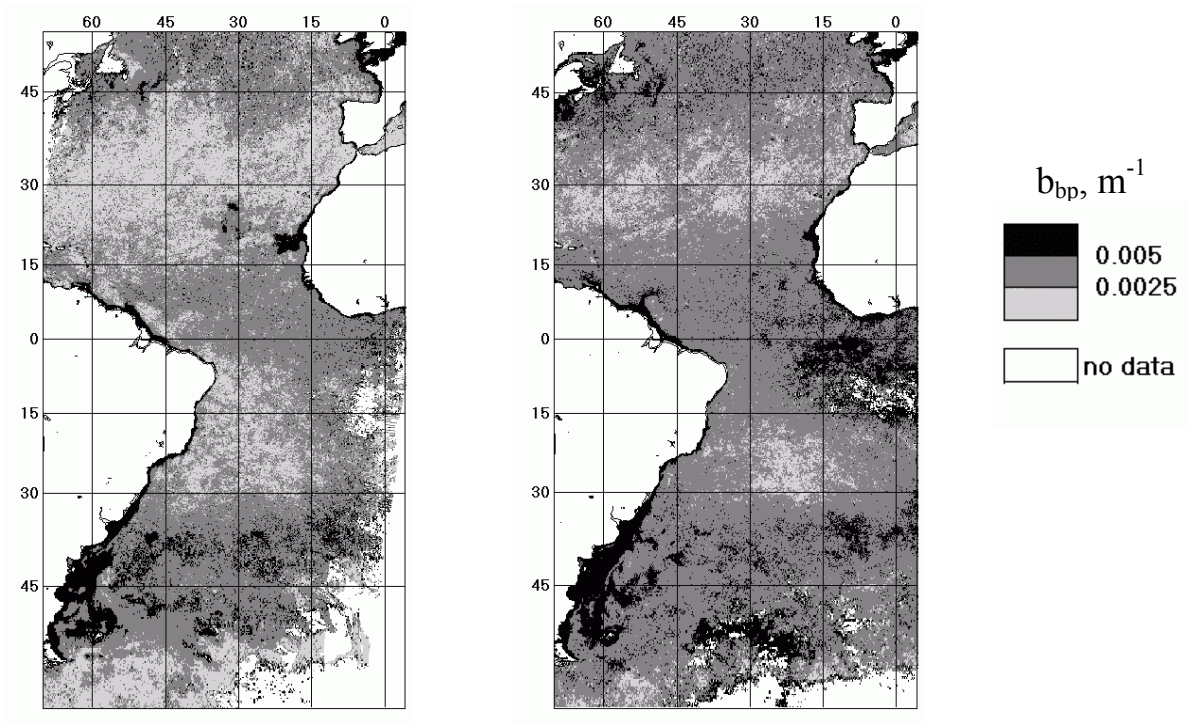

October 2001 October 2002

Figure 5.13: The mean monthly distributions of values of the particle backscattering coefficient in the Atlantic Ocean in October 2001 and 2002 derived from SeaWiFS data.

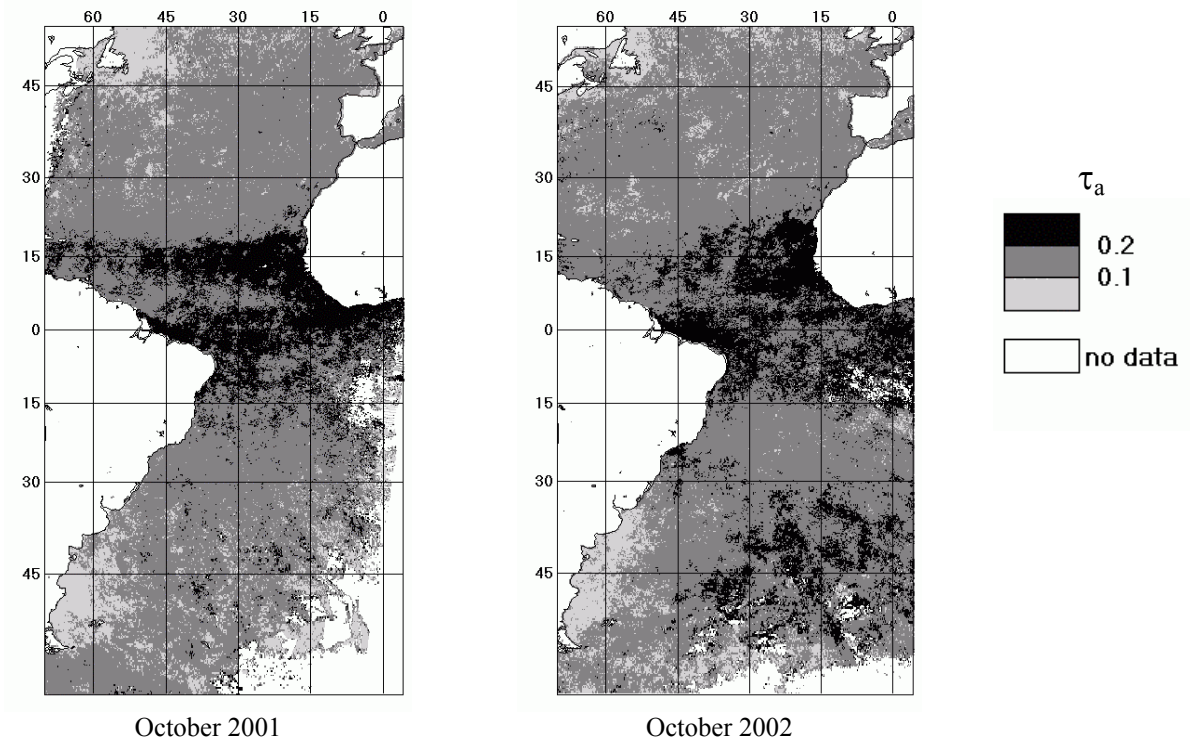

October 2001 October 2002

Figure 5.14: The mean monthly distributions of values of the aerosol optical thickness over the Atlantic Ocean in October 2001 and 2002 derived from SeaWiFS data.

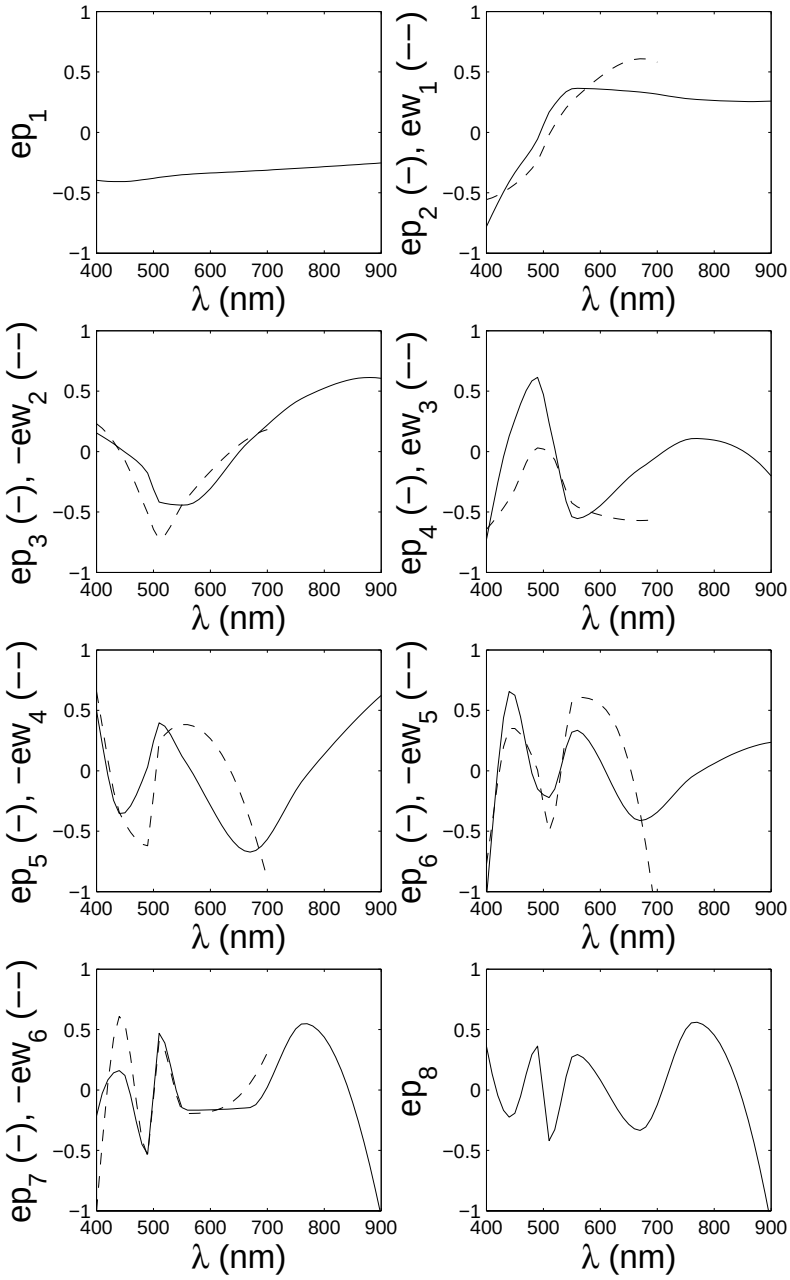

Figure 5.15: Eigenvectors of the *Rp* and *Rw* covariance matrices. The ep_i are displayed for λ ranging from 400 to 900 nm and the ew_j for λ ranging from 400 to 700 nm.

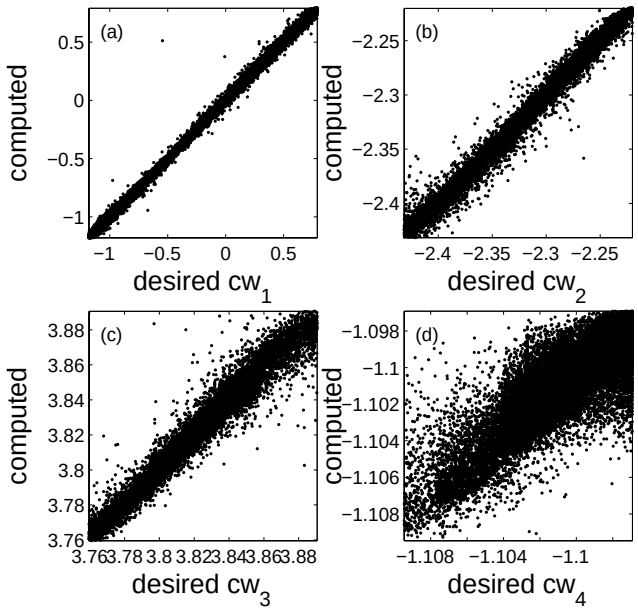

Figure 5.16. Computed versus desired principal components of marine reflectance, cw_j, for $j = 1,...,4$.

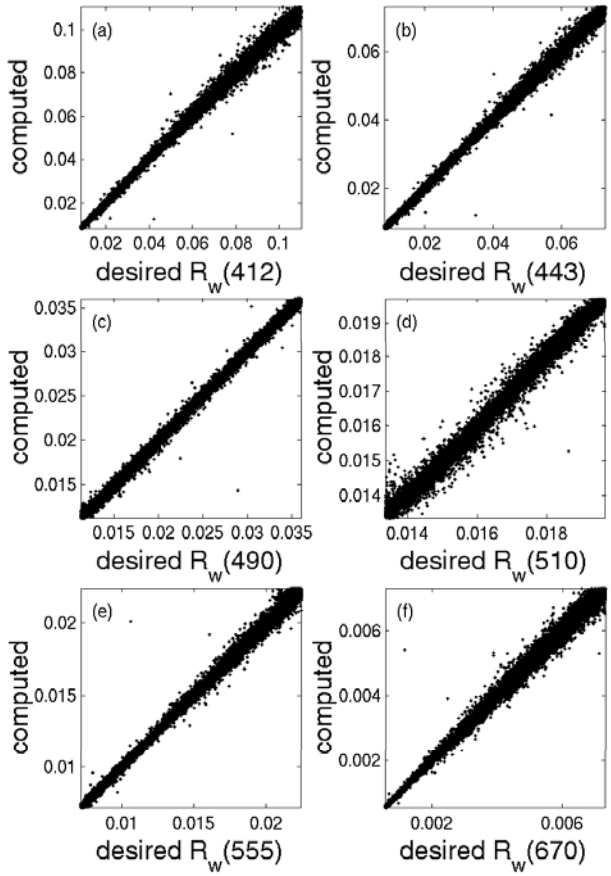

Figure 5.17: Computed versus desired marine reflectance, *Rw*, for 6 SeaWiFS wavelengths: (a) 412, (b) 443, (c) 490, (d) 510), (e) 555, and (f) 670 nm.

reflectance, the relative error on marine reflectance does not exceed 2% (Table 5.3, Fig. 5.17). Accurate retrieval of the first principal component of marine reflectance allows a global relative error of 5.4% on chlorophyll-a concentration (Table 5.3, Figs. 5.18 and 5.19). In the presence of 1% non-correlated and 5% spectrally correlated noise on satellite reflectance, the relative error is increased to 6% and 21%, respectively. Application to SeaWiFS imagery yields marine reflectance and chlorophyll-a concentration fields that resemble those obtained from the standard SeaWiFS processing (Figs. 5.20, 5.21, 5.22 & 5.23), but are generally less contrasted. The marine reflectance spectra retrieved by the two algorithms are substantially different (Fig. 5.22). A large number of SeaWiFS spectra are characterized in the blue by low values not expected in Case-I waters. Accuracy can be improved by including bio-optical variability in the simulated marine reflectance ensembles.

5.4. ACKNOWLEDGMENTS

We wish to thank the officers, technicians, and scientists that have voluntarily collected SIMBAD data and contributed to data analysis, namely Guislain Becu, Jushiro Cepeda-Morales, Martin de La Cruz, Jean-Marc Nicolas, and Haili Wang. We also gratefully John McPherson for programming support, and the SeaWiFS and SIMBIOS project staff for helping with match-up data and for stimulating discussions. This work is supported by the National Aeronautics and Space Administration under contract NAS5-00194, the Scripps Institution of Oceanography, the California Space Institute, the Centre National d'Etudes Spatiales, and the Centre National de la Recherche Scientifique.

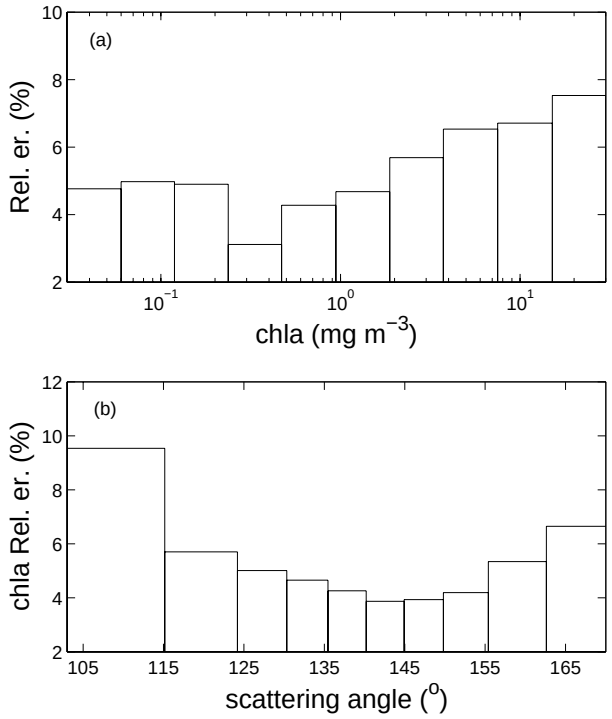

Figure 5.18: Relative error (%) on chlorophyll concentration, *chla*, as a function of (a) *chla* and (b) scattering angle.

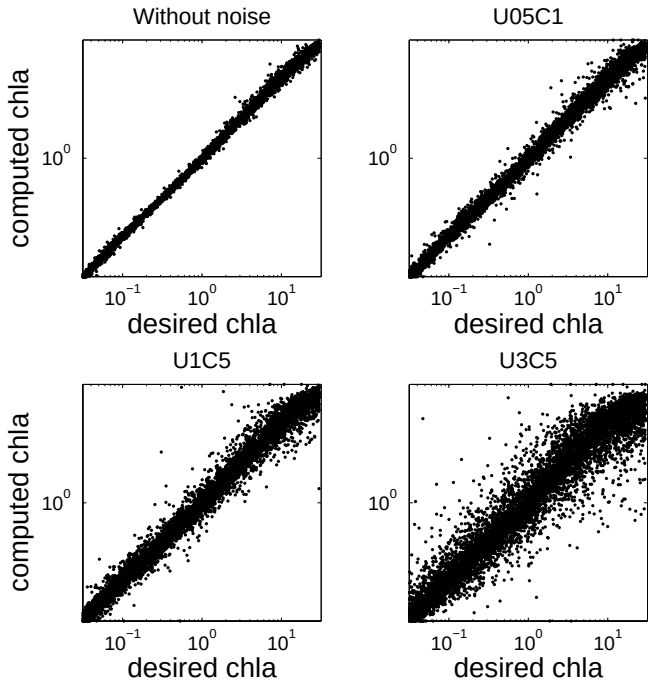

Figure 5.19: Computed versus desired chlorophyll concentration, chl *a*, for various noise figures (see text for details).

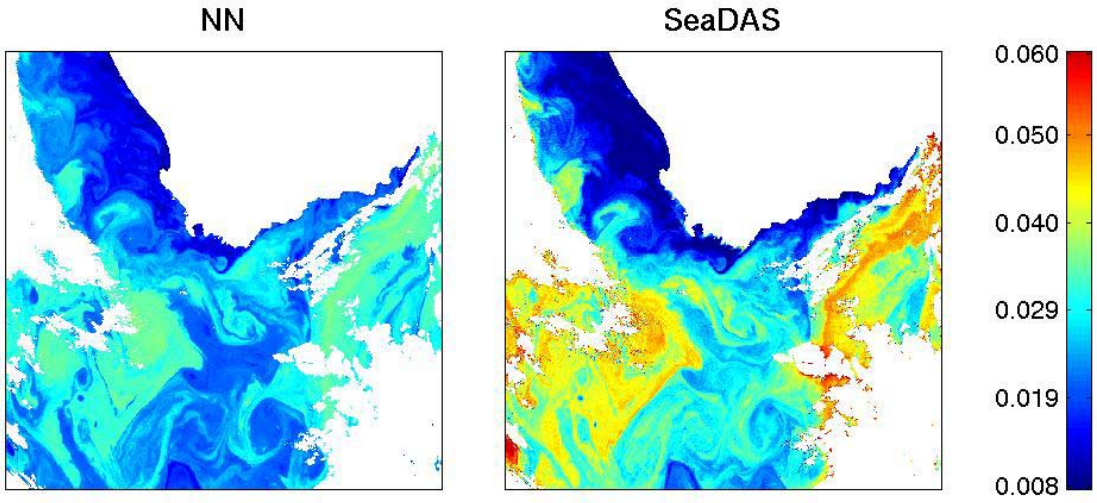

Figure 5.20: Marine reflectance at 443 nm, *Rw(443)*, derived using neural network (left) and SeaDAS (right), for SeaWiFS imagery acquired off South Africa on February 14, 1999.

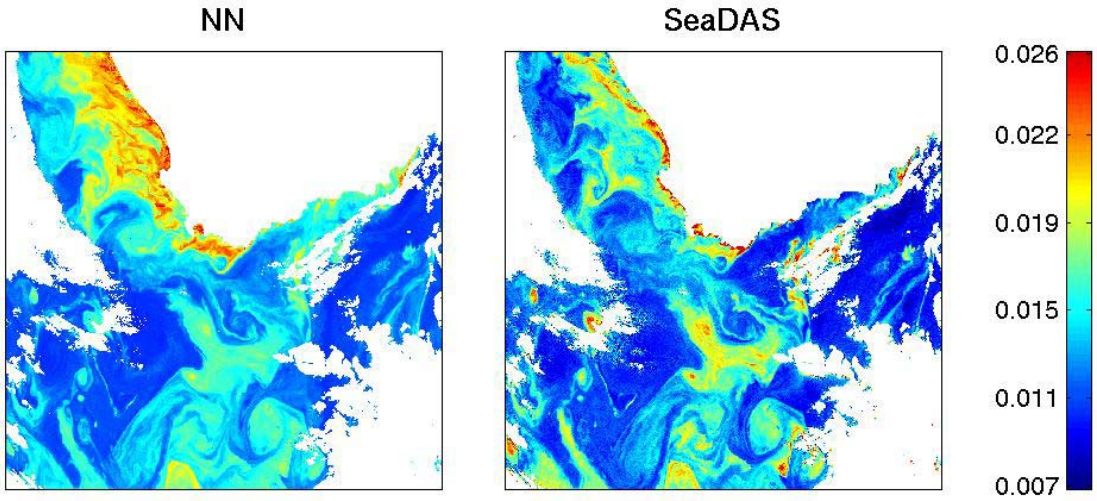

Figure 5.21: Marine reflectance at 555 nm, *Rw(555)*, derived using neural network (left) and SeaDAS (right), for SeaWiFS imagery acquired off South Africa on February 14, 1999.

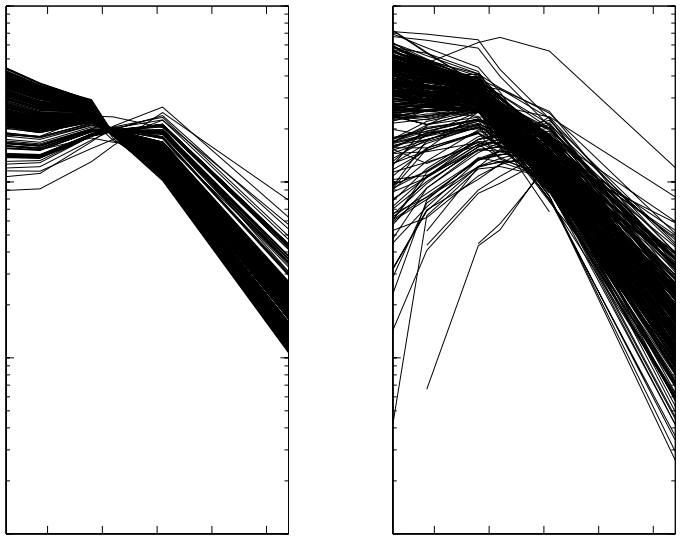

Figure 5.22: Selected marine reflectance spectra, *Rw(λ)*, obtained using neural network (left) and SeaDAS (right), for SeaWiFS imagery acquired off South Africa on February 14, 1999.

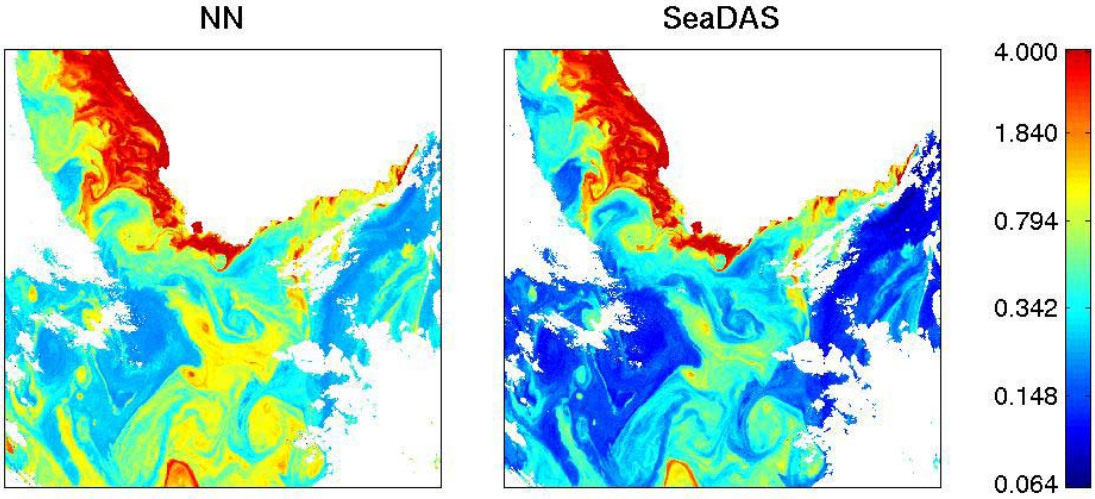

Figure 5.23. Chlorophyll concentration, chl*a*, in mgm^{-3} derived from neural network (left) and SeaDAS (right), for SeaWiFS imagery acquired off South Africa on February 14, 1999.

Table 5.2: Correlation coefficients (%) between the eight principal components of ***Rp***, cp_i, and the six principal components of ***Rw***, cw_j. The correlation coefficients between the cp_i and $\tau(550)$ and chl*a* are also indicated.

	cp_1	cp_2	cp_3	cp_4	cp_5	cp_6	cp_7	cp_8
cw_1	12.3	73.3	-39.8	-47.4	16.9	-0.1	-5.7	-8.9
cw_2	2.8	17.6	-17.4	56.0	63.6	1.8	29.8	21.2
cw_3	3.9	12.0	-2.3	46.8	10.3	-22.9	-45.2	-40.5
cw_4	1.2	3.7	-1.6	9.9	-5.3	44.1	-58.1	26.5
cw_5	0.0	-1.0	1.2	-3.1	2.0	-38.6	14.7	-14.5
cw_6	-0.2	0.1	0.2	-1.3	0.3	-12.9	-4.4	12.0
$\tau(550)$	-67.6	22.4	-4.2	15.8	-22.6	22.3	19.9	-38.2
chla	12.1	71.6	-38.0	-51.4	11.0	-0.3	-10.0	-11.3

Table 5.3: Mean performance of the neural network algorithm in the absence of noise. The tests are performed on the whole data ensemble, the RMS error and bias are computed in the physical units of each parameter (in mgm^{-3} for chl*a*).

	RMS Err.	Rel. Err. (%)	R^2 (%)	Bias
Rw(412)	0.0012	1.7	99.9	0.0000
Rw(443)	0.0007	1.4	99.9	0.0000
Rw(490)	0.0003	0.8	99.9	0.0000
Rw(510)	0.0001	0.5	99.7	0.0000
Rw(555)	0.0002	0.9	99.9	0.0000
Rw(670)	0.0001	1.8	99.9	0.0000
chla	0.841	5.4	99.3	0.0467

REFERENCES

Li, L. P., H. Fukushima, R. Frouin, B. G. Mitchell, M. X. He, T. Takamura, and S. Ohta, 2003: Influence of absorbing aerosols on SeaWiFS-derived marine reflectance during ACE-Asia. In *Ocean Remote Sensing and Applications*, R. Frouin, Y. Yuan, and H. Kawamura, Editors, Proceedings of SPIE Vol. **4892**, pp. 105-115.

Li, L. H. Fukushima, R. Frouin, B. G. Mitchell, M-X He, I. Uno, T. Takamura, and S. Ohta, 2003: Influence of sub-micron absorptive aerosol on SeaWiFS-derived marine reflectance during ACE-Asia, *J. Geophys. Res*.,in press.

Frouin, R., O. Kopelevich, V. Burenkov, A. Demidov, A. Grigoriev, A. Khrapko, S. Sheberstov, and S. Vazyulya, 2003: Variability of the bio-optical characteristics on the Atlantic transect between 50°N and 55°S in two different seasons from satellite and ship data. In *Current Problems in Optics of natural Waters*, K. Shifrin, I. Levin and G. Gilbert, Editors, Proceedings of ONW-2003, Saint-Petersburg, Russia, in press.

Gross-Colzy, L., R. Frouin, C. M. Pietras, and G. S. Fargion, 2003: Non-supervised classification of aerosol mixtures for ocean color remote sensing. *Ocean Remote Sensing and Applications*, R. Frouin, Y. Yuan, and H. Kawamura, Editors, Proceedings of SPIE Vol. **4892**, pp. 95-104.

Gross-Colzy, L., and R. Frouin, 2003: Self-organized mapping of aerosol mixtures at AERONET coastal and island sites. *IEEE Neural Network for Signal Processing Workshop 2003*, Toulouse, France, in press.

Sancak, S., S. T. Besiktepe, a. Yilmaz, M. Lee, B. G. Mitchell, and R. Frouin, 2003: Evaluation of SeaWiFS chlorophyll-a in the Black and Mediterranean Seas. *Int. J. Remote Sensing*, accepted.

Shettle E.P. and R.W. & Fenn, 1979: Models for the aerosol of the lower atmosphere and the effects of humidity variations on their optical properties. AFGL Tech. Rep., **105**, D8, 9-887-9901.

This Research was Supported by
the NASA Contract # 00194

Publications

Deschamps, P.-Y., B. Fougnie, R. Frouin, P. Lecomte, and C. Verwaerde, 2003: SIMBAD: A field radiometer for satellite ocean-color validation. *Appl. Opt*., submitted.

Dubuisson, P., D. Dessailly, M. Vesperini, and R. Frouin, 2003: Water vapor retrieval over ocean using near-infrared radiometry. *J. Geophys. Res*., submitted.

Frouin, R., and S. F. Iacobellis, 2002: Influence of phytoplankton on the global radiation budget. *J. Geophys. Res*., **107**, 4377, doi: 10.1029/2001JD000562.

Frouin, R., and G. D. Gilbert, Editors, 2002: *Remote Sensing and Underwater Imaging*. Proceedings of SPIE Vol. **4488**, 280 pp. Published by SPIE--The International Society for Optical Engineering, Bellingham, Washington, USA. [Book]

Frouin, R., G. D. Gilbert, and D. Pan, Editors, 2003*: Ocean Remote Sensing and Imaging II*. Proceedings of SPIE Vol. **5155**, in press. Published by SPIE –the International Society for Optical Engineering, Bellingham, Washington, USA.[Book]

Frouin, R., Y. Yuan, and H. Kawamura, Editors, 2003: *Ocean Remote Sensing and Applications*. Proceedings of SPIE Vol. **4892**, 620 pp. Published by SPIE--The International Society for Optical Engineering, Bellingham, Washington, USA. [Book]

Frouin, R., L. Gross-Colzy, and P.-Y. Deschamps, 2003: Ocean color remote sensing without explicit atmospheric correction. In *Ocean Remote Sensing and Applications*, R. Frouin, Y. Yuan, and H. Kawamura, Editors, Proceedings of SPIE Vol. **4892**, pp. 133-142.

Frouin, R., B. A. Franz, and P. J. Werdell, 2003: The SeaWiFS PAR product. In *Algorithm Updates for the Fourth SeaWiFS Data Reprocessing*, S. B. Hooker and E. R. Firestone, Editors, NASA/TM-2003-206892, Vol. **22**, pp. 46-50.

Frouin, R., O. Kopelevich, V. Burenkov, A. Demidov, A. Grigoriev, A. Khrapko, S. Sheberstov, and S. Vazyulya, 2003: Variability of the bio-optical characteristics on the Atlantic transect between 50^{o}N and 55^{o}S in two different seasons from satellite and ship data. In *Current Problems in Optics of natural Waters*, K. Shifrin, I. Levin and G. Gilbert, Editors, Proceedings of ONW-2003, Saint-Petersburg, Russia, in press.

Fukushima, H., M. Toratani, A. Tanaka, W. Chen, H. Murakami, R. Frouin, and B. G. Mitchell, 2003: ADEOS-II/GLI ocean color atmospheric correction: Early phase result. In *Ocean Remote Sensing and Imaging II*, R. Frouin, G. D. Gilbert, and D. Pan, Editors, Proceedings of SPIE Vol. **5155**, in press.

Gross-Colzy, L., and R. Frouin, 2003a: Self-organized mapping of aerosol mixtures at AERONET coastal and island sites. *IEEE Neural Network for Signal Processing Workshop 2003*, Toulouse, France, in press.

Gross-Colzy, L., R. Frouin, C. M. Pietras, and G. S. Fargion, 2003: Non-supervised classification of aerosol mixtures for ocean color remote sensing. In *Ocean Remote Sensing and Applications*, R. Frouin, Y. Yuan, and H. Kawamura, Editors, Proceedings of SPIE Vol. **4892**, pp. 95-104.

Gross-Colzy, L., and R. Frouin, 2003b: Remote sensing of chlorophyll concentration from space by principal component analysis of atmospheric effects. In *Ocean Remote Sensing and Imaging II*, R. Frouin, G. D. Gilbert, and D. Pan, Editors, Proceedings of SPIE Vol. **5155**, in press.

Gross-Colzy, L., C. Dupouy, R. Frouin, J.-M. André, and S. Thiria, 2003: Reducing variability due to secondary pigments in the retrieval of chlorophyll concentration from marine reflectance: A case study in the western equatorial Pacific. *Appl. Opt*., submitted.

Knapp, K., R., and R. Frouin, 2003: Separating the aerosol signal from surface effects in geostationary satellite measurements. *J. Geophys. Res*., submitted.

Li, L. H. Fukushima, R. Frouin, B. G. Mitchell, M-X He, I. Uno, T. Takamura, and S. Ohta, 2003: Influence of sub-micron absorptive aerosol on SeaWiFS-derived marine reflectance during ACE-Asia, *J. Geophys. Res*., in press.

Li, L. P., H. Fukushima, R. Frouin, B. G. Mitchell, M. X. He, T. Takamura, and S. Ohta, 2003: Influence of absorbing aerosols on SeaWiFS-derived marine reflectance during ACE-Asia. In *Ocean Remote Sensing and Applications*, R. Frouin, Y. Yuan, and H. Kawamura, Editors, Proceedings of SPIE Vol. **4892**, pp. 105-115.

Loisel, H., J.-M. Nicolas, P.-Y. Deschamps, and R. Frouin, 2002: Seasonal and inter-annual variability of particulate organic matter in the global ocean. *Geophys. Res. Lett*., **29**, doi:10.1029/2002/GL015948.

Meister, G., P. Abel, R. Barnes, J. Cooper, C. Davis, G. Fargion, R. Frouin, M. Godin, D. Korwan, R. Maffione, C. McClain, S. McLean, D. Menzies, A. Poteau, J. Robertson, and J. Sherman, 2003: Comparison of spectral radiance calibrations at oceanographic and atmospheric research laboratories. *Metrologia*, **40**, pp. S93-S96.

Miller, A. J., M. A. Alexander, G. J. Boer, F. Chai, K. Denman, D. J. Erikson, R. Frouin, A. Gabric, E. Laws, M. Lewis, Z. Liu, R. Murtugudde, S. Nakamoto, D. J. Nielson, J. R. Morris, C. Ohlman, I. Perry, N. Schneider, K. Shell, and A. Timmermann, 2003: Potential feedbacks between Pacific Ocean ecosystems and inter-decadal climate variations. *Bull. Am. Meteor. Soc*., **84**, pp. 617-633.

Nakamoto, S. S. Prasanna-Kumar, J. M. Oberhuber, H. Saito, K. Muneyama, and R. Frouin, 2002: Chlorophyll modulation of mixed layer thermodynamics in a mixed layer-sopycnal general circulation model--An example from the Arabian Sea and the Equatorial Pacific. *Proc. Indian Acad. Sci. (Earth Planet. Sci.)*, **111**, pp. 339-349.

Nakamoto, S., K. Muneyama, T. Sato, S. Prasanna Kumar, A. Kumar, and R. Frouin, 2002: Ocean bio-geophysical modeling using mixed layer-isopycnal general circulation model coupled with photosynthesis process. *Recent Research Development in Geophysics*, **4**, pp. 9-20, Researchsigpost, Trivandrum-695 023, Kerala, India.

Nakamoto, S. S. Prasanna-Kumar, K. Nakata, K. Shell, R. Frouin, K. Ueyoshi, P. Sammarco, A. Lai, H. Saito, T. Sato, and K. Muneyama, 2003: Thermophysical Interaction of Ocean Ecosystem and Geophysical system--For Understanding Carbon Circulation in the Ocean. *J. Adv. Mar. Sci. Tech. Soc*., **8**, pp. 35-48.

Sancak, S., S. T. Besiktepe, a. Yilmaz, M. Lee, B. G. Mitchell, and R. Frouin, 2003: Evaluation of SeaWiFS chlorophyll-a in the Black and Mediterranean Seas. *Int. J. Remote Sensing*, accepted.

Shell, K., R. Frouin, S. Nakamoto, and R. C. J. Somerville, 2003: Atmospheric response to solar radiation absorbed by phytoplankton, *J. Geophys. Res*., **108**, doi: 10.1029/2003JD003440.

Smirnov, A., B. N. Holben, O. Dubovik, R. Frouin, and I. Slutsker, 2003: Maritime component in aerosol optical models derived from AERONET (Aerosol Robotic Network) data, *J. Geophys. Res*., **108**, 4033, doi: 10.1029/2002JD002701.

Souaidia, N., C. Pietras, S. Brown, K. Lykke, P.-Y. Deschamps, G. Fargion, and B. C. Johnson, 2003: Sun photometer laser- and lamp-based radiometric calibrations: Comparison with the Langley technique and implications on remote sensing. In *Ocean Remote Sensing and Imaging II*, R. Frouin, G. D. Gilbert, and D. Pan, Editors, Proceedings of SPIE Vol. **5155**, in press.

Zhao, X.-P., I. Laszlo, O. Dubovik, A. Smirnov, B. H. Holben, J. Sapper, C. Pietras, K. J. Voss, and R. Frouin, 2003: Regional evaluation of the revised NOAA/NESDIS AVHRR two-channel aerosol retrieval algorithm and determination of the refractive index for key aerosol types over the ocean. *J. Geophys. Res*., in press.

Chapter 6

Merging Ocean Color Data From Multiple Missions

Watson W. Gregg
NASA Goddard Space Flight Center, Greenbelt, Maryland

6.1 INTRODUCTION

Oceanic phytoplankton may play an important role in the cycling of carbon on the Earth, through the uptake of carbon dioxide in the process of photosynthesis. Although they are ubiquitous in the global oceans, their abundances and dynamics are difficult to estimate, primarily due to the vast spatial extent of the oceans and the short time scales over which their abundances can change. Consequently, the effects of oceanic phytoplankton on biogeochemical cycling, climate change, and fisheries are not well known.

In response to the potential importance of phytoplankton in the global carbon cycle and the lack of comprehensive data, NASA and the international community have established high priority satellite missions designed to acquire and produce high quality ocean color data (Table 6.1). Ten of the missions are routine global observational missions: the Ocean Color and Temperature Sensor (OCTS), the Polarization and Directionality of the Earth's Reflectances sensor (POLDER), Sea-viewing Wide Field-of-view Sensor (SeaWiFS), Moderate Resolution Imaging Spectrometer-AM (MODIS-AM), Medium Resolution Imaging Spectrometer (MERIS), Global Imager (GLI), MODIS-PM, Super-GLI (S-GLI), and the Visible/Infrared Imager and Radiometer Suite (VIIRS) on the NPOESS Preparatory Project (NPP) and the National Polar-orbiting Operational Environmental Satellite System (NPOESS). In addition, there are several other missions capable of providing ocean color data on smaller scales. Most of these missions contain the spectral band complement considered necessary to derive oceanic chlorophyll concentrations and other related parameters. Many contain additional bands that can provide important ancillary information about the optical and biological state of the oceans.

In previous efforts, we have established that better ocean coverage can be obtained in less time if the data from several missions are combined (Gregg et al., 1998; Gregg and Woodward, 1998). In addition to improved coverage, data can be taken from different local times of day if the missions are placed in different orbits, which they are. This can potentially lead to information on diel variability of phytoplankton abundances. Since phytoplankton populations can increase their biomasses by more than double in a single day under favorable circumstances (Eppley, 1972; Doney at el., 1995), observations of their abundances at different times within a single day would be useful.

We proposed to investigate, develop, and test algorithms for merging ocean color data from multiple missions. We seek general algorithms that are applicable to any retrieved Level-3 (derived geophysical products mapped to an Earth grid) ocean color data products, and that maximize the amount of information available in the combination of data from multiple missions. Most importantly, we will investigate merging methods that produce the most complete coverage in the smallest amount of time, nominally, global daily coverage. We will emphasize 3 primary methods: 1) averaging, 2) blending, and 3) statistical interpolation.

6.2. RESEARCH ACTIVITIES

We investigated a set of 3 merging algorithms utilizing Level-3 data products. None of the candidate algorithms were limited to any Level-3 grid size or temporal frequency. The choice of grid size and frequency issue depends on how sparse the final fields are and the acceptance level for data gaps. We leave this choice to the SIMBIOS Project. For our analyses, however, we used 25-km equiangular spatial, and daily time fields.

Candidate merger algorithms under investigation in this proposed effort were: averaging, blending, and statistical (optimal) interpolation.

Averaging

This method is a simple, straightforward application of weighting data from each sensor equally. At grid points where only data from one satellite are available, it enters the merged field unadjusted.

$$C_{ij} \frac{\sum_s C_{ijs}}{\sum_s n_{ijs}}$$

where C indicates chlorophyll from sensor s, n is the number of observations from sensor s,ij represents the Level-3 grid point in question, and the summations are over the sensors. Although we use chlorophyll to represent the equation, any Level-3 data product can be used. This method has the advantage of simplicity and total objectivity, i.e., no sensor data are preferred over others. It can potentially suffer from this same objectivity in the case of relatively poorer performance. If Level-3 grid locations are common among the different sensor products, the application of the method is straightforward. If they are not, then interpolation may be required.

Blended analysis

The blended analysis has traditionally been applied to merging satellite and in situ data (Reynolds, 1988). Also known as the Conditional Relaxation Analysis Method (CRAM; Oort, 1983), this analysis assumes that in situ data are valid and uses these data directly in the final product. The satellite chlorophyll data are inserted into the final field using Poisson's equation

$$\nabla^2 C^b = \psi$$

where C^b is the final blended field of chlorophyll, and Ψ is a forcing term, which is defined to be the Laplacian of the gridded satellite chlorophyll data ($\nabla^2 S$). In situ data serve as internal boundary conditions, and are inserted directly into the solution field C^b

$$C_{ibc} = I$$

where the subscript $_{ibc}$ indicates internal boundary condition (IBC) and I is the in situ value of chlorophyll. Thus in situ data appear un-adjusted in the final blended product. In its application to multiple ocean color data sets, in situ data would be replaced by a determination of superior performance by one of the sensors data, and utilized as the IBC. This could occur across the domain for an individual sensor, if its calibration was considered superior, for example. Or it could occur by location as the environmental conditions provide for better performance of one sensor over the others (e.g., location of sun glint, individual scan problems, etc.). Where one sensor data could be established as superior, it would serve as the IBC. If no distinction could be provided, the data could simply be merged using one or more of the other methods. Then the final merged product would be blended, so that the internal boundary conditions are upheld, and the rest of the Level-3 field is adjusted according to the spatial variability of the other sensors. This can provide a bias correction to the non-IBC points, while retaining their spatial structure, and potentially produce an overall enhanced data set.

The requirement of superior data field insertion unaltered into the merged field can be relaxed. For example, the IBC weight could be 0.25 for sensor 1 and 0.75 for sensor 2 at grid point ij. This can be a useful modification of several sensor data sets are superior to others but not necessarily from one another, or if clear superiority is difficult to quantify.

Statistical Interpolation

This method is often referred to as optimal interpolation (e.g., Reynolds and Smith, 1994), but is technically only optimal when all of the error correlations are known (Daley, 1991), which is rare. In this method the weights W are chosen to minimize the expected error variance of the analyzed field (Daley,

1991). It differs from the spatial analysis method by allowing error correlations to determine the effective separation distance, and from the blended analysis by use of a statistical approach for defining the weights. A weight matrix **W** represents the error correlations, and is referred to as the error covariance matrix.

$$C_{ij} = C_{sij} + \sum W_{ijkm}(C_{S+1,km} - C_{s,km})$$

This method has the advantage of widespread use in data assimilation problems, and objectivity in selection of the weights. The disadvantage is the statistical interpretation of the merged data set, as opposed to a scientific evaluation.

It is possible that the best merging method will be one that utilizes combinations of these algorithms. For example, some level of subjective analysis will be used in data masking, and then averaged. Reynolds and Smith (1994) combine the use of blending for bias correction followed by statistical interpolation to recover the grid resolution. We may easily envision a combination of approaches.

Table 6.1. Mission characteristics of proposed and present global ocean color sensors. For node, D indicates descending, A indicates ascending. Incl. Indicate inclination (degrees). ECT means local equator crossing time on the node. GIFOV means ground instantaneous field of view at nadir. Advanced Earth Observing Satellite (ADEOS); Earth Observing System (EOS); Environmental Satellite (Envisat); NPOESS Preparatory Project (NPP) and National Polar-orbiting Operational Environmental Satellite System (NPOESS).

Sensor	Launch	Spacecraft	Altitude	Incl.	ECT	Node	Swath	Tilt	GIFOV
SeaWiFS	1997	OrbView-2	705 km	98.2	noon	D	45°	±20°	1 km
MODIS-AM	1999	EOS-Terra	705 km	98.2	10:30 AM	D	55°	none	1 km
MERIS	2002	Envisat	780 km	98.5	10:00 AM	D	41°	none	1 km
GLI	2003	ADEOS-II	803 km	98.6	10:30 AM	D	45°	±20°	1km
POLDER-II	2003	ADEOS-II	803 km	98.6	10:30 AM	D	51°	±20°	7 km
MODIS-PM	2002	EOS-Aqua	705 km	98.2	1:30 PM	A	55°	none	1 km
S-GLI	2005	ADEOS-III	803 km	98.6	10:30 AM	D	45°	±20°	1
VIIRS	2006	NPP	TBD	TBD	TBD	TBD	TBD	TBD	1 km
VIIRS	2009	NPP	TBD	TBD	TBD	TBD	TBD	TBD	1 km

6.3. RESEARCH RESULTS

The three candidate merger algorithms have been tested using SeaWiFS and MODIS data. The SeaWiFS data is Version 4 and the MODIS is Collection 4. Results indicate promising behavior from all three candidate algorithms (Figure 6.1). However, there are some problems remaining, most associated with data quality of the sensors and our ability to understand and correct for them prior to application of the algorithms. Overall the averaging method is best for data with no biases, because it is simple, objective, and computationally fast. If there are biases in either or both data sets that are uncorrected or unrecognized, this method will propagate these errors into the merged field, and produce a poor quality data set. Knowledge of biases in the new versions of each sensor is presently lacking, and requires substantial effort. The blended method is effective at eliminating biases if a "truth field" can be identified. In the analyses done so far, we assumed SeaWiFS to be a truth field unilaterally, and MODIS was the data blended to produce the final merged product. The effectiveness of the bias-correction capability of the blended analysis is quite well known in in situ-satellite data merging, but not in satellite-satellite merging. Our results indicate that significant differences in satellite data quality coupled with the very large coverage of both sensors, results in over-correction by the blended method.

The statistical (optimal) interpolation (OI) method has many of the advantages of the blended method in bias-correction. However, the over-correction behavior of the blended method is reduced to the point that it is not readily apparent in the resulting merged field. The method suffers from computational complexity and is very slow.

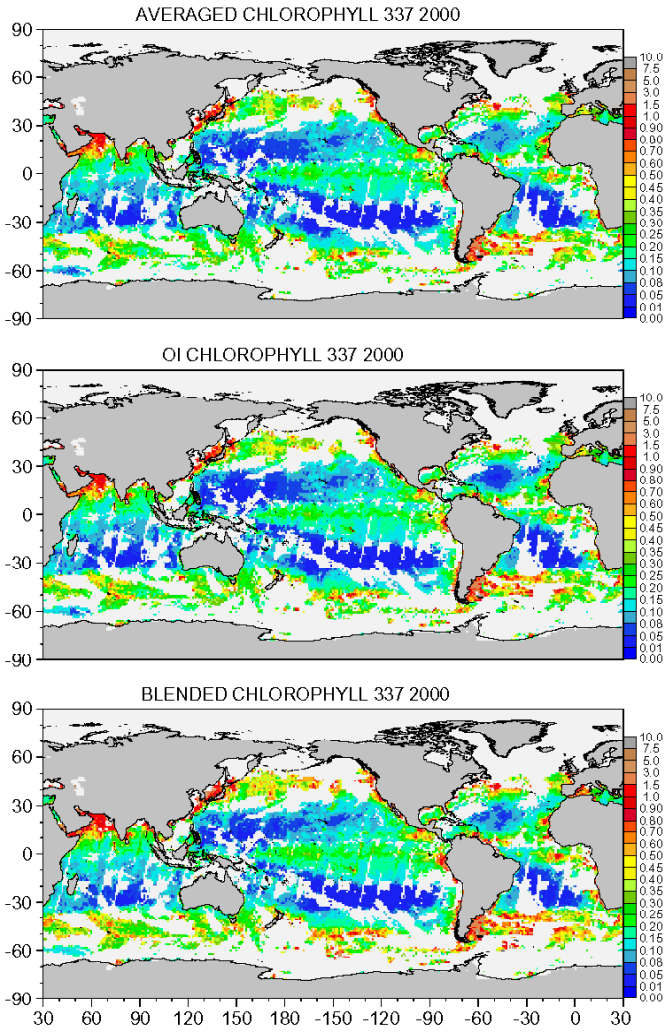

Figure 6.1: Comparison of 3 different merging methodologies for SeaWiFS and MODIS on Dec. 2, 2000

It is clear that proper selection of merging algorithms depends critically upon knowledge of the error characteristics of the data sets being merged. Consequently, we invested significant effort into analyzing the SeaWiFS and MODIS data behavior as compared against the SeaBASS data archive.

SeaWiFS Reprocessing 3 vs. Reprocessing 4

Comparisons were made between the newly reprocessed SeaWiFS Level-3 chlorophyll product (Reprocessing 4 or R4) and the previous version (Reprocessing 3 or R3) using in situ measurements. There were 2,470 SeaWiFS/SeaBASS match-up measurements of fluorometrically/spectrophotometrically-derived chlorophyll-a (mg m^{-3}) at depths of 0.0 to 10.0 meters available for the SeaWiFS mission period of September 15, 1997 through June 1, 2002 (Figure 6.2). The results showed that the newly reprocessed SeaWiFS data matched up better with the surface measurements than the previous version did (Figure 6.3). Globally, the slope of the match-ups improves to 0.85 from 0.78 in log-log scale. A significant trend that

contributed to this improvement was the overall decrease in SeaWiFS chlorophyll levels less than 1.0 mg m^{-3}. Regional analyses reveal that the match-ups improve in every oceanic basin, except the Antarctic. However, SeaWiFS continues to exhibit poor correspondence with in situ data in the North Atlantic where the match-ups have a slope of 0.54.

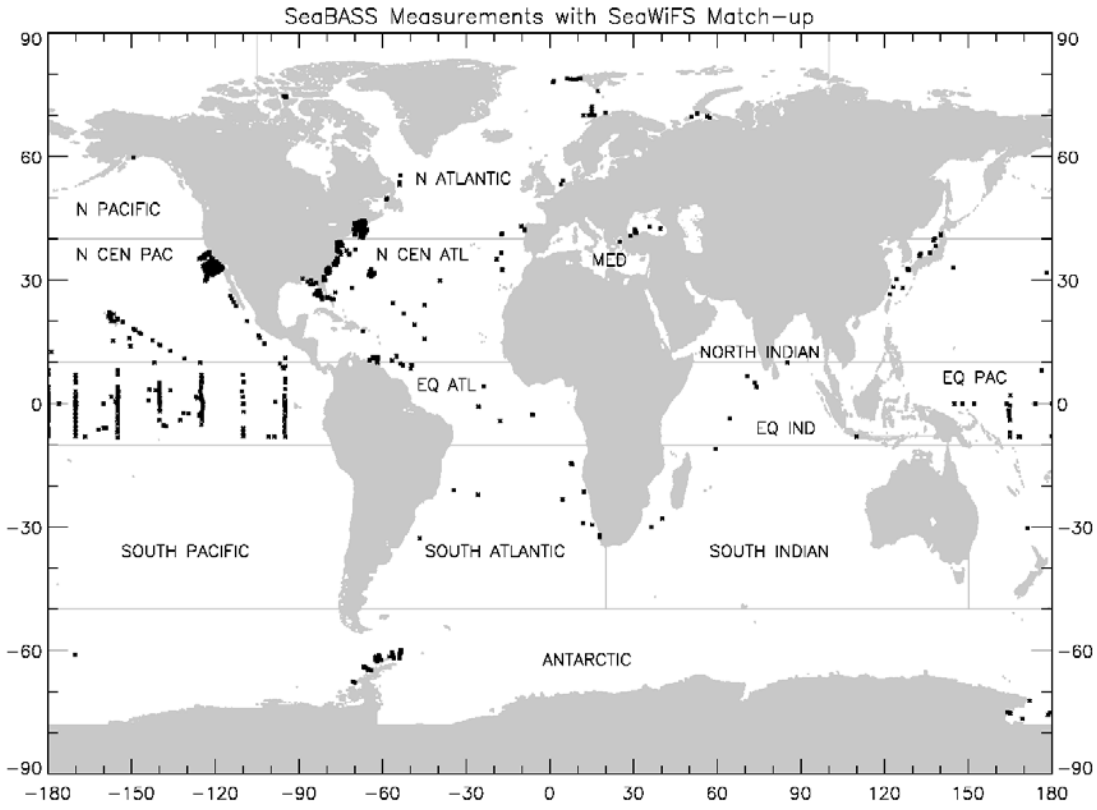

Figure 6.2: Global distribution of the SeaBASS measurements with a co-located SeaWiFS pixel for both R3 and R4 (N=2,470). The oceanic regions used for statistical comparisons are shown.

An examination of monthly images for May 1999 revealed that the number and magnitude of high-value chlorophyll pixels had increased in the high latitude open ocean of the South Pacific. There were more high-value outliers in the R4 image as compared to the R3 in the open ocean of the South Pacific, an area generally characterized by relatively homogeneous levels of low-chlorophyll. On a monthly timescale and in a largely homogenous area, increased numbers and magnitudes of high outliers in the new R4 data set as compared to the previous version is some cause for concern. The incidence of outliers should tend to be relatively low in monthly images in general due to the smoothing effects of averaging the dailies. In addition, the lower latitude areas such as the South Pacific may have fewer valid daily measurements than in other areas, but an examination of the daily images for this region exhibited the same general pattern shown in the monthly values. These results were published as a NASA Technical Memorandum (Casey and Gregg, 2003).

Global and Regional SeaWiFS Chlorophyll Data Evaluation

The SeaWiFS chlorophyll data set was compared to comprehensive archives of in situ chlorophyll data from NASA and NOAA, involving 4168 point-to-point daily matchups. The global comparison indicated

an RMS log error of 31%, with a coefficient of determination (r^2) of 0.76 (Figure 6.5). RMS log error for open ocean (defined as bottom depth > 200m) was 5% lower than for coastal regions, indicating a small deterioration of quality of the SeaWiFS data set in coastal regions. All of the Pacific oceanographic basins generally showed very good agreement with SeaWiFS, as did the South Atlantic basin. However, poorer agreement was found in the Mediterranean/Black Seas, North Central and Equatorial Atlantic basins, and the Antarctic. Optical complexity arising from riverine inputs, Saharan dust, and anomalous oceanic constituents contributed to the differences observed in the Atlantic, where a trend of overestimation by SeaWiFS occurred. The Antarctic indicated a pronounced negative bias, indicating an underestimation, especially for chlorophyll concentrations > 0.15 mg m^{-3}. The results provide a comprehensive global and geographic analysis of the SeaWiFS data set, which will assist data users and policy makers in assessing the uncertainty of estimates of global and regional ocean chlorophyll and primary production. The results have been submitted to Remote Sensing of Environment (Gregg and Casey 2003).

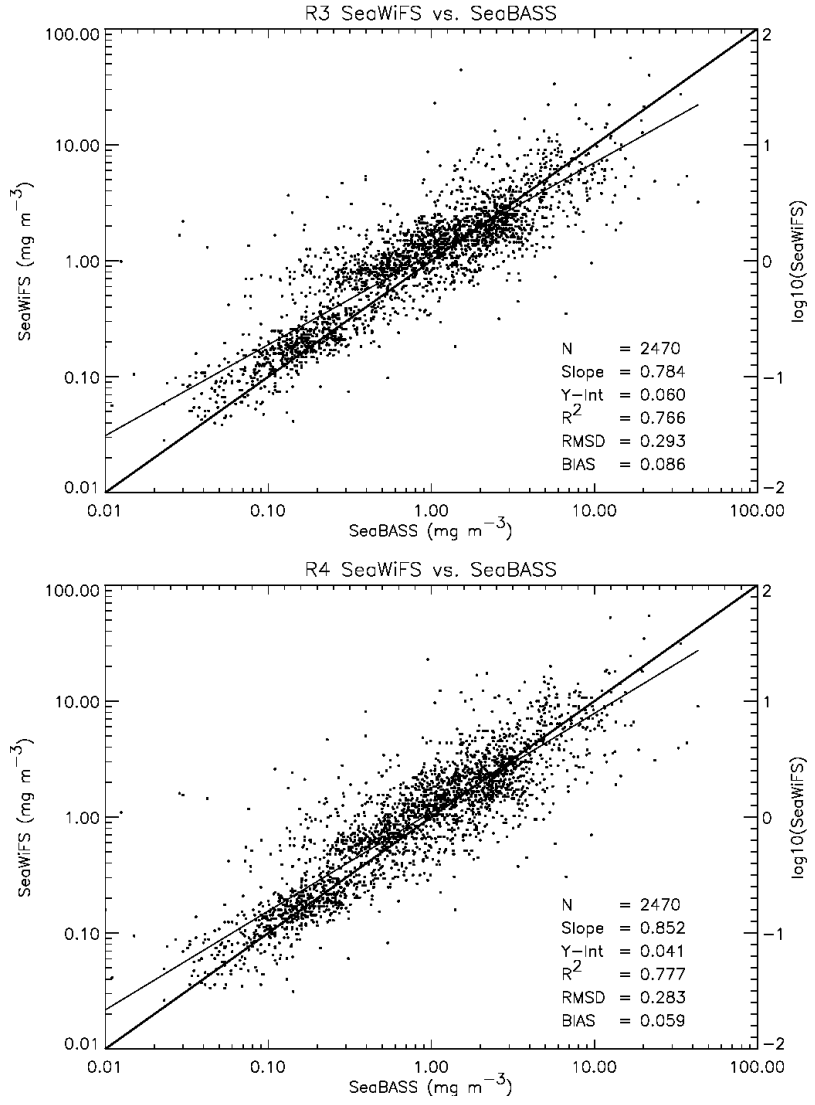

Figure 6.3: Scatterplots comparing SeaBASS chlorophyll measurements (mg m-3) with co-located SeaWiFS values for versions R3 (top) and R4 (bottom). The 1-to-1 line (thick) and the least-squares regression line (thin) are shown, as well as regression coefficients, root mean squared differences (RMSDs), and biases.

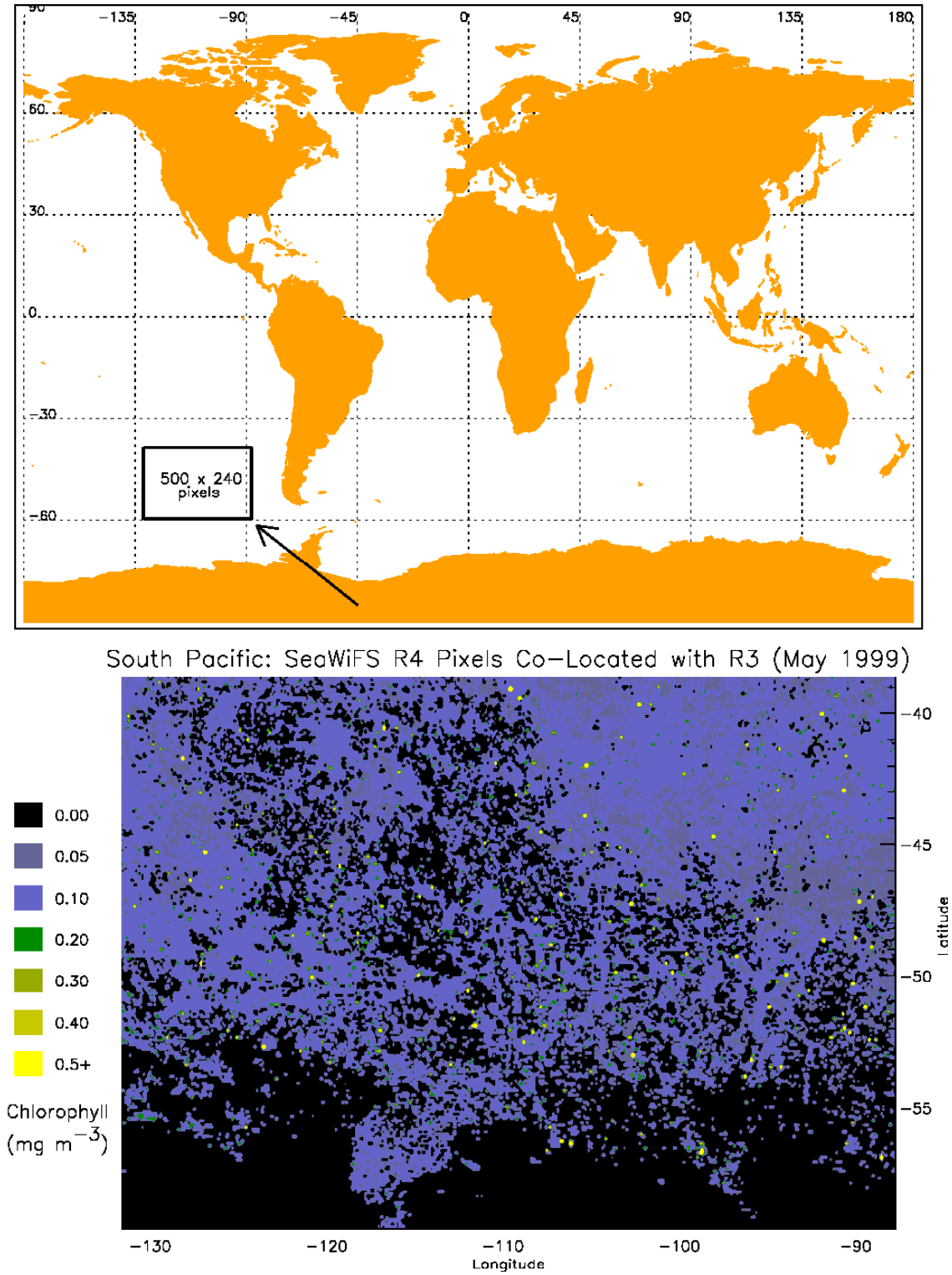

Figure 6. 4: (Top) Global map showing the location of the South Pacific region between -131.6 and -87.8 degrees longitude and -59.6 and -38.6 degrees latitude (500 x 240 pixels). (Bottom) Contour plot of the monthly SeaWiFS R4 chlorophyll values (mg m-3) which have a co-located R3 value for the South Pacific region in May 1999.

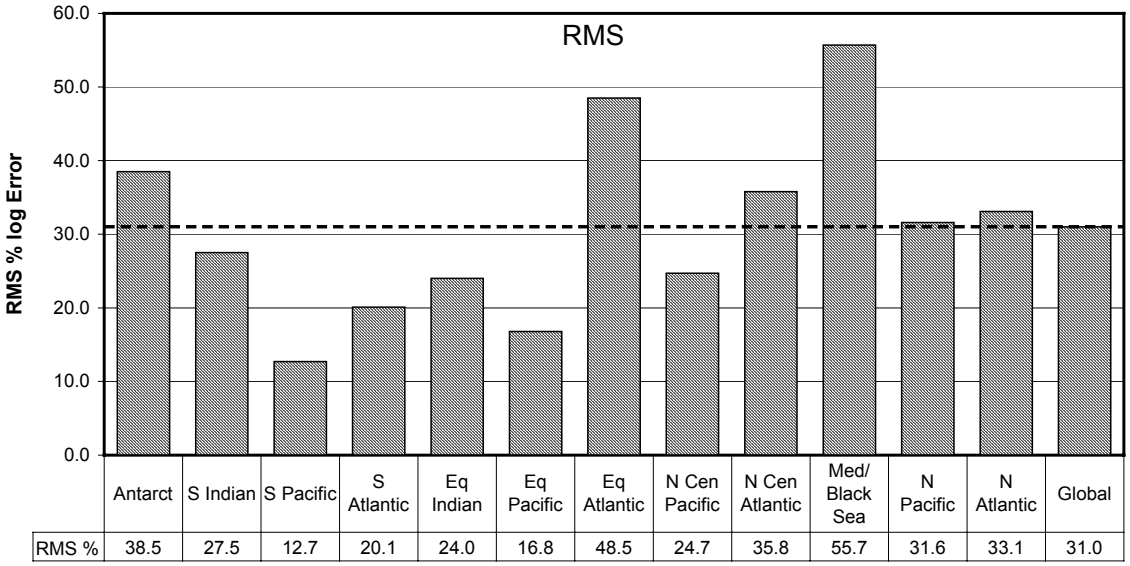

	Antarct	S Indian	S Pacific	S Atlantic	Eq Indian	Eq Pacific	Eq Atlantic	N Cen Pacific	N Cen Atlantic	Med/ Black Sea	N Pacific	N Atlantic	Global
RMS %	38.5	27.5	12.7	20.1	24.0	16.8	48.5	24.7	35.8	55.7	31.6	33.1	31.0

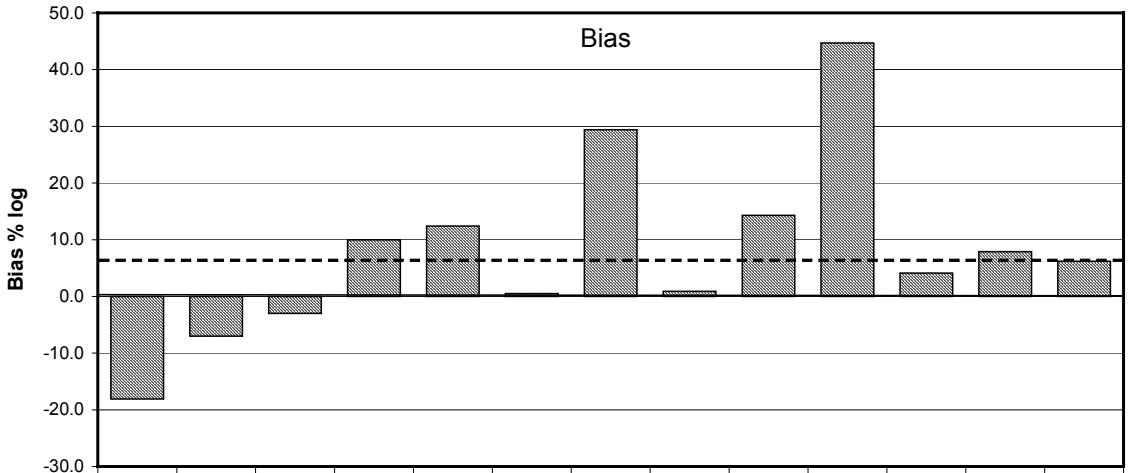

	Antarct	S Indian	S Pacific	S Atlantic	Eq Indian	Eq Pacific	Eq Atlantic	N Cen Pacific	N Cen Atlantic	Med/ Black Sea	N Pacific	N Atlantic	Global
Bias %	-18.1	-7.0	-3.0	10.0	12.4	0.5	29.4	0.9	14.3	44.7	4.1	7.9	6.2

Figure 6.5: Top: RMS error between in situ data and the SeaWiFS chlorophyll data set, separated into the 13 major oceanographic basins, and global. Bottom: average error or bias. Dashed lines indicate the global mean.

Global and Regional MODIS Chlorophyll Data Evaluation

The same methodology for evaluation of SeaWiFS was used to evaluate MODIS chlorophyll data. Only validated data from Collection 4 were used, spanning the period Nov. 2000 through Mar. 2002. In situ data were exclusively from the SeaBASS archive, as no NODC data were available.

There are 3 different bio-optical algorithms for chlorophyll from MODIS. Two (Chlor-MODIS and Chlor-a-2) are empirical expressions, while the third (Chlor-a-3) is a semi-analytic algorithm. Chlor-a-2 is the algorithm most similar to the SeaWiFS bio-optical algorithm.

All three bio-optical algorithms from MODIS produced log RMS error compared to in situ data comparable with SeaWiFS over the same time period (Figure 6.6). There were minor differences among the evaluations regionally as well. The North Atlantic basin was an exception, where the MODIS Chlor-MODIS and Chlor-a-2 algorithms performed much worse than SeaWiFS and the MODIS Chlor-a-3 algorithm. Overall these results suggest compatibility of the two chlorophyll data sets and supports initial merging analyses.

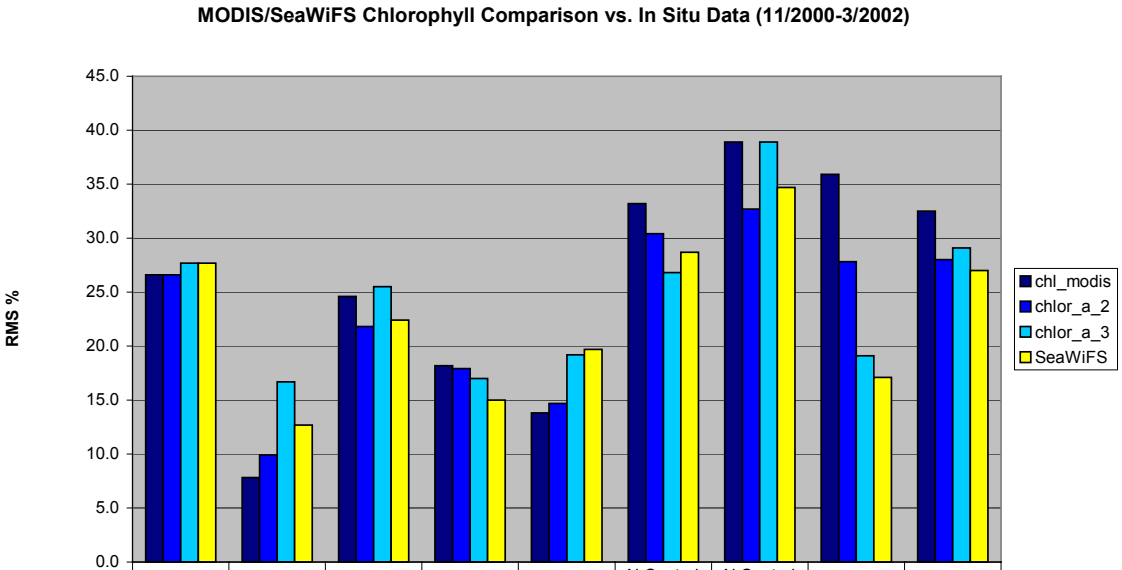

	Antarctic (n=40)	S Pacific (n=3)	S Atlantic (n=25)	Eq Pacific (n=100)	Eq Atlantic (n=10)	N Central Pacific (n=175)	N Central Atlantic (n=175)	N Atlantic (n=60)	Global (n=600)
chl_modis	26.6	7.8	24.6	18.2	13.8	33.2	38.9	35.9	32.5
chlor_a_2	26.6	9.9	21.8	17.9	14.7	30.4	32.7	27.8	28.0
chlor_a_3	27.7	16.7	25.5	17.0	19.2	26.8	38.9	19.1	29.1
SeaWiFS	27.7	12.7	22.4	15.0	19.7	28.7	34.7	17.1	27.0

Gregg and Casey, GSFC 04/03/03

Figure 6.6: Comparison of MODIS chlorophyll algorithms with SaeBASS in situ data globally and by region. SeaWiFS chlorophyll comparisons for the same time period are also shown.

Analyses of Decadal Changes in Ocean Primary Production

Although tangential to the main focus of our proposed effort, the SIMBIOS grant supported our work on analysis of decadal changes in global ocean primary production by providing in situ chlorophyll from the SeaBASS data set for blending and reduction of residual errors in the SeaWiFS data set. In this analysis, we found that satellite-in situ blended ocean chlorophyll records indicate that global ocean annual primary production has declined more than 6% since the early 1980's (Figure 6.7). Nearly 70% of the global decadal decline occurred in the high latitudes. In the northern high latitudes, these reductions in primary production corresponded with increases in sea surface temperature and decreases in atmospheric iron deposition to the oceans. In the Antarctic, the reductions were accompanied by increased wind stress. Three of four low latitude basins exhibited decadal increases in annual primary production. These results indicate that ocean photosynthetic uptake of carbon may be changing as a result of climatic changes and suggest major implications for the global carbon cycle. These results were published in Geophysical Research Letters (Gregg et al., 2003).

6.4 RECOMMENDATIONS

Comparisons between MODIS and in situ data from the SeaBASS archives for the period Nov. 2000 through Mar. 2002 indicated no significant difference from similar comparisons of SeaWiFS for the same time

period. This period is referred to as the validated MODIS time period. We therefore recommend the averaging methodology for merging MODIS and SeaWiFS chlorophyll. For time periods following the validated period, we have no knowledge of biases between the data sets, and also recommend the averaging methodology, which is the correct choice for these conditions.

For time periods preceding the MODIS validated period, biases are known to be present, and they vary in time and space. This averaging is not the proper choice for merging. However, the biases have not been fully characterized. Nevertheless, application of the blended analysis and statistical interpolation are appropriate for this time period. They both suffer from drawbacks, however, that limits their effective application. The blended analysis is subject to over-correction and produces artificially elevated chlorophyll values in places. The statistical interpolation, produces a more reasonable final merged analysis field, but is so computationally expensive as to limit its use. Further analysis is required to modify both methods prior to their implementation for satellite data merging, but both show promising results in the case where biases are known. In these circumstances one or both of these methods are superior to averaging because of the correction aspect of the methods. Averaging in the case of known biases results in degradation of the merged data set and is not recommended. If biases in the satellite data sets cannot be removed in later reprocessing, then additional effort should be expended on blending and statistical interpolation to correct for these errors in data merging.

The SeaBASS chlorophyll data set has been an invaluable resource for evaluating data merging methodologies and it or a similar data set are required for further efforts. It has also been essential in analysis of long-term trends of global satellite chlorophyll as indicated by the identification of a 6% decline in global primary production, a finding that would not have been possible without the use of SeaBASS chlorophyll data for blending with SeaWiFS to reduce residual errors in the satellite data set. It is essential to continue this effort, or something similar, to improve data merger methodologies and to further our understanding of satellite chlorophyll trends.

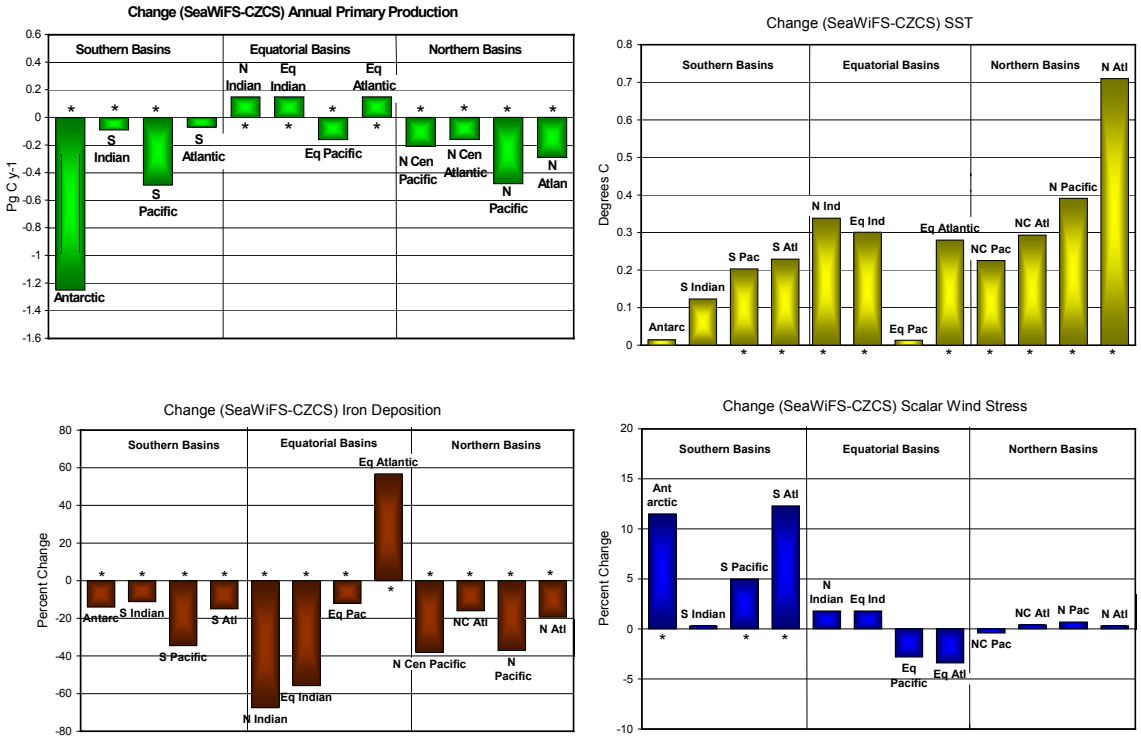

Figure 6.7: Differences between SeaWiFS (1997-2002) and CZCS (1979-1986) in the 12 major oceanographic basins. Differences are expressed as SeaWiFS-CZCS. Top left: Annual primary production (Pg C y-1). An asterisk indicates the difference is statistically significant at $P < 0.05$. Top right: SST (degrees C). Bottom left: iron deposition (%). Bottom right: mean scalar wind stress (%).

REFERENCES

Casey, N.W. and W.W. Gregg, 2003: Comparing Seawifs Reprocessing Versions (R3 vs. R4). *NASA Technical Memorandum 2003-212235*. 20 pp.

Daley, R., 1991: Atmospheric Data Analysis, Cambridge Univ. Press, Cambridge. 457 pp.

Doney, S.C., R.M. Najjar, and S.E. Stewart, 1995: Photochemistry, Mixing, and Diurnal Cycles in the Upper Ocean. *J. Mar. Res*. **53**, 341-369.

Eppley, R.W., 1972. Temperature And Phytoplankton Growth In The Sea. *Fish. Bull*., 70, 1063-1085.

Gregg, W.W. and N.W. Casey, 2003: Global And Regional Evaluation Of The Seawifs Chlorophyll Data Set. *Remote Sensing of Environment*, submitted.

Gregg, W.W., M.E. Conkright, P. Ginoux, J.E. O'Reilly, and N.W. Casey, 2003: Ocean Primary Production And Climate: Global Decadal Changes. *Geophysical Research Letters,* **30** (15) 1809, doi: 10.1029/2003GL016889.

Oort, A.H., 1983: Global Atmospheric Circulation Statistics, 1958-1973, NOAA Prof. Paper 14, 180 pp.

Reynolds, R.W., 1988: A Real-Time Global Sea Surface Temperature Analysis. *J. Clim*., **1**,75-86.

Reynolds, R.W. and T.M. Smith, 1994: Improved Global Sea Surface Temperature Analyses Using Optimum Interpolation. *J. Clim.,* **7**, 75-86.

Chapter 7

Bio-Optical and Remote Sensing Observations in Chesapeake Bay

Lawrence W. Harding Jr. and Andrea Magnuson
University of Maryland Center for Environmental Science, Cambridge, Maryland

7.1 INTRODUCTION

The high temporal and spatial resolution of satellite ocean color observations will prove invaluable for monitoring the health of coastal ecosystems where physical and biological variability demands sampling scales beyond that possible by ship. However, ocean color remote sensing of Case 2 waters is a challenging undertaking due to the optical complexity of the water. The focus of this SIMBIOS support has been to provide in situ optical measurements from Chesapeake Bay (CB) and adjacent mid-Atlantic bight (MAB) waters for use in algorithm development and validation efforts to improve the satellite retrieval of chlorophyll (chl *a*) in Case 2 waters. CB provides a valuable site for validation of data from ocean color sensors for a number of reasons. First, the physical dimensions of the Bay (> 6,500 km^2) make retrievals from satellites with a spatial resolution of ~1 km (i.e., SeaWiFS) or less (i.e., MODIS) reasonable for most of the ecosystem. Second, CB is highly influenced by freshwater flow from major rivers, making it a classic Case 2 water body with significant concentrations of chlorophyll, particulates and chromophoric dissolved organic matter (CDOM) that highly impact the shape of reflectance spectra. Finally, past and ongoing research efforts provided an extensive data set of optical observations that support the goal of this project. Our SIMBIOS contribution has the following objectives:

- To provide to SeaBASS an on-going stream of *in-situ* optical measurements from CB/MAB for use by the ocean color community in the development and validation of atmospheric correction and ocean bio-optical models;
- To evaluate the performance of SeaWiFS bio-optical algorithms in CB/MAB;
- To evaluate the performance of SeaWiFS L_{WN} and chl a products in CB/MAB on a wide range of time and space scales;
- To utilize our bio-optical database to develop a regionally-tuned algorithm for CB/MAB;
- To produce accurate satellite chl a fields that can be used in existing primary productivity models (Harding *et al*., 2002) to improve the spatial and temporal resolution of primary productivity estimates for CB/MAB.

7.2 RESEARCH ACTIVITIES

Field Program

Throughout our SIMBIOS support we have maintained a seasonal (i.e., spring, summer, fall) sampling schedule in CB proper that started in 1995 with the NSF Land-Margin Ecosystem Research (LMER) program Trophic Interactions in Estuarine Systems (TIES) cruises (1995-2000) and continued with the NSF Biocomplexity cruises (2001-2003). In addition, five separately funded Office of Naval Research (ONR) cruises were conducted in adjacent offshore waters including coverage to the Gulf Stream. All cruises collected the same suite of measurements. Vertical profiles of downwelling irradiance (E_d) and upwelling radiance (L_u) were preformed with a Biospherical Instruments MER 2040/2041. Discrete samples of particulate and dissolved fractions were collected for determination of absorption spectra of phytoplankton, $a_{ph}(\lambda)$, non-pigmented particulates, $a_d(\lambda)$, and colored dissolved material, $a_{CDOM}(\lambda)$. Discrete particulate

samples were collected for pigment analyses of chl *a* by fluorometry and a suite of pigments by HPLC. Radiometric profiles were used to calculate attenuation coefficients for downwelling irradiance (K_d) and upwelling radiance (K_u), and surface values of E_d and Lu (E_d0^- and L_u0^-, respectively) by simple linear regression. Instrument self-shading corrections were applied to each L_u0^- according to Gordon and Ding (1992).

In 2001 we expanded our sampling protocol to include two new radiometric instruments, the Satlantic MicroPro free-fall radiometer and the Satlantic Hyperspectral Tethered Spectral Radiometer Buoy (Hyper-TSRB). The MicroPro is designed for work in more turbid waters with a small sensor cross-section, and is sufficiently compact to allow deployment from small boats. The Hyper-TSRB measures surface E_d and L_u with a 120-channel detector from 400 to 800 nm. On each cruise in CB, sequential radiometric profiles were made with the MER (typically one cast) and MicroPro (2 to 5 casts). All casts were completed within ~5 to 8 minutes, depending on the number of MicroPro casts that were made. The TSRB was deployed prior to the radiometric profiles and continuously operated while on station. Since 2001 we also have been using a MicroTops sun photometer from the SIMBIOS instrument pool to measure aerosol optical thickness.

In 2002 and 2003 we participated in six EPA/NASA Atlantic Coast Estuaries Indicators Consortium (ACE INC) cruises that sampled two tributaries of CB, the Patuxent and Choptank Rivers. ACE INC cruises collected the same suite of measurements as the LMER-TIES and Biocomplexity cruises, with the exception that radiometric profiles of E_d and L_u were limited to the MicroPro because of vessel limitations.

We have submitted over 3000 in-situ measurements to SeaBASS, significantly expanding bio-optical data for Case 2 waters (Table 7.1). Data from summer and fall cruises of 2003 will be submitted prior to the end of this contract. We also participated in the CHORS/Horn Point Laboratory HPLC Round Robin. We worked together with Jason Perl to identify and minimize methodological and instrument differences between laboratories such that an internally consistent pigment database could be created.

Algorithm Evaluation/Development

We have evaluated the performance of the empirical algorithm OC4v.4 (O'Reilly *et al*., 1998) and the semi-analytical Garver-Siegel-Maritorena (GSM01) model (Maritorena et al., 2002) for the CB/MAB, using bio-optical data collected during from SIMBIOS. This entailed using regional bio-optical data as input parameters to GSM01, specifically the chl *a*-normalized absorption, $a_{ph}^*(\lambda)$, and spectral slope of the combined absorption of dissolved and non-pigmented particulate matter, S_{cdm}, to produce a regionally tuned version of the model that we termed GSM01-CB. We subsequently modified the native GSM01 parameters in the SeaWiFS Data Analysis System (SeaDAS) code to evaluate the performance of the GSM01-CB using satellite-derived radiances as input.

SeaWiFS Image Analysis

We have continued acquisition and analysis of SeaWiFS ocean color imagery from the Goddard Distributed Active Archive Center (DAAC) for CB/MAB. Approximately 100 clear images are available each year fro 1998-present. We have used in-situ data to validate SeaWiFS performance in match-up analyses and comparisons with continuous underway measurements. A three-year times series (1998-2000) has been used to determine the extent to which SeaWiFS resolves seasonal and interannual variability of chl *a* evident in the *in-situ* data.

7.3 RESEARCH RESULTS

Radiometric Comparisons

Expansion of our radiometric measurement suite allowed us to evaluate performance of each profiling instrument in nearly simultaneous (i.e., within minutes) deployments. The MicroPro is more suitable for work in Case 2 waters than the MER due to: (1) smaller diameter (MicroPro 4.8 cm relative to the MER 21 cm) that reduces instrument self-shading; (2) higher sampling frequency that gives greater depth resolution in waters where K_d is high and slight changes in the depth of the sensor have a larger effect on the measurements. The MicroPro exhibited clear advantages in waters with higher K_d. The improved depth

Table 7.1: Status of the Chesapeake Bay data set submitted to SeaBASS. Numbers for 2003 are estimated based on cruises yet to be completed.

Direct Measurements									
Direct Measurements	Derived Products	1996	1997	1998	1999	2000	2001	2002	2003
MER *									
$E_d(z,\lambda)$ $L_u(z,\lambda)$ $E_s(0^+,\lambda)$	$R_{RS}(0^+,\lambda)$ $K_d(m,\lambda)$ $K_u(m,\lambda)$	82	93	83	44	40	25	39	25
MicroPro **									
$E_d(z,\lambda)$ $L_u(z,\lambda)$ $E_s(0^+,\lambda)$	$R_{RS}(0^+,\lambda)$ $K_d(m,\lambda)$ $K_u(m,\lambda)$	---	---	---	---	---	49	130	90
$a_p(0,\lambda)$, $a_d(\lambda)$	$a_{ph}(\lambda)$	79	32	130	66	46	27	32	25
$a_{CDOM}(0,\lambda)$		79	32	130	66	46	27	32	25
Chl *a* (z)		323	709	591	514	330	189	182	60
Pigments (z)		143	95	104	63	56	49	32	20
$T(z)$, $S(z)$		---	30	55	49	43	26	31	20
MicroTops		---	---	---	---	---	---	24	15

* MER wavebands 412, 443, 455, 490, 510, 532, 550, 650, 589, 625, 671, 683, 700
**MicroPro wavebands 400, 412, 443, 455, 490, 510, 532, 555, 565, 590, 625, 670, 684, 700.

$E_d(z,\lambda)$	Downwelling irradiance depth profiles
$L_u(z,\lambda)$	Upwelling radiance depth profiles
$E_s(0^+,\lambda)$	Incident irradiance
$a_p(z,\lambda)$	Total particulate absorption (300-900 nm) of discrete samples by QFT
$a_d(z,\lambda)$	Non-pigmented particulate absorption (300-900 nm) of discrete samples by QFT with MeOH extraction
$a_{cdom}(z,\lambda)$	Colored dissolved absorption (190-820 nm) of discrete samples
Chl a (z)	Determination of chl *a* for discrete samples by Turner fluorometry
pigments (z)	HPLC analysis for a suite of pigments
$T(z)$, $S(z)$	SeaBird temperature and conductivity profiles

Derived Products	
$R_{RS}(0^+,\lambda)$	Remote sensing reflectance from calculated from radiance/irradiance profiles
$K_d(m,\lambda)$, $K_u(m,\lambda)$	Attenuation coefficients for $E_d(z,\lambda)$ and $L_u(z,\lambda)$ for the surface mixed layer, calculated from radiance/irradiance profiles
$a_{ph}(z,\lambda)$	Pigmented particulate absorption (300-900 nm), calculated as $a_p(0,\lambda)$-$a_d(0,\lambda)$

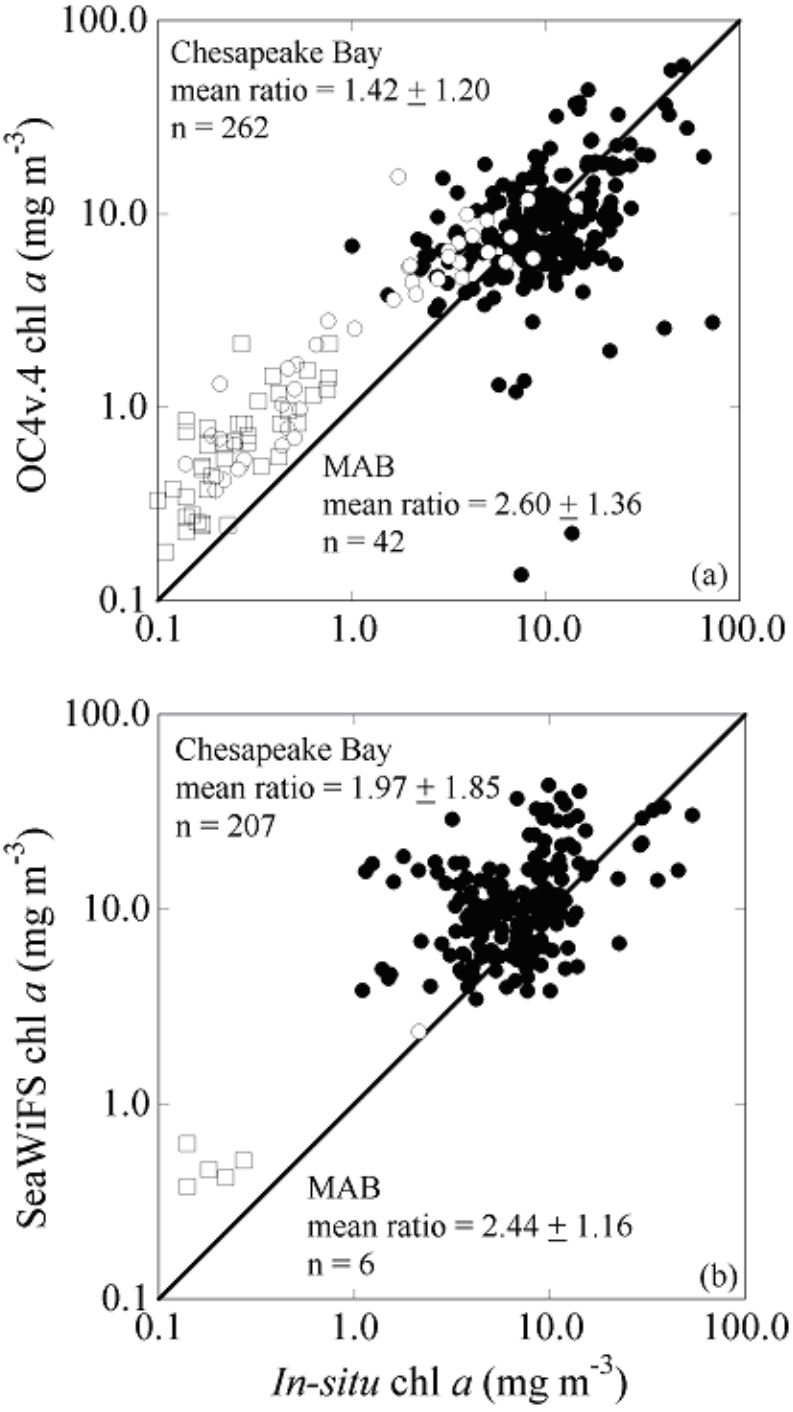

Figure 7.1: Comparisons of in-situ chl a to: (a) mean chl *a* estimated from OC4v.4 applied in-situ RRS; (b) SeaWiFS retrievals of chl *a*. SeaWiFS values represent the mean of a 3x3 pixel box centered on the station location for *in-situ* sampling. A chl *a* match-up was considered valid if the satellite observation and *in-situ* measurement occurred on the same day, and half (5 out of 9) pixels in a box centered on the latitude and longitude of the sampling station returned valid estimates. The original match-up dataset contained over 1400 chl *a* observations. Mean ratio = SeaWiFS chl *a* / *in-situ* chl *a*.

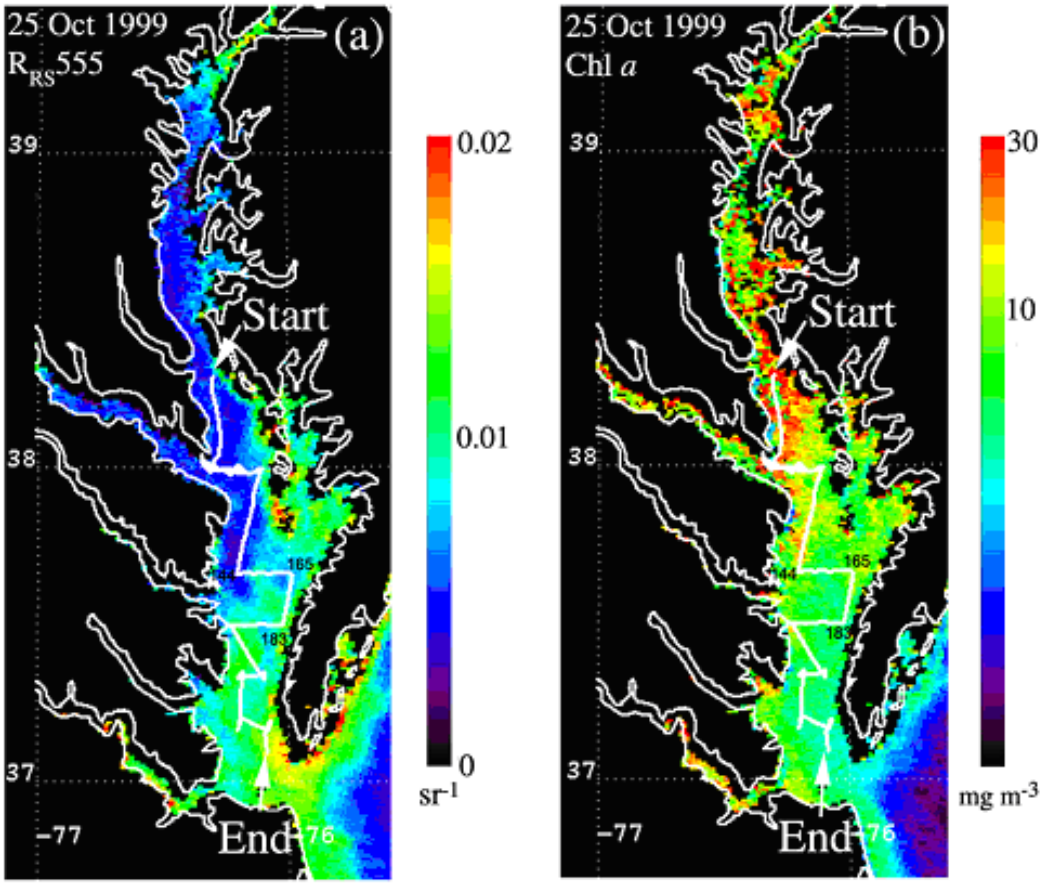

Figure 7.2: RRS555 and chl *a* from SeaWiFS for a CB scene, 15 October 1999. The white lines superimposed on these images give the ship track for concurrent measurements that included bio-optical measurements. Vertical line at ~ 150 km marks the time of the satellite pass.

resolution of the MicroPro (~25 measurements per meter) compared to the MER (~10 measurements per meter) compensated for the shallow optical depths in CB where the depth range available for the extrapolation interval was limited to the upper 4 m (or less). Measurements of E_d0^+ from the MicroPro were much easier to reconcile with surface irradiance measurements (E_s) than were those from the MER, which exhibited an increasing bias as K_d increased. Measurements of L_u0^- from the MER and MicroPro also showed increased disagreement as K_d increased. Based on advantages of the MicroPro over the MER in comparisons of E_d0^+ and E_s, we feel confident that the MicroPro measurements of L_u0^- are more accurate than the MER for the Case 2 waters in which we work. Lastly, the increased depth resolution of the MicroPro reduced the effects of small changes in the selection of the depth interval on the calculated K_d, K_u, E_d0^-, and L_u0^-. The MicroPro also allowed us to expand our radiometric sampling to more turbid waters of the tributaries, and has improved measurement capabilities in the upper reaches of CB. In addition, these comparisons of the MER and MicroPro indicated strong agreement in the clearer waters of the mesohaline and polyhaline CB, confirming confidence in our multi-year time series of radiometric measurements with the MER in the CB/MAB.

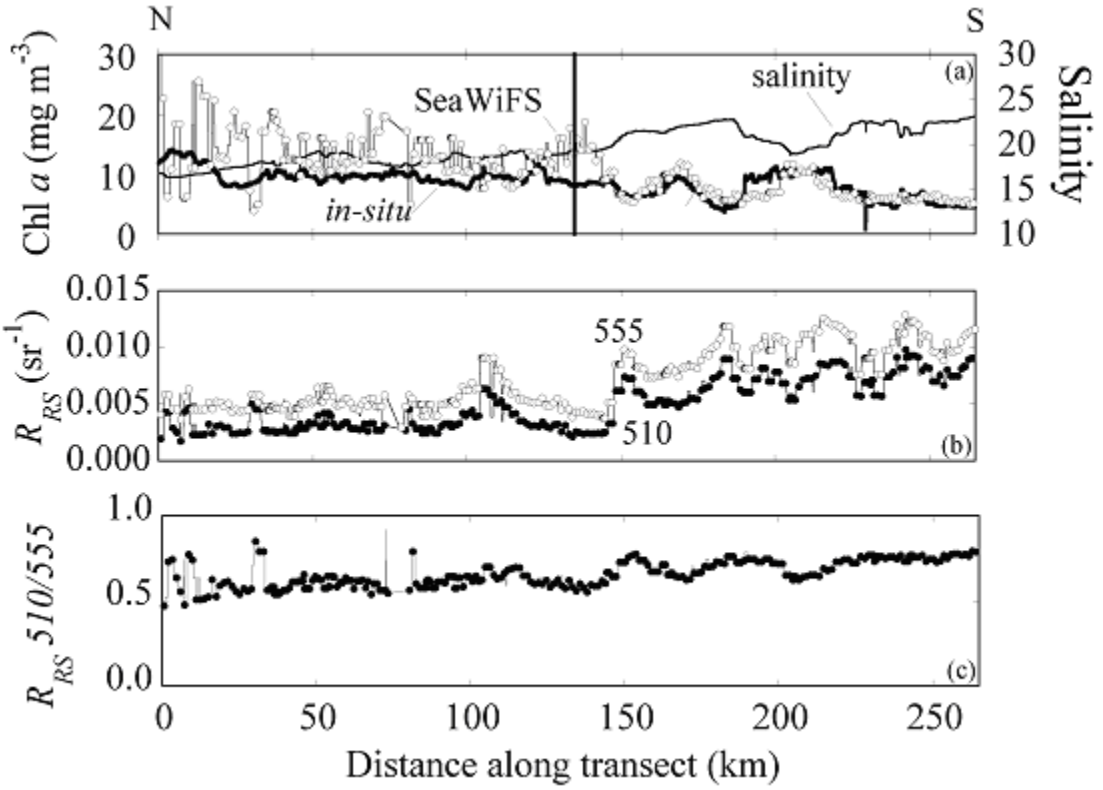

Figure 7.3: (a) Comparison of *in-situ* and SeaWiFS chl *a*; (b) SeaWiFS RRS510 and RRS555; (c) ratio of SeaWiFS RRS 510/555 along a ship track in the mesohaline to polyhaline CB.

Characterization of Bio-optical Properties in Chesapeake Bay

Distributions of inherent optical properties in CB/MAB showed the strong influence of freshwater flow that complicates retrievals of chl a from satellite ocean color measurements. $a_{ph}(440)$, $a_{CDOM}(440)$, $a_d(440)$ ranged from 0.1 to 1.0 m^{-1} in CB, and were an order of magnitude lower in the MAB. Whereas $a_d(440)$ dominated in upper CB, the magnitudes of $a_{ph}(440)$, $a_{CDOM}(440)$, $a_d(440)$ were comparable in the mid- and lower CB and inshore MAB. $a_{CDOM}(440)$ dominated water column absorption in the offshore MAB. The distribution $a_{CDOM}(440)$ was conservative in CB proper, due to its predominant terrestrial origin. $a_{ph}(440)$ and $a_d(440)$ were subject to much higher spatial variability. The distribution of dissolved and particulate materials regulated the magnitude and spectral shape of apparent optical properties such as the attenuation coefficient for downwelling irradiance, K_d, and the remote-sensing reflectance, RRS.

OC4v.4 Algorithm Evaluation

The distribution of inherent optical properties had a pronounced effect on the performance of OC4v.4 in CB/MAB (Fig. 7.1a). OC4v.4 returned chl *a* estimates for CB that had a small positive bias and high uncertainty, reflecting that a_{ph}, a_{CDOM}, ad did not co-vary. A larger positive bias of chl *a* occurred in the MAB where too much of the total absorption was attributed to phytoplankton. Match-ups of SeaWiFS chl *a* with *in-situ* data showed a larger positive bias in CB than observed for OC4v.4 applied to *in-situ* radiometric data, suggesting SeaWiFS-derived radiances introduced additional errors (Fig. 7.1b). Whereas the fourth SeaWiFS reprocessing lessened the frequency of negative LWN, comparisons of *in-situ* and satellite-derived LWN as part of this work and others have shown that low and negative LWN from SeaWiFS remain a problem in coastal and estuarine waters (Harding et al., 2003; O'Reilly and Yoder, 2003). SeaWiFS LWN at 'blue' wavebands are low in CB, causing the return of higher-than-observed chl *a*

values by OC4v.4. The lack of increased bias in chl *a* for match-ups from the MAB suggested errors in SeaWiFS chl *a* could be attributed primarily to OC4v.4 rather than errors in atmospheric correction.

Resolution of Interannual, Seasonal and Event-scale Variability by SeaWiFS

High uncertainties we detected in match-up analyses of *in-situ* and SeaWiFS chl *a* restricted the usefulness of SeaWiFS data for CB/MAB, stimulating additional analyses to lessen time-space aliasing we believed was responsible. High frequency and small-scale variability of biomass typical of estuaries virtually assures time-space aliasing of satellite observations and *in-situ* measurements. To minimize aliasing, we compared continuous shipboard measurements of chl *a* were to SeaWiFS chl *a.* along ship tracks to evaluate the extent to which SeaWiFS resolved variability on small spatial scales. We found SeaWiFS accurately captured small-scale (tens-of-kilometers) variability in the mesohaline and polyhaline regions of CB (Figs. 7.2 and 7.3) (see Harding et al., 2003). Increased noise in chl *a* with distance north corresponded to sharp gradients of RRS. We suspect that the magnitude of the RRS signal often approaches the limits of sensitivity for the SeaWiFS sensor in turbid waters with high K_d typical of mesohaline and oligohaline CB, thereby limiting the accuracy of chl *a* retrievals. This gradient of RRS was persistent in the imagery and was suggested in field radiometric measurements. Comparisons of several transects suggested axial movement of this gradient of RRS could determine the areal extent of accurate chl a retrievals.

Our evaluation of the 1998 – 2000 SeaWiFS chl *a* time series demonstrated that SeaWiFS accurately represented seasonal and interannual variability of chl *a* revealed by *in-situ* data (Fig. 7.4). Previous research has shown that the timing, position, and magnitude of the spring bloom are regulated by freshwater flow from the Susquehanna River, supplying nutrients and suspended matter to CB (Malone *et al*., 1988; Harding, 1994). We found that positive deviations of flow in 1998 resulted in a large spring bloom that extended to the polyhaline CB, shown in both satellite imagery and *in-situ* data. Measurements of chl *a* in 1999, a year of lower-than-average freshwater flow, showed a smaller bloom that was confined primarily to the mesohaline CB. Lastly, average freshwater flow in 2000 supported a bloom of intermediate magnitude that extended throughout the mesohaline and part of the polyhaline CB. As observed in transect data, the agreement of SeaWiFS and *in-situ* chl *a* improved with distance down the Bay. These comparisons with *in-situ* data confirm that SeaWiFS chl *a* retrievals are reasonable and can significantly augment the temporal resolution of shipboard measurements.

The benefit of increased temporal resolution afforded by satellite observations was demonstrated in the three-year time series of chl *a* (Fig. 7.5). Mean, daily chl *a* for a section of polyhaline CB indicated several doublings over a period of days in summer that were not captured by *in-situ* observations. We hypothesize that these doublings could be associated with short-lived, but dense blooms of dinoflagellates that have been observed before during stratified conditions in summer. The sedimentation of organic matter from the spring bloom fuels at least 50% of the primary productivity in surface waters (Kemp and Boynton, 1984). Transient destratification of the summer pycnocline provides the nutrients to support these short-lived summer blooms (Malone *et al*., 1986, 1988). The higher frequency of these events in 1998 and 2000, contrasted with 1999, may indicate a connection between these transient blooms in summer and the magnitude of the spring bloom. Further study is needed to test this hypothesis.

Regional Parameterization of GSM01

Semi-analytical models such as GSM01 have the potential to distinguish multiple constituents of the water column that absorb and scatter light. This attribute is crucial for accurate retrievals of chl *a* in optically-complex waters. The original parameterization of GSM01 was based on in-situ observations from Case 1 waters and optimized for performance in the global ocean (Maritorena et al., 2002). We hypothesized that regional parameterization was necessary to improve the accuracy of chl a retrievals in CB/MAB.

We evaluated our extensive data set of *in-situ* observations to derive regionally and seasonally (when appropriate) values for $a_{ph}^*(\lambda)$ and Scdm to produce a regional version of the model, GSM01-CB (Table 7.2) (see Magnuson et al., 2003). Regional differences of $a_{ph}^*(\lambda)$ were significant across the study area from the upper, oligohaline CB to the offshore MAB. $a_{ph}^*(\lambda)$ increased with distance offshore. This trend of increasing $a_{ph}^*(\lambda)$ can be explained by two factors: decreases of pigment packaging and increases in concentrations of accessory pigments (Yentsch and Phinney, 1989; Bricaud *et al*., 1995).

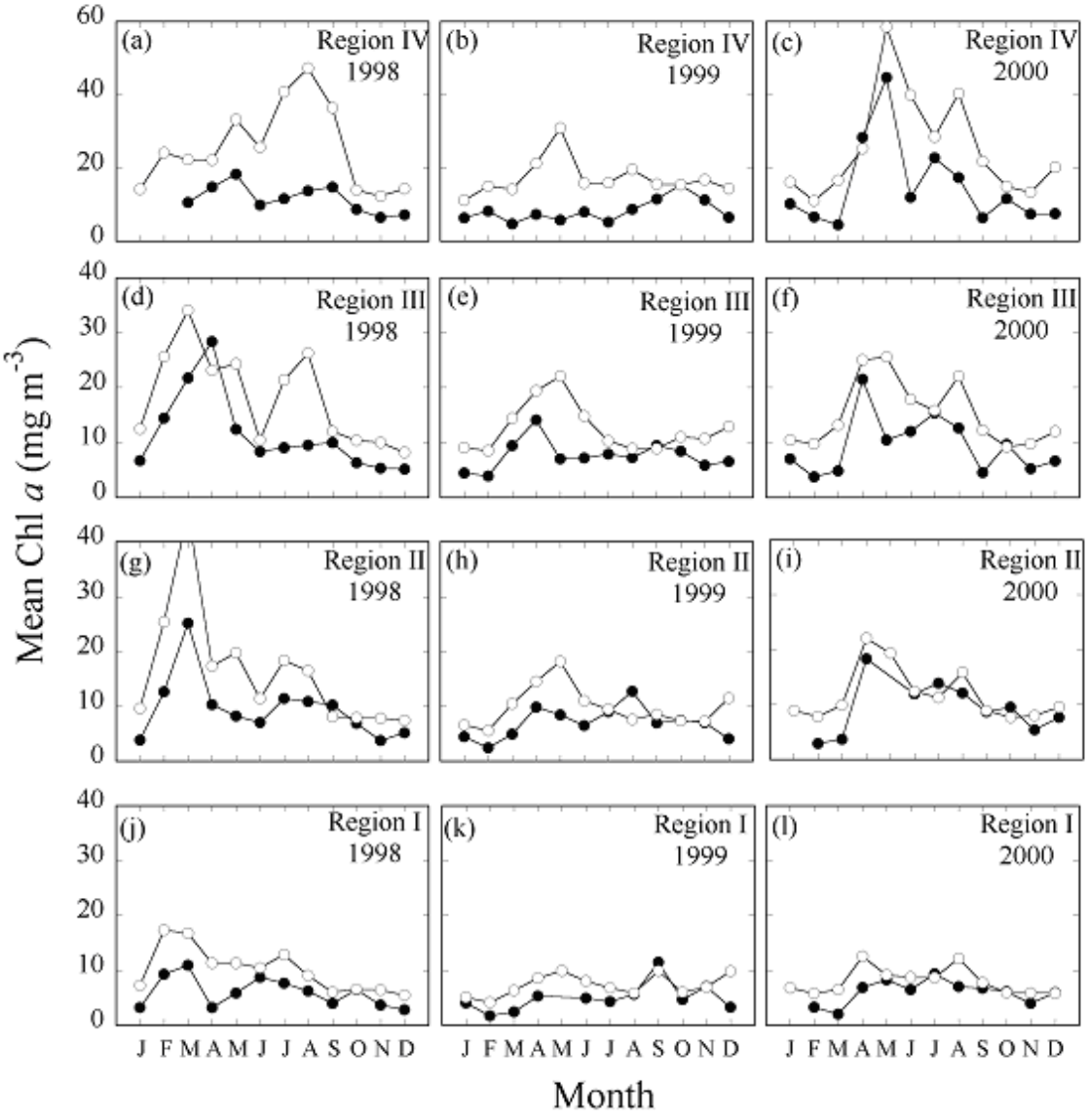

Figure 7.4: Monthly mean chl *a* for the polyhaline (I, II, south of 37.8°N) and mesohaline (III, IV, 37.8 – 38.8°N) regions of CB from in situ (closed symbols) and SeaWiFS (open symbols) data for 1998-2000.

We also found significant seasonal differences in mean $a_{ph}^*(\lambda)$ in CB that we attributed primarily to changes in floral composition and associated changes in pigment packaging. Highest $a_{ph}^*(\lambda)$ occurred in spring when phytoplankton in CB consist primarily of large cells (i.e., centric diatoms) (Malone *et al*., 1988; Marshall and Nesius, 1996). Lowest $a_{ph}^*(\lambda)$ occurred in summer when phytoplankton consist of a more diverse flora of smaller, flagellated cells (Malone *et al*., 1991; Marshall and Nesius, 1996). Scdm exhibited an increasing trend with distance offshore, reflecting the decrease in the influence of terrigenous CDOM (Blough *et al*., 1993; Nelson and Guarda, 1995; Vodecek *et al*., 1997). Small, but significant differences in S_{cdm} along the axis of CB reflected changes in the relative contributions of a_{CDOM} and ad to a_{cdm}.

Evaluation of chl *a* from OC4v.4, GSM01, and GSM01-CB for CB, inshore MAB, and offshore MAB showed that GSM01-CB improved upon OC4v.4 in all regions (Table 7.3).

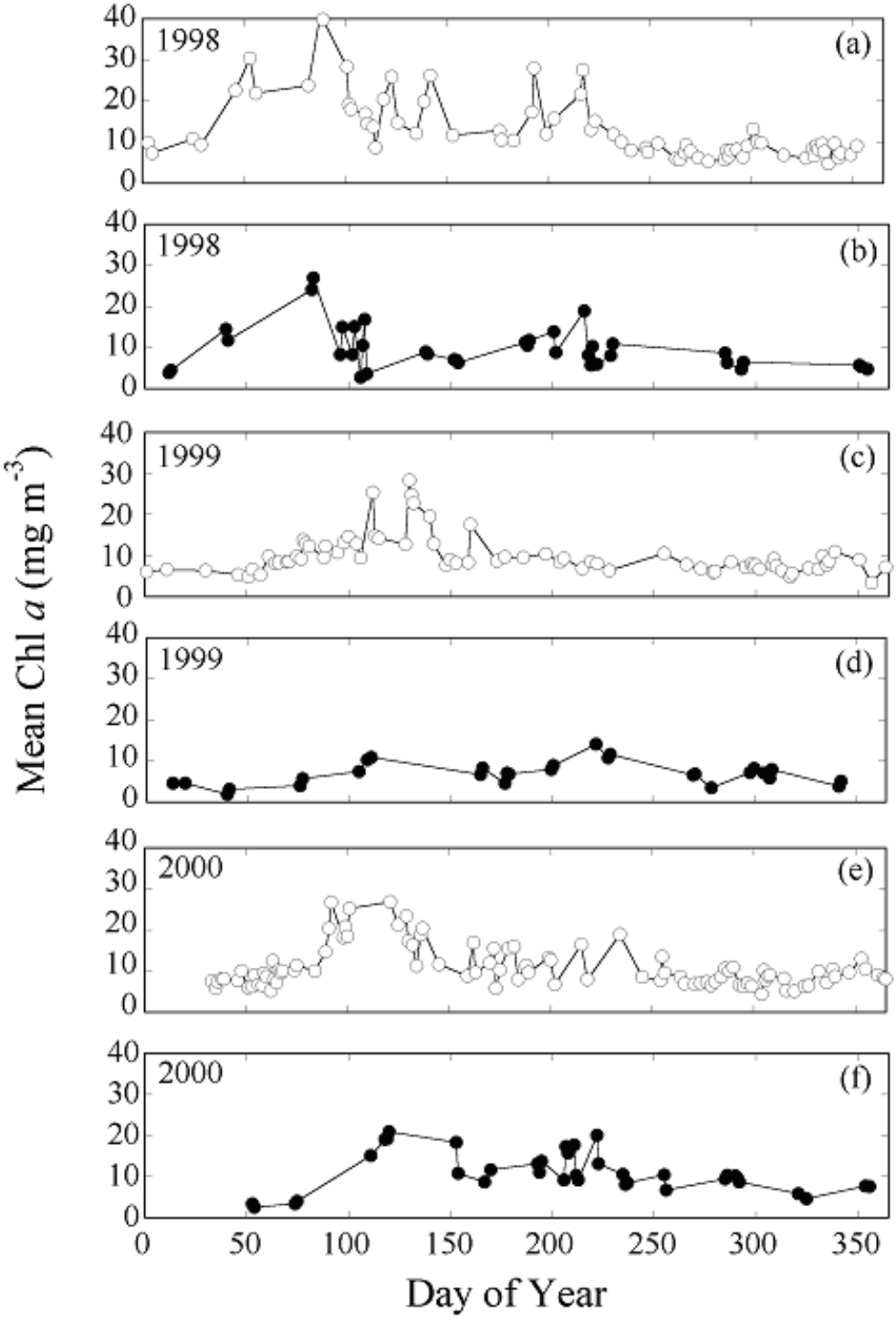

Figure 7.5: Time-series of mean, daily SeaWiFS (open symbols) and *in-situ* (closed symbols) chl *a* for a section of CB from 37.3° to 37.8°N.

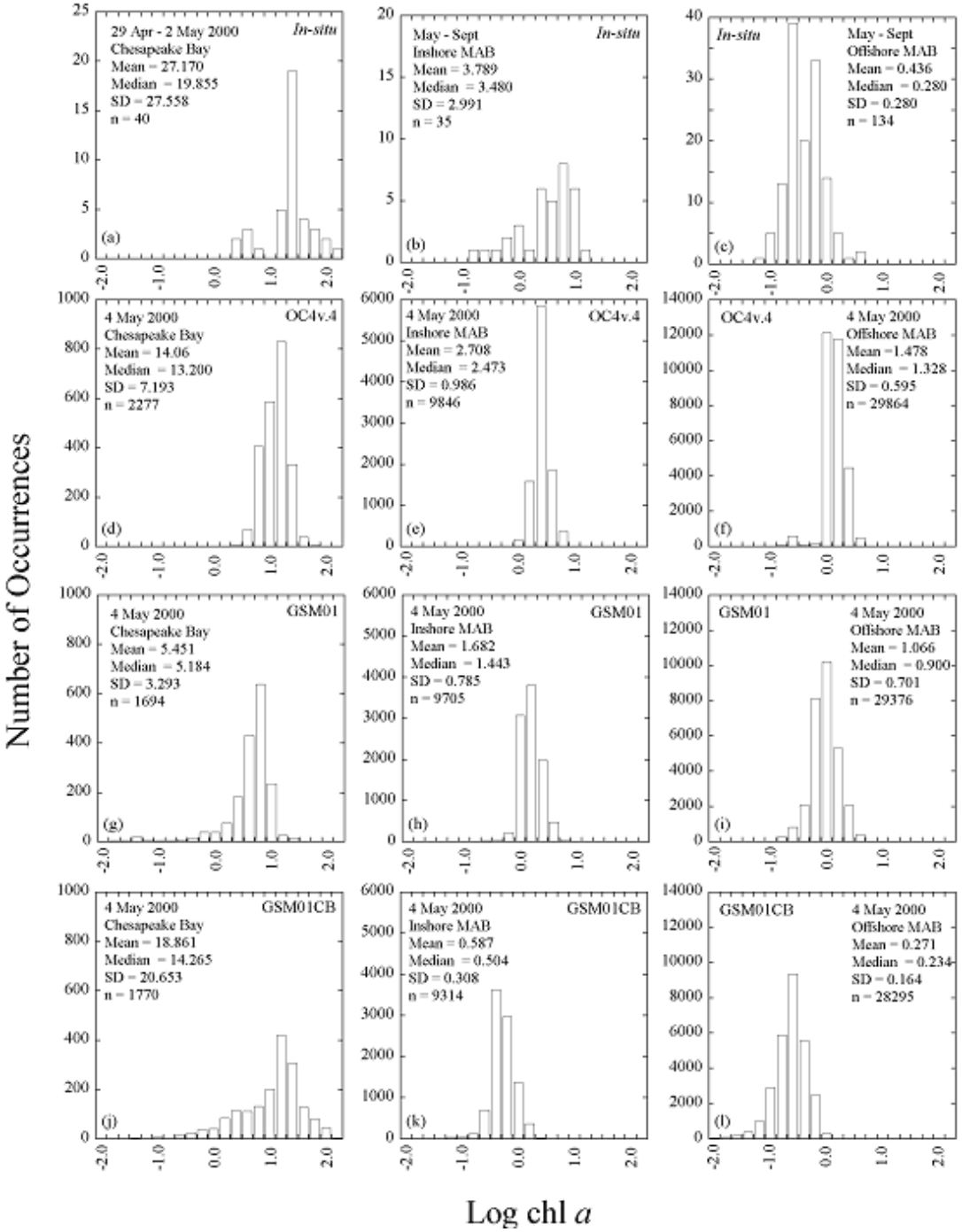

Figure 7.6: Histograms of *in-situ* and SeaWiFS chl *a* observations for CB, inshore and offshore MAB for image from 4 May 2000: (a-c) *in-situ*, (d-f) SeaWiFS OC4v.4, (g-i) SeaWiFS GSM01, and (j-l) SeaWiFS GSM01-CB. *In-situ* data from the MAB were not available for this image. The inshore and offshore MAB histograms (b-c) reflect all field data available for those regions during May-September 1996-1998.

Table 7.2. Parameter values used in GSM01 and GSM01-CB.

Region	Season	$a_{ph}^*(412)$	$a_{ph}^*(443)$	$a_{ph}^*(490)$	$a_{ph}^*(510)$	$a_{ph}^*(555)$	$a_{ph}^*(671)$	S_{cdm}	η
GSM01		0.00665	0.05582	0.02055	0.01910	0.01015	0.01424	0.02061	1.03373
GSM01-CB									
Upper Bay	Spring	0.02119	0.02509	0.01282	0.00910	0.00427	0.02087	0.01218	0
	Summer	0.02653	0.02979	0.01655	0.01208	0.00470	0.02122	0.01218	0
	Fall	0.02259	0.02573	0.01372	0.01019	0.00376	0.02066	0.01218	0
Mid-Bay	Spring	0.02001	0.02212	0.01279	0.00974	0.00449	0.01588	0.01385	0
	Summer	0.03345	0.03900	0.02318	0.01664	0.00609	0.02285	0.01385	0
	Fall	0.02758	0.03080	0.01826	0.01438	0.00691	0.02112	0.01385	0
Lower Bay	Spring	0.02001	0.02212	0.01279	0.00974	0.00449	0.01588	0.01330	0
	Summer	0.03345	0.03900	0.02318	0.01664	0.00609	0.02285	0.01330	0
	Fall	0.02758	0.03080	0.01826	0.01438	0.00691	0.02112	0.01330	0
Inshore		0.07123	0.08843	0.06024	0.04072	0.01693	0.03815	0.01236	0
Offshore		0.11331	0.14678	0.09832	0.06048	0.01920	0.04349	0.01646	1

Table 7.3: Comparison of the mean ratio (±SD) of modeled and measured chl *a* and a_{cdm} (443), and estimated b_{bp} (443) for Chesapeake Bay, inshore MAB, and offshore MAB. Mean ratio = modled/measured

	Chesapeake Bay Chl a	Inshore MAB Chl a	Offshore MAB Chl a
GSMO1	1.99 ± 2.21	1.84 ± 0.92	1.31 ± 0.68
GSM01-BAY	1.10 ± 1.08	0.59 ± 0.57	0.51 ± 0.29
OC4v.4	1.20 ± 0.71	3.12 ± 2.05	2.40 ± 1.03
	Chesapeake Bay a_{cdm} (443)	Inshore MAB a_{cdm} (443)	Offshore MAB a_{cdm} (443)
GSMO1	1.24 ± 0.58	1.01 ± 0.54	0.87 ± 0.61
GSM01-BAY	0.92 ± 0.40	1.12 ± 0.42	0.95 ± 0.67
	Chesapeake Bay b_{bp} (443)	Inshore MAB b_{bp} (443)	Offshore MAB b_{bp} (443)
GSMO1	0.94 ± 0.65	2.28 ± 1.35	1.43 ± 0.88
GSM01-BAY	1.35 ± 0.91	2.88 ± 1.64	1.34 ± 1.26

The local parameterization was essential to improve performance in CB. Both GSM01 and GSM01-CB showed improvement over OC4v.4 in the MAB where they specifically accounted for high absorption due to CDOM. Analysis of SeaWiFS products using each model supported results of evaluations using *in-situ* RRS as inputs, specifically that: (1) one or both of the semi-analytical models performed as well or better than OC4v.4; (2) both semi-analytical models clearly improved upon OC4v.4 in the offshore MAB (Fig. 7.6). Disagreement between the in-situ observations and model estimates for the inshore MAB likely reflect a sampling bias as *in-situ* observations were concentrated near the Chesapeake and Delaware Bay mouths where chl *a* are generally high, whereas mean chl *a* from SeaWiFS represented the entire inshore region.

Disregarding *in-situ* values, both semi-analytical models returned much lower mean chl *a* for the inshore MAB than did OC4v.4, and GSM01-CB chl *a* were lower than GSM01 chl *a*, consistent with results obtained using *in-situ* data as input to the models (Table 7.3). The semi-analytical models return estimates of $a_{cdm}(443)$ and $b_{bp}(443)$ in addition to chl *a*. Estimates of $a_{cdm}(443)$ were closer to *in-situ* values than were estimates of chl *a* (Table 7.3). Meaningful evaluation of the $b_{bp}(443)$ product was not possible due to the lack of direct measurements of scattering. Relatively high uncertainties remained for all models, reflecting the difficulty of working in bio-optically complex waters. It is notable that the performance of GSM01 was surprisingly good, considering the parameterizations differed significantly from bio-optical properties of CB. The relatively strong performance of GSM01 in CB likely reflects the robust tuning procedures used by Maritorena et al. (2002) to derive global parameters for GSM01.

7.4 CONCLUSIONS

It is useful and necessary to assess the performance of satellite products at various stages to recognize limitations, as well as to demonstrate strengths and identify the types of applications for which current products are suitable. We have made use of an extensive database of bio-optical measurements to provide several different evaluations of SeaWiFS performance. We have identified several factors that inhibit the accuracy of the standard chl a product, including: (1) use of an empirical algorithm that does not account for all of the absorbing and scattering components of the water column; (2) atmospheric correction errors in coastal waters resulting in low satellite radiances; (3) RRS signals approaching the lower sensitivity limits of the sensor. Nonetheless, the importance of these factors lessened, and SeaWiFS recoveries improved, with increasing water clarity. We found that in mesohaline and polyhaline CB, SeaWiFS accurately and reliably represented seasonal and interannual variability of biomass, resolved event-scale phenomena that were missed in our field sampling, and resolved small-scale (i.e., tens-of-kilometers) regional variability. We are encouraged by our initial attempts to improve chl *a* estimates by tuning a semi-analytical model for regional conditions. We are exploring modifications to the parameterization that could lessen the use of abrupt transitions in parameter values at seasonal and regional boundaries. Improvements in SeaWiFS radiances also will be necessary for maximal performance of semi-analytical models in Case 2 waters.

REFERENCES

Blough, N.V., O.C. Zafirou, and J. Bonilla, 1993: Optical absorption spectra of waters from the Orinoco River outflow: terrestrial input of colored organic matter to the Caribbean. *Journal of Geophysical Research* **98**, 2,271-2,278.

Bricaud, A., M. Babin, A. Morel, & H. Claustre, 1995: Variability in the chlorophyll-specific absorption coefficients of natural phytoplankton: analysis and parameterization, *Journal of Geophysical Research* 100, **13**,321-13,332.

Gordon, H.R. and K. Ding. 1992. Self-shading of in-water optical instruments. *Limnology and Oceanography.*, **37**, 491-500.

Kemp, W.M., & W.R. Boynton, 1984: Spatial and temporal coupling of nutrient inputs to estuarine primary production: the role of particulate transport and decomposition, *Bulletin of Marine Science* ,**35**, 242-247.

Harding, L.W., Jr., E.C. Itsweire, and W.E. Esaias, 1994: Estimates of phytoplankton biomass in the Chesapeake Bay from aircraft remote sensing of chl-a, 1989-1992, *Remote Sensing of Environment* ,**49**, 41-56.

Harding, L.W., Jr., A. Magnuson, and M.E. Mallonee, 2003: Bio-Optical and Remote Sensing Observations in Chesapeake Bay, *Estuarine, Coastal, and Shelf Science* (in review).

Magnuson, A., L.W. Harding, Jr., M.E. Mallonee, and J.E. Adolf, 2003: Bio-optical modeling in the Middle Atlantic Bight, Estuarine, *Coastal, and Shelf Science* (to be submitted).

Malone, T.C., W.M. Kemp, H.W. Ducklow, W.R. Boynton, J.H. Tuttle, and R.B. Jonas, 1986: Lateral variation in the production and fate of phytoplankton in a partially stratified estuary, *Marine Ecology Progress Series* , **32**, 149-160.

Malone, T.C., L.H. Crocker, S.E. Pike, and B.W. Wendler, 1988: Influences of river flow on the dynamics of phytoplankton production in a partially stratified estuary, *Marine Ecology Progress Series* ,**48**, 235-249.

Malone, T.C., H.W. Ducklow, E.R. Peele, and S.E. Pike, 1991: Picoplankton carbon flux in Chesapeake Bay, *Marine Ecology Progress Series*, **78**, 11-22.

Maritorena, S., D.A Siegel, and A.R. Peterson, 2002: Optimization of a semianalytical ocean color model for global-scale applications, *Applied Optics*, **41**, 2,705-2,714.

Marshall, H.G. and K.K. Nesius, 1996: Phytoplankton composition in relation to primary production in Chesapeake Bay, *Marine Biology*, **125**, 611-617.

Nelson, J.R. and S. Guarda, S. 1995: Particulate and dissolved spectral absorption on the continental shelf of the southeastern United States, Journal of Geophysical Research 100, 8,715-8,732.

O'Reilly, J.E., S. Maritorena, B.G. Mitchell, D.A. Siegel, K.L. Carder, S.A. Garver, M.Kahru, & C.R. McClain, 1998: Ocean color algorithms for SeaWiFS, *Journal of Geophysical Research* ,**103**, 24,937-24,953.

O'Reilly, J.E. and J.A. Yoder, 2003: A comparison of SeaWiFS LAC Products from the Third and Fourth Reprocessing: Northeast US Ecosystem, in Algorithm Updates for the Fourth SeaWiFS Data Reprocessing (S.B. Hooker & E.R. Firestone, eds). *NASA Tech. Memo. 2003-206892*, NASA Goddard Space Flight Center, Greenbelt, MD, pp. 60-67.

Vodecek, A., N.V. Blough, M.D. DeGrandpre, E.T. Peltzer, and R.K. Nelson, 1997: Seasonal variation of CDOM and DOC in the Middle Atlantic Bight: Terrestrial inputs and photooxidation, *Limnology and Oceanography* ,**42**, 674-686.

Yentsch, C.S. and D.A. Phinney, 1989: A bridge between ocean optics and microbial ecology, *Limnology and Oceanography*, **34**, 1,694-1,705.

This Research was Supported by the
NASA Contract # 00195

Publications

Harding, L.W., W. . Miller, R.N. Swift, and C.W. Wright, 2001: Aircraft remote sensing, In: Steele, J., S. Thorpe, and K. Turekian, (eds.), Encyclopedia of Ocean Sciences, Academic Press, London, UK, 113-122.

Harding, L.W., Jr., M.E. Mallonee, and E.S. Perry, 2002: Toward a predictive understanding of primary productivity in a temperate, partially stratified estuary, Estuarine, *Coastal and Shelf Science*, **55**, 437-463.

Harding, L.W., Jr., A. Magnuson, and M.E. Mallonee, 2003: Bio-Optical and remote sensing observations in Chesapeake Bay, Estuarine, *Coastal, and Shelf Science* (in review).

Magnuson, A., L.W. Harding, Jr., M.E. Mallonee, and J.E. Adolf, 2003: Bio-optical modeling in the middle Atlantic bight, Estuarine, *Coastal, and Shelf Science* (to be submitted).

Presentations

Harding, L.W., Jr., Seasonal and inter-annual variability of primary productivity in Chesapeake Bay from remotely sensed aircraft observations, at Phytoplankton Productivity - An Appreciation of 50 Years of the Study of Production in Oceans and Lakes, 19 March 2002, Bangor, Wales, United Kingdom.

Magnuson, A., L.W. Harding, Jr., and M.E. Mallonee, Progress toward a case II bio-optical algorithm optimized for Chesapeake Bay and the adjacent waters of the mid-Atlantic bight. Ocean Optics XVI, 18-22 November 2002, Sante Fe, NM.

Magnuson, A., L.W. Harding, Jr., M.E. Mallonee, and W.D. Miller, Comparison of In Situ radiometric measurements in turbid waters, poster presented at the 5th SIMBIOS Science Team Meeting, 15-17 January 2002, Baltimore, MD.

Chapter 8

Refinement of Protocols for Measuring the Apparent Optical Properties of Seawater

Stanford B. Hooker
NASA/GSFC Greenbelt, Maryland

Giuseppe Zibordi and Jean-François Berthon
JRC/IES/Inland and Marine Waters, Ispra, Italy

André Morel and David Antoine
CNRS/UPMC/Laboratoire d'Océanographie de Villefranche, Villefranche-sur-Mer, France

8.1 INTRODUCTION

Ocean color satellite missions, like the Sea-viewing Wide Field-of-view Sensor (SeaWiFS) or the Moderate Resolution Imaging Spectroradiometer (MODIS) projects, are tasked with acquiring a global ocean color data set, validating and monitoring the accuracy and quality of the data, processing the radiometric data into geophysical units using a set of atmospheric and bio-optical algorithms, and distributing the final products to the scientific community. The long-standing requirement of the SeaWiFS Project, for example, is to produce spectral water-leaving radiances, $L_W(\lambda)$, to within 5% absolute (λ denotes wavelength) and chlorophyll *a* concentrations to within 35% (Hooker and Esaias 1993), and most ocean color sensors have the same or similar requirements. Although a diverse set of activities are required to ensure the accuracy requirements are met (Hooker and McClain 2000), the perspective here is with field observations. Assuming half of the total uncertainty budget is apportioned to the satellite sensor and that the uncertainties sum in quadrature (the square root of the sum of the squares), the allowed uncertainty in the *in situ* data is approximately 3.5% ($\sqrt{5^2 / 2}$).

The accurate determination of upper ocean apparent optical properties (AOPs) is essential for the vicarious calibration of ocean color data and the validation of the derived data products, because the sea-truth measurements are used to evaluate the satellite observations (Hooker and McClain 2000). The uncertainties with *in situ* AOP measurements have various sources: a) the sampling procedures used in the field, including the environmental conditions encountered; b) the absolute characterization of the radiometers in the laboratory; c) the conversion of the light signals to geophysical units in a processing scheme, and d) the stability of the radiometers in the harsh environment they are subjected to during transport and use. Assuming ideal environmental conditions, so this aspect can be neglected, the SeaWiFS ground-truth uncertainty budget can only be satisfied if each uncertainty is on the order of 1–2%, or what is generally referred to as *1% radiometry*.

In recent years, progress has been made in estimating the magnitude of some of these uncertainties and in defining procedures for minimizing them. For the SeaWiFS Project, the first step was to convene a workshop to draft the SeaWiFS Ocean Optics Protocols (hereafter referred to as the Protocols). The Protocols initially adhered to the Joint Global Ocean Flux Study (JGOFS) sampling procedures (JGOFS 1991) and defined the standards for optical measurements to be used in SeaWiFS calibration and validation activities (Mueller and Austin 1992). Over time, the Protocols were revised (Mueller and Austin 1995), and then recurringly updated on essentially an annual basis (Mueller 2000, 2002, and 2003) as part of the Sensor Inter-comparison and Merger for Biological and Interdisciplinary Oceanic Studies (SIMBIOS) project.

This report summarizes advances in ocean optics protocols derived from a variety of inquiries brought to completion within the last year of the SIMBIOS project. The presentation is restricted to minimizing instrument characterization, *in situ* sampling, and data processing uncertainties for AOP sensors normally used in vicarious calibration activities. The full inquiry included the uncertainties associated with the determination of pigment concentrations using high performance liquid chromatography (HPLC), because pigment concentrations are an essential part of a complete validation program. The results for the latter are not described here, because they are not part of AOP investigations. The complete details, however, are presented in Claustre et al. (2003) and Hooker et al. (2003a).

8.2 INSTRUMENT CHARACTERIZATION PROTOCOLS

The immersion factor, $If\ (\lambda)$, is a necessary part of the spectral characterization of an in-water irradiance sensor, because when a cosine collector is immersed in water, its light transmissivity is less than it was in air. Irradiance sensors are calibrated in air, however, so a correction for this change in collector transmissivity must be applied when the in-water raw data are converted to physical units. The immersion factor must be determined experimentally, using a laboratory protocol, for each collector.

Depth (z) profiles of the downward and upward irradiances, $E_d\ (z,\lambda)$ and $E_u(z,\lambda)$, respectively, are directly influenced by uncertainties in the characterization of immersion factors. Although irradiances do not appear explicitly in the determination of $L_W\ (\lambda)$—which is derived primarily from a profile of the upwelled radiance, $L_u(z,\lambda)$—vicarious calibration activities frequently rely on measurements, normalized variables, or alternative methods for producing $L_W\ (\lambda)$ which require irradiance variables:

1. The Q-factor, which requires $E_u\ (z,\lambda)$ and $L_u\ (z,\lambda)$, or the use of Q-factor look-up tables with measurements of $E_u\ (z,\lambda)$to derive $L_u\ (z,\lambda)$;
2. The irradiance reflectance $R(z,\lambda)$, when computed with $E_u\ (z,\lambda)$ and $E_d\ (z,\lambda)$ obtained from different radiometers;
3. The normalized water-leaving radiance, $L_{WN}\ (\lambda)$, as well as the remote sensing reflectance, $R\text{rs}(\lambda)$, when the solar irradiance, $E_d\ (0^+,\lambda)$, is computed from subsurface $Ed(0^-,\lambda)$values (0^+ and 0^- denote measurements immediately above and below the sea surface, respectively);
4. Determination of the near-surface extrapolation interval, and thus the water-leaving radiance, for those processing schemes taking advantage of the convergence of $E_d\ (0^+,\lambda)$ and $E_d\ (0^-,\lambda)$to select the interval limits; and
5. Derived quantities formed from band ratios of $R\ (\lambda)$, $L_{WN}\ (\lambda)$, or $R\text{rs}(\lambda)$at different wavelengths.

The latter are the input variables for algorithms inverting the optical measurements to derive the chlorophyll *a* concentration (O'Reilly et al. 1998).

Studies of immersion effects date back to the work of Atkins and Poole (1933), who attempted to experimentally estimate the internal and external reflections for an opal glass diffuser. Additional investigations by Berger (1958 and 1961) refined the laboratory procedures and Westlake (1965) gave detailed explanations for the internal and external reflection contributions. A comprehensive description of a protocol for a more modern Plexiglas diffuser was given by Smith (1969). The culmination of these early investigations was the incremental method, or what is now referred to as the *traditional* method.

The traditional method has been in use for the past 25 years, and originated with the protocol revisions suggested by Aas (1969) and communicated more widely by Petzold and Austin (1988). They all advocated using a lamp as a light source and including a geometric correction factor as a function of the lamp–collector distance, incremental changes in the water depth, and the water refractive index. The advantage of the geometric correction factor is it minimizes the effects caused by changes in the flux reaching the collector as a function of the change in water depth.

The traditional method involves a relatively simple procedure and a small number of components (Mueller and Austin 1995). A lamp of suitable wattage is needed to provide a flux of light at all sensor wavelengths well above dark values, with the appropriate baffing and apertures to minimize diffuse light contributions into the tank. A lamp with a small filament is preferred, because it better approximates a point source, and a regulated power supply should be used to ensure the emitted flux from the lamp is stable over the time period of each characterization trial. The water vessel or tank should have a removable aperture

sized or adjusted to ensure the direct beam of light from the lamp projects onto an area that is only slightly larger than the area of the diffuser. The interior of the tank must be *flat* black, and contain a sensor support system that permits an accurate horizontal leveling of the diffuser and an accurate alignment of the sensor with respect to the centerline of the lamp filament.

Two alternatives for characterizing immersion factors were recently evaluated by Hooker and Zibordi (2003a). For the first method, the optical measurements taken at discrete water depths are substituted by continuous profiles created by removing the water with a pump. In the second method, the commonly used large tank is replaced bya small water vessel with sidewall baffes, which permits the use of a quality-assured and reproducible volume of water. The latter was achieved by refining the capabilities of the Compact Portable Advanced Characterization Tank (ComPACT), which had already been built for experimenting with immersed sensors.

The continuous method takes advantage of having a pump (with an almost constant discharge rate) to drain the water vessel. For a cylindrical tank, the water depth can be approximated as a linear function of time as the water is pumped out. Consequently, there is no need to stop at discrete depths to record the diffuser measurements. This means the total characterization time is the time needed to prepare, fill, and empty the tank (about 40 min for a large, 350 L, tank), which is considerably shorter than the traditional method (which usually requires about 100 min, but for some setups as much as 300 min).

The ComPACT apparatus originated from a desire to perform quality tests on immersed radiometers either in the field (measuring the response of bio-fouled sensors while still wet) or in the laboratory (the characterization of immersion factors). The original concept was to have a small (portable) water vessel, with baffing elements to minimize light reflections inside the tank if an extended source was used for illumination. The basic elements of the Com-PACT measurement protocol involve many elements associated with the traditional method, e.g, leveling, aligning, and adjusting the components before the experimental process can be executed. These and many other finer levels of detail are not recounted here, because they are provided by Zibordi et al. (2003a). The primary advantages of the ComPACT apparatus in the characterization of immersion factors is a) it only requires 3 L of water, which means pure water, manufactured shortly before use, can be used, and b) the small size places minimal requirements on work spaces and waste water requirements.

The validation of the continuous and ComPACT methodsis accomplished by comparing them to the traditional method. Specifically, the $If(\lambda)$values from an alternative method and a specific sensor (Y) are differenced with respect to the $If(\lambda)$values for that sensor as provided by the traditional method (X). Relative percent difference (RPD) values,

$$\varphi = 100\frac{Y - X}{X} \tag{8.1}$$

are used to evaluate the performance characteristics of the methods. The overall capabilities are derived by averaging across all sensors or all wavelengths (which are identical for all the sensors).

The intercomparison of the alternative and traditional methods is given in Fig. 8.1. The results show a significant convergence of the two new methods with the traditional method with individual sensor differences generally well below 1%. The histogram of RPD values (inset panel) has a significant central peak, but a slightly distorted gaussian distribution—there is a small net positive bias; the average RPD is 0.1%. The average repeatability for single-sensor characterizations (across seven wavelengths) of the three methods are very similar and approximately 0.5%.

The evaluation of the continuous method demonstrates its full applicability in the determination of immersion factors with a significant time savings. The evaluation of the small water vessel demonstrates the possibility of significantly reducing the size of the tank (along with decreasing Fig. 8.1. A comparison of the traditional $If(\lambda)$ method versus the continuous (open circles) and ComPACT (solid circles) methods. The experimental trials for the new methods were executed in as small a time difference with respect to the traditional method as possible. The sensors involved are the same ones characterized during the eighth SeaWiFS Intercalibration Round-Robin Experiment (SIRREX-8) for investigating uncertainties in the traditional method (Zibordi et al. 2003b). The sensors had identical (nominal) center wavelengths and were usually characterized more than once, although one of the radiometers was selected as a so-called *reference* sensor and was measured more frequently than the others. The mix of sensors used with the ComPACT method is different than those used with evaluating the continuous method, but five are common to both

and between the two types of experiments, all 12 of the sensors used during SIRREX-8 are represented. The anomalously low *If* (λ)value at approximately 1.275 is a confirmed feature of one of the sensors. The inset panel shows the histogram of RPD values, with the traditional method used as the reference in the RPD calculation.

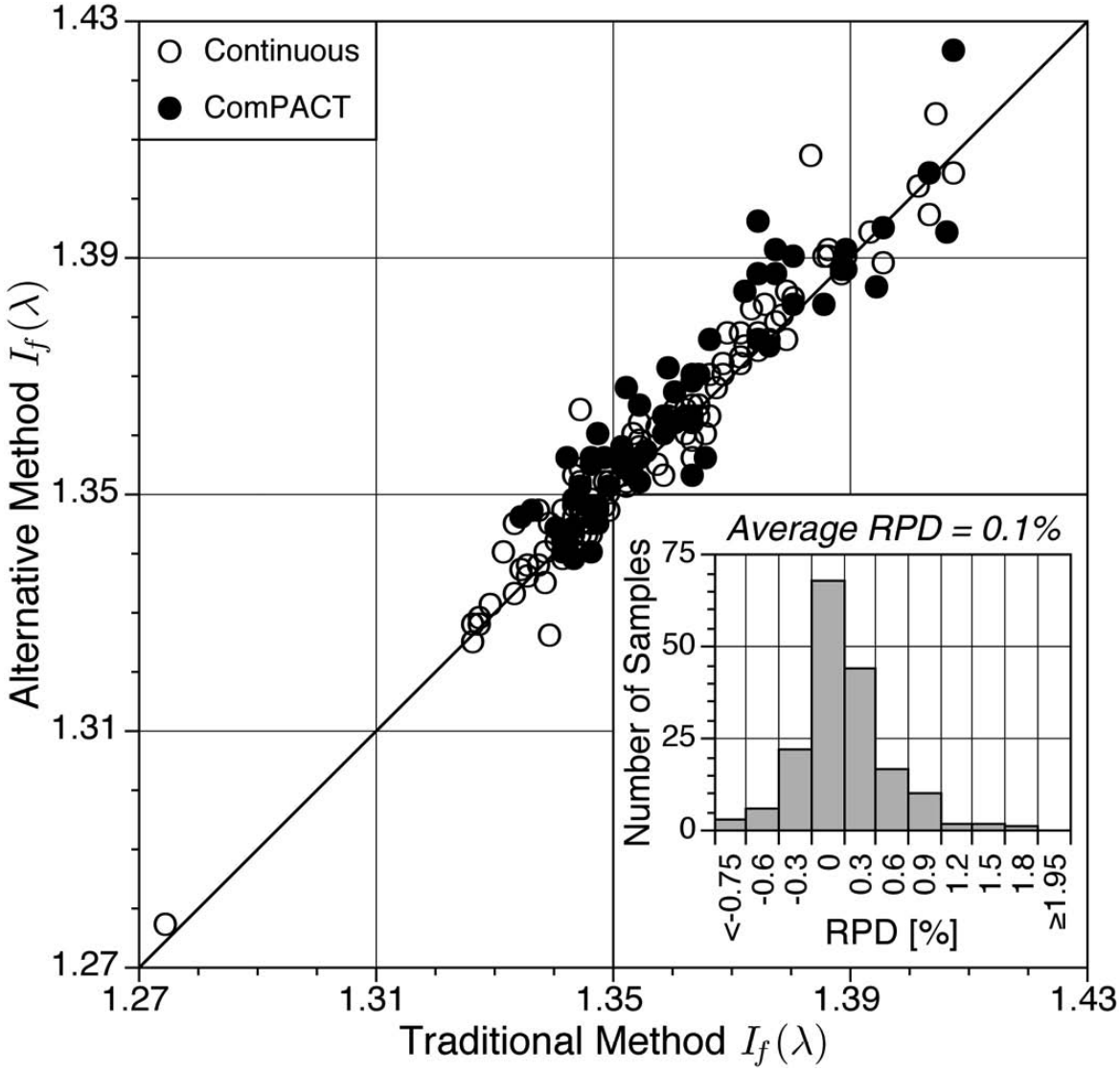

Figure 8.1:A comparison of the traditional I_f (λ) method the continuous (open circles) and ComPACT (solid circles) methods. The experimental trials for the new methods were executed in as small a time difference with respect to the traditional method as possible. The sensors involved are the same ones characterized during the eight SeaWiFS Intercalibration Round Robin Experiments (SIRREX-8) for investigating uncertainties in the traditional method (Zibordi et al. 2003b). The sensors had identical (nominal) center wavelengths and were usually characterized more than once, although one of the radiometers was selected as a so-called *reference* sensor and was measured more frequently than others. The mix of sensors used with the ComPACT method is different than those used with evaluating the continuous method, but five are common to both and between the two types of exeperiments, all 12 of the sensors used during SIRREX-8 are represented. The inset panel shows the histogram of RPD values, with the traditional method used as the reference in the RPD calculation.

the execution time) and permitting a completely reproducible methodology (based on the use of pure water). The results also show sidewall reflections can be properly minimized with internal baffes. Within the context of experimental effciency and reproducibility, this study suggests the combination of a properly baffed small tank with a constant flow pump would be an optimal system.

8.3 IN SITU SAMPLING PROTOCOLS

Achieving working at the 1% level is achievable in the laboratory, doing so in the field is much more diffcult, which is well demonstrated by considering the magnitude of the perturbations in the proximity of a large structure as a specific example. This is an appropriate choice, because platform effects are a recurring problem for *in situ* optical methods. These perturbations are made more complex according to the sun orientation with respect to the structure, and differentially influence the data obtained by above-and in-water methods. For example, from the perspective of the in-water light field, investigations within 15–20 m of an offshore tower show significant effects of the structure: approximately 3–8% for clear-sky conditions, and as much as 20% under overcast conditions (Zibordi et al. 1999). Similar uncertainties have been estimated for in-water measurements from a ship (Voss et al. 1986).

From a measurement perspective, the above-water approach is more restrictive, because there is presently no reliable mechanism for floating an above-water system away from a platform (which is easily and effectively accomplished for an in-water system), so all above-water measurements are made in close proximity to a large structure. For the purposes of the results presented here, the proximity of the sampling platform is parameterized as the perpendicular distance x from the side of the sampling platform to the center of the area on the sea surface observed by the sea-viewing sensor, the so-called *surface spot*. The possible values of x range from approximately 0 (the field of view of the sensor must view only water and no part of the sampling platform), to a maximum value approximately equal to the height of the sensor above the water, H.

The team assembled to study platform perturbations imagined a horizontal deployment system (HDS) that would be easy to operate by one person, and modular for conventional transportation to the sampling platform. The idea wastobe able to extend an above-water system about 10 m away from the platform. The above-water instruments commonly in use are too large to safely use such a system on a moving platform, like a ship. The unique stability of a tower offered the best opportunity to satisfy all the design requirements, but only if the size of the radiometers could be significantly reduced. Prior to the initial design of the HDS, there was already a concerted effort to produce smaller and lighter sensors for SeaWiFS field campaigns. A next-generation (very small) version of the SeaWiFS Surface Acquisition System, called microSAS, was available for testing at the same time when the HDS design was being initiated, so this new sensor system was used to set the design criteria for the HDS (Hooker et al. 2003b).

The microSAS system measures the radiances required for the above-water approach used here, the so-called *modified Fresnel reflectance glint correction* as presented in the version 1 revision of the Protocols (Mueller and Austin 1995), hereafter referred to as S95. This method assumes the total radiance measured at the sea surface, $L_T(\lambda)$, is a combination of $L_W(\lambda)$ plus two sources of reflected light or *glint*: the sky and the sun. If the latter is minimized by pointing the measurement instruments at least 90◦ away from the sun plane (but not into any perturbations associated with the platform), the only quantity needed to retrieve $L_W(\lambda)$ from $L_T(\lambda)$isan estimate of the sky radiance, $L_i(\lambda)$, contribution. Removing the sky glint also requires an estimate of the surface reflectance, ρ.In the original formulation of S95, ρ wasa constant, but more realistic values for ρ as a function of the viewing geometry and the wind speed are available from Mobley (1999). The incorporation of the latter is hereafter referred to as the S01 method (Hooker et al. 2003b):

$$\hat{L}w_W^{S01}(\lambda) = L_T(\lambda) - \rho(W)L_i(\lambda), \tag{8.2}$$

where the pointing angles are omitted for brevity.

The tower-perturbation field measurements were carried out on the *Acqua Alta* Oceanographic Tower (AAOT) and within the framework of the Coastal Atmosphere and Sea Time Series (CoASTS) Project (Zibordi et al. 2002a). The tower is located in the northern Adriatic Sea approximately 15 km offshore of

the Venice Lagoon in a frontal region that can be characterized by Case-1 or Case-2 conditions, although the former predominate (Berthon et al. 2002). The HDS was mounted on the topmost level (Fig. 8.2), and consists of a tubular horizontal mast sliding between rollers mounted within five rigid support frames. The HDS can carry an instrument package weighing approximately 10 kg, and to deploy it up to as much as 12 m away from the tower with a vertical deflection of the mast less than 1% (Van der Linde 2003). Although the HDS can be moved an arbitrary distance, 10 distance or *mast index* markers were placed on the horizontal mast in 1 m intervals. A mast index origin was established at the first mast support, so a quick determination of the relative position of the mast with respect to the tower could be determined (and reliably reproduced).

Following the work by Hooker and Morel (2003), the presence of an artificial perturbation in an above-water measurement can be detected (after wave effects have been removed) with the ratio

$$r(865) = \frac{L_T(865) / L_i(865)}{\rho(W)} \tag{8.3}$$

where the numerator comes from the Morel (1980) assumption that the sea surface is essentially *black* at a near-infrared wavelength (i.e., the above-water radiance measured is entirely due to surface reflection, principally from sky radiation once the sensor is pointed at least 90◦ away from the sun), and the denominator is the modeled surface reflectance from Mobley (1999). Under *natural* circumstances (i.e., in the absence of platform perturbations) and in Case-1 water conditions, $\rho(W) = L_T(865)/L_i(865)$, within the accepted variance, and $r(x, 865) = 1$. Any other reflected radiation added to the sky-reflected radiance leads to an increase in $L_T(x, 865)$, and $r(x, 865) > 1$.

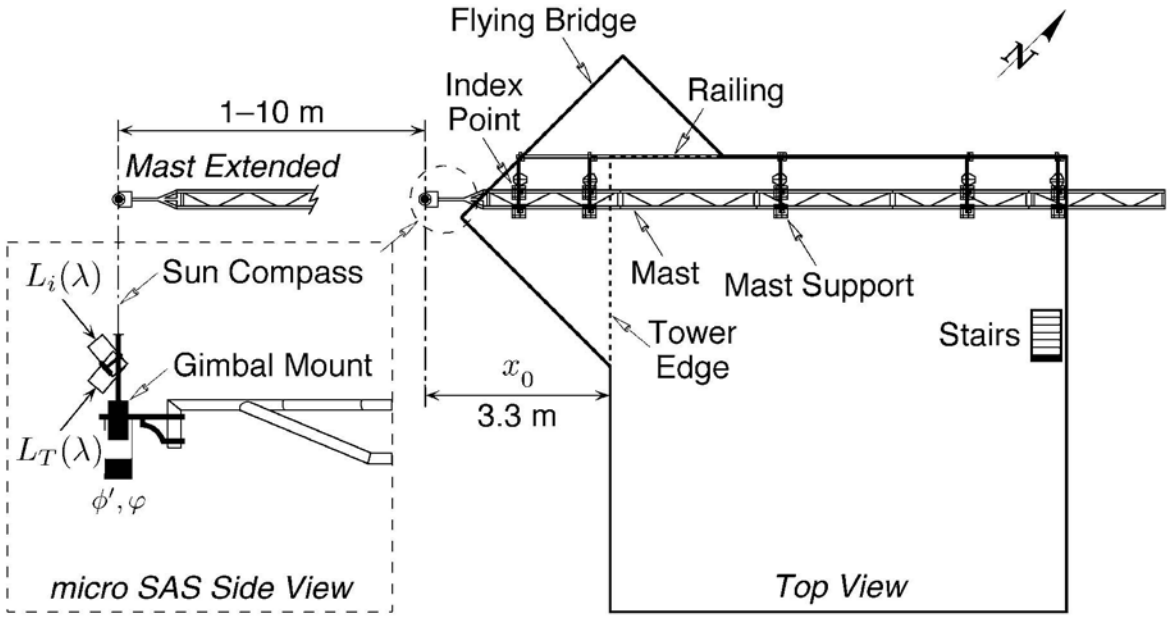

Fig. 8.2. Aschematic of the top view of the AAOT. The HDS is installed along the northwest edge and extends over the flying bridge that projects out over the main body of the tower. The microSAS sensors are mounted in a cardanic gimbal whose axes are aligned in the direction of, and perpendicular to, the HDS mast. Sensors inside the gimbal ballast confirm the azimuthal angle with respect to the solar azimuth, φ', is appropriate, and that the vertical (two-axis) tilt, φ, is less than 1^0. The latter confirms the nadir and zenith viewing angles (denoted υ hereafter) are correct. A complete experiment is made up of a set of approximately 10 microSAS measurement sequences, or casts. The casts are made at different mast index positions, m_i, which were sequentially set going from 1 to 10 or 10 to 1 (in 1 m increments).

The most important aspects of r (865) as an analytical variable are as follows:

1. It intrinsically includes the effects of changing solar illumination, because the sea-viewing observations are normalized by the sky radiance; and
2. It can be used to create a severity index, in the sense that the stronger the artificial increase in LT (x, 865), the larger the increase in r (x, 865), and the magnitude of the departure from unity (or an appropriate reference value) is an estimate of the severity of the contamination.

In Case-2 water conditions, or if the water type is close to the threshold of Case-1 and Case-2 conditions, r (x, 865) is not expected to be unity even far from the tower, so the last point requires some qualification: over the course of atower-perturbation experiment (usually requiring about 45 min), and in the absence of a source of artificial reflections, r (x, 865) is expected to remain essentially constant.
In other words, if the tower were not present, r (865) might not be unity, but it would remain constant over the time period of an experiment.

Departures from constancy (i.e., above the level of environmental variability) as a function of x are expected to be an indicator of the presence of platform perturbations, particular if they show a significant increase as x decreaess. The constancy of r (865) can be quantified by selecting one of the most distant far-field observations within an experiment as a reference point, x. The RPD, ψ, is again used to quantify the difference between an observation Y with respect to a reference value X. For the specific case of determining changes in r (865) as a function of x, the RPD (1) is computed as

$$\varphi(x) = 100\frac{r(x,865) - r(x^1,865)}{r(x^1,865)} \tag{8.4}$$

where x^1 is the reference point in the calculation and $\psi(x)$, the RPD value, is the so-called severity index.

An ensemble description of the perturbation field, in terms of the severity index, can be created by binning the RPD data as a function of x and averaging the values in each bin. Scaling the x values by the height of the sensor above the water (also approximating the height of the tower), H, permits a more generalized description of the data. The result of this process is shown in Fig. 8.3, along with delineations of the original minimum and maximum extents of the RPD values. The intersection of the perturbation curves with the scaled surface spot distance (x/H) gives the minimum, (expected) average, and maximum severity indexes. The curves show three important aspects of the tower-perturbation field:

1. The maximum perturbations occur very close to the tower (small values of x/H);
2. As x/H increases and approaches 1 (i.e., as the surface spot becomes as far away as the platform is high), the platform perturbation curves converge towards smaller and smaller values; and
3. For $x>H$, the platform perturbation is negligible.

It is important to remember the perturbation here is modeled only in terms of the severity index. The azimuthal-viewing arcs in Fig. 3 (based on $\upsilon = 40^{\circ}$) allow the RPD curves to be used to predict the severity index for a particular azimuthal-viewing angle. Conversely, the data in Fig. 8.3 can be used to determine what maximum azimuthal-viewing angle can be used while maintaining a certain severity index. For example, for a severity index of 3%, an instrument mounted on the edge of a platform (x_0 =0.0m) can be azimuthally rotated up to $\pm 23.1^0$ (α is assumed symmetrical), and an instrument displaced 3.3 m from the edge of the platform can be rotated up to $\pm 51.6^0$.

A topic deserving additional consideration is the spectral aspects of the tower perturbation in the near field. It is important to remember that the severity index is only a relative diagnostic and cannot be used as an absolute predictor. The primary reason why a severity index versus spectral radiance approach will yield a different description of the tower perturbation is the geometry at the time of sampling, both in terms of the sun and the mechanical pointing of the instruments. The geometry controls the importance of platform shading versus superstructure reflections, and the resulting net perturbation from these contamination effects is strongly spectrally dependent.

Alternative spectral analyses for the tower perturbation investigation based on above-water normalized water-leaving radiances are presented by Hooker and Zibordi (2003b). These analyses confirm the

generalized metric established with the original work by Hooker and Morel (2003): the primary avoidance principal for a sea-viewing sensor mounted on the illuminated side of a platform is that it must be pointed to a spot on the sea surface that is at least as far away as the platform is high. The successful application of the generalized sampling metrics established here to an automated above-water sampling system is presented by Zibordi et al. (2003c).

It is important to remember this study was based on a simplistic and symmetric (box-like) structure. It is likely that some of the results will not be immediately applicable to asymmetric or highly reflective platforms, and some extra considerations will have to be applied. For example, a sensor mounted on the bow of a ship, with the main superstructure set far back from the bow, will probably have to view a surface spot that is as far away as the height of the bow railing. Ships with superstructures set much closer to the bow, especially those painted white, will probably require a surface viewing distance that approximates the full height of the superstructure.

In any case, each platform is a particular case, and each instrument mounting location a separate challenge. Although this study can provide guidance, it cannot answer all questions for all platforms. The most important lesson is that a perturbation analysis needs to be conducted for each above-water instrument location to determine the level of contamination as a function of the pointing parameters. For calibration and validation activities, sampling of the unperturbed far field will be a necessity that might not be easily satisfied without specially-designed mounting hardware.

8.4 DATA PROCESSING PROTOCOLS

Although above-water determinations of water-leaving radiances are part of the databases used to create global bio-optical models, the majority of the data for these activities are from in-water measurements (O'Reilly et al. 2000). Part of this disparity is historical, in-water measurements have been conducted for a longer time period, and part of it is the consequence of the poor agreement that is frequently obtained when the two methods are intercompared (Rhea and Davis 1997, Fougnie et al. 1999, Toole et al. 2000, and Hooker et al. 2002a), so traditional in-water measurements have been preferred.

Aportion of the discrepancy between the two methods was recently shown to be caused by wave effects (Hooker et al. 2002a and Zibordi et al. 2002b), platform perturbations (Hooker and Morel 2003 and Hooker and Zibordi 2003b), and the anisotropy of the upwelled radiance field (Morel and Gentili 1996). The latter is particularly important, because in-water systems are usually nadir viewing, whereas above-water systems are not). The study presented here builds on these accomplishments by analyzing simultaneous above-and in-water optical observations, wherein one of the two measurements was unequivocally free of platform perturbations, and implementing an above-water method with corrections for many problems unique to above-water methods. This data set is then used for the following objectives, which are examined within the generalized requirements of calibration and validation activities (i.e., the generalized 1% radiometry needed to satisfy the SeaWiFS absolute uncertainty requirement): a) evaluate the capabilities of above-water radiometry in shallow, coastal waters; and b) determine if the above-and in-water methods converge to within the uncertainties associated with the two methods.

For a meaningful comparison with the (nadir-viewing) in-water sensors, the above-water methodology needs to be corrected to account for the bidirectional dependency of the upward radiance field below the surface with that exiting the surface. The basic equations for this transformation (Morel and Gentili 1996 and Mobley 1999) are an established part of the Protocols (Morel and Mueller 2002) and have been successfully incorporated into above-water measurements (Hooker and Morel 2003, Hooker and Zibordi 2003b, and Hooker et al. 2003c), so only only a brief summary is presented here.

The radiance bidirectionality is parameterized by the so-called Q-factor, which takes a particular value, denoted Q_n, for the nadir-viewing measurements. For above-water measurements, the angular parameters are imposed by the pointing angles of the sensors, as well as the surface effects of reflection and refraction. When dealing exclusively with Case-1 waters, the functional dependence of the variables can be simplified. In particular, it is assumed that the inherent optical properties are universally related to the chlorophyll a concentration (Morel and Prieur 1977), Ca.

Because a nadir-transformed, above-water estimate of L_W is equivalent to the in-water value, a formulation can be produced (Morel and Mueller 2002) to correct the S01 method, and is hereafter referred to as the Q02 method:

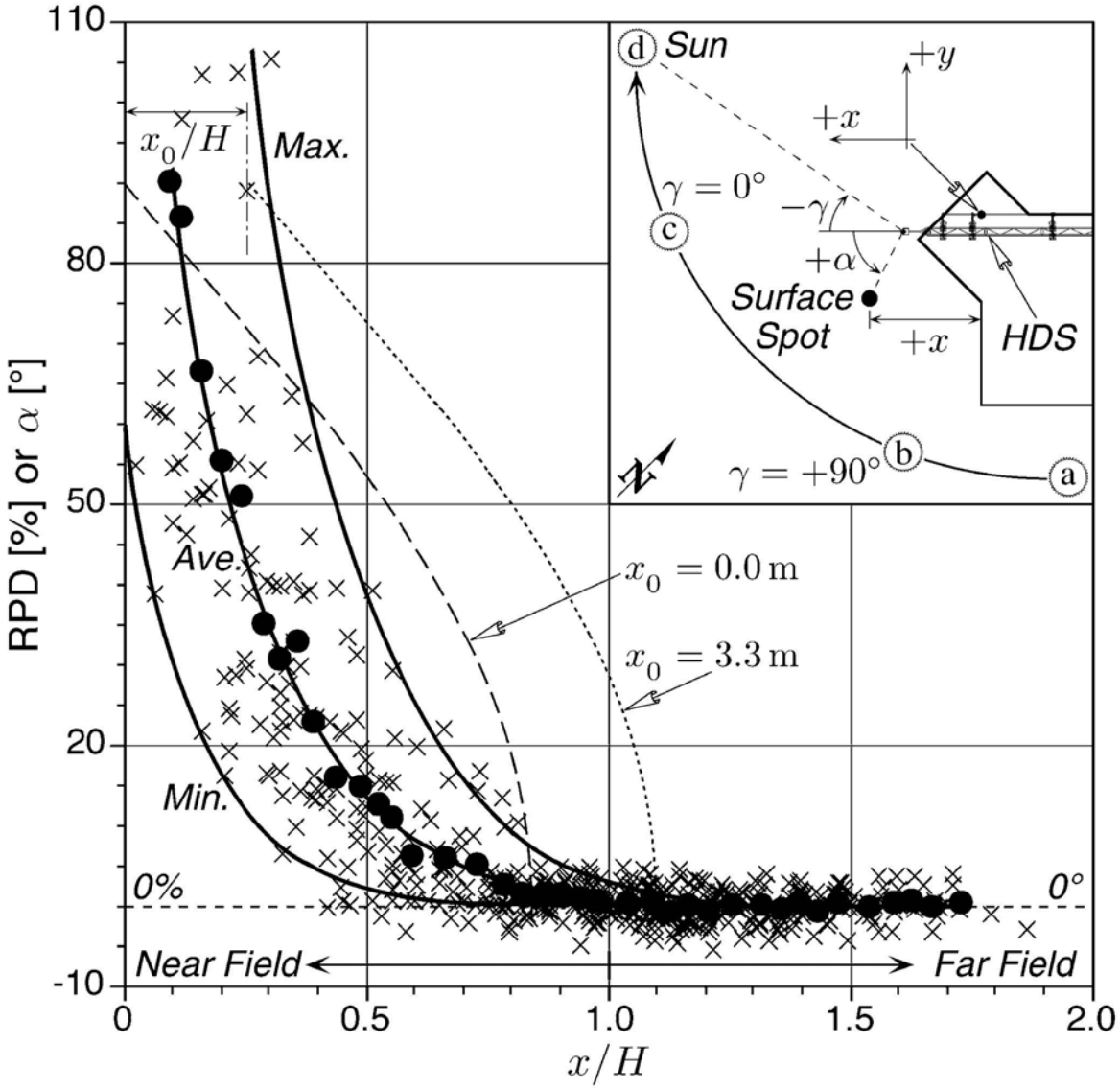

Fig. 8.3. The bin-averaged *r* (865) RPD values (solid circles and associated curve) as a function of *x/H*. Also shown are the curves delineating the minimum and maximum RPD values associated with the full data set (the x symbols). Superimposed on these curves are the azimuthal-viewing arcs based on υ =40◦ for a sensor mounted on the edge of a platform (x_0 =0.0m) and one mounted at *mi* =1 (the first mast index position) on the HDS (x_0 =3.3 m). Each viewing arc gives the scaled distance to the surface spot (*x/H*) asa function of α. The x_0 =3.3m arc ends at x_0/H =0.25 (α =90◦), although, lower *x/H* values could be measured. The inset panel shows a schematic of the localized (*x,y*) coordinate system, along with the geometry for the pointing angles with respect to the sun (γ) and the surface spot viewed by the sea-viewing sensor (α). Note the origin of the localized coordinate system (denoted by the intersection of the +*x* and +*y* axes) is a point at the northwest corner of the tower within the area associated with the flying bridge.

$$\hat{L}_W^{Q02}(\lambda) = \frac{\Re_0}{\Re(\theta^1, W)} \frac{Q(\lambda, \theta, \phi^1, C_a)}{Q_n(\lambda, \theta, C_a)} \hat{L}1(\lambda) \tag{8.5}$$

where the *Q* terms are evaluated at null depth ($z = 0^-$), θ is the solar zenith angle, θ' is the above-water viewing angle (υ) refracted by the air–sea interface, and the factor merges all the effects of reflection and

refraction (the 0 term is evaluated at nadir, i.e., $\theta = 0$). All the correction terms are computed here from look-up tables (Morel et al. 2002). An above-water instrument system cannot be floated away from a sampling platform, but this is easily and effectively accomplished with many in-water profiler designs. Within the context of this generalized difference between the two methods, an above-water acquisition effort—even if platform perturbations are recognized and minimized—is still more likely to contain platform-contaminated acquisition sequences than profiles from a simultaneous in-water method. There are exceptions to this generality, but it remains more true than not, and is one of the reasons why in-water calibration and validation exercises predominate. Using these arguments as an overall rationale for prioritizing the data used in this study, the analytical perspective adopted here is as follows:

1. Use the in-water observations as the reference measurement for evaluation purposes.
2. When matching the above-and in-water observations, use only simultaneous or nearly simultaneous (within ± 5 min) data acquisition sequences to minimize environmental influence.
3. Use radiometers with absolute calibrations from separate calibration facilities (the usual case for most investigators), but intercalibrate the sensors to quantify the effect of eliminating differences in the calibration standards and procedures.

Although the discussion contained within the aforementioned rationale readily supports a decision to use the in-water measurements as the analytical reference, another reason for doing so is the in-water data processor used here has been evaluated in a data processor round robin and its uncertainties are well quantified (Hooker et al. 2001).

An intercomparison of the intercalibrated above-and in-water methods, for all the Case-1 and Case-2 data (Loisel and Morel 1998) is presented in Fig. 8.4. With the exception of a small number of values at 555 nm, the majority of the data are well distributed around the 1:1 line, although the lower edge of the variance is defined by a large number of the values at 510 nm. The AAOT above-water measurements were unequivocally free of platform perturbations, whereas for the ADRIA-2000 data, the in-water observations were free of perturbations. Because the Fig. 8.4 data do not show any significant biases, platform perturbations were properly avoided, and the Case-2 data are not substantially different from the Case-1 data. The average RPD of all the intercalibrated data is approximately 1.8%, and if the independently calibrated data are considered, the average RPD increases to about 2.3%. In either case, the average RPD values are to within the uncertainties associated with the absolute calibration of the radiometers (Hooker et al. 2002b). Additional details on the total uncertainty budget of both methods are presented by Hooker et al. (2003c).

An interesting aspect of the Fig. 8.4 results is the very good agreement for the overcast data (much of the data at approximately 0.3 $\mu Wcm^{-2}\,nm^{-2}\,sr^{-1}$ and below are from overcast stations). This is an added capabilitiy of the above-water method used here, and shows an enhanced flexibility of the method. It can be particularly important in some circumstances, because cloud conditions are not predetermined by any means, and many field expeditions get only limited opportunities to sample certain regimes.

The importance of properly accounting for bidirectional effects and accurately determining the surface reflectance is demonstrated by replacing (λ) with $\hat{L}_W^{Q02}(\lambda)$ with $\hat{L}_W^{S95}(\lambda)$ in the intercomparisons of the intercalibrated results (the S95 method assumes ρ =0.028 and there is no Q-factor correction). The results of this substitution is a significant bias—almost all the data are above the 1:1 line—that is, the S95 method overestimates the water-leaving radiances across all bands. The average magnitude of the overestimation is approximately 6.6%, which is about 4.8% above the Q02 intercalibrated results. This level of difference is in keeping with the differences in above-and in-water methods documented by Hooker et al. (2002a), wherein the former were not bidirectionally corrected.

The SeaWiFS uncertainty requirements were based primarily on an open ocean perspective. The data presented here were collected in the coastal environment, so the level of agreement that has been achieved is significantly better than originally anticipated. The convergence of the Q02 above-water method with the traditional in-water technique was primarily the result of careful metrology, platform perturbation avoidance, state-of-the-art corrections to the primary variables, plus comprehensive and independent evaluations of the calibration and data processing schemes. If this level of effort is reproduced in similar or simpler environments (coastal waters predominated by Case-1 conditions or the open ocean), there is every reason to believe that the Q02 above-water method can be used at the same level of effcacy as an in-water

method. Furthermore, this should be equally true both for calibration and validation activities and bio-optical modeling requirements.

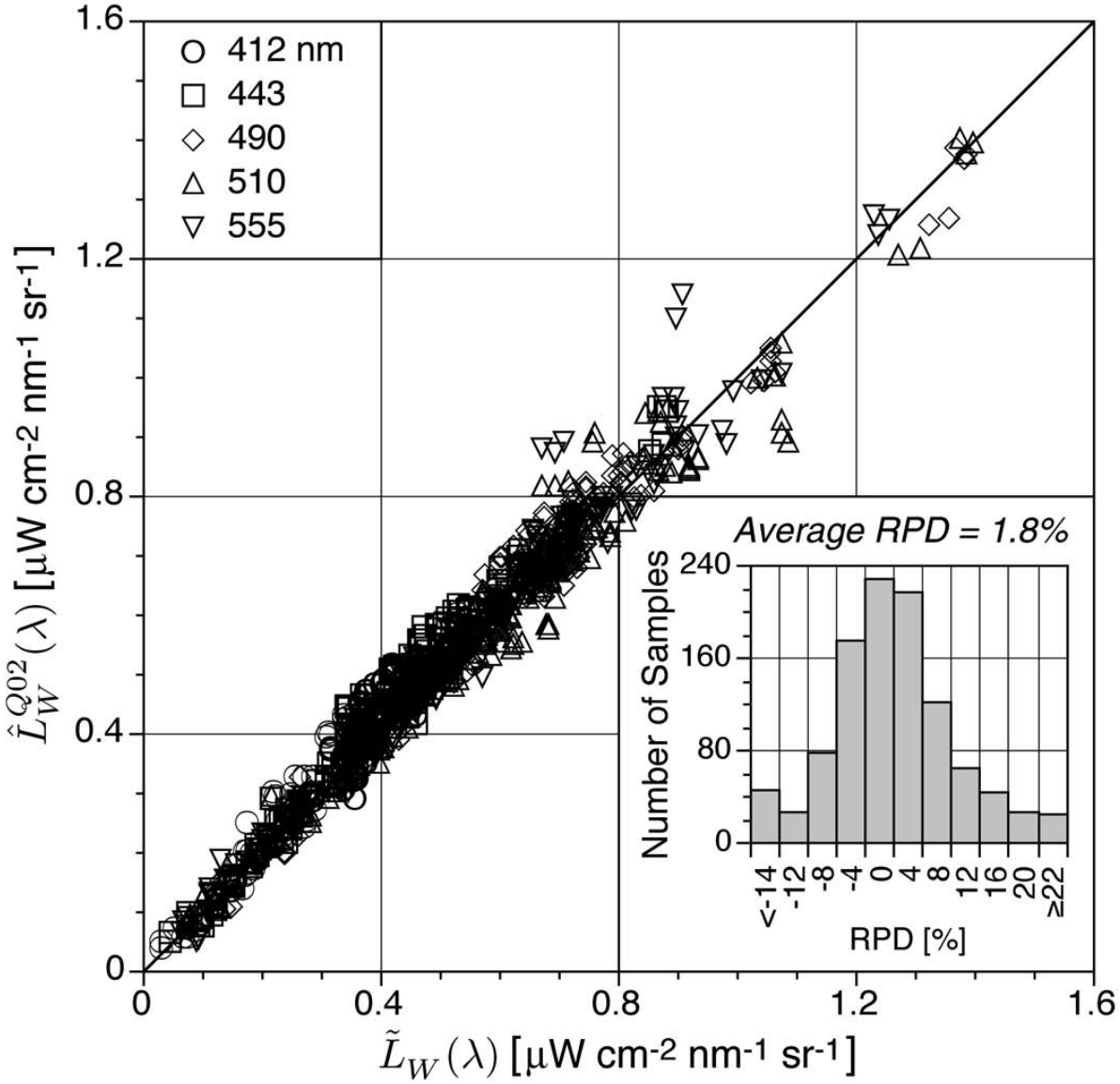

Fig. 8.4. An intercomparison of intercalibrated (*Q*-corrected) above-water determinations of water-leaving radiances, $\hat{L}_W^{Q02}(\lambda)$, with simultaneous in-water determinations, $\tilde{L}_W(\lambda)$, for Case-1 and Case-2 conditions. The data were collected at the AAOT under sampling geometries that avoided all platform perturbations and during the Adriatic Data collection for Research on marine Inherent and Apparent optical properties field campaign (conducted in 2000 and referred to hereafter as ADRIA-2000). The majority of the data are for Case-1 conditions (about 85%), and the Case-2 stations were close to the threshold between the two water typesas defined by Loisel and Morel (1998). The vast majority of all optical data were collected under clear-sky conditions, and the average environmental conditions were excellent: cloud cover was less than 2/10, wind speed was less than 5 m s^{-1}, and wave height was 0.3 m or less. Water depth at the AAOT is 17 m, wheras it ranged from 7.4–32.3 m during ADRIA-2000.

8.6 DATA ARCHIVE

The SIRREX-8 activity established that the immersion factors originally supplied with the SeaWiFS Field Team profiling equipment were significantly incorrect (by more than 10% in the blue part of the spectrum). Consequently, the entire archive of *in situ* optical measurements are being reprocessed. This activity has been coordinated with the production of a new optical data processor, so many of the data processing protocols that were refined during the investigations for the SIMBIOS project could be utilized. The reprocessing is in the final stages of quality assurance, and a preliminary assessment indicates a substantial improvement in many of the primary and bio-optical variables. A final set of water-leaving radiances and ancillary parameters for those campaigns that were not specialized experiments (like the tower perturbation investigations) will be delivered to the SeaWiFS Bio-Optical Archive and Storage System (SeaBASS) before the end of 2003.

REFERENCES

Aas, E., 1969: On Submarine Irradiance Measurements. *University of Copenhagen Report No. 6*, University of Copenhagen Institute for Physical Oceanography, Copenhagen, Denmark, 23 pp plus tables and figures.

Atkins, W.R.G., and H.H. Poole, 1933: The photo-electric measurement of the penetration of light of various wave lengths into the sea and the physiological bearing of results. *Phil. Trans. Roy. Soc. London,* **222**, 129–164.

Berger, F., 1958: Uber die ursache des “oberflacheneffekts” bei lichtmessungen unter wasser. *Wetter ü. Leben,* **10**, 164– 170 (translated from German).

Berger, F., 1961: Uber den “Taucheffekt” bei der lichtmessunguber und unter wasser. *Arch. Meteorol. Wien.,* **11**, 224–240 (translated from German).

Berthon, J-F., G. Zibordi, J.P. Doyle, S. Grossi, D. Van der Linde, and C. Targa, 2002: Coastal Atmosphere and Sea Time Series (CoASTS), Part 2: Data Analysis. *NASA Tech. Memo. 2002–206892,* Vol. **20**, S.B. Hooker and E.R. Firestone, Eds., NASA Goddard Space Flight Center, Greenbelt, Maryland, 25 pp.

Claustre, H., S.B. Hooker, L. Van Heukelem, J-F. Berthon, R. Barlow, J. Ras, H. Sessions, C. Targa, C. Thomas, D. van der Linde, and J-C. Marty, 2003: An intercomparison of HPLC phytoplankton pigment methods using *in situ* samples: Application to remote sensing and database activities. *Marine Chem.,* (accepted).

Fougnie, B., R. Frouin, P. Lecomte, and P-Y. Deschamp, 1999: Reduction of skylight reflection effects in the above-water measurement of diffuse marine reflectance. *Appl. Opt.,* **38**, 3,844–3,856.

Hooker, S.B., and W.E. Esaias, 1993: An overview of the Sea-WiFS project. *Eos, Trans., Amer. Geophys. Union,* **74**, 241–246. ,

Hooker, S.B., and C.R. McClain, 2000: The Calibration and Validation of SeaWiFS Data. *Prog. Oceanogr.,* **45**, 427–465.

Hooker, S.B., G. Zibordi, J-F. Berthon, D. D’Alimonte, S. Maritorena, S. McLean, and J. Sildam, 2001: Results of the Second Sea-WiFS Data Analysis Round Robin, March 2000 (DARR-00). *NASA Tech. Memo. 2001–206892,* Vol. **15**, S.B. Hooker and E.R. Firestone, Eds., NASA Goddard Space Flight Center, Greenbelt, Maryland, 71 pp.

Hooker, S.B., G. Lazin, G. Zibordi, and S. McLean. 2002a. An evaluation of above-and in-water methods for determining water-leaving radiances. *J. Atmos. Oceanic Technol.,* **19**, 486– 515.

Hooker, S.B., S. McLean, J. Sherman, M. Small, G. Lazin, G. Zibordi, and J.W. Brown, 2002b: The Seventh SeaWiFS Inter-calibration Round-Robin Experiment (SIRREX-7), March 1999. *NASA Tech. Memo. 2002–206892,* Vol. **17***,* S.B. Hooker and E.R. Firestone, Eds., NASA Goddard Space Flight Center, Greenbelt, Maryland, 69 pp.

Hooker, S.B.,, and A. Morel, 2003: Platform and environmental effects on above-and in-water determinations of water-leaving radiances. *J. Atmos. Oceanic Technol.,* **20**, 187–205.

Hooker, S.B., and G. Zibordi, 2003a: Advanced methods for characterizing the immersion factor of marine radiometers. *Appl. Opt.,* (submitted).

Hooker, S.B., and , 2003b: Platform perturbations in above-water radiometry. *Appl. Opt.,* (submitted).

Hooker, et al., 2003a: The Second SeaWiFS HPLC Analysis Round-Robin Experiment (SeaHARRE-2). *NASA Tech. Memo. 2003,* NASA Goddard Space Flight Center, Greenbelt, Maryland, (in prep.).

Hooker, S.B., G. Zibordi, J-F. Berthon, D. D'Alimonte, D. van der Linde, and J.W. Brown, 2003b: Tower-Perturbation Measurements in Above-Water Radiometry. *NASA Tech. Memo. 2003–206892, Vol. 23,* S.B. Hooker and E.R. Fire-stone, Eds., NASA Goddard Space Flight Center, Greenbelt, Maryland, 35 pp.

Hooker, S.B., and G. Zibordi, J-F. Berthon, and J.W. Brown, 2003c: Above-water radiometry in shallow, coastal waters. *Appl. Opt.,* (submitted).

Joint Global Ocean Flux Study, 1991: JGOFS Core Measurements Protocols. *JGOFS Report,* No. **6***,* Scientific Committee on Oceanic Research, 40 pp.

Loisel, H., and A. Morel, 1998: Light scattering and chlorophyll concentration in case 1 waters: A reexamination. *Limnol. Oceanogr.,* **43**, 847–858.

Mobley, C.D., 1999: Estimation of the remote-sensing reflectance from above-surface measurements. *Appl. Opt.,* **38**, 7,442– 7,455.

Morel, A., 1980: In-water and remote measurements of ocean color. *Bound.-Layer Meteorol.,* **18**, 177–201.

Morel, A., and L. Prieur, 1977: Analysis of variations in ocean color. *Limnol. Oceanogr***., 22**, 709–722.

Morel, A., and B. Gentili, 1996: Diffuse reflectance of oceanic waters, III. Implication of bidirectionality for the remote sensing problem. *Appl. Opt.,* **35**, 4,850–4,862.

Morel, A., and J.L. Mueller, 2002: "Normalized Water-Leaving Radiance and Remote Sensing Reflectance: Bidirectional Reflectance and Other Factors." In: J.L. Mueller and G.S. Fargion, Ocean Optics Protocols for Satellite Ocean Color Sensor Validation, Revision 3, Volume 2. *NASA Tech. Memo. 2002–210004/Rev3–Vol2,* NASA Goddard Space Flight Center, Greenbelt, Maryland, 183–210.

Morel, A., D.Antoine, and B. Gentilli, 2002: Bidirectional reflectance of oceanic waters: Accounting for Raman emission and varying particle scattering phase function. *Appl. Opt.,* **41**, 6,289–6,306.

Mueller, J.L., 2000: "Overview of Measurement and Data Analysis Protocols" In: G.S. Fargion and J.L. Mueller, Ocean Optics Protocols for Satellite Ocean Color Sensor Validation, Revision **2**. *NASA Tech. Memo. 2000–209966,* NASA Goddard Space Flight Center, Greenbelt, Maryland, 87– 97.

Mueller, J.L., 2002: "Overview of Measurement and Data Analysis Protocols." In: J.L. Mueller and G.S. Fargion, Ocean Optics Protocols for Satellite Ocean Color Sensor Validation, Revision 3, Volume **1**. *NASA Tech. Memo. 2002– 210004/Rev3–Vol1,* NASA Goddard Space Flight Center, Greenbelt, Maryland, 123–137.

Mueller, J.L., 2003: "Overview of Measurement and Data Analysis Methods." In: Mueller, J.L., and et al., Ocean Optics Protocols for Satellite Ocean Color Sensor Validation, Revision 4, Volume III: Radiometric Measurements and Data Analysis Protocols. *NASA Tech. Memo. 2003– 211621/Rev4–Vol.III*, NASA Goddard Space Flight Center, Greenbelt, Maryland, 1–20.

Mueller, J.L., and R.W. Austin, 1992: Ocean Optics Protocols for SeaWiFS Validation. *NASA Tech. Memo. 104566*, Vol. **5***,* S.B. Hooker and E.R. Firestone, Eds., NASA Goddard Space Flight Center, Greenbelt, Maryland, 43 pp.

Mueller, J.L. and R.W. Austin, 1995: Ocean Optics Protocols for Sea- WiFS Validation, Revision 1. *NASA Tech. Memo. 104566*, Vol. **25**, S.B. Hooker, E.R. Firestone, and J.G. Acker, Eds., Vol. 25, S.B. Hooker, E.R. Firestone, NASA Goddard Space Flight Center, Greenbelt, Maryand J.G. Acker, Eds., land, 66 pp.

Mueller, J.L., F. M«elin, S.B. Hooker, D. D'Alimonte, and B. Holben, 2003c: An autonomous above-water system for the vali dation of ocean color radiance data. *Trans. IEEE Trans. Geosci. Remote Sensing*., (accepted).

O'Reilly, J.E., S. Maritorena, B.G. Mitchell, D.A. Siegel, K.L. O'Reilly, J.E., S. Maritorena, B.G. Mitchell, D.A. Siegel, K.L. O'Reilly, J.E., S. Maritorena, B.G. Mitchell, D.A. Siegel, K.L. Carder, S.A. Garver, M. Kahru, and C. McClain, 1998: Ocean color chlorophyll algorithms for SeaWiFS, *J. Geo phys. Res.,* 103, 24,937–24,953.

O'Reilly, and 24 Coauthors, 2000: SeaWiFS Postlaunch Calibration and Validation Analyses, Part 3. *NASA Tech. Memo. 2000–206892, Vol. 11,* S.B. Hooker and E.R. Firestone, Eds., NASA Goddard Space Flight Center, 49 pp.

Petzold, T.J., and R.W. Austin, 1988: Characterization of MER 1032. *Tech. Memo. EN–001–88t*, Vis. Lab., Scripps Institution of Oceanography, La Jolla, California, 56 pp. plus appendices.

Rhea, W.J., and C.O. Davis, 1997: A coparison of the SeaWiFS chlorophyll and CZCS pigment algorithms using optical data from the 1992 JGOFS Equatorial Pacific Time Series. *Deep Sea Res. II,* 44, 1,907–1,925.

Smith, R.C., 1969: An underwater spectral irradiance collector. *J. Mar. Res.,* 27, 341–351.

Toole, D.A., D.A. Siegel, D.W. Menzies, M.J. Neumann, and R.C. Smith, 2000: Remote sensing reflectance determinations in the coastal ocean environment—impact of instrumental characteristics and environmental variability. *Appl. Opt.,* 39, 456–469.

Van der Linde, D., 2003: The AAOT Deployment Systems: An Overview. *EUR Report 20548 EN,* Joint Research Centre, Ispra, Italy, 13 pp.

Voss, K.J., J.W. Nolten, and G.D. Edwards, 1986: Ship shadow effects on apparent optical properties. *Proc. Soc. Photo Opt., Instrum. Eng.,* Ocean Optics XII, 2,258, 815–821.

Westlake, D.F., 1965: Some problems in the measurement of radiation under water: A review. *Photochem. Photobiol.,* 4, 849–868.

Zibordi, G., J.P. Doyle, and S.B. Hooker, 1999: Offshore tower shading effects on in-water optical measurements. *J. At mos. Ocean. Tech.,* 16, 1,767–1,779.

Zibordi, G., J-F. Berthon, J.P. Doyle, S. Grossi, D. van der Linde, C. Targa, and L. Alberotanza, 2002a: Coastal Atmosphere and Sea Time Series (CoASTS), Part 1: A Tower-Based Long-Term Measurement Program. *NASA Tech. Memo. 2002–206892, Vol. 19,* S.B. Hooker and E.R. Firestone, Eds., NASA Goddard Space Flight Center, Greenbelt, Maryland, 29 pp.

Zibordi, G., S.B. Hooker, J-F. Berthon, and D. D'Alimonte, 2002b: Autonomous above-water radiance measurements from an offshore platform: A field assessment experiment. *J. At mos. Oceanic Technol.,* 19, 808–819.

Zibordi, G., S.B. Hooker, J. Mueller, G. Lazin, 2003a: Characterization of the immersion factor for a series of underwater opti cal radiometers. *J. Atmos. Oceanic Technol.,* (accepted).

Zibordi, G.,D. D'Alimonte, D. van der Linde, S.B. Hooker, J.W. Brown, 2003b: New Laboratory Methods for Characterizing the Immersion Factors of Irradiance Sensors. *NASA Tech. Memo. 2003–206892, Vol. 26,* S.B. Hooker and E.R. Firestone, Eds., NASA Goddard Space Flight Center, Greenbelt, Maryland, 34 pp.

This Research was Supported by the NASA SIMBIOS Program

Hooker, S.B., and A. Morel, 2003: Platform and environmental effects on above-and in-water determinations of water-leaving radiances. *J. Atmos. Oceanic Technol.,* **20**, 187– 205.

Johnson, B.C., S.W. Brown, K.R. Lykke, C.E. Gibson, G. Fargion, G. Meister, S.B. Hooker, Brian Markham, and J.J. Butler, 2003: Comparison of cryogenic radiometry and thermal radiometry calibrations at NIST using multichannel filter radiometers. *Metrologia,* **40**, S216–S219.

Claustre, H., S.B. Hooker, L. Van Heukelem, J-F. Berthon, R. Barlow, J. Ras, H. Sessions, C. Targa, C. Thomas, D. van der Linde, and J-C. Marty, 2003: An intercomparison of HPLC phytoplankton pigment methods using *in situ* samples: Application to remote sensing and database activities. *Marine Chem.,* (accepted).

Zibordi, G., S.B. Hooker, J. Mueller, G. Lazin, 2003: Characterization of the immersion factor for a series of underwater optical radiometers. *J. Atmos. Oceanic Technol.,* (accepted).

McClain, C.R., G.C. Feldman, S.B. Hooker, 2003: An overview of the SeaWiFS project and strategies for producing a climate research quality global ocean bio-optical time series. *Deep Sea Res.,* (submitted).

Zibordi, G., F. Mélin, S.B. Hooker, D. D'Alimonte, and B. Holben, 2003: An autonomous above-water system for the validation of ocean color radiance data. *Trans. IEEE Trans. Geosci. Remote Sensing.,* (accepted).

Hooker, S.B., and G. Zibordi, 2003: Platform perturbations in above-water radiometry. *Appl. Opt.,* (submitted).

Hooker, S.B., and G. Zibordi, J-F. Berthon, and J.W. Brown, 2003: Above-water radiometry in shallow, coastal waters. *Appl. Opt.,* (submitted).

Hooker, S.B., and G. Zibordi, 2003: Advanced methods for characterizing the immersion factor of marine radiometers. *Appl. Opt.,* (submitted).

Hooker, S.B., G. Zibordi, J-F. Berthon, D. D'Alimonte, D. van der Linde, and J.W. Brown, 2003: Tower-Perturbation Measurements in Above-Water Radiometry. *NASA Tech. Memo. 2003–206892,* Vol. **23***,* S.B. Hooker and E.R. Fire-stone, Eds., NASA Goddard Space Flight Center, Greenbelt, Maryland, 35 pp.

Doyle, J., G. Zibordi, J-F. Berthon, D. van der Linde, and S.B. Hooker, 2003: Validation of an In-Water, Tower-Shading Correction Scheme. *NASA Tech. Memo. 2003–206892,* Vol. **25***,* S.B. Hooker and E.R. Firestone, Eds., NASA Goddard Space Flight Center, Greenbelt, Maryland, 32 pp.

Zibordi, G., D. D'Alimonte, D. van der Linde, S.B. Hooker, J.W. Brown, 2003: New Laboratory Methods for Characterizing the Immersion Factors of Irradiance Sensors. *NASA Tech. Memo. 2003–206892, Vol.* **26***,* S.B. Hooker and E.R. Firestone, Eds., NASA Goddard Space Flight Center, Greenbelt, Maryland, 34 pp.

Barlow, R., H. Sessions, N. Silulwane, H. Engel, S.B. Hooker, J. Aiken, J. Fishwick, V. Vicente, A. Morel, M. Chami, J. Ras, S. Bernard, M. Pfaff, J.W. Brown, and A. Fawcett, 2003: BENCAL Cruise Report. *NASA Tech. Memo. 2003– 206892,* Vol. **27***,* S.B. Hooker and E.R. Firestone, Eds., NASA Goddard Space Flight Center, Greenbelt, Maryland, 64 pp.

Hooker, S.B., L. Van Heukelem, C.S. Thomas, H. Claustre, J. Ras, L. Schl¬uter, J. Perl, C. Trees, V. Stuart, E. Head, R. Barlow, H. Sessions, L. Clementson, J. Fishwick, and J. Aiken, 2003: The Second SeaWiFS HPLC Analysis Round-Robin Experiment (SeaHARRE-2). *NASA Tech. Memo. 2003,* NASA Goddard Space Flight Center, Greenbelt, Maryland, (in prep.).

Chapter 9

Optimization Of Ocean Color Algorithms: Application To Satellite And In Situ Data Merging.

Stéphane Maritorena and David A. Siegel

Institute for Computational Earth System Science, UCSB, Santa Barbara, CA 93106-3060, USA

André Morel

Laboratoire de Physique et Chimie Marines, Villefranche Sur Mer, France

9.1 INTRODUCTION

The objective of our program is to develop and validate a procedure for ocean color data merging which is one of the major goals of the SIMBIOS project (McClain et al., 1995). The need for a merging capability is dictated by the fact that since the launch of MODIS on the Terra platform and over the next decade, several global ocean color missions from various space agencies are or will be operational simultaneously. The apparent redundancy in simultaneous ocean color missions can actually be exploited to various benefits. The most obvious benefit is improved coverage (Gregg et al., 1998; Gregg & Woodward, 1998). The patchy and uneven daily coverage from any single sensor can be improved by using a combination of sensors. Beside improved coverage of the global ocean the merging of ocean color data should also result in new, improved, more diverse and better data products with lower uncertainties. Ultimately, ocean color data merging should result in the development of a unified, scientific quality, ocean color time series, from SeaWiFS to NPOESS and beyond.

Various approaches can be used for ocean color data merging and several have been tested within the frame of the SIMBIOS program (see e.g. Kwiatkowska & Fargion, 2003, Franz et al., 2003). As part of the SIMBIOS Program, we have developed a merging method for ocean color data. Conversely to other methods our approach does not combine end-products like the subsurface chlorophyll concentration (chl) from different sensors to generate a unified product. Instead, our procedure uses the normalized water-leaving radiances ($L_{wN}(\lambda)$) from single or multiple sensors and uses them in the inversion of a semi-analytical ocean color model that allows the retrieval of several ocean color variables simultaneously. Beside ensuring simultaneity and consistency of the retrievals (all products are derived from a single algorithm), this model-based approach has various benefits over techniques that blend end-products (e.g. chlorophyll): 1) it works with single or multiple data sources regardless of their specific bands, 2) it exploits band redundancies and band differences, 3) it accounts for uncertainties in the $L_{wN}(\lambda)$ data and, 4) it provides uncertainty estimates for the retrieved variables.

9.2 RESEARCH ACTIVITIES

Development of an ocean color database and algorithm development

Over the past 3 years, we have assembled a large comprehensive in situ ocean color data set that contains inherent (IOP) and apparent (AOP) optical properties as well as chlorophyll a concentration data from various locations. This database is designed for ocean color algorithm development and is well suited for semi-analytical algorithm development in particular. Since it contains both IOPs and AOPs, this database is better suited for semi-analytical algorithms development than data sets like the one used during SeaBAM (O'Reilly et al., 1998) which only contained chl and remote sensing reflectance data. Most of the data included in the database come from the NASA SIMBIOS SeaBASS archive but several investigators

have provided data sets or subsets directly to us. Various quality control (QC) procedures have been developed (Fargion & McClain, 2003) to identify corrupted data, outliers or specific bio-optical situations. The database contains chlorophyll a concentration, diffuse attenuation coefficients, L_{wN}□, particulate backscattering and component absorption (phytoplankton, detrital, dissolved). Most of the absorption data are hyperspectral. The current status of the IOP/AOP data set is described in Table 9.1.

Table 9.1: Status of the AOP/IOP data set. The first number in each cell indicates the number of stations for which data are available. The numbers in parentheses indicate the number of available wavelengths

EXPERIMENT	Chl a	Kd	Rrs	bb	ad	ag	ap
AAOT	94	-	35 (5)	-	-	-	-
Aerosols Indoex	53	3367 (12)	5309 (6)	-	70 (225)	70 (200)	73 (225)
Ace-Asia	116	696 (18)	903 (18)	780 (6)	48 (225)	69 (200)	48 (225)
AMLR	268	1060 (18)	1302 (18)	-	101 (225)	91 (200)	101 (225)
Atlantic Meridional Transect	281	281 (5)	281 (5)	-	-	-	-
Bermuda Bio-Optics Project	406	4024 (16)	6505 (12)	-	77 (520)	77 (520)	77 (520)
Arc00	159	-	7262 (5)	-	-	-	-
BIOCOMPLEXITY	300	-	6505 (13)	-	74 (500)	74 (315)	74 (500)
CALCOFI	430	938 (12)	1064 (23)	-	159 (225)	130 (200)	143 (225)
CaTS	11	-	16 (5)	-	-	-	-
CoJet	53	-	74 (15)	-	-	-	-
CSC	23	-	23 (5)	-	-	-	-
DOER	10	-	10 (5)	-	-	-	-
ECOFRONT	37	3142 (6)	2168 (7)	-	16 (225)	16 (200)	16 (225)
Ecology of Harmful Algal Blooms	429	-	246 (200)	-	422 (200)	398 (200)	422 (200)
EPIC	152	1988 (5)	3179 (5)	-	-	-	-
JGOFS-EQPAC	125	1785-	1737 (5)	-	-	-	-
Globec Biomapper	45	-	-	-	43 (200)	43 (200)	43 (200)
GOCAL	NA	-	1328 (7)	28 (6)	-	-	-
NASA-Gulf of Maine	148	-	-	-	150 (200)	137 (200)	150 (200)
NOAA-Gulf of Maine	316	-	-	-	-	-	-
JGOFS-SIO	89	1671 (12)	1875 (12)	-	23 (225)	23 (225)	23 (225)
JGOFS-Arabian Sea	2693	3085 (5)	3083 (5)	-	-	-	-
Kieber Photochemistry 2002	427	1791 (5)	1772 (5)	-	-	-	-
Lab2000	51	-	3191 (5)	-	-	-	-
Lab1997	204	-	-	-	-	-	-
Lab1996	42	-	113 (12)	-	122 (500)	74 (500)	122 (500)
LMER-TIES	237	-	76 (7)	-	85 (250)	85 (200)	85 (250)
MBARI	34	-	34 (5)	-	-	-	-
MOCE	13	-	13 (5)	-	-	-	-
North Atlantic Bloom Experiment	110	609 (5)	431 (5)	-	-	-	-
Ocean Research Consortium	17	-	18 (10)	14 (6)	16 (470)	16 (470)	16 (470)
Plumes and Blooms	786	7702 (7)	10330 (12)	3867 (7)	500 (13)	431 (13)	505 (13)
ROAVERRS	162	-	162 (5)	-	-	-	-
Sea of Japan	54	593 (12)	777 (12)	666 (6)	51 (225)	51 (200)	51 (225)
Scotia Prince Ferry	7420	-	60 (5)	7147 (3)	-	6591 (9)	6478 (9)
Tongue of the Ocean	88	-	86 (200)	16 (6)	95 (200)	95 (225)	95 (200)
World Ocean Circulation Experim	68	-	68 (5)	-	-	-	-
Total Measurements	**15951**	**32732**	**60036**	**12518**	**2052**	**8471**	**8522**

The IOP/AOP database is designed in part to help the development of our merging model. The transformation of the model into a fully hyperspectral mode (which would make it usable right away with any sensor) and improved parameterizations of some of the components of the model are the major modifications we are trying to implement. A preliminary version of the hyperspectral model has been developed and optimized using data from the AOP/IOP database. Although it shows some good overall results for all three retrieved variables this preliminary hyperspectral version does not always perform well

at the extremes of the chlorophyll range (either in very clear or very rich waters). This new version of the model still requires some work and a more conservative, step-by-step approach is now used for its development.

Satellite Ocean Color Data Merging

Our approach for ocean color data merging is based on the inversion of a semi-analytical model that relates L_{wN} to the backscattering and absorption coefficients (Eq. 9.1) as described in Gordon et al. (1988).

$$L_{wN}(\lambda) = \frac{t\,F_0(\lambda)}{n_w^2} \sum_{i=1}^{2} g_i \left(\frac{b_{bw}(\lambda) + b_{bp}(\lambda)}{b_{bw}(\lambda) + b_{bp}(\lambda) + a_w(\lambda) + a_{ph}(\lambda) + a_{cdm}(\lambda)} \right)^i \qquad (9.1)$$

Each of the non-water components in a and b_b is expressed as a known shape function with an unknown magnitude:

$$a_{ph}(\lambda) = \text{Chl}\, a_{ph}^*(\lambda) \qquad (9.2)$$

$$a_{cdm}(\lambda) = a_{cdm}(443) \exp(-S(\lambda - 443) \qquad (9.3)$$

$$b_{bp}(\lambda) = b_{bp}(443)\,(\lambda/443)^{-\eta} \qquad (9.4)$$

where t, n_w, g_i, $F_o(\lambda)$, $a_w(\lambda)$ and $b_{bw}(\lambda)$ at taken from the literature whereas η, S, $a_{ph}^*(\lambda)$ were determined by "tuning" the model against a large in situ data set (Maritorena et al., 2002). A non-linear least-square fitting technique is used to solve for the unknowns (chl, $a_{cdm}(443)$ and $b_{bp}(443)$) from $L_{wN}(\lambda)$ data at 4 or more wavelengths. The model also provides uncertainty estimates for each of the retrievals using a linear approximation to the calculation of non-linear regression inference regions (Bates & Watts, 1988). The model, hereafter referred to as the GSM01 model, is fully described in Garver & Siegel (1997) and Maritorena et al. (2002).

Since the model retrievals are generated using a curve-fitting technique that minimizes the least-squares differences between the measured and modeled $L_{wN}(\lambda)$, it is straightforward to use the GSM01 model with multiple data sets like in data merging. When multiple data sets are used (e.g. two or more sensors have L_{wN} measurements over a given pixel), the $L_{wN}(\lambda)$ data from all available sources are concatenated (as are the relevant wavebands information) allowing the curve-fitting step to be conducted with more data points than with a single source. When data sources have different bands, the fitting procedure also benefits from an increased spectral resolution. A key aspect of the procedure is that there is no transformation or averaging of the input L_{wN} data, they are used "as is" in the curve-fitting technique. A schematic of the input and output products of the merging model is presented in figure 9.1.

Our model-based approach for ocean color data merging was first tested using SeaWiFS and MOS data and results were presented during the SIMBIOS science Team meeting in Baltimore (Jan. 15-17, 2002). Since then, we have successfully used SeaWiFS and MODIS data (from both the Terra and Aqua platforms). We have tested our merging approach using daily level-3 data from SeaWiFS (reprocessing # 4, 9 km) and MODIS (collection # 4, 4.6 km) for 18 dates between December 4, 2000 and March 22, 2003. Only the MODIS "best quality" data (i.e. quality 0) were used during these tests. Since the SeaWiFS and MODIS $L_{wN}(\lambda)$ data products have different spatial resolution, it is necessary to first adapt the MODIS data to the SeaWiFS resolution by averaging four 4.6 km bins into a 9 km bin and to have the 2 data sources set to a common binned grid. The data are processed between 65 degrees North and 65 degrees South. We have focused most of our effort on the period for which MODIS Terra collection # 4 products are validated (11/1/2000-3/19/2002). Some data outside this time window were also used to illustrate SeaWiFS/Terra/Aqua data merging and to assess improvement in coverage when merging 3 different ocean color data sources.

9.3 RESEARCH RESULTS

The aim of our SIMBIOS work is to demonstrate the feasibility of an ocean color data merging procedure based on a semi-analytical mode that uses $L_{wN}(\lambda)$ data from one or more sources. It is out of the scope of this report to document the accuracy of the model retrievals with in situ or satellite data (but see Maritorena et al., 2002; Siegel et al., 2002 and Siegel et al., 2003. Examples of global maps of chlorophyll a concentration, $a_{cdm}(443)$ and $b_{bp}(443)$ generated by the GSM01 merging model with SeaWiFS and MODIS-Terra $L_{wN}(\lambda)$ data are presented in figure 9.2. Global maps of chl, $a_{cdm}(443)$ and the $b_{bp}(443)$ images generated by the GSM01 merging model using the Terra and SeaWiFS data show very good consistency overall (Maritorena et al., 2003). In general, the retrieved fields do not show discontinuities when the model switched from an area with a single data source to an area where both SeaWiFS and MODIS $L_{wN}(\lambda)$ data were used. This reflects the generally good agreement between the $L_{wN}(\lambda)$ data from both sources and the robustness of the model. The level of agreement between the two sensors also has an influence on the estimated uncertainties of the derived products. When considering the pixels that are covered by both sensors, a very large majority of them show reduced uncertainties in the merged products compared to those generated from a single data source. Figure 9.3 shows the frequency distribution of the ratio of the Chl uncertainties using either SeaWIFS or MODIS L_{wN} data alone over the Chl uncertainties when both sources are used. Overall, the uncertainties tend to decrease when multiple sources are used and this is true for all 3 products generated by the GSM01 model. This decrease in the uncertainties of the derived products is observed for all products and at all the dates we have processed. In the worst case, 70% of the pixels showed lower uncertainties in the merged products. Uncertainties are generally higher in the merged products when L_{wN} data do not agree well between the data sources.

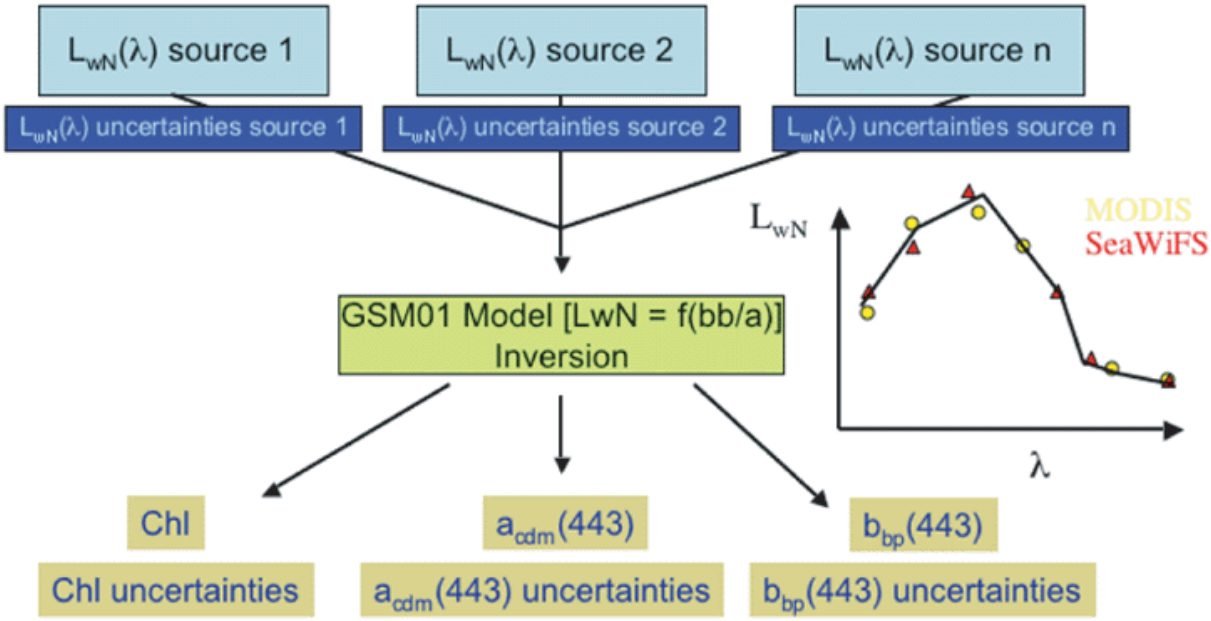

Figure 9.1: Schematic of the input and output data of the semi-analytical ocean color merging model.

This is illustrated in figure 9.4 where $L_{wN}(443)$ from both sensors are compared when uncertainties improved in the merged product (merged/unmerged uncertainty ratio of 0.5 or less) and when they got worse (uncertainty ratio > 1). When the uncertainties are lower in the merged product, the agreement between both sets of $L_{wN}(\lambda)$ is generally very good with most of the data points on or very close to the 1:1 line (figure 9.4 shows the 443 data but this is true for all bands). When the uncertainties were higher in the

merged images, the $L_{wN}(\lambda)$ data showed some clear differences between SeaWiFS and MODIS. Areas where the products uncertainties are actually higher in the merged image are frequently next to gaps caused by sun glint, gaps between the swaths or clouds. They also appear to be mostly located in the south hemisphere. Further analyses are needed to assess what causes these features.

Improvement in coverage is obvious. The daily surface area effectively covered by any individual sensor depends upon various factors such as the sensor's technical and orbital characteristics, sun glint, cloud cover and season. The increased coverage that results from the use of multiple data sources is illustrated in figure 9.5 for the 18 dates we have used. Daily coverage jumps from ~12-15% of the ocean surface (in the 65N to 65S range) when SeaWiFS is used alone to ~25% when it is used with MODIS-Terra. When MODIS-Aqua data are used in the merging process along with SeaWiFS and Terra the daily percentage coverage reaches ~30-35% to the ocean surface. These numbers agree well with those derived from a theoretical analysis prior to SeaWiFS and MODIS launches (Gregg and Woodward, 1998) as well as with those obtained by the SIMBIOS Project with their Level-3 merged chlorophyll product (Franz et al.).

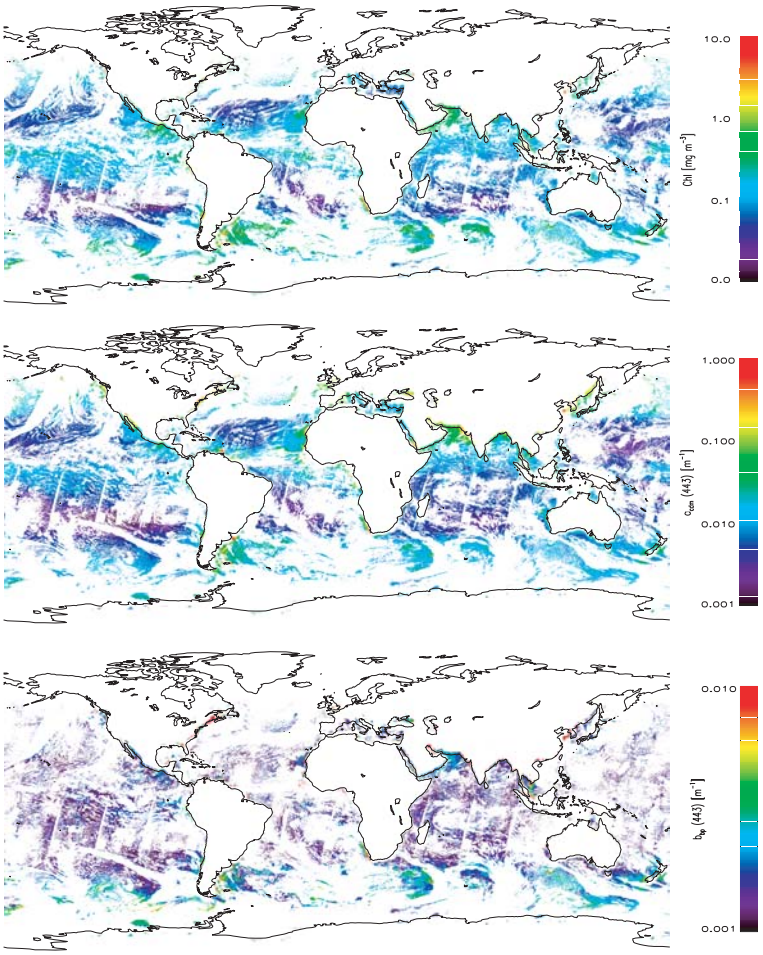

Figure 9.2: Example of daily images (December 4, 2000) of chl (upper panel), $a_{cdm}(443)$ (center panel) and $b_{bp}(443)$ (lower panel) generated by the GSM01 merging model using daily level-3 $L_{wN}(\lambda)$ data from SeaWiFS and MODIS-Terra.

The absence of marked discontinuities in the mapped product and the lower products uncertainties are two important results. At this point, it should be mentioned that some of the features of our merging approach cannot be used to their full efficiency mostly because the MODIS data are not fully characterized or stabilized. For example, the direct use of all available L_{wN} data in the fitting procedure assumes they agree well and have similar or close uncertainty levels and that none of the data sources contains noticeable

bias. This may not be always true. Although not used in the results presented here, the merging model has the ability of weighting each individual $L_{wN}(\lambda)$ data to insure that the best observations are given a higher weight in the fitting procedure that leads to the derivation of the retrievals. Uncertainties ($\sigma_i(\lambda_j)$) of input $L_{wN}(\lambda)$ can be accounted for in the the least squares minimization (LSM) procedure as

$$LSM = \sum_{i=1}^{N_{sat}} \sum_{j=1}^{N_{\lambda i}} \left[\frac{L_{wN\text{-}i}(\lambda_j)_{mod.} - L_{wN\text{-}i}(\lambda_j)_{meas.}}{\sigma_i(\lambda_j)} \right]^2 \qquad (9.5)$$

where N_{sat} is the number of data source and $N\lambda$ is the number of bands for each source. This has not yet been used mostly because the uncertainties associated with the MODIS bands of Terra and Aqua cannot yet be fully assessed in time and space. This requires matchup analyses from a large and diverse set of in situ and satellite data. These analyses are available for SeaWiFS but more matchup points are needed to complete the analysis for the MODIS data. It is also necessary to have some knowledge of the uncertainties variability in space and time. Once the characterization of Terra and Aqua is detailed enough, it should be possible to implement uncertainty weighting functions. A consistent BRDF correction scheme for the sensors involved in the data merging would also represent an improvement and upcoming reprocessings of SeaWiFS and MODIS data should take care of that particular aspect.

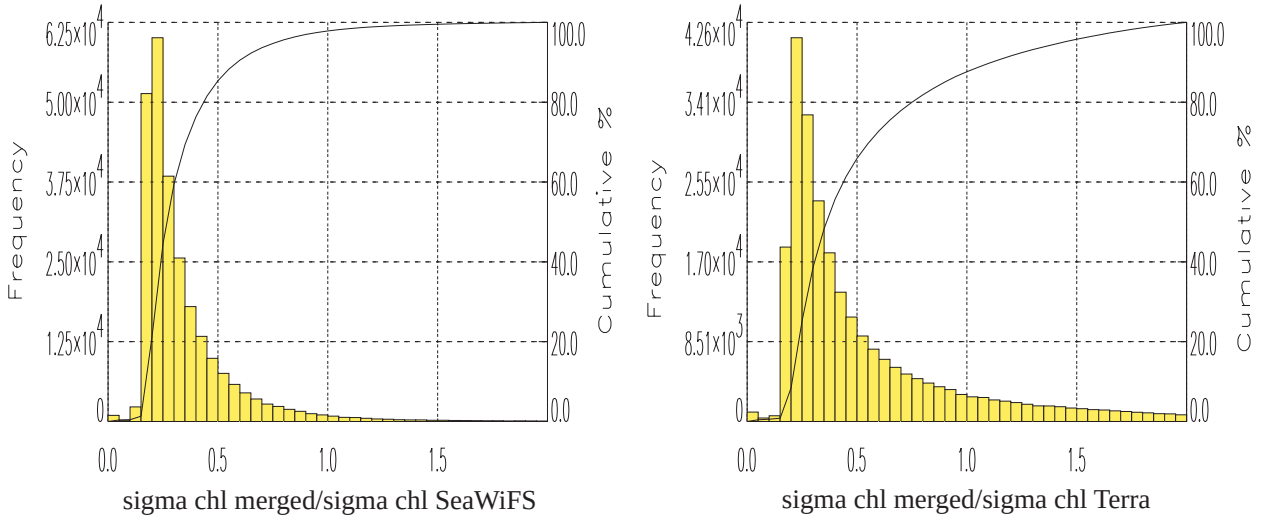

Figure 9.3: Frequency distribution of the ratio of the chl uncertainties using either SeaWiFS or MODIS-Terra L_{wN} data alone (December 4, 2000) over the chl uncertainties when both sources are used (for the same pixels). Ratios < 1 show an improvement in the uncertainties of the merged products.

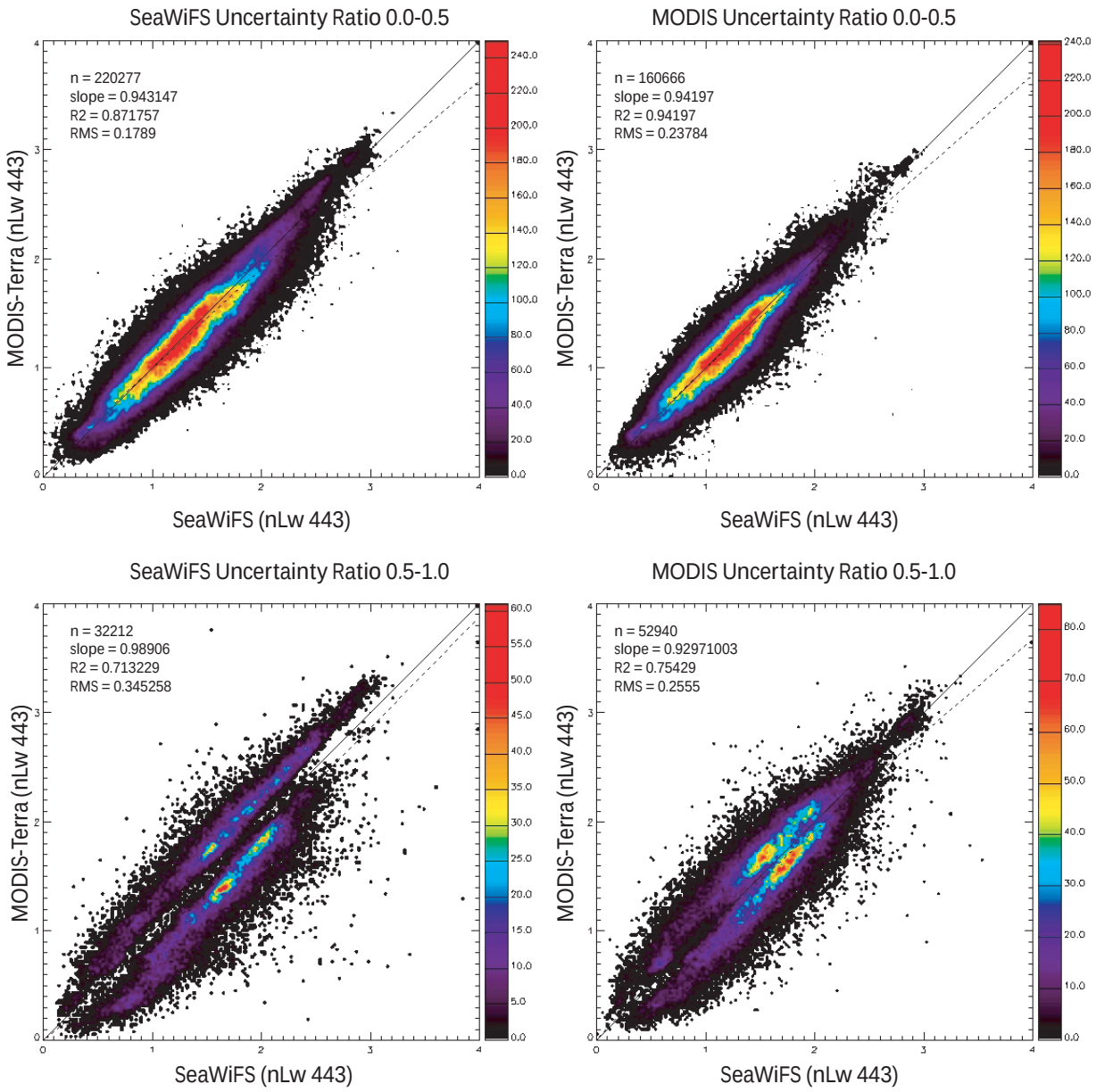

Figure 9.4: Comparison of $L_{wN}(443)$ data from SeaWiFS and MODIS-Terra data when uncertainties improved in the merged chl product (merged/unmerged uncertainty ratio of 0.5 or less, upper panels) and when they got worse (uncertainty ratio > 1, lower panels).

In this project, we have demonstrated that ocean color data merging can effectively be conducted using L_{wN} data and the inversion of a semi-analytical algorithm. The method can be applied straightforwardly to any suite of ocean color sensors. Beside the feasibility aspect, the improvement in daily coverage and the lower uncertainties in the merged products are two important results of our work. Some refinements (e.g. weighting functions based on the uncertainty levels of the input $L_{wN}(\lambda)$ data, BRDF correction) can be added to the current approach in the future when some of the satellite data will be more mature

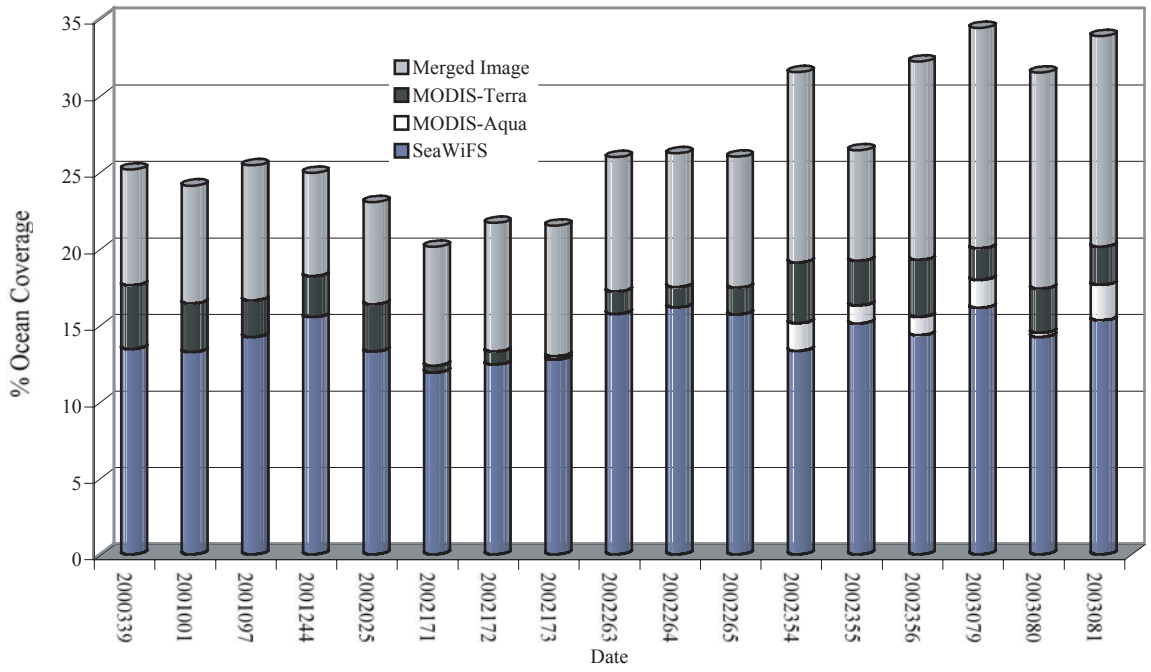

Figure 9.5: Daily coverage resulting from the merging of SeaWiFS, MODIS-Terra and MODIS-Aqua for the 18 dates used in this study. The coverage is computed as the percentage of the total ocean area (between 65 degrees North and 65 degrees South).

REFERENCES

Bates, D.M., and D.G. Watts, 1988: *Nonlinear Regression Analysis and its Applications*. Wily, 365 pp.Garver, S.A., and D.A. Siegel, 1997: Inherent optical property inversion of ocean color spectra and its biogeochemical interpretation: I. Time series from the Sargasso Sea. *J. Geophys. Res.*, **102**, 18,607-18,625.

Fargion G.S. and C.R. McClain, 2003: SIMBIOS Project Annual Report 2002, *NASA Technical Memorandum*, **TM-2003-211622**, NASA/GSFC, Greenbelt, Maryland, p157.

Franz B.A., J.G. Wilding and J.M. Gales, 2003: Operational Merging of MODIS and SeaWiFS Ocean Color Products at Level-3. In "MODIS Validation, Data Merger and Other Activities by the SIMBIOS Project:2002-2003", Fargion G.S. and C.R. McClain, NASA Technical Memorandum, TM-2003-, NASA/GSFC, Greenbelt, Maryland, (In Press).

Garver, S.A., and D.A. Siegel, 1997: Inherent optical property inversion of ocean color spectra and its biogeochemical interpretation: I. Time series from the Sargasso Sea. *J. Geophys. Res.*, 102, 18,607-18,625.

Gordon, H.R., O.B. Brown, R.H. Evans, J.W. Brown, R.C. Smith, K.S. Baker, and D.K. Clark. 1988: A semi-analytic radiance model of ocean color. *J. Geophys. Res.,* **93**, 10,909-10,924.

Gregg, W.W., W.E. Esaias, G.C. Feldman, R. Frouin, S.B. Hooker, C.R. McClain and R.H. Woodward. 1998: Coverage opportunities for global ocean color in a multimission era. IEEE Transactions On Geoscience And Remote Sensing, **36** :1620-1627.

Gregg, W.W. and R.H. Woodward. 1998: Improvements in coverage frequency of ocean color: Combining data from SeaWiFS and MODIS. IEEE Transactions On Geoscience And Remote Sensing, **36** :1350-1353.

Kwiatkowska, E.J. & G.S. Fargion, 2003. Merger of ocean color data from multiple satellite missions within the SIMBIOS project. Ocean remote sensing and applications, R. Frouin, Y. Yuan and H. Kawamura [Eds.], Proceedings of SPIE, Vol. **4892**, 168-182.

McClain, C.R., W. Esaias, G. Feldman, R. Frouin, W. Gregg and S. Hooker. 2002: The Proposal for the NASA Sensor Intercalibration and Merger for Biological and Interdisciplinary Oceanic Studies (SIMBIOS) Program, 1995. NASA Technical Memorandum, *TM-2002-210008*, NASA/GSFC, Greenbelt, Maryland, p54.

Maritorena S., D.A. Siegel and A. Peterson. 2002: Optimization of a Semi-Analytical Ocean Color Model for Global Scale Applications. *Applied Optics*. **41**(15): 2705-2714.

Maritorena, S., D.A. Siegel and D.B. Court, 2003: Ocean Color Data Merging Using a Semi-Analytical Algorithm. In preparation for Remote sensing of Environment.

O'Reilly J. E., S. Maritorena, B. G. Mitchell, D. A. Siegel, K. L. Carder, S. A. Garver, M. Kahru and C. R. McClain. 1998. Ocean Color Chlorophyll Algorithms for SeaWiFS. *J. Geophys. Res.*, **103**(C11): 24,937-24,953.

Siegel, D.A., S. Maritorena, N.B. Nelson, D.A. Hansell & M. Lorenzi-Kayser. 2002. Global Distribution and Dynamics of Colored Dissolved and Detrital Organic Materials. *Journal of Geophysical Research*. **107**(C12): 10.1029/2001JC000965.

Siegel, D.A., S. Maritorena, N.B. Nelson, 2003: Independence and interdependencies of ocean optical properties viewed using SeaWiFS. In preparation for *Journal of Geophysical Research*.

This Research was Supported by
the NASA Contract # 00196

Publications

Behrenfeld, M.J., E. Boss, D.A. Siegel and D.M. Shea, 2003: Global remote sensing of phytoplankton physiology. Submitted to *Science*.

Chomko, R.M., H.R. Gordon, S. Maritorena and D.A. Siegel, 2003: Simultaneous determination of oceanic and atmospheric parameters for ocean color imagery by spectral optimization: a validation. *Remote Sensing of the Environment*, **84**, 208-220.

Maritorena S., D.A. Siegel & A. Peterson. 2002: Optimization of a Semi-Analytical Ocean Color Model for Global Scale Applications. *Applied Optics*. 41(15): 2705-2714.

Maritorena, S., D.A. Siegel and D.B. Court, 2003: Ocean Color Data Merging Using a Semi-Analytical Algorithm. In preparation for Remote sensing of Environment.

Morel A. and S. Maritorena. 2001: Bio-optical properties of oceanic waters: a reappraisal. *J. Geophys. Res.*, 106(C4) : 7163-7180.

Siegel, D.A., S. Maritorena, N. B. Nelson, D.A. Hansell and M. Lorenzi-Kayser, 2002: Global ocean distribution and dynamics of colored dissolved and detrital organic materials. *Journal of Geophysical Research*, **107**, 3228, DOI: 10.1029/2001JC000965.

Siegel, D.A., S. Maritorena, N.B. Nelson, 2003: Independence and interdependencies of ocean optical properties viewed using SeaWiFS. For *Journal of Geophysical Research*.

Chapter 10

The Marine Fast-Rotating Shadow-band Network: Status Report and New Retrieval Techniques

Mark A. Miller, R.M Reynolds, A. Vogelmann and M.J. Bartholomew
The Brookhaven National Laboratory, Earth Systems Science Division, New York

10.1 INTRODUCTION

The radiation transfer characteristics of certain types of aerosols and mixtures of aerosols found over the world's oceans are poorly known. To simulate the radiative impacts of these aerosols requires detailed knowledge of five basic physical characteristics: the size distribution, chemical composition, optical thickness, single scattering albedo, and the asymmetry parameter. The single scattering albedo describes the total amount of incoming energy that is scattered by the aerosol particle and the asymmetry parameter describes the angular distribution of this scattered energy relative to the incident direction. Given this information, it is possible to accurately simulate the interaction of these aerosols with incoming solar radiation and the radiant energy scattered into space from the upper layers of the ocean, which is known as the water-leaving radiance. At present, the atmospheric correction schemes that are applied to satellite ocean color measurements are based primarily on the results of radiation transfer codes, which are supplied information about the physical characteristics of the aerosols from measurements made in the late 70's (Gordon and Wang, Shettle and Fenn). These aerosol measurements and the radiation-transfer-based atmospheric correction algorithms that result from them have been recently shown to be inadequate to describe the observed distribution of Angstrom Exponent that has resulted from a subset of the SIMBIOS measurements (Knoblespiesse *et al*., 2003). This implies that the aerosol models that are currently used to develop atmospheric correction algorithms do not adequately describe the physical characteristics of some of the aerosols that are present in the marine environment.

At the onset of SIMBIOS, there were virtually no aerosol optical thickness measurements from over the world's oceans. This lack of data was due mostly to a lack of appropriate instrumentation to make the measurements on a routine basis. To address this deficiency, SIMBIOS deployed newly developed off-the-shelf hand held radiometers (Microtops) and funded the development of a marine shadow-band radiometer. A network of ship-mounted marine shadow-band radiometers (FRSRs) and broadband radiometers have been deployed over the past five years on several backbone ships, along with periodic ships of opportunity, as part of the atmospheric correction exercises conducted by SIMBIOS (Reynolds *et al*., 2002). These radiometers operate continuously and automatically during daylight hours. As a result of these developments and the SIMBIOS program, a relatively large database of aerosol optical thicknesses measured from ships at sea has been amassed. To date, there are over 150 independent cruises in the FRSR database, ranging in duration from a week to nearly two years. Data have been collected from all three oceans, as well as during important field campaigns such as Aerosols99, INDOEX, Nauru99, ACE-Asia, and the Northeast Aerosol Characterization Experiment (Voss *et al*. 2001; Quinn *et al*., 2001). The database consists of over 140,000 individual measurements of the radiation budget over the world's oceans, including approximately 50,000 measurements of aerosol optical thickness in clear and partly cloudy skies.

The fundamental measurements made by the FRSRs in the network are the direct-normal irradiance and diffuse irradiance in six 10-nm wide channels that span the visible and near-infrared wavelengths (440 nm, 500 nm, 610 nm, 660 nm, 870 nm, and 936 nm) and a broadband channel. These measurements are complemented by broadband solar and infrared irradiance using standard Eppley pyranometers and pyrgeometers. Most importantly, a thorough evaluation of FRSR measurement uncertainty has shown that the accuracy of FRSR aerosol optical thickness measurements is approximately 0.02-0.03 (Miller *et al*., 2003). It has also been shown that the accuracy of FRSR measurements of the Angstrom Exponent is

strongly dependent on the aerosol optical thickness such that measurements in polluted air masses are more accurate than those made in clean maritime conditions.

An important and, currently, untapped resource within the database is the potential ability of the FRSR diffuse irradiance field to enable retrievals of the single scattering albedo and asymmetry parameter, and to evaluate atmospheric correction models. At present, a retrieval algorithm for the single scattering albedo has been developed and tested on FRSR data collected during ACE-Asia, as detailed in this report. Examples of model evaluation exercises using FRSR diffuse and global data have been reported in previous SIMBIOS TMs and will not be discussed here. The results of these two efforts are presented in this report. The report also provides a final summary of current status of the network and a summary of recommendations for future activities based on the past five years of operation.

10.2. RETRIEVING THE AVERAGE SINGLE SCATTERING ALBEDO USING THE FRSR

This section details our initial attempt to retrieve information in addition to the aerosol optical thickness about the radiation transfer characteristics of the aerosol in the column. Specifically, we have worked with Andy Vogelmann, a NASA and ARM PI, to develop a new single-scattering albedo retrieval scheme for the FRSR. While this work is in the development phase, we are relatively encouraged by our early results.

The ratio of direct-to-diffuse radiation for each FRSR channel is effectively an aggregate scattering property that combines the effects of the single-scattering albedo and the scattering phase function. The challenge is to untangle these two parameters for a given solar zenith angle and aerosol optical depth. This problem was first addressed by Herman *et al*. (1975) and King and Herman (1979), who were able to retrieve surface albedo and aerosol absorption using prescribed aerosol optical models. Recent work by Anikin et al. (2002) provide an elegant set of closed equations that parameterize the direct-diffuse ratio in terms of the aerosol optical depth, single-scattering albedo, asymmetry parameter, and a set of tuned coefficients.

We have tested these equations and found them to provide excellent agreement with Modtran multiple scattering radiative transfer calculations for the aerosol types within the Modtran database. However, inverting these equations to obtain the aerosol single-scattering albedo requires the aerosol asymmetry parameter, which they obtain from a parameterization based on the Angstrom exponent. The parameterization captures the first-order size-dependence of the asymmetry parameter, but necessitates having sufficient prior knowledge of the aerosol refractive index, which again would be difficult for our application. Several innovative studies have developed methods for retrieving the aerosol single-scattering properties by inverting sky radiances obtained from specific angles relative to the Sun (e.g., the principle plane and almucantar) that have been extremely successful (Nakajima *et al.*, 1996; Dubovik and King, 2000; Devaux *et al*., 1998; Gordon and Zhang, 1995; Zhang and Gordon, 1997). However, it has been found to be very difficult to apply these techniques to ship data owing to the difficulty of scanning the required sky planes on a rolling and pitching platform (Smirnov *et al*., 2000).

The fundamentals of our trial approach are based on the original direct-diffuse approach (Herman et al., 1975; King and Herman, 1979) as rendered by Anikin et al. (2002). This approach will eventually be augmented by the generalized radiance considerations provided in the formulations by Devaux et al. (1998), Gordon and Zhang (1995) and Zhang and Gordon (1997), who developed their retrievals to be independent of the aerosol model information. Relative to other research, our retrieval problem is greatly simplified owing to the low and relatively constant ocean surface albedo. As for Anikin *et al*. (2002), we will also use the Angstrom exponent, obtained from the direct-beam measurements, to obtain a general indication of the aerosol particle size (within a specific aerosol type). Fortunately, the retrieved single-scattering albedos do not appear overly sensitive to the asymmetry parameter. For example, sensitivity studies indicate that a ±0.05 uncertainty in the aerosol asymmetry parameter results in only a ± 0.02 uncertainty in the retrieved single-scattering albedo.

Results from an initial attempt to use the FRSR diffuse irradiance in a retrieval procedure are shown in Figure 10.1. Results from the retrieval are compared with surface measurements of the single scattering albedo made on the Ron Brown during Ace-Asia. As the figure shows, the retrieval algorithm is

reasonably successful on days 95-100, 107 and 109, but fails on days 102, 103, and 104. The reasons for failure on these days are under investigation, but the overall results are quite encouraging.

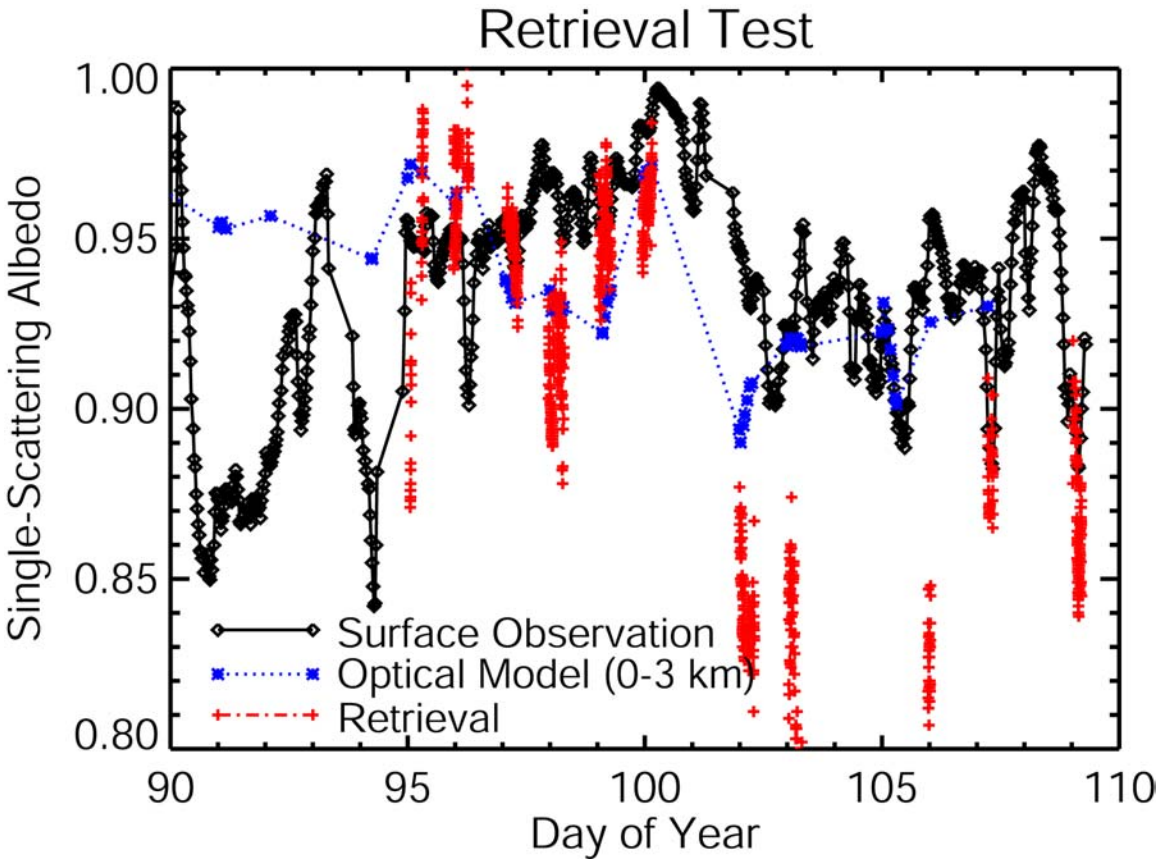

Figure 10.1: Results from a prototype retrieval of the single scattering albedo from FRSR data collected during aboard the R/V Ronald H. Brown ACE-Asia. The black diamonds are surface measurements of the single scattering albedo. The red pluses are the results of the FRSR retrieval algorithm and the blue crosses are the results of a retrieval based on a 0-3 km deep aerosol optical model.

10.3 ANALYSIS OF A LONG-TERM FRSR DATA SET: THE EXPLORER OF THE SEAS

We have discussed the size and scope of the FRSR database in past NASA TMs. In this final TM, we shall concentrate on the analysis of the data from the Explorer of the Seas, which is a cruise ship operated by Royal Caribbean. The ship has a full complement of atmospheric and oceanic sensors operated by the University of Miami. We deployed an FRSR on the Explorer nearly two years ago. It has operated continuously during successive one-week transects and the FRSR unit has remained highly stable. We are in the process of analyzing the first year of the data set and some of the results are shown here.

The observed relationship between wind direction and aerosol optical thickness is shown in Figure 10.2. Each panel shows a 30-degree span in wind direction and the size of the plotted circle reflects the magnitude of the observed optical thickness in this range of wind directions. The observations clearly show increased optical thicknesses when the winds have a northeasterly component, as compared to east or southeast. As expected, there are relatively few observations when the winds are westerly because the climatological wind direction contains an easterly component. The presence of African dust in the Caribbean has been known for decades, but the Explorer of the Seas data set suggests that the wind direction observed when the aerosol optical thickness is typically the largest is not southeasterly, as might be expected if there was a straight flow from Africa. We are in the process of analyzing these data to

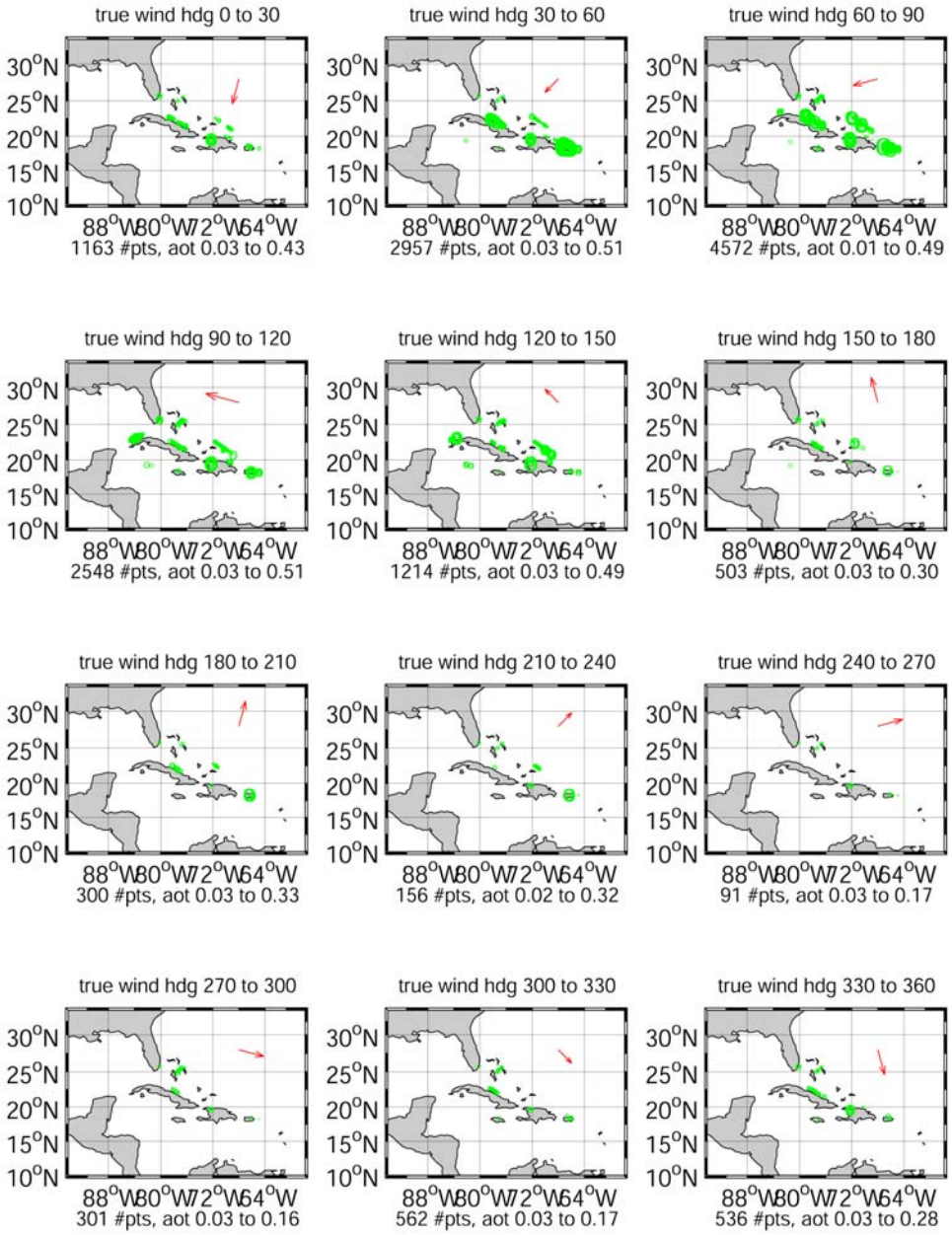

Figure 10.2: Each subplot shows the aerosol optical thickness for each cloud-free observation along the cruise track of the Explorer of the Seas when the wind direction is observed to be within the listed 30-degree passband, which is centered on the direction of the small plotted arrow. The radius of each plotted circle represents the magnitude of the observed aerosol optical thickness and the largest radii indicate the highest aerosol optical thickness.

determine whether the aerosol that we are observing has the physical characteristics of African dust (Angstrom Exponent), or whether it is a mixture of different aerosol, some potentially generated locally.

The Explorer of the Seas has a full complement of sensors include standard meteorological variables. Scatterplots of the relationship between aerosol optical thickness and relative humidity, temperature, and winds are shown in Figure 10.3. It is surprising to find that the relative humidity appears to have little correlation with the aerosol optical thickness. We have observed the same lack of a predicted relationship in some of our other analyses, but they have been made on smaller data sets. While we are in the process of further processing these data and doing additional filtering, the indication is that relative humidity does not play a significant role in determining the optical thickness in the Caribbean. Examination of the true wind direction appears to show two distinct populations of aerosol with the most polluted air clearly associated with wind directions in the 0-100 degree range. No relationship between wind speed or temperature and aerosol optical thickness is indicated, although wind speed is the primary governing factor in determining the concentration of sea-salt in the marine atmosphere.

These observations may be consistent with theory despite the lack of strong signals showing high correlations between wind speed and aerosol optical thickness and relative humidity and aerosol optical thickness in this region. What is apparent is that the relative humidity and wind speed do no appear to vary through a wide enough dynamic range to enable the signals to be observed in the tropics. This would appear to be an important attribute of the tropical marine environment for a number of reasons. It suggests that observations of relative humidity and wind may not significantly improve atmospheric correction algorithms in these tropical regions because they do not change enough to be of importance in selecting a model. From a climate perspective, it also suggests the direct aerosol effects in the topics may not be modulated by atmospheric water vapor as they may be in continental regions.

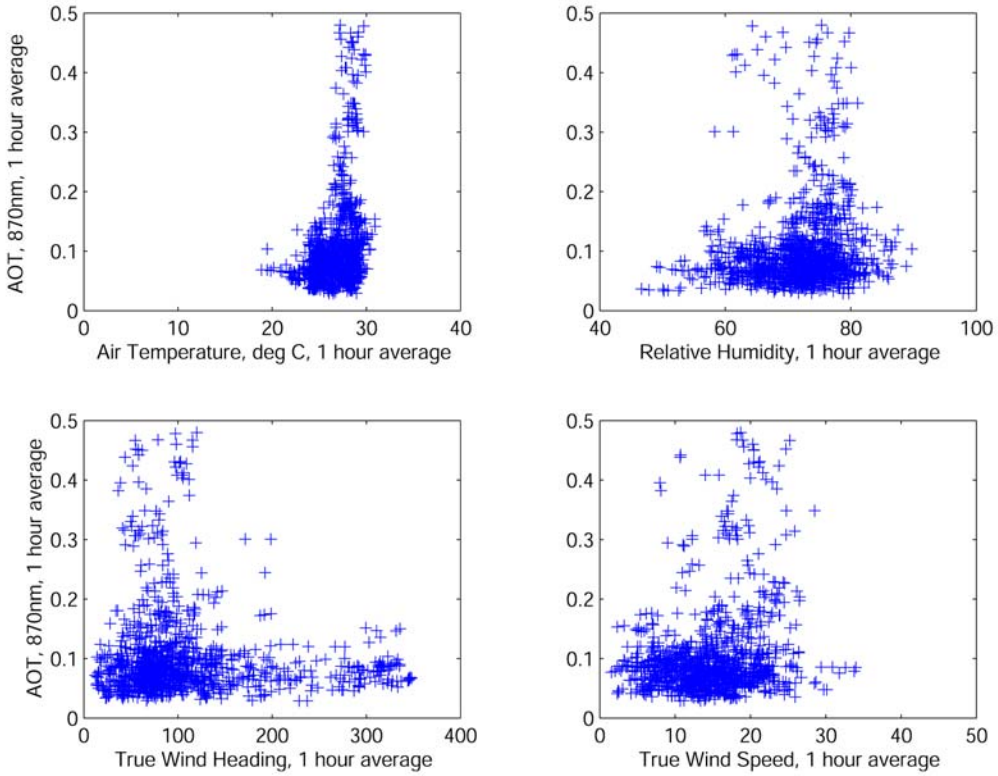

Figure 10.3: Each subplot shows a scatter plot of 1-hour average meteorological variables and one-hour average aerosol optical thickness.

10.4 CONCLUSIONS

We have amassed a large and important database over the four years of operation of the FRSR network. While the data requires careful analysis and quality control before summary conclusions can be reached, we expect that the data set will prove to be extremely useful for the atmospheric and oceanographic communities. There is considerable value in the data set that has yet to be realized. Most notably, the focus of optical thickness must be broadened to include the other radiative parameters of interest, namely the single scattering albedo and the asymmetry parameter. As we have demonstrated, it may be possible to retrieve one or both of these variables using FRSR data. This is the path forward with regard to aerosol physics in the marine boundary layer. In our opinion, the utility of aerosol optical thickness measurements alone is limited because model improvements are only possible when the other aerosol radiative forcing variables are known, along with related data such as in situ chemical measurements and meteorological variables. The other aspect of the data that is largely untapped is information about cloud optical thickness over the world's oceans.

REFERENCES

Anikin, P., M.A. Sviridenkov, and E. V. Romashova, 2002: Estimation of Aerosol Single-Scattering Albedo Over ZSS from MFRSR Data. In Proceedings of the Twelfth Atmospheric Radiation Measurement (ARM) Science Team Meeting, April 8-12, St. Petersburg, Florida. (http://www.arm.gov/docs/documents/technical/ conf_0204/anikin-p.pdf).

Devaux, C, A. Vermeulen, J.L. Deuze, P. Dubuisson, M. Herman, R. Santer, and M. Verbrugghe, 1998: Retrieval of aerosol single-scattering albedo from ground-based measurements: application to observational data. *J. Geophys. Res*., **103**, 8753-8761.

Dubovik, O, and M.D. King, 2000: A flexible inversion algorithm for retrieval of aerosol optical properties from Sun and sky radiance measurements. *J. Geophys. Res*., **105**, 20673-20696.

Herman, B.M., R.S. Browning, and J.J. De Luisi, 1975: Determination of the effective imaginary term of the complex refractive index of atmospheric dust by remote sensing: The diffuse-direct radiation method. *J. Atmos. Sci*., **32**, 918-925.

Gordon, H.R., and T. Zhang, 1995: Columnar aerosol properties over oceans by combining surface and aircraft measurements: simulations. *Appl. Opt*., **34** (24), 5552-5555.

King, M.D., and B.M. Herman, 1979: Determination of the ground albedo and the index of absorption of atmospheric particulates by remote sensing. *I. Theory. J. Atmos. Sci*., **36**, 163-173.

Miller, M.A., M.J. Bartholomew, and R.M. Reynolds, 2003: The accuracy of marine shadow-band measurements of aerosol optical thickness and Angstrom exponent. *J. Atmos. Ocean. Tech*. (submitted).

Nakajima, T, G. Tonna, R. Rao, P. Boi, Y. Kaufman, and B. Holben, 1996: Use of sky brightness measurements from ground for remote sensing of particulate polydispersions. *Appl. Optics*, **35** (15), 2672-2686.

P.K. Quinn, D.J. Coffman, T.S. Bates, T.L. Miller, J.E. Johnson, E.J. Welton, C. Neusüss, M.A.Miller, and P. Sheridan: Aerosol Optical Properties during INDOEX 1999, 2001: Means,Variability, and Controlling Factors, *J. Geophys. Research*, **107**(D18), 10.1029/2000JD000037, 2002 **.**

Reynolds, M.R., M.A. Miller, and M.J. Bartholomew, 2002: A fast-rotating, spectral shadowband radiometer for marine applications. *J. Atmos. Ocean. Tech*., Vol. **18**, No. 2, pp. 200–214

Smirnov, A., B.N. Holben, O. Dubovik, N.T. O'Neill, L.A. Remer, T.F. Eck, L. Slutsker, and D Savoie, 2000: Measurement of atmospheric optical parameters on U.S. Atlantic coast sites, ships, and Bermuda during TARFOX. *J. Geophys. Res*., **105**, 9887-9901.

Vogelmann, A.M., Miller, M.A., Flatau, P.J., Markowitz, K.M., 2003: Aerosol radiative effects and single-scattering properties in the Tropical Western Pacific. 2003 ARM Science Team Meeting.

Voss, K.J., E.J. Welton, P.K. Quinn, R. Frouin, M.A. Miller, and R.M. Reynolds, 2001: Aerosol optical depth measurements during the Aerosols99 experiment, *J. Geophys. Research*, 106, 20811-20820.

Zhang, T., and H.R. Gordon, 1997: Columnar aerosol properties over oceans by combining surface and aircraft measurements: sensitivity analysis. *Appl. Optics*, **36** (12), 2650-2662.

Chapter 11

Bio-Optical Measurement and Modeling of the California Current and Southern Oceans

B. Greg Mitchell

Scripps Institution of Oceanography, University of California San Diego, La Jolla, California

11.1 INTRODUCTION

This SIMBIOS project contract has supported *in situ* ocean optical observations in the California Current, and in the north Pacific, Southern and Indian Oceans. Our principal goals are to validate standard or experimental ocean color products through detailed bio-optical and biogeochemical measurements, and to combine ocean optical observations with modeling to contribute to satellite vicarious radiometric calibration and algorithm development. In collaboration with major oceanographic ship-based observation programs (CalCOFI, JGOFS, AMLR, INDOEX, and ACE Asia) our SIMBIOS effort has resulted in data from diverse bio-optical provinces. For these global deployments we generate a methodologically consistent data set encompassing a wide-range of oceanic conditions. We have initiated several collaborations with scientists in East Asian countries to study the complex Case-2 waters of their marginal seas. Global data collected in recent years are routinely evaluated relative to our CalCOFI time-series. The combined database we have assembled now comprises more than 1000 stations and includes observations for the clearest oligotrophic waters, highly eutrophic blooms, red-tides and coastal Case-2 conditions. The data has been used to validate water-leaving radiance estimated with OCTS, SeaWiFS, MODIS and GLI as well as bio-optical algorithms for chlorophyll pigments. During the past year we continued to process and quality control our data and carried out a detailed calibration/validation exercise in the California Current for the Japanese GLI instrument. For this GLI initialization effort, we coordinated with the Mexico IMECOCAL program to get extra data to complement our CalCOFI data for the simultaneous April, 2003 cruises. The comprehensive data is utilized for development of standard and experimental algorithms.

11.2 RESEARCH METHODS AND DATA

We continue to participate on CalCOFI cruises to the California Current System (CCS) for which we have an 8-year time-series. This region experiences a large dynamic range of coastal and open ocean trophic structure and has experienced strong interannual forcing associated with the El Niño – La Niña cycle from 1997-2000 (Kahru and Mitchell, 2000; Kahru and Mitchell, 2002). CalCOFI data provide an excellent reference for evaluating our other global data sets (O'Reilly et al. 1998; Mitchell et al. 2002b, 2002c). During the third year of our contract, we participated in 2 CalCOFI cruises, a cruise to the Southern Ocean (AMLR), and received data from colleagues in Korea and Hong Kong for East Asian coastal cruises. The April 2003 CalCOFI cruise (CAL0304) was coordinated with the simultaneous IMECOCAL cruise (IME0304) off Mexico. The combined April data are being used for a comprehensive campaign for calibration and validation of GLI algorithms. A preliminary analysis of the water-leaving radiances and fluorometric chlorophyll concentration was presented at the SPIE 2003 conference (Fukushima et al., 2003) and at the subsequent meeting at Scripps Institution of Oceanography on August 7, 2003. Work on the GLI calibration/validation using the combined dataset is continued .

The global distribution of our data collected during 6 years of SIMBIOS funding is shown in Figure 1.11. On most cruises, an integrated underwater profiling system was used to collect optical data and to

characterize the water column. The system included an underwater radiometer (Biospherical Instruments MER-2040 or MER-2048) measuring depth, downwelling spectral irradiance (E_d) and upwelling radiance (L_u) in 13 spectral bands. A MER-2041 deck-mounted reference radiometer (Biospherical Instruments) provided simultaneous measurements of above-surface downwelling irradiance. Details of the profiling procedures, characterization and calibration of the radiometers, data processing and quality control are

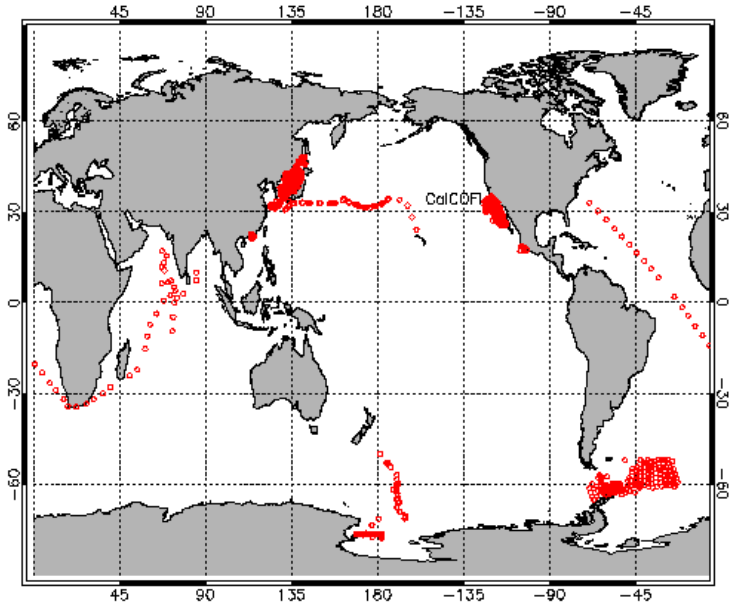

Figure 11.1: Global distribution of bio-optical stations accomplished in the past 5 years by the Scripps Photobiology Group (SPG). All stations include spectral reflectance and fluorometric chlorophyll. Most include particle and soluble absorption and HPLC pigments. For many cruises since 1997 we have deployed Hydroscat backscatter and AC9 absorption and attenuation meters to better understand the variables that govern remote sensing reflectance.

described in Mitchell and Kahru (1998). The underwater radiometer was also interfaced with 25 cm transmissometers (SeaTech or WetLabs), a fluorometer, and SeaBird conductivity and temperature probes. When available, additional instrumentation integrated onto the profiling package included AC9 absorption and attenuation meters (WetLabs Inc.), and a Hydroscat-6 backscattering meter (HobiLabs). For two AMLR, ACE Asia and recent CalCOFI cruises we deployed our new Biospherical Instruments PRR-800 freefall radiometer that included 19 channels of surface irradiance (312-865 nm) and three geometries of underwater radiometry (L_u, E_u, E_d) from 312 to 700 nm. We have shown that measuring these three radiometric geometries with our MER 2048 allowed us to retrieve backscatter and absorption coefficients (Stramska et al., 2000). Our colleagues in Hong Kong and Korea use PRR-800 profilers and collect samples for chlorophyll and absorption with methods consistent with ours. At *in situ* optical stations discrete water samples were collected from a CTD-Rosette immediately before or after each profile for additional optical and biogeochemical analyses. Pigment concentrations were determined fluorometrically and with HPLC. All HPLC samples acquired in the past year have been submitted to San Diego State University for analysis under a separate SIMBIOS contract. Spectral absorption coefficients (300-800 nm) of particulate material were estimated by scanning particles concentrated onto Whatman GF/F filters (Mitchell, 1990) in a dual-beam spectrophotometer (Varian Cary 1). Absorption of soluble material was measured in 10 cm cuvettes after filtering seawater samples through 0.2 µm pore size polycarbonate filters.

Absorption methods are described in more detail in Mitchell et al. (2002a). For some cruises we collected measurements of other optical and phytoplankton properties including photosynthesis, particulate organic matter (carbon and nitrogen), phycoerythrin pigment, and size distribution using flow cytometry and a Coulter Multi-sizer.

For most of our field work in association with CalCOFI and AMLR we submit all data directly to NASA SIMBIOS including supporting CTD and water bottle information. For the collaborations with Asian colleagues, we process their optical data and with their permission we will submit some of the Asian data to SIMBIOS in 2003. On the SOFEX cruise to the Southern Ocean we did not deploy a profiling radiometer, but we collected data for particle absorption; other SOFEX PIs collected samples for fluorometric chlorophyll and HPLC pigments. Our absorption data from SOFEX will be submitted to SIMBIOS and we will request approval to submit the pigment data.

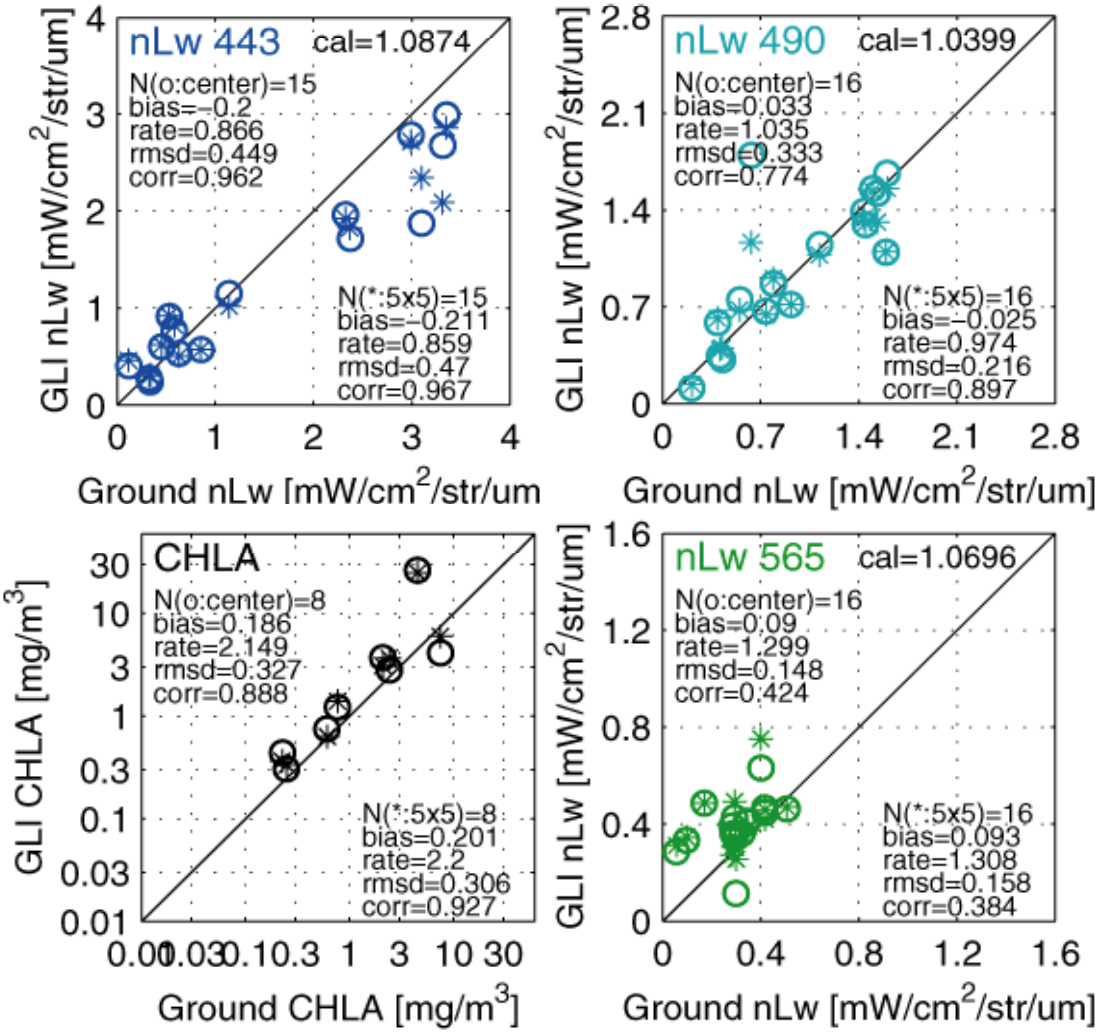

Figure 11.2: Validation of GLI water-leaving radiances (nLw) at 443, 490 and 565 nm, and of the empirical OC4-GLI chlorophyll algorithm during CalCOFI 0304 cruise. The in situ nLw were measured with the PRR-800. The GLI match-ups were estimated both as the value of the nearest pixel (o) and as average for a 5 x 5 pixel area (*) centered at the nearest pixel. The chl-a match-ups show very good performance of the OC4-GLI algorithm. The only station with a significant difference was a near-shore station with expected problems like small-scale spatial variability, terrestrial aerosols and stray light.

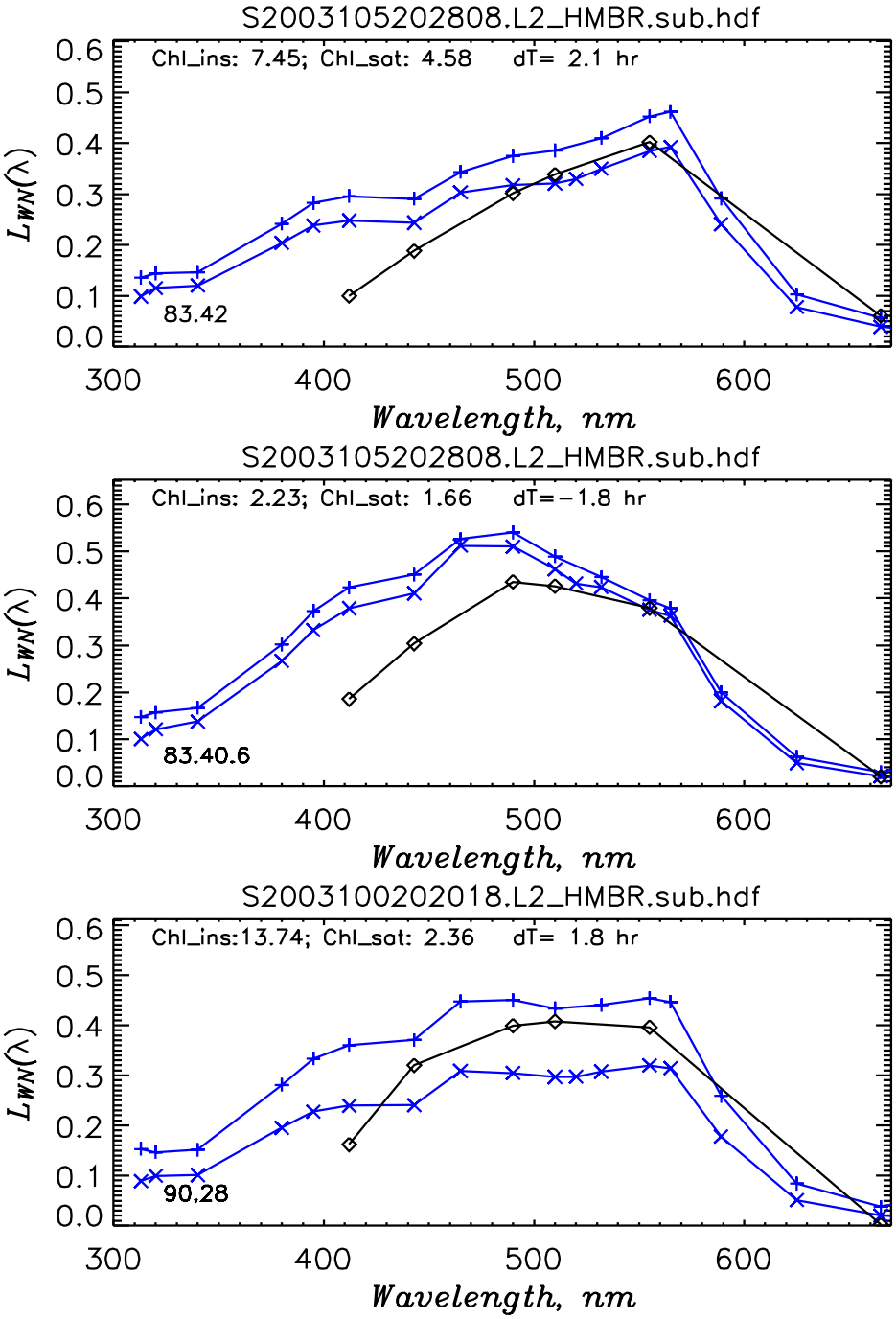

Figure 11.3: Validation of SeaWiFS water-leaving radiance spectra with three match-ups within a 3-hour time lag during the CalCOFI 0304 cruise. At each station two casts of PRR-800 were made to get in situ nLw spectra between 313 and 700 nm (continuous line with X). The SeaWiFS nLw spectra were estimated with SeaDAS version 4.4 and the default options. While at longer wavelengths the SeaWiFS-derived nLw values are within the in-station variability range of in situ values, at 412 and even at 443 nm SeaWiFS is still under-predicting the in situ nLw. It should be noted that all three match-ups were near-shore and had high to very high chl-a concentration (7.45, 2.23 and 13.74 mg m-3). At near-shore stations the discrepancies may be caused by small-scale spatial variability, terrestrial aerosols and stray light. In fact, the large small-scale variability in in situ nLw is shown at the bottom panel.

11.3 RESEARCH RESULTS

Remote sensing reflectance (Rrs) derived from the in-water measurements, defined as the ratio of upwelling radiance (Lu) and downwelling irradiance (Ed), is closely related to the normalized water-leaving radiance (Lwn) product of satellite ocean color data. Rrs (λ) in Case-1 waters is well correlated to chl-a. As chl-a increases, Rrs generally decreases for SeaWiFS wavelengths 412, 443, 490, 510 nm due to increased absorption, but increases at SeaWiFS wavelength 555 and 665 nm due to increased backscatter (Mitchell and Kahru, 1998; O'Reilly et al., 1998). To explore issues with Case-2 waters we have collaborated with colleagues in Korea (NFRDI), and Hong Kong (HKUST) to assemble a large regional data set from the East China Sea, South China Sea and coastal waters of Eastern Asia. Relationships between Rrs and chl-a for HKUST and NFRDI data can be both lower and higher than the Case-1 (CalCOFI) relationships, depending on whether absorption or scattering is the dominant process (data not shown).

Typical ocean color algorithms take ratios of reflectance for different spectral bands. The standard SeaWiFS chl-a algorithm is currently OC4v4 [O'Reilly et al., 1998; O'Reilly et al., 2000]. CalCOFI data set is a good reference data set since it covers a large range of chl-a, was acquired with very consistent methodology, and comprises approximately 25% of the data used for development of the SeaWiFS OC4v4 algorithm (O'Reilly et al., 2000). Kahru and Mitchell (1999; 2001) have shown that the chl-a retrieved by satellite in the CalCOFI region is in good agreement with our ship data when computed with our regional algorithm or NASA's OC4v4. Thus the CalCOFI region is an ideal location to evaluate new ocean color missions. We collaborated closely with Japanese colleagues and NASDA to execute a comprehensive calibration and validation program for GLI on the April CalCOFI and IMECOCAL cruises. The GLI empirical chlorophyll algorithm OC4-GLI (Mitchell and Kahru, unpublished) that uses the same maximum band ratio algorithm as OC4v4 of SeaWiFS (O'Reilly et al., 1998) but a different set of bands (443, 460, 520, 545 nm) seems to be working very well (Figure 11.2). The ratio of GLI-detected chlorophyll to SeaWiFS-detected chlorophyll (not shown) is close to one. The GLI water-leaving radiances correspond well to in situ measurements (Figure 2), especially considering the early phase of the cal/val process. However, we are still seeing significant discrepancies between satellite-derived nLw and in situ values at near-shore CalCOFI stations (Figure 11.3). While the negative water-leaving radiances have disappeared in our match-ups, the SeaWiFS-derived nLw412 and even nLw443 are still often lower than in situ values. The maximum band ratio algorithms compensate for the decreased nLw values at 412 and 443 nm by switching to longer wavelength bands but the distortion in the satellite-derived nLw spectra causes severe problems for semi-analytic algorithms.

11.4 CONCLUSIONS

Since this is the final year of NASA SIMBIOS, NASA should define an explicit program for in situ support of ocean color satellites. Even for Case 1 waters, algorithm problems persist and this will be the focus of a session at the ASLO Ocean Sciences meeting in 2004. Our SIMBIOS data have demonstrated that the Southern Ocean should continue to be a high priority since it is evident that standard algorithms for chl-a do not perform well in this region (Mitchell and Holm-Hansen, 1991; Mitchell, 1992; Mitchell et al., 2002b; Reynolds et al., 2001). Furthermore, it is essential to broaden the in situ data sets to include detailed information on spectral absorption and backscattering, particle size distributions, mineral and organic mass, and the optical differentiation of bio-geochemically important taxa like diazotrophs, diatoms and coccolithophores. To understand the details of how community structure regulates spectral reflectance so that advanced algorithms can be developed requires a commitment to supporting detailed in situ studies.

REFERENCES

Carder, K.L., F.R. Chen, Z.P. Lee and S.K. Hawes, 1999: Semianalytic moderate-resolution imaging spectrometer algorithms for chlorophyll a and absorption with bio-optical domains based on nitrate-depletion temperatures. *Journal of Geophysical Research*. **104**(C3): 5,403-5,421

Fukushima, H., M. Toratani, A. Tanaka, W.-Z. Chen, H. Murakami, R. Frouin , G. Mitchell and M. Kahru, 2003: ADEOS-II/GLI ocean color atmospheric correction: early phase results. SPIE 48th Annual Meeting, San Diego, August 5, 2003.

Garver, S.A. and D.A. Siegel, 1997: Inherent Optical Property Inversion of Ocean Color Spectra and its Biogeochemical Interpretation: 1. Time series from the Sargasso Sea. *Journal of Geophysical Research*. **102**(C8): 18,607-18,625

Kahru, M. and B.G. Mitchell, 1999: Empirical chlorophyll algorithm and preliminary SeaWiFS validation for the California Current. *International Journal of Remote Sensing*. **20**(17): 3,423-3,430

Kahru, M. and B.G. Mitchell, 2000: Influence of the 1997-98 El Niño on the surface chlorophyll in the California Current. *Geophysical Research Letters*. **27**(18): 2,937-2,940

Kahru, M. and B.G. Mitchell, 2001: Seasonal and non-seasonal variability of satellite-derived chlorophyll and colored dissolved organic matter concentration in the California Current. *Journal of Geophysical Research*. **106**(C2): 2517-2529

Kahru, M., B.G. Mitchell, J. Wieland, J.C. Chen, N.W. Man, Y.S. Suh, M. Stramska, and D. Stramski, 2002: Evaluation of Satellite Ocean Color Algorithms for East Asian Marginal Seas. *ASLO*, Honolulu, Hawaii, February 2002.

Kahru, M. and B.G. Mitchell, 2002: Influence of El Niño – La Niña cycle on satellite-derived primary production in the California current. *Geophysical Research Letters*, **29**(9), doi: 10.1029/2002GL014963

Li, L.-P., H. Fukushima, R. Frouin, B.G. Mitchell, M. -X. He, I. Uno, T. Takamura, and S. Ohta (In Press) Influence of sub-micron absorptive aerosol on SeaWiFS-derived marine reflectance during ACE-Asia. *Journal of Geophysical Research – Atmospheres.*

Loisel, H., D. Stramski, B.G. Mitchell, F. Fell, V. Fournier-Sicre, B. Lemasle, and M. Babin, 2001: Comparison of the ocean inherent optical properties obtained from measurements and inverse modeling. *Applied Optics*. **40**(15): 2384-2397

Mitchell, B.G. , 1990: Algorithms for determining the absorption coefficient of aquatic particulates using the quantitative filter technique (QFT). In: Spinrad, R., ed., Ocean Optics X, Bellingham, Washington, *SPIE*, pp. 137-148

Mitchell, B.G. , 1992: Predictive bio-optical relationships for polar oceans and marginal ice zones. *Journal of Marine Systems*. **3**: 91-105

Mitchell, B.G. and M. Kahru, 1998: Algorithms for SeaWiFS standard products developed with the CalCOFI bio-optical data set. *Cal. Coop. Ocean. Fish. Invest***. R. 39**: 133-147.

Mitchell, B.G. and O. Holm-Hansen (1991) Bio-optical properties of Antarctic Peninsula waters: Differentiation from temperate ocean models. *Deep-Sea Research I*. **38**(8/9): 1,009-1,028.

Mitchell B. G., M. Kahru, J. Wieland and M. Stramska, 2002a: Determination of spectral absorption coefficients of particles, dissolved material and phytoplankton for discrete water samples. In: Fargion, G.S. and J.L. Mueller, Eds. Ocean Optics Protocols for Satellite Ocean Color Sensor Validation, *NASA Technical Memorandum 2002-210004*/Rev 3-Vol 2, Chapter 15, P. 231-257.

Mitchell, B.G., M. Kahru, R. Reynolds, J. Wieland, D. Stramski, C. Hewes, and O. Holm-Hansen, 2002b: Chlorophyll-a Ocean Color Algorithms for the Southern Ocean and their Influence on Satellite Estimates of Primary Production. *ASLO*, Honolulu, Hawaii, February 2002.

Mitchell, B.G., M. Kahru, J. Wieland, and H. Wang, J.C. Chen, N.W. Man, and Y.S. Suh, 2002c: Case 2 Optical relationships for East Asian marginal seas. *Ocean Optics XVI Conference*. Santa Fe, New Mexico, November 18–22, 2002.

O'Reilly, J.E., S. Maritorena, B.G. Mitchell, D.A. Siegel, K.L. Carder, S.A. Garver, M. Kahru and C. McClain, 1998: Ocean color chlorophyll algorithms for SeaWiFS. Journal of Geophysical Research**.** **103**(C11): 24,937-24,953.

O'Reilly, J.E., S. Maritorena, D.A. Siegel, M.C. O'Brien, D.A. Toole, B.G. Mitchell, M. Kahru, et al. ,2000: Ocean color chlorophyll a algorithms for SeaWiFS, OC2 and OC4: Version 4. In: NASA, SeaWiFS Postlaunch Calibration and Validation Analyses.

Reynolds, R.A., D. Stramski and B.G. Mitchell, 2001: A chlorophyll-dependent semianalytical reflectance model from derived from field measurements of absorption and back scattering coefficients within the Southern Ocean. *Journal of Geophysical Research*. **106**(C4): 7125-7138.

Stramska, M., D. Stramski, B.G. Mitchell and C.D. Mobley, 2000: Estimation of the absorption and backscattering coefficients from in-water radiometric measurements. Limnology and Oceanography. **45**(3): 628-641.

Chapter 12

Variability in Ocean Color Associated with Phytoplankton and Terrigenous Matter: Time Series Measurements and Algorithm Development at the FRONT Site on the New England Continental Shelf.

John R. Morrison and Heidi M. Sosik

Woods Hole Oceanographic Institution, Woods Hole, Massachusetts

12.1 INTRODUCTION

Fronts in the coastal ocean describe areas of strong horizontal gradients in both physical and biological properties associated with tidal mixing and freshwater estuarine output (e.g. Simpson, 1981 and O'Donnell, 1993). Related gradients in optically important constituents mean that fronts can be observed from space as changes in ocean color as well as sea surface temperature (e.g., Dupouy et al., 1986). This research program is designed to determine which processes and optically important constituents must be considered to explain ocean color variations associated with coastal fronts on the New England continental shelf, in particular the National Ocean Partnership Program (NOPP) Front Resolving Observational Network with Telemetry (FRONT) site. This site is located at the mouth of Long Island sound and was selected after the analysis of 12 years of AVHRR data showed the region to be an area of strong frontal activity (Ullman and Cornillon, 1999). FRONT consists of a network of modem nodes that link bottom mounted Acoustic Doppler Current Profilers (ADCPs) and profiling arrays. At the center of the network is the Autonomous Vertically Profiling Plankton Observatory (AVPPO) (Thwaites et al. 1998). The AVPPO consists of buoyant sampling vehicle and a trawl-resistant bottom-mounted enclosure, which holds a winch, the vehicle (when not sampling), batteries, and controller. Three sampling systems are present on the vehicle, a video plankton recorder, a CTD with accessory sensors, and a suite of bio-optical sensors including Satlantic OCI-200 and OCR-200 spectral radiometers and a WetLabs ac-9 dual path absorption and attenuation meter. At preprogrammed times the vehicle is released, floats to the surface, and is then winched back into the enclosure with power and data connection maintained through the winch cable. Communication to shore is possible through a bottom cable and nearby surface telemetry buoy, equipped with a mobile modem, giving the capability for near-real time data transmission and interactive sampling control.

12.2 RESEARCH ACTIVITIES

AVPPO deployments

The AVPPO was deployed during 2003 at the Martha's Vineyard Coastal Observatory (MVCO) as part of the Coastal Carbon Time-series (CCTS, J. Campbell and D. Vandemark – PIs) project of the Coastal Ocean Observation and Analysis (COOA) center of the University of New Hampshire (UNH). The Martha's Vineyard Coast Observatory, which came on-line in June 2001, was designed as a highly flexible facility to provide investigators, from school students to scientists, the means to collect long-term environmental data. It is located off the south shore of the island Martha's Vineyard on the northeastern seaboard of the U.S. between the highly productive waters of the Gulf of Maine (GOM) and the Mid Atlantic Bight (O'Reilly et al. 1987). The cabled facility provides power and communications at an underwater node and at the Air Sea Interaction Tower (ASIT), which is 3 km offshore in 15 m of water. Fast Ethernet communications and large power supply facilitates high bandwidth realtime sampling which

is not possible in moorings traditionally used for coastal measurements. The AVPPO was reconfigured to take advantage of the MVCO infrastructure with power and telemetry obtained from the ASIT and deployed on

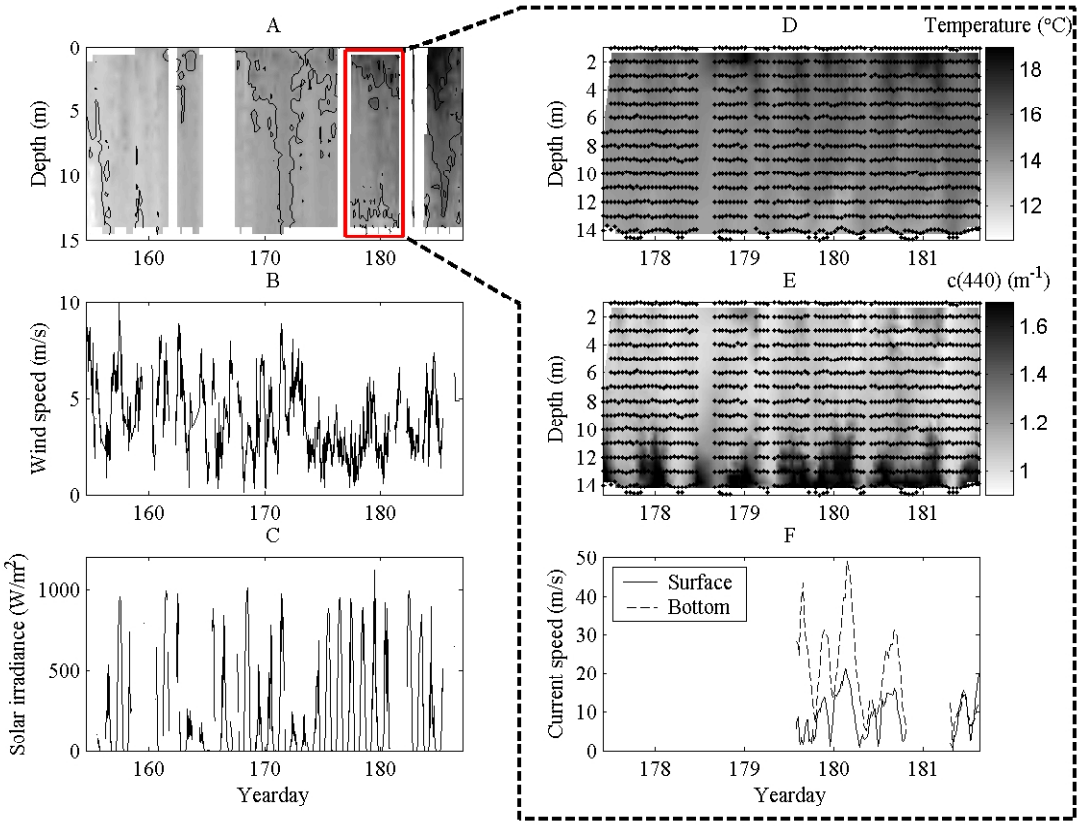

Figure 12.1: Processes at MVCO from AVPPO measurements between 4 June and 8 July 2003. A) The onset of thermal stratification as indicated by interpolated temperature values. High wind (B) events apparently mixed the water column. Stratification intensified with high solar irradiance (C) and low winds after day 172. Expansion of the data between Day 179 and 182 (D-F) shows warm water intrusions at tidal frequencies together with particulate resuspension events (beam attenuation coefficient at 440 nm). Resuspension appears correlated with periods of strong bottom current speeds.

May, 30 2003 at 41 19.412 °N, 70 33.954 °W in approximately 15 m of water. Realtime processing of data was implemented and contour plots are automatically updated at the AVPPO website (http://4dgeo.whoi.edu/vpr).

12.3 RESEARCH RESULTS

Ongoing observations from the AVPPO illustrate some of the important forcing on the coastal ocean around MVCO. Vertical temperature profiles clearly illustrate warming and the onset of summer stratification modified by mixing induced by surface winds (Fig. 12.1). Initial analysis of beam attenuation coefficient, c (λ), measured from the AVPPO during this time period also illustrated the effects of tidal forcing. Tidal currents resuspended bottom sediment and appeared to advect differing water masses over the study sight (Fig. 12.1). On maintenance cruises these fronts were clearly visible as distinct lines of surface debris. Wind driven resuspension of sediment is also an important process in coastal oceans and has been observed in previous deployments of the AVPPO in New England coastal waters (Morrison and Sosik 2002a) and in deeper waters south of Martha's Vineyard (Chang 2001).

Using solar stimulated fluorescence (SSF) Morrison (2003) presented evidence of three types of quenching in natural phytoplankton populations, 1) photochemical quenching, 2) rapidly varying energy dependent quenching, qE, of which the xanthophyll cycle is an example (Demmig-Adams and Adams 1992), and 3) quenching associated with photoinhibition, qI, with longer relaxation timescales (Horton et al. 1996). The last two are examples of non-photochemical quenching.

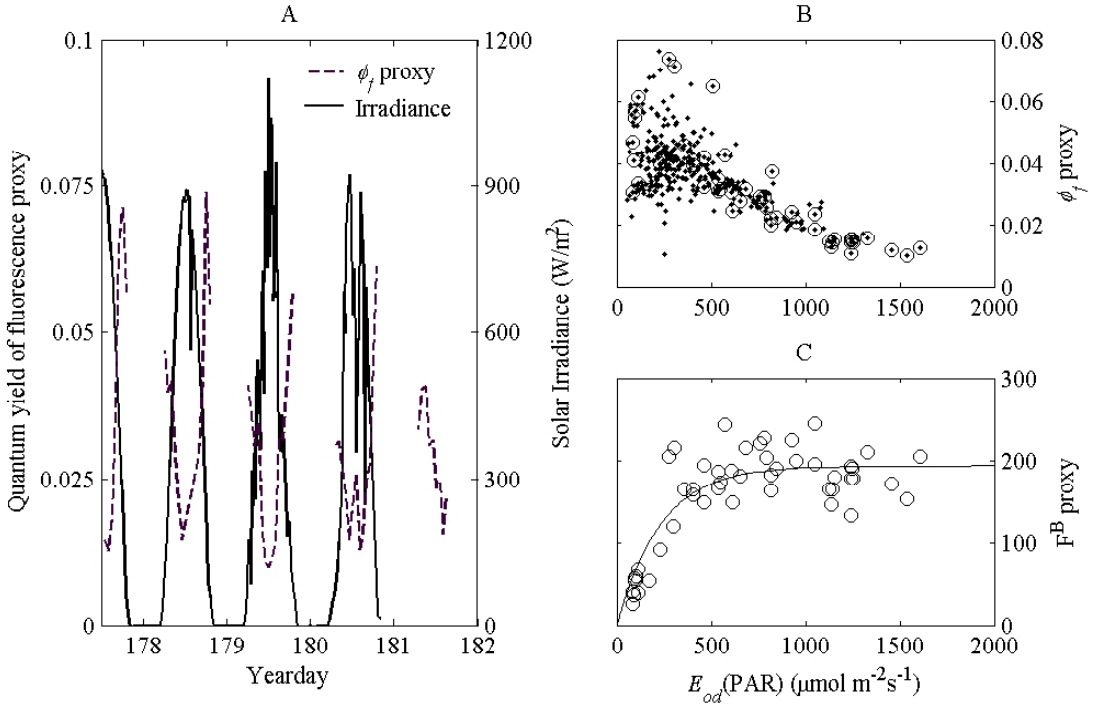

Figure 12.2: Quantum yield of fluorescence proxy from the 25 June – 1 July, 2003. A) Surface φf values demonstrated non-photochemcial quenching decreasing φf during the majority of daytime. Day 180 clearly shows this modulated by surface irradiance. B) Decreases in φf at low irradiances were indicative of photochemical quenching (blue – all depths, red – surface data from A). C) Biomass normalized fluoresce – irradiance showed similar relationships to those reported previously (e.g., Schallenberg et al. 2002)

Similar trends were also observed at MVCO during the summer of 2003. Proxy values of the quantum yield of fluorescence (upwelling radiance at 665 nm used to correct for back- and Raman scattered light) were calculated from radiometric measurements from the AVPPO with the formulations of Morrison (2003, phytoplankton absorption was obtained from ac-9 measurements). The fluorescence yield was suppressed at high irradiances in the middle of the day and responded to varying irradiance conditions induced by clouds (Fig. 12.2A). The transition from photochemically to non-photochemically dominated quenching was apparent both at fixed depths and throughout the water column (Fig. 12.2A and B). To our knowledge, these observations represent one of the most detailed studies of the diurnal variability of the fluorescence yield of natural phytoplankton populations to date.

We have shown previously that absorption spectra measured with an ac-9 can be decomposed into that from phytoplankton and non-algal material (Morrison and Sosik 2002a). This was achieved by assigning characteristic spectral shapes to each fraction and iteratively varying constituent concentrations to minimize the sum of square deviations between observed and predicted spectra. The spectral slope of non-algal material, *S*, was also iteratively varied to account for different spectral shapes but the phytoplankton absorption shape remained constant. Ciotti et al. (2002) described the phytoplankton absorption shape as a mixing series between two normalized spectra representative of pico- and micro-phytoplankton or minimal and maximal packaging, $\hat{a}_{ph}^{pico}(\lambda)$ and $\hat{a}_{ph}^{micro}(\lambda)$, respectively. Greater than 80% of the variability in the spectral shape of phytoplankton was explained using this method. This parameterization of the phytoplankton absorption shape was included in the previous absorption model and used in the

decomposition. To test the ability of the method to accurately reproduce spectral variation 478 groups of absorption spectra of particles, non-algal particles, and colored dissolved organic material ($a_p(\lambda)$, $a_{NAP}(\lambda)$, and $a_{CDOM}(\lambda)$, respectively) from the North East Atlantic were used to assess the absorption decomposition methods (Morrison and Sosik in prep). Phytoplankton absorption, $a_{ph}(\lambda)$, was calculated as the difference between $a_p(\lambda)$ and $a_{NAP}(\lambda)$. Spectra were measured with bench-top spectrophotometers either by ourselves or as part of the Bermuda Bio-Optics Project (Siegel et al. 1995) using standard protocols (Mitchell et al. 2000) and are archived at the NASA Seabass database.

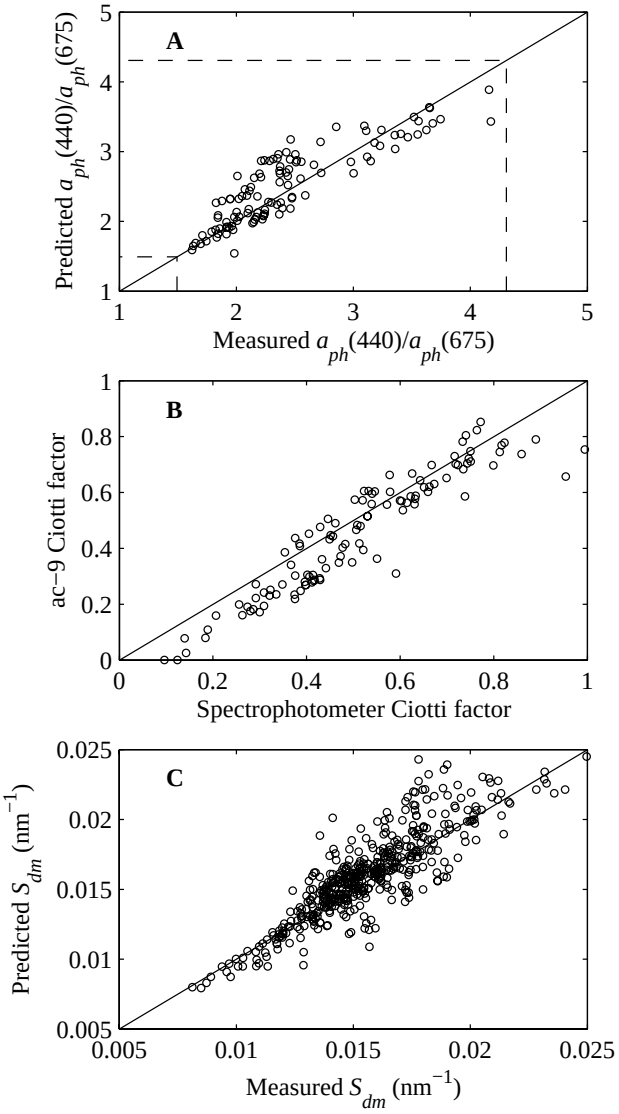

Figure 12.3: Spectral information of the original data was also retrieved by the inversion. (A) The ratio of the phytoplankton absorption maxima, aph(440)/aph(675), from the inversion was significantly related to that from the original aph(λ) when aph(440)/anw(440) ≥ 0.40, r2 = 0.77 N=135. (B) The ciotti factor from the inversion was significantly related to that obtained from the original phytoplankton spectra, same data as in 3A r2 = 0.87. (C) Spectral shapes of non-algal absorption were also retrieved as indicated by the significant relationship between the slope, Sdm, r2 = 0.77 for all data.

Comparison of the ratios of the phytoplankton absorption, $a_{ph}(440)/a_{ph}(675)$, and the Ciotti factors, f_c, retrieved from the inversion with those calculated from the original phytoplankton absorption spectra indicated that spectral variations in $a_{ph}(\lambda)$ were retrieved with the inversion, Figure 12.3A and B. Similarly, comparison of the spectral slopes of the non-algal absorption from the inversion with those calculated with the original data demonstrated that the inversion retrieved spectral variation of $a_{dm}(\lambda)$, Figure 12.3C.

Babin et al. (2003) showed theoretical normalized scattering spectra for both phytoplankton and non-algal particles which varied with particle size and refractive index. Theoretically, scattering shapes for non-algal particles can be described as a power law with slope γ which increases with decreasing particle size. The exponent γ is related to the Junge exponent of the particle size distribution, j, through $\gamma = j - 3$ (Babin et al. 2003; Boss et al. 2001; Morel 1973). Inclusion of absorbing bands, such as with phytoplankton, is accompanied by decreases in the scattering coefficient. Evidence of the variation in the range of scattering shapes was present in the 25,276 one meter depth-binned ac-9 measurements obtained with the AVPPO deployments prior to 2003 and the 5 minute time-binned data from the cruise EN372 (Fig. 12.4, Morrison and Sosik 2002b). Further analysis demonstrated that greater than 99 % of the variation in the spectral scattering shape could be explained by three normalized scattering spectra, small and large non-algal particles (slopes of 1.63 and -0.20 nm^{-1}, respectively) and large phytoplankton. The spectral shape of small phytoplankton was indistinct from the others and was similar to small particles mixed with large phytoplankton.

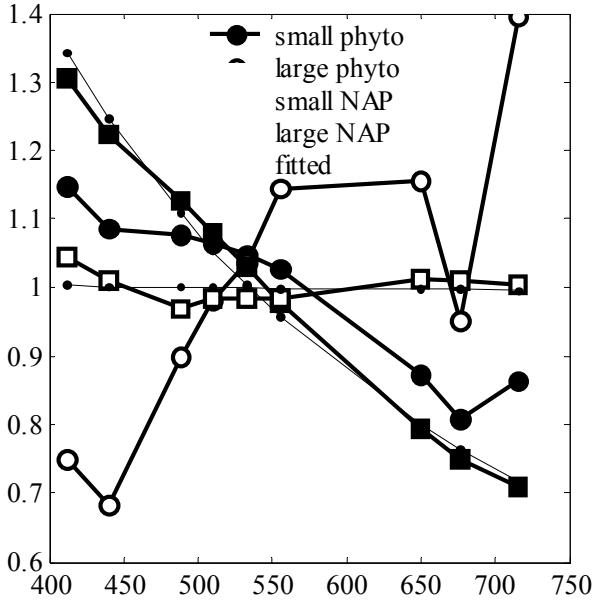

Figure 12.4: The normalized scattering spectra for both small and large phytoplankton and non-algal particles (NAPs) determined from AVPPO ac-9 measurements prior to 2003. Note the troughs in the phytoplankton scattering spectra associated with absorption peaks. The slopes of the fitted values are 1.136 and 0.012 nm-1 for the small and large NAPs, respectively.

12.4 **CONCLUSIONS**

Parameterizing the variability in inherent optical properties associated with optically important constituents is fundamental to understanding variations in ocean color, especially in optically complex regions such as the coastal ocean. Measurements with sufficient resolution, both temporal and spatial, are necessary to encompass the range of possible IOPs and to understand their forcings. Much of this detail has been captured by the Autonomous Vertically Profiling Plankton Observatory during deployments at the FRONT site, in Massachusetts Bay, and at the MVCO. We have explained the majority of the variation in

the measured IOPs by developing models based on characteristic shape vectors. We are currently working to improve ocean color remote sensing inversion algorithms in Case II by including this increased understanding of the natural range of IOPs. This includes approaches utilizing the increased information associated with hyperspectral measurements.

Rigorous use of solar stimulated fluorescence depends on a quantitative understanding the variability of the quantum yield of fluorescence of phytoplankton. Inherent in this is determining the rates of onset and relaxation of non-photochemical quenching. As demonstrated by the data presented herein (Fig. 12.3), the Autonomous Vertically Profiling Plankton Observatory provides an ideal platform for such a study of solar stimulated fluorescence.

REFERENCES

Babin, M., A. Morel, V. Fournier-Sicre, F. Fell, and D. Stramski. 2003: Light scattering properties of marine particles in coastal and open ocean waters as related to the particle mass concentration. Limnology and Oceanography **48:** 843-859.

Boss, E., M. S. Twardowski, and S. Herring. 2001: Shape of the particulate beam attenuation spectrum and its inversion to obtain the shape of the particulate size distribution. Applied Optics **40:** 4885-4893.

Chang, G. C. 2001: Sediment resuspension over a continental shelf during Hurricanes Edouard and Hortense (vol 106, pg 9517, 2001). Journal of Geophysical Research-Oceans **106:** 19995-19995.

Ciotti, A. M., M. R. Lewis, and J. J. Cullen. 2002: Assessment of the relationships between dominant cell size in natural phytoplankton communities and the spectral shape of the absorption coefficient. Limnology and Oceanography **47:** 404-417.

Demmig-Adams, B., and W. W. I. Adams. 1992: Photoprotection and other responses of plants to high light stress. Annual Review of Plant Physiology and Plant Molecular Biology **43:** 599-626.

Horton, P., A. V. Ruban, and R. G. Walters. 1996: Regulation of light harvesting in green plants. Annual Review of Plant Physiology and Plant Molecular Biology **47:** 655-684.

Mitchell, B. G. and others 2000: Determination of spectral absorption coefficients of particles, dissolved material and phytoplankton for discrete water samples. *In* G. S. Fargion and J. L. Mueller [eds.], Ocean optics protocols for satellite ocean color sensor validation, revision 2, NASA Technical Memoradum, 2000-209966. NASA.

Morel, A. 1973: Diffusion de la lumiere par les eaux de mer: Resultats experimentaux et approche theorique, p. 3.1.1-3.1.76, Optics of the sea. AGARD lecture series. North Atlantic Treaty Orginisation.

Morrison, J. R. 2003: In situ determination of the quantum yield of phytoplankton chlorophyll *a* fluorescence: a simple algorithm, observations, and a model. Limnology and Oceanography **48:** 618-631.

Morrison, J. R., and H. M. Sosik. 2002a: Inherent optical properties in New England coastal waters: decomposition into contributions from optically important constituents, p. 1-10, Ocean Optics XVI.

Morrison, J. R., and H. M. Sosik. 2002b: Variability in ocean color associated with phyoplankton and terrigenous matter: time series measurements and algorithm development at the FRONT site on the New England continental shelf, p. 91-97. *In* G. S. Fargion and C. R. McClain [eds.], SIMBIOS project 2002 annual report. NASA.

Morrison, J. R., and H. M. Sosik. in prep. Analysis of nine channel absorption-attenuation meter data: Scattering correction and decomposition of constituent contributions to absorption and scattering. to be submitted to Limnology and Oceanography Methods.

Schallenberg, C., M. R. Lewis, D. E. Kelley, and J. J. Cullen. 2002: Variability in the quantum yield of sun-induced fluorescence in the Bering Sea: effects of light and nutrients, p. 1-13, Ocean Opticx, XVI.

Siegel, D. A., A. F. Michaels, J. C. Sorensen, M. C. O'Brien, and M. A. Hammer. 1995: Seasonal variability of light availability and utilization in the Sargasso Sea. Journal of Geophysical Research **100:** 8695-8713.

This Research was Supported by
the NASA Contract # 00198

Publications

Morrison, J. R. 2003: In situ determination of the quantum yield of phytoplankton chlorophyll *a* fluorescence: a simple algorithm, observations, and a model. *Limnology and Oceanography* **48:** 618-631.

Morrison, J. R., and N. B. Nelson. 2003: Seasonal cycle of phytoplankton UV absorption at the Bermuda Atlantic Time-series Study (BATS) site. *Limnology and Oceanography* (in press).

Presentations

Morrison, J.R., Sosik, H.M., 2002: Inherent optical properties in New England coastal waters: Decomposition into contributions from optically important constituents. Presented at Ocean Optics XVI, Santa Fe, NM.

Chapter 13

Ocean Optics Protocols and SIMBIOS Protocol Intercomparison Round Robin Experiments (SPIRREX).

James L. Mueller

Center for Hydro-Optics and Remote Sensing, San Diego State University, California

13.1 INTRODUCTION

The objective of research under this contract is the maintenance and annual revision of the document "Ocean Optics Protocols for Satellite Ocean Color Sensor Validation (e.g. Fargion and Mueller 2000; Mueller et al. 2002; Mueller et al. 2003a – 2003e; Pegau et al. 2003).

13.2 RESEARCH ACTIVITIES

The research activities under the third year of this contract were devoted to completing final touches on Vol. IV (Pegau et al. 2003) and Vol. VI of "Ocean Optics Protocols for Satellite Ocean Color Validation, Revision 4" (Mueller et al. 2002), and in the preparation and completion of Revision 5. Revision 5 consists of a small number of important corrections to some of the volumes of Revision 4, a revised Volume V containing one new chapter, and a new Volume VI, Part 2 containing two new "Special Topics" chapters. The important updates, additions and revisions in the Revision 5 document are summarized in the next section.

13.3 RESEARCH RESULTS

Revision 4 to the ocean optics protocol document was reorganized, from the format of Revision 3 (Mueller et al. 2000a) into 6 separate volumes (Mueller et al. 2003a through 2003e, Pegau et al. 2003). This multi-volume format was adopted to allow timely future protocol revisions to be made reflecting important evolution of instruments and methods in some areas, without reissuing the entire document. Revision 5 consists of Errata to these Volumes (published in PDF form on the SIMBIOS Web Page), a revised version of Volume V (Biogeochemical and Bio-Optical Protocols) and a new Volume VI, Part II (Special Topics). Revision 5 to Vol. V contains corrections to the HPLC Pigment Protocols (Chapter 2) and a new Chapter 4 covering protocols for measurements of scattering and Calcium Carbonate concentrations associated with coccolithophorids. Volume VI, Part 2, contains two new chapters: "Advances in Radiometry for Ocean Color" and "Progress in Self Shading Corrections for In-Water Measurements of Upwelled Radiance".

13.4 CONCLUSIONS

Together, Revisions 4/5 comprise the final version of the "Ocean Optics Protocols for Satellite Ocean Color Sensor Validation" that will be issued under the auspices of the NASA SIMBIOS and SeaWiFS Programs. The scope and detail of this document has, at this stage, increased enormously over the decade since the first version was issued (Mueller and Austin 1992), as evidenced by comparing the slim 45pp of that first document to the more than 450 pages of the multi-volume present version. The present version also benefits greatly from the direct involvement of a broader authorship.

There are currently no plans for continued evolution of the Ocean Optics Protocols. It is hoped that at some point in the next few years, someone will revisit and update them, for they will always be a "work in progress".

REFERENCES

Fargion, G.S. and J.L. Mueller, 2000: Ocean Optics Protocols for Satellite Ocean Color Sensor Validation, Revision 2, NASA TM 2001-209955, NASA Goddard Space Flight Center, Greenbelt, Maryland, 184 pp.

Mueller, J.L. and R.W. Austin, 1992: Ocean Optics Protocols for SeaWiFS Validation. NASA Tech. Memo. 104566, Vol. 5, S.B. Hooker and E.R. Firestone (Eds.), NASA Goddard Space Flight Center, Greenbelt, Maryland, 45pp.

Mueller, J.L., et al., 2002: Ocean Optics Protocols for Satellite Ocean Color Sensor Validation, Revision 3, NASA TM 2002-210004, Mueller, J.L. and G. Fargion (Eds.), NASA Goddard Space Flight Center, Greenbelt, Maryland, 308pp.

Mueller, J.L., et al., 2003a: Ocean Optics Protocols for Satellite Ocean Color Sensor Validation, Revision 4, Volume I: Introduction, Background and Conventions. NASA TM 2003-211621/Rev.4-Vol.I, Mueller, J.L., G. Fargion and C.R. McClain (Eds.), NASA Goddard Space Flight Center, Greenbelt, Maryland, 50pp.

Mueller, J.L., et al., 2003b: Ocean Optics Protocols for Satellite Ocean Color Sensor Validation, Revision 4, Volume II: Instrument Specifications, Characterization, and Calibration.. NASA TM 2003-211621/Rev.4-Vol.II, Mueller, J.L., G. Fargion and C.R. McClain (Eds.), NASA Goddard Space Flight Center, Greenbelt, Maryland, 56pp.

Mueller, J.L., et al., 2003c: Ocean Optics Protocols for Satellite Ocean Color Sensor Validation, Revision 4, Volume III: Radiometric Measurements and Data Analysis Protocols. NASA TM 2003-211621/Rev.4-Vol.III, Mueller, J.L., G. Fargion and C.R. McClain (Eds.), NASA Goddard Space Flight Center, Greenbelt, Maryland, 78pp.

Mueller, J.L., et al., 2003d: Ocean Optics Protocols for Satellite Ocean Color Sensor Validation, Revision 4, Volume V: Biogeochemical and Bio-optical Measurements and Data Analysis Protocols, NASA TM 2003-211621/Rev.4-Vol.V, Mueller, J.L., G. Fargion and C.R. McClain (Eds.), NASA Goddard Space Flight Center, Greenbelt, Maryland, 25pp.

Mueller, J.L., et al., 2002e: Ocean Optics Protocols for Satellite Ocean Color Sensor Validation, Revision 4, Volume I: Special Topics in Ocean Optics Protocols and Appendices. NASA TM 2003-211621/Rev.4-Vol.VI, Mueller, J.L., G. Fargion and C.R. McClain (Eds.), NASA Goddard Space Flight Center, Greenbelt, Maryland, 139pp.

Pegau, S., et al., 2003: Ocean Optics Protocols for Satellite Ocean Color Sensor Validation, Revision 4, Volume IV: Inherent Optical Properties: Instruments, Characterizations, Field Measurements and Data Analysis Protocols. NASA TM 2003-211621/Rev.4-Vol.VI, Mueller, J.L., G. Fargion and C.R. McClain (Eds.), NASA Goddard Space Flight Center, Greenbelt, Maryland, 76pp.

Chapter 14

Bermuda Bio Optics Project

Norm Nelson

Institute for Computational Earth Science, UCSB, Santa Barbara, California

14.1 INTRODUCTION

The Bermuda BioOptics Project (BBOP) is a collaborative effort between the Institute for Computational Earth System Science (ICESS) at the University of California at Santa Barbara (UCSB) and the Bermuda Biological Station for Research (BBSR). This research program is designed to characterize light availability and utilization in the Sargasso Sea, and to provide an optical link by which biogeochemical observations may be used to evaluate bio-optical models for pigment concentration, primary production, and sinking particle fluxes from satellite-based ocean color sensors. The BBOP time-series was initiated in 1992, and is carried out in conjunction with the U.S. JGOFS Bermuda Atlantic Time-series Study (BATS) at the Bermuda Biological Station for Research. The BATS program itself has been observing biogeochemical processes (primary productivity, particle flux and elemental cycles) in the mesotrophic waters of the Sargasso Sea since 1988. Closely affiliated with BBOP and BATS is a separate NASA-funded study of the spatial variability of biogeochemical processes in the Sargasso Sea using high-resolution AVHRR and SeaWiFS data collected at Bermuda (N. Nelson, P.I.). The collaboration between BATS and BBOP measurements has resulted in a unique data set that addresses not only the SIMBIOS goals but also the broader issues of important factors controlling the carbon cycle.

14.2 RESEARCH ACTIVITIES

BBOP personnel participate on all BATS cruises, which are conducted monthly with additional cruises during the spring bloom period, January through May. Table 1 contains a list of data products relevant to SIMBIOS. The BBOP project collects continuous profiles of apparent optical properties (AOPs) in the upper 140m and deployments are planned to optimize match-ups with the BATS primary production incubations and with SeaWiFS overpasses. In 1999, a free-falling Satlantic profiling radiometer system (SPMR/SMSR s/n 028) became our primary profiling instrument. The primary optical measurements are downwelling vector irradiance and upwelling radiance, $E_d(z,t,l)$ and $L_u(z,t,l)$, respectively. Derived products include remote sensing reflectance ($R_{rs}(z,l)$) and down- and upwelled attenuation coefficients ($K_d(z,l)$, $K_u(z,l)$). The sampling package also includes a second mast-mounted radiometer with wavebands matching those on the underwater instrument for measuring incident downwelling vector irradiance, $E_d(0^+,t,l)$. The instruments are calibrated three times annually at UCSB. Sky radiance measurements were collected early in the year, but the Microtops photometer began malfunctioning and it was returned to the project in the spring of 2003.

Bottle samples for fluorometric chlorophyll-*a* and inherent optical properties (IOPs) are also collected. Chlorophyll-*a* is collected once or twice daily during each cruise. Discrete samples for determining the absorption spectra of particulates, $a_{ph}(z,l)$ and $a_d(z,l)$, and CDOM ($a_g(z,l)$) are collected according to Nelson *et al* (1998). Particulate absorption spectra are determined using the quantitative filter technique (Mitchell, 1990) (with a regionally specified beta correction factor) and CDOM absorption according to Nelson *et al* (1998). During the past year, BBOP has participated in 14 BATS cruises. We have submitted 260 optics profiles, 70 fluorometric Chlorophyll-a profiles, 150 IOP spectra, and 4 Microtops scans for sky radiance.

14.3 RESEARCH RESULTS

Instrument Calibration

We have continued our documentation of the long-term calibration behavior of our SPMR systems using several lamps traceable to our own NIST standard. Channels greater than 500nm continue to show no obvious drift, and overall scatter is ~1% and ~2% for irradiance and radiance detectors, respectively. The coefficients of variation these channels are less than 1%. In general, the radiance channels are more stable than the irradiance channels. This suggests that the fault is most likely to be the materials used in the cosine collectors. The tendency for the UV and blue channels to vary more than the red is in part due to the lower output of calibration lamps at lower wavelengths. The most extreme changes were noted at the shortest UV channels in both irradiance heads: up to 50-60% for Ed325 and Es325, and about half that for Ed340 and Es340. It appears that this decrease in sensitivity occurred during the first year, and that these sensors are now stabile, although the response is still quite variable. The additional year of data now shows that two UV radiance and the blue irradiance channels have undergone significant drift toward lower sensitivity. The drift in the blue radiance sensors was less apparent, and smaller, about 1-2%, not significantly different from variation observed in the green-red channels. All affected data for these channels was recalculated using a predicted coefficient rather than a long-term average, and resubmitted.

Collaborative and Project-Related Activities

As in past years, the BBOP data set 1) contributed to the validation of satellite data products within in the SIMBIOS project and 2) used to make original contributions to scientific literature. In particular, BBOP is among the clearest ocean sites observed within the SIMBIOS program on a consistent basis. This means that BBOP has consistently been the clear water end member in match-up analyses made between field and satellite observations. The present version (August 2003) of the SIMBIOS SeaWiFS LAC-field observation match-up data set (Bailey et al. 2000) contains 383 independent field and satellite observations of water-leaving radiance. Thirty of these observations are from the BBOP project. As always these data are available via the world wide web (www.icess.ucsb.edu/bbop.html).

A primary science result from BBOP has been the observation that the optical properties of open ocean are greatly affected by concentrations of colored dissolved organic materials or CDOM (Siegel and Michaels, 1996; Nelson et al. 1998; Nelson and Siegel, 2002; Siegel et al. 2002). We have shown that CDOM dominates the optical properties in the blue region of the spectrum using knowledge gained at BBOP and available field and satellite data sets (many field observations were supported by the SIMBIOS program). Globally, 45% of the non-water absorption at 440 nm is due to CDOM (Siegel et al. 2002). Retrieval algorithms for CDOM were developed (Maritorena et al. 2002) and used to assess its global distribution and variability (Siegel et al. 2002). We have recently shown that the open ocean source of CDOM is the heterotrophic cycling of DOM by bacteria (Nelson et al. 2003) where CDOM can be created and destroyed by microbes. The interesting result from these microbe batch culture experiments is that the net CDOM produced mirrors the “complexity” of the DOM source (i.e., high molecular weight DOM leads to more long-lasting CDOM produced). We are presently testing these hypotheses on a new project looking at open ocean CDOM cycling supported by NSF.

Our work on CDOM has lead us to consider its interactions with other photoactive materials. One interesting candidate is dimethyl sulfide (DMS). Using existing time series (Dacey et al. 1998) and new experimental data, we have calculated the rates that DMS is photolysed by exposure to ultraviolet radiation (Toole et al. 2003). Using these results and new observations of microbial DMS (and DMSP) cycling by bacteria, we have made new and important estimates of the biological cycling of DMS (Toole and Siegel, 2003). Our supports the notion that DMS is important as an intracellular anti-oxidant removing radicals and superoxides within a cell. (Sunda et al. 2002). These results have a critical bearing on how climate feedbacks due to marine emissions of DMS might occur (Toole and Siegel, 2003).

REFERENCES

Bailey, S.W., C.R. McClain, P.J. Werdell and B.D. Schieber, 2000:Normalized water-leaving radiance and chlorophyll a match-up analyses. Chapter 7, In: SeaWiFS Postlaunch Calibration and Validation

Analyses, Part 2. *NASA Tech. Memo. 2000-206892*, Vol. **10**, S.B. Hooker and E.R. Firestone, Eds., NASA Goddard Space Flight Center, Greenbelt MD.

Dacey, J.W.H., F.A. Howse, A.F. Michaels, and S.G. Wakeham. 1998: Temporal variability of dimethylsulfide and dimethylsulfoniopropionate in the Sargasso Sea. *Deep-Sea Research* **45**: 2085-2104.

Nelson, N.B., and D.A. Siegel, 2002: Chromophoric DOM in the Open Ocean. In: *Biogeochemistry of Marine Dissolved Organic Matter,* D.A. Hansell and C.A. Carlson, eds. p. 547-578, Academic Press, San Diego, CA.

Maritorena, S., D.A. Siegel and A.R. Peterson, 2002: Optimal tuning of a semi-analytical model for global applications. *Applied Optics-LP*, **41**, 2705-2714.

Mitchell, B.G., 1990: Algorithms for determining the absorption coefficient for aquatic particles using the quantitative filter technique. *Ocean Optics X, Proceedings of S.P.I.E.*, **1302**, 137-142.

Mueller, J. L. and R. W Austin. 1995. Ocean optics protocols for SeaWiFS Validation, revision 1. NASA Tech. Memo. 104566, v. 25: (Hooker, S, E. Firestone and J. Acker, eds.), 67 pp.

O'Brien, M.C., D.W Menzies, D.A. Siegel, and R.C. Smith, 2000: Long-Term Calibration History of Several Marine Environmental Radiometers (MERs). *NASA Tech. Memo, SeaWiFS Postlaunch Calibration and Validation Analyses*, Vol. **11**, Part 3, Chap. 4.

Nelson, N.B., D.A. Siegel, and A.F. Michaels, 1998: Seasonal dynamics of colored dissolved material in the Sargasso Sea, *Deep Sea Research I,* **45**, 931-957.

Siegel, D.A., and A.F. Michaels, 1996: Quantification of non-algal light attenuation in the Sargasso Sea: Implications for biogeochemistry and remote sensing. *Deep-Sea Research II*, **43**, 321-345.

Siegel, D.A., S. Maritorena, N. B. Nelson, D.A. Hansell and M. Lorenzi-Kayser, 2002: Global ocean distribution and dynamics of colored dissolved and detrital organic materials. *Journal of Geophysical Research,* **107,** 3228, DOI: 10.1029/2001JC000965.

Sunda,W., D.J. Kieber, R. P. Kiene & S. Huntsman, 2002, An antioxidant function for DMSP and DMS in marine algae. *Nature*, **418**, 317 – 320.

Toole, D.A., and D.A. Siegel, 2003: Light and the open ocean cycling of dimethyl sulfide (DMS). Submitted to *Nature*.

Toole, D.A., D.J. Kieber, R.P. Kiene, D.A. Siegel and N.B. Nelson, 2003: Photolysis and the dimethylsulfide (DMS) summer paradox in the Sargasso Sea. *Limnology and Oceanography*, **48**, 1088-1100.

Table 14.1: Partial List of Measurements Made by BBOP & BATS

BBOP	
Direct Measurements:	
$E_d(z,l)$	Downwelling vector irradiance (325, 340, 380, 412, 443, 488, 510, 555, 565, 665 & 683 nm)
$E_d(0^+,l)$	Incident irradiance (325, 340, 380, 412, 443, 488, 510, 555, 565, 665 & 683 nm)
$L_u(z,l)$	Upwelling radiance (325, 340, 380, 412, 443, 488, 510, 555, 565, 665 & 683 nm)
chl-fl(z)	Chlorophyll fluorescence with a WetStar fluorometer
T(z) & S(z)	Temperature and conductivity with Ocean Sensors probes (calibrations by Satlantic)
$a_{tp}(l)$	Particulate absorption spectrum by QFT
$a_d(l)$	Detrital particle absorption spectrum by MeOH extraction
$a_{ys}(l)$	Colored dissolved absorption spectrum
chl-a(z)	Discrete chlorophyll *a* determinations via Turner fluorometry
Primary Derived Products:	
$L_{wN}(l)$	Normalized water leaving radiance (325, 340, 380, 412, 443, 488, 510, 555, 565, 665 & 683 nm)
$R_{RS}(0^-,l)$	In-water remote sensing reflectance (325, 340, 380, 412, 443, 488, 510, 555, 565, 665 & 683 nm)
$K_d(z,l)$	Attenuation coefficient for $E_d(z,l)$ (325, 340, 380, 412, 443, 488, 510, 555, 565, 665 & 683 nm)
$K_l(z,l)$	Attenuation coefficient for $L_u(z,l)$ (325, 340, 380, 412, 443, 488, 510, 555, 565, 665 & 683 nm)
$a_{ph}(l)$	Phytoplankton absorption spectrum (= $a_p(l) - a_{det}(l)$)
<PAR(z)>	Daily mean photosynthetically available radiation at depths of the *in situ* C^{14} incubations

U.S. JGOFS BATS (NSF) AND RELATED BIOGEOCHEMISTRY SAMPLING PROGRAMS	
Primary Production (*in situ* ^{14}C incubation)	Sinking flux (sediment trap array)
Phytoplankton pigments (fluorometric & HPLC)	Nutrients (NO_3+NO_2, SiO_4, PO_4)
CO_2 system (alkalinity, TCO_2 and pCO_2)	Continuous atmosphere & surface pCO_2
Dissolved oxygen (continuous & discrete)	Zooplankton biomass & grazing
POC & PON (POP infrequently)	DOC & DON (DOP infrequently)
Full water column, WOCE-standard CTD profile	Bacterial abundance and rates
Validation spatial cruises (5 days, 4cruises/year)	Deep ocean sediment sinking fluxes

This Research was Supported by
the NASA Contract # 00200

Publications

Siegel, D.A., S. Maritorena, N. B. Nelson, D.A. Hansell and M. Lorenzi-Kayser, 2002: Global ocean distribution and dynamics of colored dissolved and detrital organic materials. *Journal of Geophysical Research,* **107,** 3228, DOI: 10.1029/2001JC000965.

Chomko, R.M., H.R. Gordon, S. Maritorena and D.A. Siegel, 2003: Simultaneous determination of oceanic and atmospheric parameters for ocean color imagery by spectral optimization: a validation. *Remote Sensing of the Environment*, **84**, 208-220.

Westberry T.K., and D.A. Siegel, 2003: Phytoplankton natural fluorescence in the Sargasso Sea: Prediction of primary production and eddy induced nutrient fluxes. *Deep-Sea Research, Part I*, **50**, 417-434.

Toole, D.A., D.J. Kieber, R.P. Kiene, D.A. Siegel and N.B. Nelson, 2003: Photolysis and the dimethylsulfide (DMS) summer paradox in the Sargasso Sea. *Limnology and Oceanography*, **48**, 1088-1100.

Nelson, N.B., C.A. Carlson, and D.A. Steinberg. 2003, Production of chromophoric dissolved organic matter by Sargasso Sea microbes. In press, *Marine Chemistry*.

Nelson, N.B., D.A. Siegel, and J.A. Yoder, 2003, The spring bloom in the northwestern Sargasso Sea: Spatial extent and relationship with winter mixing. Accepted for publication in *Deep-Sea Research, Part II.*

Submitted

Behrenfeld, M.J., E. Boss, D.A. Siegel and D.M. Shea, 2003, Global remote sensing of phytoplankton physiology. Submitted to *Science*.

Toole, D.A., and D.A. Siegel, 2003: Light and the open ocean cycling of dimethyl sulfide (DMS). Submitted to *Nature*.

Presentations

Toole, D.A., R.P. Kiene, and D. Slezak, D.J. Kieber, and D.A. Siegel, Rates and Quantum Yields of Dimethylsulfide Photo-oxidation in the Western Atlantic Ocean, 2002 3rd international symposium on biological and environmental chemistry of DMS(P) and related compounds, September 2002, Rimouski, Quebec, Canada, poster presentation.

Maritorena, S., D.A. Siegel and D.B. Court, 2002: Ocean color data merging using a semi-analytical model. Poster presented at the Ocean Optics XIII meeting, Sante Fe, NM, November 2002.

Westberry, T., D.A. Siegel and A. Subramaniam, 2002: New techniques for the remote sensing of Trichodesmium. Poster presented at the 2002 AGU Fall Meeting, San Francisco, CA, December 2002.

Toole, D.A., D.A. Siegel, D. Slezak, R.P. Kiene, N.B. Nelson and J.W. Dacey, 2002: A light driven upper-ocean dimethylsulfide (DMS) biogeochemical cycling model for the Sargasso Sea. Poster presented at the 2002 AGU Fall Meeting, San Francisco, CA, December 2002.

Siegel, D.A., J.C. Ohlmann, S.C. Doney, C.R. McClain, 2002: Variability of ocean radiant heating in the Eastern Tropical Pacific. Poster presented at the 2002 AGU Fall Meeting, San Francisco, CA, December 2002.

Siegel, D.A., 2003: Sverdrup's critical depth hypothesis and the North Atlantic spring bloom. Presentation made for the International JGOFS North Atlantic Synthesis Group, Toulouse, FR., January 2003.

Klamberg, J.L., N.B. Nelson and D.A. Siegel, 2003: One-dimensional modeling of seasonal colored dissolved organic matter dynamics in the Sargasso Sea. Poster presented at the 2003 ASLO Aquatic Sciences meeting, Salt Lake City, UT, February 2003.

Siegel, D.A., N.B. Nelson, S. Maritorena, C.A. Carlson, A.F. Michaels, D.A. Hansell and D.K. Steinberg, 2003: Distribution, dynamics and biogeochemical implications of colored dissolved organic materials in the open ocean. Poster presented at the NASA Ocean Color Science Team Meeting, Miami FL, April 2003.

Maritorena, S., D.A. Siegel and D.B. Court, 2003: Ocean color data merging using a semi-analytical model. Poster presented at the NASA Ocean Color Science Team Meeting, Miami FL, April 2003.

Siegel, D.A., 2003: Reenvisioning the Ocean: The View from Space A RESPONSE, Invited rebuttal presented at the JGOFS Open Science Conference, Washington DC, May 2003.

Siegel, D.A., N.B. Nelson, S. Maritorena, C.A. Carlson, A.F. Michaels, D.A. Hansell and D.K. Steinberg, 2003: Distribution, dynamics and biogeochemical implications of colored dissolved organic materials in the open ocean: discoveries made during the JGOFS era. Poster presented at the JGOFS Open Science Conference, Washington DC, May 2003.

Chapter 15

Plumes and Blooms: Modeling the Case II Waters of the Santa Barbara Channel

D.A. Siegel, S. Maritorena and N.B. Nelson

Institute for Computational Earth System Science, University of California, Santa Barbara, California

15.1 INTRODUCTION

The goal of the Plumes and Blooms (PnB) project is to develop, validate and apply to imagery state-of-the-art ocean color algorithms for quantifying sediment *plumes* and phytoplankton *blooms* for the Case II environment of the Santa Barbara Channel. We conduct monthly to twice-monthly transect observations across the Santa Barbara Channel to develop an algorithm development and product validation data set. The PnB field program started in the summer of 1996. At each of the 7 PnB stations, a complete verification bio-geo-optical data set is collected. Included are redundant measures of apparent optical properties (remote sensing reflectance and diffuse attenuation spectra), as well as *in situ* profiles of spectral absorption, beam attenuation and backscattering coefficients. Water samples are analyzed for component *in vivo* absorption spectra, fluorometric chlorophyll, phytoplankton pigment (by the SDSU CHORS laboratory), and inorganic nutrient concentrations (Table 15.1). A primary goal is to use the PnB field data set to objectively tune semi-analytical models of ocean color for this site and apply them using available satellite imagery (SeaWiFS and MODIS). In support of this goal, we have also been addressing SeaWiFS ocean color and AVHRR SST imagery (Otero and Siegel, 2003). We also are using the PnB data set to address time/space variability of water masses in the Santa Barbara Channel and its relationship to the 1997/1998 El Niño. However, the comparison between PnB field observations and satellite estimates of primary products has been disappointing. We find that field estimates of water-leaving radiance, $L_{wN}(\lambda)$, correspond poorly to satellite estimates for both SeaWiFS and MODIS local area coverage imagery. We believe this is due to poor atmospheric correction due to complex mixtures of aerosol types found in these near-coastal regions. Last, we remain active in outreach activities.

15.2 RESEARCH ACTIVITIES

We have conducted 12 one-day cruises since November 2002 and anticipate conducting two more before the end of the contract. To date combination, we have completed 70 stations (up to 14 more by the end of the project) comprised of CTD/rosette casts, spectroradiometer profiles and in situ IOP determinations (AC9 & hydroscat). All available processed data has been submitted to the SeaBASS system and we will complete this task by November 1, 2003.

In January of 2003, the Channel Islands National Marine Sanctuary (CINMS) received delivery of its new research vessel, the *R/V Shearwater*. This finally has given us consistent platform to work from since the loss of the *R/V Ballena* in 2001. However, it hasn't come easy. We have experienced several aborted cruises early this year due to "new ship issues". This has been frustrating but we are now finally over the top. We have worked with CINMS and NOAA/NOS staff throughout this process and I think we finally have a stable field observation configuration for PnB cruises. We have continued our acquisition and analysis of satellite ocean color (SeaWiFS) and thermal imagery (AVHRR) from the UCSB HRPT ground station (HUSC). The UCSB ground station presently supported by SIMBIOS and NOAA/NESDIS.

The PnB project has an extensive education and outreach component. Typically, two undergraduate students volunteer on each one day cruise and the PnB data is presently being used in the theses and dissertations of three graduate students at UCSB. We also participated in the California Fish & Game workshops on monitoring the status of no-take marine protected areas around the CINMS. Satellite and field data supported by SIMBIOS are being used in this public process.

Table 15.1: Plumes and blooms measurements and data products

Direct Measurements:	
$E_d(z,\lambda)$	Downwelling vector irradiance (325, 340, 380, 412, 443, 490, 510, 555, 565, 665 & 683 nm)
$E_d(0^+,\lambda)$	Incident irradiance (325, 340, 380, 412, 443, 490, 510, 555, 565, 665, 683 & 350-1050 nm)
$L_u(z,\lambda)$	Upwelling radiance (325, 340, 380, 412, 443, 490, 510, 555, 565, 665 & 683 nm)
$a(z,\lambda)$	*In situ* absorption spectrum using WetLabs AC-9 (410,440,490,520,565,650,676 & 715 nm)
$c(z,\lambda)$	*In situ* beam attenuation spectrum (same as above)
$b_b(z,\lambda)$	*In situ* backscattering spectrum - HOBI Hydroscat (442,470,510,532, 590 & 671 nm)
T(z) & S(z)	SeaBird temperature and conductivity probes
$a_p(z_o,\lambda)$	*In vivo* particulate absorption spectrum by Mitchell (1990)
$a_{det}(z_o,\lambda)$	*In vivo* detrital particle absorption spectrum by MeOH extraction
$a_g(z_o,\lambda)$	*In vivo* colored dissolved absorption spectrum
chl-a(z_o)	Discrete chlorophyll *a* determinations by Turner fluorometry
pigs(z_o)	Discrete phytoplankton pigment sample to be run by HPLC (SDSU CHORS analysis)
nuts(z_o)	Discrete inorganic nutrient concentrations (NO_3, SiO_4, PO_4, NO_2)
$L_{sat}(x,y,\lambda)$	SeaWiFS and AVHRR imagery from the HUSC ground station

Primary Derived Products:	
$R_{rs}(0^-,\lambda)$	In-water remote sensing reflectance from profiling radiometry (see above)
$L_{WN}(\lambda)$	Normalized water leaving radiance calculated from $R_{RS}(0^+,\lambda)$ and $R_{RS}(0^-,\lambda)$
$a_{ph}(z_o,\lambda)$	*In vivo* phytoplankton absorption spectrum (= $a_p(z_o,\lambda)$ - $a_{det}(z_o,\lambda)$)
$K_d(z,\lambda)$	Attenuation coefficient for $E_d(z,\lambda)$ from profiling radiometry (also $K_L(z,\lambda)$)
$b(z,\lambda)$	*In situ* total scattering spectrum (= $c(z,\lambda)$ - $a(z,\lambda)$)
Chl(x,y), etc.	Processed SeaWiFS and AVHRR imagery

15.3 RESEARCH RESULTS

Academic research has gone along two major fronts; 1) the validation and development of satellite data products using the PnB data set (Siegel et al. 2002; 2003a; Otero and Siegel, 2003; Warrick et al. 2003a) and 2) the analyses of field and satellite data to assessment of the time/space variability in the Santa Barbara Channel (Shipe et al. 2002; Siegel et al. 2003b; Otero and Siegel, 2003; Warrick et al. 2003b; 2003c). We have used the PnB data set extensively in validation and development of satellite data products. This includes work related to development and application of global algorithms (Maritorena et al. 2002; Siegel et al. 2002; 2003c) and at the local scale (Warrick et al. 2003a). In particular, we have developed a simple mixing model to estimate suspended sediment concentrations for the Santa Clara River outflow plume (Warrick et al. 2003a). Jon Warrick, a recent PhD graduate from our group, has applied this algorithm to SeaWiFS imagery to examine the fate of river-borne sediment concentrations as they enter the Santa Barbara Channel (Mertes and Warrick, 2001; Warrick et al. 2003b; 2003c). We are still in progress in developing a regional semi-analytical model for this site (following Maritorena et al. 2002) and a new graduate student researcher (Tihomir Kostadinov) has taken this on as his Masters project.

Unfortunately, the hard part about building detailed predictive models of Case II ocean color variability is that matchups between satellite and in situ observations of water-leaving radiance, $L_{wN}(\lambda)$, are often poor and this suggests that significant improvements are required in the assumptions used to drive the atmospheric correction procedure (Siegel et al. 2003a). For example, figure 1 shows that both MODIS and SeaWiFS often, though not always, dramatically underestimate $L_{wN}(\lambda)$, particularly for the violet to blue wavebands. It is premature to make more definitive statements of the comparisons between the two satellite sensors due to the comparatively fewer number of matchup observations found using MODIS (29

as compared with as many as 314 found for SeaWiFS were available when this work was performed). However, these discrepancies are not due to problems with the field data as the satellite retrieved $L_{wN}(412)$ and $L_{wN}(443)$ values shown are much lower than typical values expected (Siegel et al. 2003a). The fact that the retrievals sometimes work and sometimes do not suggests that issues with the satellite's radiometric calibration are also not at fault either. That is, there is no obvious trending the discrepancy with the field observed $L_{wN}(412)$ and $L_{wN}(443)$ values as one would expect with for a static calibration error arising from the difference between two large numbers (measured and modeled top of the atmosphere radiance). Both sensors do a fair job (though clearly not spectacular) predicting $L_{wN}(555)$ and chlorophyll concentrations (r^2 = 0.50 [$L_{wN}(555)$] & 0.56 [Chl] for SeaWiFS and r^2 = 0.68 & 0.62 for MODIS for the same quantities). This reasonable success gives some confidence in the scientific application of these data to near-coastal regions (see also Otero and Siegel, 2003).

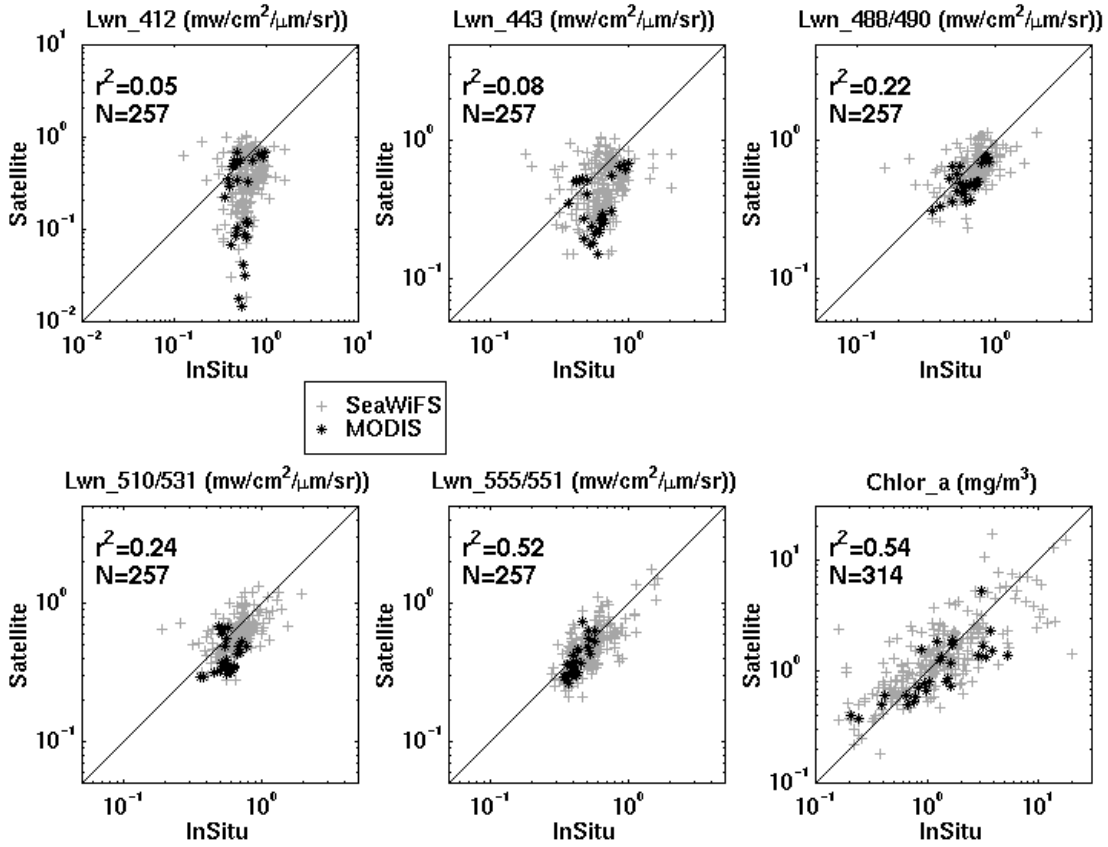

Figure 15.1: Matchup comparisons of satellite vs. field observations for normalized water-leaving radiance and chlorophyll a concentration for both SeaWiFS (+) and MODIS (*). Only MODIS data from Terra are shown and all data pass the quality zero flag. The OC3M chlorophyll estimate for MODIS is shown as there are 29 retrievals with this algorithm vs. 13 available from the MODIS semi-analytical algorithm (failures in the chl_a3 MODIS data product are quality flagged).

This simple matchup analysis suggests that substantial improvements are needed in the procedures used to correct satellite radiance for the complicating effects of the atmosphere. This may be true for global ocean retrievals, but it will be particularly acute for the coastal zone where state-of-the-art ocean color algorithms cannot be used due to the poor performance of present atmospheric correction procedures. We believe these difficulties are algorithmic (due to processing procedures and codes) and NOT to inadequacies in the field observations or in the radiometric calibration of satellite observations. Present techniques used by both SeaWiFS and MODIS to correct for the effects of the atmosphere are based on the initial framework of Gordon and Wang [1994] (see also Gordon and Voss, 1999). The Gordon and Wang (1994) algorithm uses spectral bands in the near infrared (NIR) to assess the aerosol's contribution to the

reflectance in the visible. This approach is applicable only for a non- or weakly-absorbing aerosol (Gordon, 1997). When the aerosol is strongly absorbing, associated with soot, pollution, biomass burning, pollen or dust aerosols, the NIR reflectance provides no clue to the path radiance that an atmospheric correction algorithm must correct for. This means that the two-step atmospheric correction process implemented in the retrieval of MODIS ocean color products will fail in the presence of strongly absorbing aerosols. The advantage of the spectral mixing approach of Warrick et al. [2003a] is that anomalies in the atmospheric path radiance due to complex aerosol distributions can be treated in an ad hoc manner enabling the sediment signal to be quantified. Semi-analytical methods (such as Maritorena et al. 2002) will NOT perform well under these conditions. We have ideas (in pending proposals!!) to develop novel correction procedures that simultaneously account for complex atmosphere and ocean interactions following approaches outline by Chomko et al. [2003].

We have continued our analyses of oceanographic processes using the six-year PnB observational record. Of continuing interest is our work assessing the sources and modes of ocean color variability within the Santa Barbara Channel (Toole and Siegel, 2001; Siegel et al. 2003b). The characterization of the substances, processes, and mechanisms that regulate coastal ocean color variability is crucial for the application of ocean color imagery to the management of marine resources. Using an empirical orthogonal function (EOF) analysis, we find that nearly two-thirds of the observed variability in remote sensing reflectance is contained in a backscattering mode. Phytoplankton absorption makes a much smaller contribution to the observed variance in the water-leaving radiance spectrum. Hence, particulate backscattering associated with suspended sediment concentrations is the dominant driver of ocean color variability for this environment. However, sediment plumes appear to play a much smaller role on biological processes. An empirical partitioning of physical, biological and chemical oceanographic parameters suggests that physical oceanographic processes (i.e., upwelling and horizontal advection) have the dominant role in determining phytoplankton pigment biomass for this region. One goal is to use these spectral EOF modes with satellite data to map out where and when blooms occur. Using EOF analysis of the space/time patterns of satellite ocean color imagery, we find a similar partitioning (Otero and Siegel, 2003). This work attempts to differentiate between the role of local (wind-driven upwelling and seasonal heating) vs. non-local (i.e., advection and ENSO) processes in regulating biological distributions in the Santa Barbara Channel (Otero and Siegel, 2003). A similar analysis is looking at the water quality measurements (nutrients, chlorophyll and optical properties, etc.) to address how physical processes are regulating optical variability in the Santa Barbara Channel (Siegel et al. 2003b). Further, a new graduate student supported by the Santa Barbara Coastal-LTER program, Clarissa Anderson, is working with the HPLC pigment data set to look at phytoplankton succession processes and their control by physical oceanographic proceses (Anderson et al. 2003).

On a last technical note, throughout the PnB time series we have noticed that our observations of the specific absorption of phytoplankton at 676 nm [$a^*_{ph}(676)$] often exceed the theoretical maximum of 0.0206 $m^2.mg^{-1}$. We now know that the reason for this overestimate was the use of previously published pathlength amplification factors (β) suggested by Mitchell (1990) from experiments using mixed phytoplankton cultures. To assess this source of bias, we conducted a set of experiments to test the relationship between the optical density in suspension (OD_s) and the optical density of the same sample on a GF/F filter (OD_f) of natural samples from PnB waters enabling us to determine our own β factor for our own spectrophotometer (Guillocheau, 2003). We conducted three independent determinations of the β factor which were consistent with each other (within a factor of 10%). However, the composite PnB β factor is a factor of 1.7 times lower than the Mitchell (1990) coefficients. Procedures used are documented in Guillocheau [2003]. We subsequently corrected all of our filter-pad absorption data and have submitted these to the SeaBASS data set.

REFERENCES

Anderson, C.R., D.A. Siegel, M.A. Brzezinski, N. Guillocheau and D.A. Toole, 2003: A time series assessment of phytoplankton community structure in the Santa Barbara Channel. Poster presented at the 2003 ASLO Aquatic Sciences meeting, Salt Lake City, UT, February 2003.

Chomko, R.M., H.R. Gordon, S. Maritorena and D.A. Siegel, 2003: Simultaneous determination of oceanic and atmospheric parameters for ocean color imagery by spectral optimization: a validation. *Remote Sensing of the Environment*, **84**, 208-220.

Guillocheau, N., 2003: Beta-Correction Experiment Report. ICESS Internal document, UCSB, April 2003, www.icess.ucsb.edu/~davey/MyPapers/beta_corr_report2.doc.

Mertes, L.A.K., and J.A. Warrick, 2001. Measuring flood output from 110 coastal watersheds in California with field measurements and SeaWiFS. *Geology*, **29**, 659-662.

Otero, M.P., and D.A. Siegel, 2003: Spatial and temporal characteristics of sediment plumes and phytoplankton blooms in the Santa Barbara Channel. Accepted for publication in *Deep-Sea Research, Part II*.

Shipe, R.F., U. Passow, M.A. Brzezinski, D.A. Siegel and A.L. Alldredge, 2002: Effects of the 1997-98 El Nino on seasonal variations in suspended and sinking particles in the Santa Barbara Basin. *Progress in Oceanography*, **54**, 105-127.

Siegel, D.A., S. Maritorena, N. B. Nelson, D.A. Hansell and M. Lorenzi-Kayser, 2002: Global ocean distribution and dynamics of colored dissolved and detrital organic materials. *Journal of Geophysical Research*, **107**, 3228, DOI: 10.1029/2001JC000965.

Siegel, D.A., E. Fields O. Polyakov, N. Guillocheau and D.W. Menzies, 2003a, Plumes and Blooms Field-Satellite Matchup Analyses. ICESS internal report. Available at www.icess.ucsb.edu/~davey/MyPapers/PnB_Matchups_March2003.doc.

Siegel, D.A., L. Washburn, J. Warrick, D.A. Toole, J. Sorensen, O. Polyakov, M.P. Otero, M.J. Neumann, L.A.K. Mertes, N. Guillocheau, D. Fernamburg and M.A. Brzezinski, 2003b: A time-series assessment of sediment plumes and phytoplankton blooms in the Santa Barbara Channel, California, To be submitted to Continental-Shelf Research.

Toole, D.A., and D.A. Siegel, 2001: Modes and mechanisms of ocean color variability in the Santa Barbara Channel. *Journal of Geophysical Research*, **106**, 26,985-27,000.

Warrick, J.A., L.A.K. Mertes, D.A. Siegel and C. MacKenzie, 2003a: Estimating suspended sediment concentrations in turbid coastal waters with SeaWiFS. In press *International Journal of Remote Sensing*.

Warrick J.A., L.A.K. Mertes, L. Washburn, and D.A. Siegel, 2003b: A conceptual model for river water and sediment dispersal in the Santa Barbara Channel, California. Submitted to *Continental Shelf Research*.

Warrick J.A., L.A.K. Mertes, L. Washburn, and D.A. Siegel, 2003c: Dispersal forcing of southern California river plumes, based on field and remote sensing observations. Submitted to *Geo-Marine Letters*.

Warrick J.A., L. Washburn, M.A. Brzezinski, and D.A. Siegel, 2003d: Nutrient contributions to the Santa Barbara Channel, California, from the ephemeral Santa Clara River. Submitted to *Estuarine, Coastal and Shelf Research*.

This Research was Supported by
the NASA Contract # 00201

Publications (denotes student papers)*

Behrenfeld, M.J., E. Boss, D.A. Siegel and D.M. Shea, 2003: Global remote sensing of phytoplankton physiology. Submitted to *Science*.

Chomko, R.M., H.R. Gordon, S. Maritorena and D.A. Siegel, 2003: Simultaneous determination of oceanic and atmospheric parameters for ocean color imagery by spectral optimization: a validation. *Remote Sensing of the Environment*, **84**, 208-220.

Guillocheau, N., 2003: Beta-Correction Experiment Report. ICESS Internal document, UCSB, April 2003, www.icess.ucsb.edu/~davey/MyPapers/beta_corr_report2.doc.

McPhee-Shaw, E., D.A. Siegel, L. Washburn, M.A. Brzezinski, and J.A. Jones, 2003, Mechanisms for nutrient delivery to the inner shelf: Observations from the Santa Barbara Channel. For *Limnology and Oceanography*.

Otero, M.P., and D.A. Siegel, 2003: Spatial and temporal characteristics of sediment plumes and phytoplankton blooms in the Santa Barbara Channel. Accepted for publication in *Deep-Sea Research, Part II*. (*)

Shipe, R.F., U. Passow, M.A. Brzezinski, D.A. Siegel and A.L. Alldredge, 2002: Effects of the 1997-98 El Nino on seasonal variations in suspended and sinking particles in the Santa Barbara Basin. *Progress in Oceanography*, **54**, 105-127. (*)

Siegel, D.A., .P. Kinlan, B. Gaylord and S.D. Gaines, 2003: Lagrangian descriptions of marine larval dispersion. *Marine Ecology Progress Series*, **260**, 83-96.

Siegel, D.A., S. Maritorena, N. B. Nelson, D.A. Hansell and M. Lorenzi-Kayser, 2002: Global ocean distribution and dynamics of colored dissolved and detrital organic materials. *Journal of Geophysical Research*, **107**, 3228, DOI: 10.1029/2001JC000965.

Siegel, D.A., L. Washburn, J. Warrick, D.A. Toole, J. Sorensen, O. Polyakov, M.P. Otero, M.J. Neumann, L.A.K. Mertes, N. Guillocheau, D. Fernamburg and M.A. Brzezinski, 2003: A time-series assessment of sediment plumes and phytoplankton blooms in the Santa Barbara Channel, California, To be submitted to Continental-Shelf Research.

Siegel, D.A., E. Fields O. Polyakov, N. Guillocheau and D.W. Menzies, 2003, Plumes and Blooms Field-Satellite Matchup Analyses. ICESS internal report. Available at www.icess.ucsb.edu/~davey/MyPapers/PnB_Matchups_March2003.doc.

Siegel, D.A., S. Maritorena, N.B. Nelson, 2003, Independence and interdependencies of ocean optical properties viewed using SeaWiFS. For *Journal of Geophysical Research*.

Warrick, J.A., L.A.K. Mertes, D.A. Siegel and C. MacKenzie, 2003: Estimating suspended sediment concentrations in turbid coastal waters with SeaWiFS. In press *International Journal of Remote Sensing*. (*)

Warrick J.A., L.A.K. Mertes, L. Washburn, and D.A. Siegel, 2003: A conceptual model for river water and sediment dispersal in the Santa Barbara Channel, California. Submitted to *Continental Shelf Research*. (*)

Warrick J.A., L.A.K. Mertes, L. Washburn, and D.A. Siegel, 2003: Dispersal forcing of southern California river plumes, based on field and remote sensing observations. Submitted to *Geo-Marine Letters*.

Warrick J.A., L. Washburn, M.A. Brzezinski, and D.A. Siegel, 2003: Nutrient contributions to the Santa Barbara Channel, California, from the ephemeral Santa Clara River. Submitted to *Estuarine, Coastal and Shelf Research*. (*)

Presentations

Anderson, C.R., D.A. Siegel, M.A. Brzezinski, N. Guillocheau and D.A. Toole, 2003: A time series assessment of phytoplankton community structure in the Santa Barbara Channel. Poster presented at the 2003 ASLO Aquatic Sciences meeting, Salt Lake City, UT, February 2003.

McPhee-Shaw, E.E., L. Washburn, D.A. Siegel, and M.A. Brzezinski, 2002: The Santa Barbara Channel LTER (Long-term ecological research) study. Oceanographic time-series data from nearshore stations, 2001, with implications for nutrient delivery to kelp reefs. Talk given at EPOC (Eastern Pacific Ocean Conference) meeting, Mt Hood, OR, September 25028, 2002.

McPhee-Shaw, E.E., M.A. Brzezinksi, D.A. Siegel, and L. Washburn, 2002: The Santa Barbara Channel LTER Oceanographic data from near-shore stations, 2001-2002, with implications for nutrient delivery to kelp reefs. Poster presented at the California and World Ocean ’02 Conference, Santa Barbara, CA, October 27-30, 2002.

Ow, L., L. Washburn, D.A. Siegel, and E.E. McPhee-Shaw, 2003: Moored observations of biological and physical variability near kelp reefs in the Santa Barbara Channel. Poster presented at the 2003 ASLO Aquatic Sciences meeting, Salt Lake City, UT, February 2003.

Senyk, N., and D.A. Siegel, 2002: Using remotely sensed data to describe spatial and temporal habitat distributions of the giant kelp, Macrocystis pyrifera. Poster presented at the California and World Ocean '02 Conference, Santa Barbara, CA, October 27-30, 2002.

Siegel, D.A., 2002: Flow, fish and fishing or the modeling of marine protected area efficiency. Colloquium presented at the UCSB Geography Department, November, 2002.

Siegel, D.A., N.B. Nelson, S. Maritorena, C.A. Carlson, A.F. Michaels, D.A. Hansell and D.K. Steinberg, 2003: Distribution, dynamics and biogeochemical implications of colored dissolved organic materials in the open ocean: discoveries made during the JGOFS era. Poster presented at the JGOFS Open Science Conference, Washington DC, May 2003.

Siegel, D.A., O. Polyakov, E. Fields and N. Guillocheau, 2003: Comparison of SeaWiFS and MODIS water leaving radiance spectra with in situ observations from the Santa Barbara Channel: Role of aerosol absorption, Poster presented at the NASA Ocean Color Science Team Meeting, Miami FL, April 2003.

Chapter 16

Algorithms for Processing and Analysis of Ocean Color Satellite Data for Coastal Case 2 Waters

Richard P. Stumpf
NOAA National Ocean Service, Silver Spring, Maryland

Robert A. Arnone and Richard W. Gould, Jr.
Naval Research Laboratory (NRL), Stennis Space Center, Mississippi

Varis Ransibrahmanakul
Technology Planning and Management Corporation, Silver Spring, Maryland

Patricia A. Tester
NOAA National Ocean Service, Beaufort, North Carolina

16.1 INTRODUCTION

SeaWiFS has the ability to enhance our understanding of many oceanographic processes. However, its utility in the coastal zone has been limited by valid bio-optical algorithms and by the determination of accurate water reflectances, particularly in the blue bands (412-490 nm), which have a significant impact on the effectiveness of all bio-optical algorithms. We have made advances in three areas: algorithm development (Table 16.1), field data collection, and data applications.

Table 16.1: Issues and advances to atmospheric correction.

Issues	Advances
1. The previous atmospheric correction poorly estimates water leaving radiance in the near infrared (NIR) when detritus and chlorophyll don't co-vary.	1. We offer an NIR correction, which draws on coupling the atmospheric and oceanic models (Stumpf et al., 2003), to better estimate water reflectance. NASA has implemented this correction to process of SeaWIFS data in July 2002.
2. The current atmospheric correction neglects the effects of absorbing aerosols associated such as pollution.	2. We offer a technique to estimate and remove the unresolved absorbing aerosol component in water reflectance (Ransibrahmanakul and Stumpf, 2003).

Data Collection

We have collected data sets of bio-optical properties in turbid Case 2 waters, which are relatively few in SeaBASS database. We have collected over 300 stations of AC9, remote sensing reflectance spectra, and HPLC (Table 16.2).

These data sets will provide the basis for improving and evaluating *in situ* bio-optical and atmospheric correction algorithms for coastal waters. The coastal waters with a high sediment load and/or high concentrations of colored dissolved organic matter (CDOM), standard processing algorithms typically fail (negative or erroneous retrievals of water-leaving radiance) due to invalid assumptions related to the atmospheric correction. Our efforts have focused on describing the reflectance properties at near-infrared (NIR) and blue wavelengths in coastal waters, and utilization these properties to improve the atmospheric

correction. We have modified and developed new coastal bio-optical algorithms, as well as validated the algorithms and atmospheric corrections.

We are also preparing for MODIS. We have implemented MODCOLOR and MODSST into the NRL processing software. This has included modifying the MODIS processing software in cooperation with NASA and University of Miami to use the same NIR atmospheric correction SEADAS is using.

Table 16.2: Number of stations of various data collected.

AC9/CTD	ASD/remote sensing reflectance	HPLC
352	404	413

Data Applications

In addition to algorithm development, we also utilize the new products to monitor and predict harmful algal blooms along the west Florida shelf and develop new products for SeaWiFS and MODIS.

16.2. RESEARCH ACTIVITIES

Cruises

We have collected in situ bio-optical data on twenty-five cruises. Measurements in the Northern Gulf of Mexico include absorption coefficient, beam attenuation coefficient, scattering coefficient (ac9), remote sensing reflectance (above water method), aerosol optical thickness (Microtops), and HPLC pigments (Table 16.2). A substantial number of these stations were collected during minimum cloud cover and matched up with SeaWIFS and MODIS passes. Measurements in North Carolina waters include water samples, water profile measurements (YSI), and remote sensing reflectance. The water samples were collected to determine chlorophyll, CDOM, filter pad absorption, HPLC, total suspended solids (TSS), and nutrients. Measurements along the Gulf coast include remote sensing reflectance from 400-900 nm, spectral absoprtion and scattering profiles (from an ac9), water samples, and aersol optical depth (MICROTOPS sunphotometer). The water samples were collected to determine chlorophyll, CDOM, filtered pad absorption, HPLC (through CHORS), total suspended solids (TSS), and nutrients.

The Use of LIDAR to Improve Bio-optical Algorithms (NOAA)

The current chlorophyll algorithm fails in high CDOM areas. We have collected simultaneous SeaWIFS, LIDAR, hyperspectral radiance, and water samples from Pamlico Sound to develop a more robust Case 2 bio-optical algorithm. Airborne LIDAR have been used to determine synoptic chlorophyll-*a* and CDOM in coastal North Carolina. Pat Tester has started a collaborative research project with Bob Swift at NASA Wallops Island. She has contracted for six more over flight windows to use LIDAR during the spring and fall from 2003 through 2005. In addition to the utility of CDOM (and organic C), CDOM signals may serve as mimics for salinity or nutrients pulses after runoff events.

16.3. RESEARCH RESULTS

NIR atmospheric correction implemented to latest SEADAS (NOAA & NRL)

We submitted NIR atmospheric correction code and manuscript to Sean Bailey in March and September 2002, respectively. After Gene Feldman compared the products derived from many atmospheric corrections and posted them to SeaWiFS community for review, NASA implemented our NIR-correction approach into SEADAS 4.4 (released July 2002). In addition to NASA's evaluation, we independently compared the products derived from different atmospheric corrections against measured data. The comparison shows that the proposed NIR reduced both the bias and root-mean square error. Description NIR correction may be found in Volume 22 of a NASA technical memo: Algorithm Updates for the Fourth SeaWiFS Data Processing.

Table 16.3: Summary of Data Collected

Experiment	Cruise	Date	Ac9/CTD Etc.	ASD rrs	HPLC
Cojet 3–Northern Gulf of Mexico	Mopex	5/16/01	26	36	0
Cojet 3–Northern Gulf of Mexico	Lgssur	5/16/01	31	31	29
Cojet 3–Northern Gulf of Mexico	Ocolor	5/16/01	22	22	25
NGLI Lake Bourne Apr01	Ocolor	04/01	4	3	4
NGLI Biloxi 11Sep01	Ocolor2	09/01	8	8	8
Leo2001- East Coast –New jersey	R/V NorthStar	7/31- 8/02/01	15	28	23
Cojet 4 – Barrier Islands, Mobile Bay		9/2/01 – 9/6/01	17	16	33
Cojet 5 – Barrier Is., Mobile Bay	Pelican	12/3/01-12/7/01	26	25	26
Cojet 6- Barrier Is., Mobile Bay	Pelican	3/5/02-3/6/02	8	9	9
Cojet 7 – Barrier Island	Pelican	5/17/02-5/26/02	29	17	27
Cojet 7 – Barrier Island	Ocolor	5/17/02-5/26/02	24	25	25
NGLI Biloxi 19Nov01		5/01			5
ECOHAB- West Florida Shelf	ECOHAB	9/25/00-9/29/00			25
NC-04/01- North Carolina	Pamlico	4/10/01-4/11/01	8	10	14
NC-05/01 – North Carolina		5/24/01		4	4
NC 07/01 North Carolina	Pamlico	7/24/01 – 7/26/01		4	11
NC 08/01	Pamlico/NC shelf	08/1/01-8/2/01			5
NC-10/01	NC Shelf/Pamlico	10/16/01-10/19/01		8	13
NC-02/02	Pamlico	2/19/02-2/21/02		8	8
CA-03/02	Offshore San Francisco, Gulf of Farallones	3/2/02-3/4/02		7	20
NC-07/02	Pamlico	7/3/02		2	6
Dolche-Vita	Adriatic Sea	Feb 03	35	35	
Monterey		April 03	59	55	60
Fort Lauderdale		Aug 8 – 10, 2003	18	18	0
Horn Island, near Biloxi, MS		Sep 17- 19, 2003	22	22	22
NC03		4/15/03-4/16/03		11	11
		TOTALS	352	404	413

Absorbing aerosol correction

Although the NIR correction improves the accuracy of the derived water reflectance, the correction only corrects for the Rayleigh and aerosol scattering but neglects absorption due to aerosols. Thus, the current 'water absorption' is an overestimate of true water absorption when absorbing aerosols are present. The overestimated water absorption begets underestimated reflectance and underestimated chlorophyll. We have a proposed algorithm to correct for absorbing aerosols and will submit the manuscript to Applied Optics.

Calibration (NOAA)

At the AGU meeting in San Francisco, December 2001, Ransibrahmanakul and Stumpf (2001) presented a new method for validating calibration gain values in the blue bands.

Background & Problem

The current calibration of SeaWiFS involves two steps: correction for temporal changes using lunar observations and periodic vicarious calibration of the radiance based on comparison with the Marine Optical Buoy (MOBY) sites. The later has potential uncertainty of 0.5 % in the top-of-atmosphere (TOA) radiance calibration (Barnes et al. 2000), partly because each band is calibrated independently. In coastal areas, the calibration of the 412 nm band is of particular concern owing to the need to correct for absorbing aerosols in the atmosphere and the need to monitor and compensate for colored dissolved organic matter (CDOM) in the water. Calibration errors of 0.5-1% between bands in the blue (412 nm, 443 nm, 490 nm) can introduce significant errors in the retrieved water reflectance (5-10% in case 1 water, and 20-100% in case 2 water).

We proposed two methods: one involving examination of case 2 water; another, in all water types. Both methods use an inter-band relationship found in the field (and assumed to be intrinsic) to validate the spectral shape observed in satellite data. The coastal method examines spectral curvature in the blue bands. Satellite data typically shows a convex shape from 412 to 490 nm, while field data shows a concave shape. By defining coastal water spectra as those with remote sensing reflectance at 443 nm greater than remote sensing reflectance at 412 nm, we found that 90% of the 420 field coastal water spectra are concave (index < 0). In contrast, 90% of the satellite coastal water spectra are convex (index > 0).

Using the latest calibration and software, we found the calibration at 412 nm appears to be underestimated by about 1%. For validation, we computed the overall bias and root mean square error (rms) from 105 pairs of satellite and same-day cloud-free measured remote sensing reflectance in US waters. Using the adjusted calibration, the bias at 412 nm is reduced by four folds. Adding a component to the current protocol to calibrate multiple bands simultaneously may improve the total calibration.

Remote Sensing Relectance at 670 nm (NOAA)

Remote sensing reflectance at 670 nm is used in the NIR correction. Inaccurate remote sensing reflectance at 670 nm would contribute errors in all bands. We have observed large patches of negative remote sensing reflectance at 670 nm near the coast in the North Atlantic. In an effort to identify the problem, we compared SeaWiFS remote sensing reflectance at 670 nm with two modeled estimates in the Sargasso Sea. This area was chosen because of its extremely low chlorophyll characteristics, therefore reducing the number of assumptions made in the models. We observed satellite remote sensing reflectance at 670 nm to be higher than both modeled estimates. This was unexpected, considering that negative remote sensing reflectance has been observed. In conclusion, adjusting the calibration at 670 nm in any direction is not a global solution, indicating that a local problem, possibly in some of the atmospheric correction models, may be producing the negative radiances at 670 nm.

Validation of Atmospheric Correction and Chlorophyll Algorithms for Processing SeaWiFS data (NOAA)

With at least four atmospheric corrections and chlorophyll algorithms for SeaWiFS available, a user may be interested in their performances in different water types. To facilitate this comparison, Zhong Ping Lee and Bob Arnone have started an Ocean-Color-Algorithm working Group (OCAG), where the first meeting will take place on November 17, 2002, Sata Fe, NM, prior to the Ocean Optics Conference.

We presented the results comparing atmospheric corrections and five chlorophyll algorithms in different water types at the 7th International Conference on Remote Sensing for Marine and Coastal Environments, Miami, May 2002 (Ransibrahamanakul et al., 2002). We have developed an evaluation protocol to evaluate the performance of the available atmospheric corrections (including the NOAA/NRL developmental atmospheric correction) and chlorophyll algorithms. To date, we have used 159 same-day field-satellite pairs of remote sensing reflectance spectra to determine the best atmospheric correction applicable to the entire US coastline. The five atmospheric corrections considered were developed by Gordon & Wang (1994), Siegel et al. (2000), Gould et al. (1998), Ruddick et al. (2000), and NOAA/NRL (Stumpf et al., 2003). We did not include the atmospheric correction developed by Hu et al. (2000) because it requires manual interaction and is not appropriate for automated processing.

Similarly, we have developed protocols and software for evaluating multiple chlorophyll algorithms for regional application. The analysis involves examination of spatial matches and ranking of the procedures. In both the evaluations of atmospheric correction and chlorophyll algorithms, the selection procedure was designed to determine an algorithm that works best over a range of water types and compensates for distribution biases. The process also allows comparison of the chlorophyll with unique optical properties where algorithms may fail. This occurs in Pamlico Sound, North Carolina, during flood conditions, and in Atchafalaya Bay, Louisiana, under high flow. We are examining the potential factors.

MODIS Terra processing (NRL)

We are working with the University of Miami and NASA Goddard for processing MODIS ocean color data. We have obtained MODCOLOR and MODSST and implemented on our Linux operating system and integrated it into the Automated Processing System (APS) (Navy's satellite processing software). We have modified the MODIS software with the NIR atmospheric correction used in SeaWIFS processing and implemented coastal algorithms. The output of all the APS is an HDF file format that is directly input into SEADAS or ENVI. Our efforts in MODIS processing required that we closely coordinate efforts with the MODIS Science team and MODIS calibration Science Team. These required updated calibration, level 0 and 2 processing etc. We have worked with the programmers and scientists at University of Miami (Evans group), and Goddard (Esaisas group, and C. Lyons group). They have provided quality data and cooperative efforts which have allowed us the ability to do our research. This cooperation is strongly acknowledged.

We are generating the standard NASA products (Chlorophyll, absorption and scattering) in addition to bio-optical navy algorithms (over 50 products) in both MODIS (TERRA) and SeaWIFS. We are comparing the differences in the sensors for a 2 year period in the Gulf of Mexico by looking at weekly composites. These results are being presented at the Ocean Optics Conference in Nov 02.

We have implemented routine processing of MODIS-TERRA for selected ocean regions in the US (Gulf of Mexico, and Chesapeake Bay) and other areas. We have automated the procedure for transfer and processing of MODIS data from the "MODIS Direct Broadcasting" and the NOAA/NASA Project. We have obtained software and data from MODIS –AQUA but are not currently processing this data routinely.

We have added the capability to process MODIS AQUA data with the NRL Automated Processing System (APS), in addition to our capabilities for TERRA imagery. We have worked closely with folks at University of Miami, NOAA, and NASA/Goddard on this effort. We are implementing the new NIR algorithms we developed for SeaWiFS under SIMBIOS. The processing is now implemented and we process daily MODIS AQUA and TERRA imagery from several regions, including the Gulf of Mexico, Adriatic Sea, Persian Gulf, Arabian Sea, and New York Bight.

We have automated transfer of MODIS data to our APS. Automated MODIS data streams are in place from both NASA/Goddard and NOAA, and we generally process scenes within about 6-8 hours of the satellite overpass. The processed imagery is archived at NRL/Stennis and is accessible via our web browser.

We are working with NASA/Stennis to receive MODIS data over the Gulf of Mexico in real time. We have successfully captured, transferred, and processed a test scene from their X-band receiving system. We developed preliminary MODIS c660, absorption, scattering, and diver visibility products at 250m resolution for the Persian Gulf (in support of Operation Iraqi Freedom). Work is underway to improve the products and the atmospheric correction routines used for the 250m MODIS channels, including both Rayleigh and aerosol corrections.

Work is underway to implement new bio-optical optimization algorithms for MODIS into the NRL APS. We are in the process of validating MODIS TERRA-retrieved estimates of remote sensing reflectance (Rrs), through comparisons with our in situ shipboard measurements. After completing this effort, we will validate the derived optical properties (absorption, backscattering) for TERRA, then we will conduct similar comparisons for AQUA. We have implemented new SQL search engines on our web page to facilitate browsing for daily and composited MODIS scenes in our image archive.

Other SeaWiFS activities

- We have developed new methods to understand terrestrial flux from coastal rivers. By unravelling the ocean color signatures into the basic in water constituents; we developed a 2 year time series of

SeaWIFS optical properties. We established the covariance of this 2 year satellite time series with river discharge of the Mississippi river.

- We developed new algorithms for extending the satellite near surface chlorophyll algorithms to depth. We assimilate the mixed layer depth and surface wind stress from NCOM with the latest satellite observations and define a vertical profile. This is being performed daily and has been automated for the Gulf of Mexico.

- We developed methods to limit cloud cover by using the spatially and temporally varying time series of satellite imagery. We developed methods of compositing more recent imagery into latest pixel composite. This method has created new products for optimizing ocean color products. We are using these methods for SeaWIFS and MODIS in the Gulf of Mexico.

- We have used the data collected in SIMBIOS to validate the coastal algorithms. We have tested the algorithms used for bio-optical properties (absorption and scattering derived from SeaWIFS). We have published this in Sea Technology.

- We have organized a real time data base on our web server to provide real time access to ocean products. These include SeaWIFS and MODIS sensors. Real time access is available to test algorithm products and determine the sensitivity of the algorithms for SeaWIFS and MODIS. http://www7333.nrlssc.navy.mil

- We developed a relationship between absorption and salinity, to derive surface salinity maps from coastal SeaWiFS imagery.

- We developed a relationship between b(555) and total suspended solids (TSS), to derive surface TSS maps from SeaWiFS.

- We linked physical processes (currents, tides, winds, wave resuspension) to optical distribution patterns in northern Gulf of Mexico.

- We developed new algorithms to estimate particulate inorganic matter (PIM) and particulate organic matter (POM) from SeaWiFS imagery.

- We developed new SeaWiFS algorithms to estimate separate CDOM and detritus absorption coefficients, rather than a single combined term. This will facilitate development of a new optical water mass classification system.

- We have improved coastal SeaWiFS optical algorithms through investigation of b_b/b and F/Q parameters.

- We have implemented a new Quasi- Analytical Algorithms (QAA) into the NRL APS processing of SeaWIFS and MODIS for coastal bio-optical algorithms. The QAA s a linearized version of the optimization algorithms which accounts for the majority of the optimization within the computation required. Products of chlorophyll, scattering and absorption from CDOM, phytoplankton and particles are currently being generated. They are available on the web. (Lee et al 2002).

- We have developed automated methods for collection and processing *in situ* ocean optics data for processing of field data. These methods have been applied to all our advanced *in situ* instrumentation. We have organized a calibration laboratory and track all our instrumentation. These include the ac9 and above water reflectance instruments and particle size instrument measurements. Additionally we have developed methods for partitioning particles into organic and inorganic fraction. These new methods are providing measurements for advanced algorithms.

- Work is underway to implement new bio-optical optimization algorithms for SeaWiFS into the NRL APS.

- We have developed new methods to understand terrestrial flux from coastal rivers, using new algorithms to estimate total suspended sediments (partitioned into organic and inorganic components). We calculated particle mass and areal plume extent, for the Mississippi River and Mobile Bay plumes. Results were presented at the Ocean Optics meeting in Santa Fe in November, 2002, and at the Oceanography Society meeting in New Orleans in June, 2003.

- We developed a new optical water mass classification system to trace water masses. The technique is based on the separation of the total absorption coefficient into components due to detritus, phytoplankton, and CDOM. It can be used to quantitatively characterize and trace coastal features over time. Results were presented at Ocean Optics and will be presented at the Optics of Natural Waters Conference in St. Petersburg, Russia, in September 2003.

- Work is underway to implement algorithm changes into our APS, for consistency with changes made by NASA/Goddard during the 4th SeaWiFS reprocessing. Following the algorithm updates, we will validate the SeaWiFS Rrs and optical products through comparison with our shipboard in situ data.

- We have implemented new SQL search engines on our web page to facilitate browsing for daily and composited SeaWiFS scenes in our image data base. Work is underway to add the capability to search for level 1 imagery and in situ data from our web page, to facilitate validation and reprocessing efforts (http://www7333.nrlssc.navy.mil).

16.4 CONCLUSIONS

Between the two groups, NOAA and NRL, we are developing an extensive data set for coastal and case 2 waters. We are in the process of merging the information for examination of remote sensing reflectance and chlorophyll. NRL has a data set from over 21 cruises. There are now 218 vertical profiles, 263 field spectra, and 320 HPLCs. NOAA has approximately 100 same-day match-ups of remote sensing reflectance and chlorophyll from the southeast and Gulf of Mexico. We assembled a database of *in situ* optical properties to evaluate SeaWIFS-derived properties collected from 1997 to present in a variety of coastal regions (Mississippi Bight, Mississippi River, West Florida Shelf, Loop Current, North Carolina, New Jersey). The data cover a broad range of absorption ($0.4 – 15\ m^{-1}$) and scattering ($0.1 – 27\ m^{-1}$) coefficients and remote sensing reflectance. The collected data set contributes to the SEABASS database, particular its Case 2 component. In addition to data collection, our groups produced the NIR-iterative technique used by the SeaWiFS project for the fourth reprocessing (repro4).

REFERENCES

Barnes, R.A., R.E. Eplee Jr., W.D. Robinson, G.M. Schmidt, F.S. Patt, S.W. Bailey, M. Wang, and C.R McClain, 2000: The calibration of SeaWiFS on orbit, Earth Observing Systems V, William L. Barnes (eds.), Proceedings of SPIE Vol. **4135**, 281-293.

Carder, K.L., F.R. Chen, Z.P. Lee, S.K. Hawes, and D. Kamykowski, 1999: Semianlytical moderate resolution imaging spectrometer algorithms for chlorophyll a and absorption with bio-optical domains based on nitrate-depletion temperatures, *Journal of Geophysical Research*, **104**, 5403-5421.

Fu, G., K.S. Baith, and C.R. McClain, 1998: SEADAS: The SeaWiFS Data Analysis System, Proceedings of the 4th Pacific Ocean Remote Sensing Conference, Qingdao, China, July 28-31.

Gordon, H.R., and M. Wang, 1994: Retrieval of water leaving radiance and aerosol optical thickness over the oceans with SeaWiFS: a preliminary algorithm, *Applied Optics*, **33**, 443-452.

Gould, R.W. Jr., R.A. Arnone, and M. Sydor, 1998: Testing a new remote sensing algorithm to estimate absorption and scattering in CASE 2 waters, SPIE Ocean Optics XII, Hawaii, November, 1998.

Hu, C., K.L. Carder, and F.E. Muller-Karger, 2000: Atmospheric correction of SeaWiFS imagery over turbid coastal waters: a practical method, *Remote Sensing of Environment*, **74**, 195-206.

Kahru, K., and G.B. Mitchell, 1999: Empirical chlorophyll algorithm and preliminary SeaWiFS validation for the California Current, *International Journal of Remote Sensing*, **20**, 34323-3429.

O'Reilly, J.E., S. Maritorena, G.B. Mitchell, D.A. Siegel, K.L. Carder, S.A. Garver, M. Kahru, and C. McClain, 1998: Ocean color chlorophyll algorithms for SeaWiFS, *Journal of Geophysical Research*, **103**, 24937-24953.

Ransibrahmanakul, V., and R.P. Stumpf, 2001: Refining SeaWiFS Vicarious Calibration Using Spectra Slopes. American Geophysical Union, 2001 Fall Meeting, San Francisco, CA, December 10-14, 2001.

Ransibrahmanakul, V., R.P. Stumpf, S. Ramachandran, H. Gu, R. Sinha, and K. Hughes: Evaluation of atmospheric correction and chlorophyll algorithms for processing SeaWiFS data. Seventh International Conference on Remote Sensing for Marine and Coastal Environments, Miami, FL. May 20-22, 2002.

Ruddick, K., F. Ovidio, and M. Rijkeoboer, 2000: Atmospheric correction of SeaWiFS imagery for turbid coastal and inland waters, *Applied Optics*, **39**, 897-912.

Siegel, D., M. Wang, S. Maritorena, and W. Robinson 2000: Atmospheric correction of satellite ocean color imagery: the black pixel assumption, *Applied Optics*, **39**, 3582-3591.

Sigel, S., 1956: *Nonparametric statistics for the behavioral sciences*. McGraw-Hill Book Company, New York.

Stumpf, R.P., R.A. Arnone, R.W. Gould, P. Martinolich, V. Ransiabrahmanakul, P.A. Tester, R.G. Steward, A. Subramaniam, M.E. Culver, and J.R. Pennock, 2000: SeaWiFS ocean color data for US Southeast coastal waters. Sixth International Conference on Remote Sensing for Marine and Coastal Environments. Charleston, SC. Veridian ERIM Intl. Ann Arbor, MI, USA, p. 25-27.

Stumpf, R.P., R.A Arnone, R.W. Gould, Jr., P. Martinolich, V. Ransibrahmanakul, 2003: A Partially-Coupled Ocean-Atmosphere Model for Retrieval of Water-Leaving Radiance from SeaWiFS in Coastal Waters: Chapter 9 In: Patt, F.S., and et al., 2003: Algorithm Updates for the Fourth SeaWiFS Data Reprocessing. *NASA Tech. Memo. 2003-206892*, Vol. **22**, S.B. Hooker and E.R. Firestone, Eds., NASA Goddard Space Flight Center, Greenbelt, Maryland, 74 pp.

Stumpf, R.P., M.E. Culver, P.A. Tester, M. Tomlinson, G.J. Kirkpatrick, B.A. Penderson, E. Truby, V. Ransibrahmanakul, M. Soracco. Monitoring *Karenia brevis* blooms in the Gulf of Mexico using satellite ocean color imagery and other data. *Harmful Algae*, 2, 147-160.

This Research was Supported by the NASA
Interagency Agreements # S-44796-X & S-44791-X

Publications

Arnone, R.A. and R.W. Gould, 2001: Mapping Coastal Processes with Optical Signatures, *Backscatter*, **12**, 17-24.

Arnone, R.A, L. ZhongPing, P. Martinolich, and S.D. Ladner. Characterizing the optical properties of coastal waters by coupling 1 km and 250 m channels on MODIS Terra. Proceedings, Ocean Optics XVI, Santa Fe, New Mexico, 18-22 November, 2002.

Bissett, W., H. Arango, R.A. Arnone, S. Glenn, C. Mobley, M.A. Moline, O.M. Scofield, R. Stewart, L. Sundman, and J. Wilkin. The Prediction Of Remote Sensing Reflectance At Leo-15. Proceedings, Ocean Optics XVI, Santa Fe, New Mexico, 18-22 November, 2002.

Casey, B., R.A. Arnone, P.M. Martinolich, S.D. Ladner, M. Montes, D. Kohler, and W.P. Bissett. Characterizing The Optical Properties Of Coastal Waters Using Fine And Course Resolution. Proceedings, Ocean Optics XVI, Santa Fe, New Mexico, 18-22 November, 2002.

Davis, C. O., M. Moline, P. Bissett, R.A. Arnone, O. Schofield, B. Snyder, M. Montes, and B. Gao. Impact Of Spatial Resolution On The Observation Of Coastal Environmental Features. Proceedings, Ocean Optics XVI, Santa Fe, New Mexico, 18-22 November, 2002.

Gould, R.W., Jr., R.A. Arnone, and M. Sydor, 2001: Absorption, scattering, and particle size relationships in coastal waters: Testing a new reflectance algorithm, *Journal of Coastal Research*, **17**, 328-341.

Gould, R.W., Jr. and R.A. Arnone. 2003. Coastal Transport of Organic and Inorganic Matter. *2003 NRL Review*.

Gould, R.W., Jr. 2003. Optical water mass classification for coastal waters. NRL web page feature article, http://www.nrl.navy.mil/pressRelease.php?Y=2003&R=30-03r, and NRL Labstracts article, http://pipeline.nrl.navy.mil/publications/labstracts/issues/03-04-07.pdf.

Gould, R.W., Jr., and R.A. Arnone. 2002. Coastal optical properties estimated from airborne sensors. *Remote Sensing of Environment*, 79(1): 138-142.

Gould, R.W., Jr., R.H. Stavn, M.S. Twardowski, and G.M. Lamela. Partitioning optical properties into organic and inorganic components from ocean color imagery. Proceedings, Ocean Optics XVI, Santa Fe, New Mexico, 18-22 November, 2002.

Gould, R.W., Jr. and R.A. Arnone. Optical Water Mass Classification for Ocean Color Imagery. Proceedings, Second International Conference, Current Problems in Optics Of Natural Waters, 8-12 September, 2003, St. Petersburg, Russia.

Gould, R.W., Jr., and R.A. Arnone. Temporal and spatial variability of satellite sea surface temperature and ocean color in the Japan/East Sea. *International Journal of Remote Sensing*, In Press.

Haltrin, V.I., M.E. Lee, E.B. Shybanov, R.A. Arnone, A.D. Weidemann, and W.S. Pagau. Relationship between backscattering and beam scattering coefficients derived from new measurements of light scattering phase functions. Proceedings, Ocean Optics XVI, Santa Fe, New Mexico, 18-22 November, 2002.

Haltrin, V.I., R.A. Arnone, and V.A. Urdenko. 2002. Effective Wavelength as a Universal Parameter of Hyperspectral Light Radiance Upwelling from the Sea,pp.133-142,in Ocean Optics: Remote Sensing and Underwater Imaging, Proceedings of SPIE,Vol.4488, Robert J. Frouin,and Gary D.Gilbert, Editors, Bellingham, WA, USA.

Johnson, D.R., A.D. Weidemann, R.A. Arnone, and C.O. Davis. The Chesapeake Bay Outflow Plume and Coastal Upwelling Events Optical /Physical Properties. June 2001. *Journal of Geophysical Research* .

Johnson, D., A. Weidemann, R.A. Arnone, W. Goode, R. W. Gould, Jr., and S. Ladner. Seasonal variations in optical conditions associated with the Mobile Bay outflow plume. Proceedings, Ocean Optics XVI, Santa Fe, New Mexico, 18-22 November, 2002.

Ladner, S., R.A. Arnone, R. Gould, A. Weidemann, V.I. Haltrin, Z. Lee, P. Martinolich, and T. Bergmann. Variability in the backscattering to scattering and F/Q ratios observed in natural waters. Proceedings, Ocean Optics XVI, Santa Fe, New Mexico, 18-22 November, 2002.

Ladner, S., R.A. Arnone, R.W. Gould, Jr., and P.M. Martinolich. 2002. Evaluation of SeaWiFS optical products in coastal regions. *Sea Technology,* 43(10): 29-35.

Lee, Z., K.L. Carder, and R.A. Arnone. 2002. Deriving inherent optical properties from water color: A multiband quasi-analytical algorithm for optically deep waters. *Applied Optics,* Vol 41, No27, Sept 2002. pp 5755-5772.

Martinolich, P.M., R.A. Arnone, and R.W. Gould. Coupling the MODIS and SeaWiFS optical Products. Proceedings, Ocean Optics XVI, Santa Fe, New Mexico, 18-22 November, 2002.

Rochford, P. A., A. B. Kara, A.J. Walcraft, and R.A. Arnone. The Importance of Solar Subsurface Heating in Ocean General Circulation Models, *Journal of Geophysical Research*, Vol 106, No C12 Dec 2001. pp 30923- 30938.

Stavn, R.H., R.W. Gould, Jr., and G.M. Lamela. The biogeo-optical model: The database and testing. Proceedings, Ocean Optics XVI, Santa Fe, New Mexico, 18-22 November, 2002.

Stumpf, R.P., M.E. Culver, P.A. Tester, M. Tomlinson, G.J. Kirkpatrick, B.A. Penderson, E. Truby, V. Ransibrahmanakul, M. Soracco, 2003. Monitoring *Karenia brevis* blooms in the Gulf of Mexico using satellite ocean color imagery and other data. *Harmful Algae*, 2: 147-160.

Stumpf, R.P., R.A Arnone, R.W. Gould, Jr., P. Martinolich, V. Ransibrahmanakul. 2003. A Partially-Coupled Ocean-Atmosphere Model for Retrieval of Water-Leaving Radiance from SeaWiFS in Coastal Waters: Chapter 9 In: Patt, F.S., and et al., 2003: Algorithm Updates for the Fourth SeaWiFS Data Reprocessing. NASA Tech. Memo. 2003--206892, Vol. 22, S.B. Hooker and E.R. Firestone, Eds., NASA Goddard Space Flight Center, Greenbelt, Maryland, 74 pp.

Tester, P.A., S.M. Varam, M. Culver, D.L. Eslinger, R.P. Stumpf, R. Swift, J. Yungel, R.W. Litaker. Airrborne detection of ecosystem responses to an extreme event: phytoplankton displacement and abundance after hurricane induced flooding in the Pamlico-Albemarle Sound system, North Carolina, *Estuaries*, 26 (5), in press.

Wynne, T.T., R.P. Stumpf, M.C. Tomlinson, V. Ransibrahmanakul, T.A. Villareal. 2003. A new method for detecting Karenia brevis blooms in the western Gulf of Mexico with satellite ocean color imagery. Proceedings of the 13th Biennial Coastal Zone Conference, Baltimore, MD, July 13-17, 2003; NOAA Coastal Services Center. NOAA/CSC/20322-CD. Charleston SC.

Publications submitted

Ransibrahmanakul, V., and R.P. Stumpf. Absorbing aerosol correction for SeaWiFS. Submitted, *Applied Optics*.

Wood, A.M., R.A. Arnone, R.W. Gould, W. Li, S. Pegau, and C. Trees. Optical Biogeography of Spectrally Distinct Forms of Picocyanobacteria in the Coastal Ocean. Abstract submitted to the International Photosynthetic Procaryote Meeting, August 2003.

Presentations

Arnone, R.A., R.W. Gould, Jr., C.O. Chan, and S.D. Ladner, 2000: Uncoupling CDOM, scattering and chlorophyll properties in coastal waters using SeaWiFS ocean color. Abstract Published to Oceans from Space 2000, Venice, Italy, 9-13 October, 2000. (Invited talk)

Arnone, R.A., R.W. Gould, Jr., A.D. Weidemann, S.C. Gallegos, and V.I. Haltrin, 2000: Using SeaWiFS ocean color absorption, backscattering properties to discriminate coastal waters. Abstract published Ocean Optics XV, Monaco, 16-20 October, 2000.

Arnone, R.A., R.W. Gould, Jr., S.D. Ladner, A. Weidemann, and T. Bowers. Seasonal Bio-Optical Properties of the Coastal Gulf of Mexico and Influence of Riverine Inputs. ASLO Summer Meeting 2002, Victoria, British Columbia, 10-14 June, 2002.

Arnone, R.A., R.W. Gould, Jr., S.D. Ladner, B. Jones, P.J. Hogan, and G.A. Jacobs. Bio-Optical and Temperature Climatology of the Japan/East Sea. AGU/ASLO Ocean Sciences Meeting 2002, Honolulu, HI, 11-15 February, 2002. *EOS Trans. AGU*, 83(4), Ocean Sciences Meeting. Supplemental Abstract OS11C-41, 2002.

Arnone, R.A., R.W. Gould, Jr., and S.D. Ladner. CDOM Variability in the Coastal Zone from SeaWiFS. AGU/ASLO Ocean Sciences Meeting 2002, Honolulu, HI, 11-15 February, 2002. *EOS Trans. AGU*, 83(4), Ocean Sciences Meeting. Supplemental Abstract OS22J-01, 2002.

Arnone, R.A., R.W. Gould, Jr., P.M. Martinolich, and S.D. Ladner. Improved algorithms for retrieving optical properties in coastal waters from ocean color sensors. Abstract submitted to the AGU Fall Meeting 2001, San Francisco, CA, 10-14 December, 2001.

Arnone, R.A, Lee, ZhongPing, Martinolich, P. and Ladner, S.D "Characterizing the optical properties of coastal waters by coupling 1 km and 250 m channels on MODIS – Terra" Proceedings, Ocean Optics XVI, Santa Fe, New Mexico, 18-22 November, 2002.

Arnone, R., R. Gould, Z. Lee, P. Martinolich, B. Casey, C. Hu, and A. Weidemann. Uncoupling the optical signatures in coastal waters with ocean color sensors. Oceanography Society Annual Meeting, 4-6 June, 2003, New Orleans, LA.

Arnone, R.A., R.W. Gould, A. Weidemann, S.D. Ladner, and P. Martinolich. Satellite ocean color products for real-time navy applications. International Geoscience and Remote Sensing Symposium, 21-25 July, 2003, Toulouse, France.

Bissett, W. Arango, H., Arnone, R.A. Glenn, S., Mobley, C., Moline, M.A. Scofield, O.M., Stewart, R. Sundman, L., Wilkin, J. The Prediction Of Remote Sensing Reflectance At Leo-15, Proceedings, Ocean Optics XVI, Santa Fe, New Mexico, 18-22 November, 2002.

Bowers, T., R.A. Arnone, S.D. Ladner, R.W. Gould, Jr., and D. Fox. Modeling the Vertical Bio-Optical Properties Based on the Surface SeaWiFS Properties. Seventh International Conference on Remote Sensing for Marine and Coastal Environments, Miami, FL, 20-22 May, 2002.

Casey, B., Arnone, R.A., Martinolich, P., Ladner, S.D., Montes. M., Kohler, D., Bissett, W.P., "Characterizing The Optical Properties Of Coastal Waters Using Fine And Coarse Resolution." Proceedings, Ocean Optics XVI, Santa Fe, New Mexico,18-22 November, 2002.

Culver, M.E., M.C. Tomlinson, T.H. Orsi, and R.P. Stumpf. Access to harmful algae data in the Gulf of Mexico. 10th International Conference on Harmful Algae, St. Petersburg, FL. 21-25 October, 2002.

Davis C, O , Moline, M. Bissett, P. Arnone, R.A. , Schofield, O., Snyder, B., Montes, M., Gao, Bo-Cai. Impact Of Spatial Resolution On The Observation Of Coastal Environmental Features, Proceedings, Ocean Optics XVI, Santa Fe, New Mexico, 18-22 November, 2002.

Gould, R.W., Jr., R.A. Arnone, and C.O. Chan, 2000: Temporal and spatial variability of satellite sea surface temperature and ocean color. Oceans from Space 2000, Venice, Italy, 9-13 October, 2000.

Gould, R.W. Jr., R.A. Arnone, C.M. Lee, and B.H. Jones, 2000: Characterizing surface and subsurface thermal and bio-optical fields in the Japan/East Sea during a spring bloom: Shipboard measurements and satellite imagery. Proceedings, Ocean Optics XV, Monaco, 16-20 October, 2000.

Gould, R.W., Jr., T.R. Keen, R.A. Arnone, R.H. Stavn, A.-R. Diercks, 2001: Bio-Optical variability in a barrier-island coastal environment: Coupling remote sensing imagery, shipboard measurements, and modeling results. Ocean Odyssey 2001 Meeting, Joint meeting of IAPSO and IABO, Mar del Plata, Argentina, 21-28 October, 2001.

Gould, R.W., Jr., R.A. Arnone, S.D. Ladner, P.M. Martinolich, A.R. Diercks, and R.H. Stavn. Optical Variability Linked to Physical Forcing in the Northern Gulf of Mexico using Satellite, Shipboard, and CODAR observations. AGU/ASLO Ocean Sciences Meeting 2002, Honolulu, HI, 11-15 February, 2002. *EOS Trans. AGU*, 83(4), Ocean Sciences Meeting. Supplemental Abstract OS12J-06, 2002.

Gould, R.W., Jr., R.H. Stavn, M.S. Twardowski, and G.M. Lamela. Partitioning optical properties into organic and inorganic components from ocean color imagery. Proceedings, Ocean Optics XVI, Santa Fe, New Mexico, 18-22 November, 2002.

Gould, R.W., Jr., R.A. Arnone, R. Smith, S. D. Ladner, and P. M. Martinolich. Coastal Transport of Organic and Inorganic Matter from Ocean Color Remote Sensing. Oceanography Society Annual Meeting, 4-6 June, 2003, New Orleans, LA.

Greene, R.M., T.A. Villareal, R.P. Stumpf, K.A. Steidinger, J. Simons, J.R. Pennock, T. Orsi, C.A. Moncreiff, K. Hamilton, S.C. Gallegos, W.S. Fisher, and Q. Dortch: Harmful Algal BloomS Observing System (HABSOS) pilot project. 10th International Conference on Harmful Algae, St. Petersburg, FL. 21-25 October, 2002.

Gould, R.W., Jr. and R.A. Arnone. Optical Water Mass Classification for Ocean Color Imagery. Proceedings, Second International Conference, Current Problems in Optics Of Natural Waters, 8-12 September, 2003, St. Petersburg, Russia.

Haltrin, V.I., W. McBride, and R.A. Arnone. A Spectral Approach to Calculate Spectral Reflection of Light from a Wavy Water Surface, ONW 2001 International Conference, St. Petersburg, Russia, 25 Sept, 2001.

Haltrin, V.I., Lee., M.E., Shybanov, E.B., Arnone R.A. Weidemann A.D., and Pagau, W.S. Relationship between backscattering and beam scattering coefficients derived from new measurements of light scattering phase Functions " Proceedings, Ocean Optics XVI, Santa Fe, New Mexico,18-22 November, 2002.

Holderied, K., D. Pirhalla, V. Ransibrahmanakul, and R.P. Stumpf. 2003. Application of Improved SeaWiFS Chlorophyll Data in Estuarine and Coastal Waters. Presentation at the 2003 Estuarine Research Federation Conference, 15-18 Sep 2003, Seattle, Washington.

Holt, A., R.P. Stumpf, M.C. Tomlinson, V. Ransibrahmanakul, V. Trainer, D. Woodruff, 2003. Applications of satellite ocean color imagery for detecting and monitoring harmful algal blooms in the Olympic Penisula region. Proceedings of the 13th Beennial Coastal Zone Conference, Baltimore, MD July 13-17, 2003.

Hughes, D.C., R.J. Holyer, and R.A. Arnone. Removal of Bottom Reflectance Contribution to Remote Sensing Reflectance in Coastal SeaWiFS Imagery AGU/ASLO Ocean Sciences Meeting 2002, Honolulu, HI, 11-15 February, 2002. *EOS Trans. AGU*, 83(4), Ocean Sciences Meeting Supplemental Abstract OS11C-41, 2002.

Hughes, D.C., R.J. Holyer, and R.A. Arnone. Estimating Depth and Bottom Contributions Using Optimization and Neural Network Methods for Hyperspectral Imagery, Seventh International Conference on Remote Sensing for Marine and Coastal Environments, Miami, FL, 20-22 May, 2002.

Johnson, D., A. Weidemann, R. Arnone, W. Goode, R. W. Gould, Jr., and S. Ladner. Seasonal variations in optical conditions associated with the Mobile Bay outflow plume. Proceedings, Ocean Optics XVI, Santa Fe, New Mexico, 18-22 November, 2002.

Jones, B.H., C.M. Lee, R.A. Arnone, R.W. Gould, and K. Brink. A Comparison of Bio-Optical Characteristics of the Subpolar Front in the Japan/East Sea in Spring and Winter. AGU/ASLO Ocean Sciences Meeting 2002, Honolulu, HI, 11-15 February, 2002. *EOS Trans. AGU*, 83(4), Ocean Sciences Meeting Supplemental Abstract OS12O-04, 2002.

Ladner, S.D., R.A. Arnone, R.W. Gould, Jr., and P.M. Martinolich. Evaluation of SeaWiFS bio-optical products in coastal regions. Abstract submitted to the AGU Fall Meeting 2001, San Francisco, CA, 10-14 December, 2001.

Ladner, S., R. Arnone, R. Gould, A. Weidemann, V.I. Haltrin, Z. Lee, P. Martinolich, and T. Bergmann. Variability in the backscattering to scattering and F/Q ratios observed in natural waters. Proceedings, Ocean Optics XVI, Santa Fe, New Mexico, 18-22 November, 2002.

Ladner, S., R.Gould, Jr., R. Arnone, A. Weidemann, P. Martinolich, and B. Casey. Coupling In Situ and Satellite Data to Validate Satellite Optical Properties. Oceanography Society Annual Meeting, 4-6 June, 2003, New Orleans, LA.

Lee, C.M., B.H. Jones, K.H. Brink, L.N. Thomas, R.A. Arnone, R.W. Gould, C. Dorman, and R. Beardsley. Evidence of Wintertime Subduction at the Subpolar Front of the Japan/East Sea. AGU/ASLO Ocean Sciences Meeting 2002, Honolulu, HI, 11-15 February, 2002. *EOS Trans. AGU*, 83(4), Ocean Sciences Meeting. Supplemental Abstract OS120-02, 2002.

Ly, L.N., R.P. Stumpf, T.F. Gross, and F. Aikman III. Modeling of cross-shelf transport in support of monitoring and forecasting of harmful algal blooms along the West Florida coast, 10th International Conference on Harmful Algae. St. Petersburg, FL. October 21-25, 2002.

Martinolich, P.M., R.A. Arnone, R.W. Gould, Jr., and S.D. Ladner. Coupling MODIS and SeaWiFS optical products. Abstract submitted to the AGU Fall Meeting 2001, San Francisco, CA, 10-14 December, 2001.

Martinolich, P. Arnone, R.A. and Gould, R.W. " Coupling the MODIS and SeaWIFS optical Products." Proceedings, Ocean Optics XVI, Santa Fe, New Mexico, 18-22 November, 2002.

Ransibrahmanakul, V., R.P. Stumpf, A. Robertson, K. Casey, and K. Buja, 2001: Temporal patterns in chlorophyll and temperature around the coastal US, from September 1997 through 2001. 16th Biennial Conference of the Estuarine Research Federation, St. Pete Beach, Fl, November 4-8, 2001.

Ransibrahmanakul, V., R.P. Stumpf, S. Ramachandran, H. Gu, R. Sinha, and K. Hughes. Evaluation of atmospheric correction and chlorophyll algorithms for processing SeaWiFS data, Seventh International Conference on Remote Sensing for Marine and Coastal Environments, Miami, FL. 20-22 May, 2002.

Ransibrahmanakul, V., and R.P. Stumpf. Refining SeaWiFS Vicarious Calibration Using Spectra Slopes, American Geophysical Union, 2001 Fall Meeting. San Francisco, CA, 10-14 December, 2001.

Ransibrahmanakul V., R.P. Stumpf, A. Robertson, and K.S. Casey. Temporal patterns in chlorophyll and temperature around the coastal US from September 1997 through 2001, Estuarine Research Federation, 16th Biennial Conference. St. Pete Beach, FL. 4-8 November, 2001.

Ransibrahmanakul, V., R. Stumpf, K. Holderied, P. Tester, and J.W. Budd. 2003. Retrieval of Chlorophyll in U.S. Estuaries and Lakes. Presentation at the 2003 Estuarine Research Federation Conference, 15-18 Sep 2003, Seattle, Washington.

Sandidge, J., P.M. Martinolich, R.A. Arnone, S.D. Ladner, and R.W. Gould, Jr. Compositing Ocean Color Imagery, Seventh International Conference on Remote Sensing for Marine and Coastal Environments, Miami, FL, 20-22 May, 2002.

Stavn, R.H., R.W. Gould, W.S. Pegau, G. Korotaev, and A.D. Weidemann. Biogeo-optics: Predicting the Optical Properties of Coastal New Jersey at the LEO-15 Site, AGU/ASLO Ocean Sciences Meeting 2002, Honolulu, HI, 11-15 February, 2002. *EOS Trans. AGU*, 83(4), Ocean Sciences Meeting Supplemental Abstract OS31T-06, 2002.

Stavn, R.H., R.W. Gould, Jr., and G.M. Lamela. The biogeo-optical model: The database and testing. Proceedings, Ocean Optics XVI, Santa Fe, New Mexico, 18-22 November, 2002.

Stavn, R.H. and R.W. Gould, Jr. Biogeo_optics: Organic Matter Scattering in Case 2 Waters. Oceanography Society Annual Meeting, 4-6 June, 2003, New Orleans, LA.

Stumpf, R.P. and M.E. Culver: Forecasting harmful algal blooms in the Gulf of Mexico, 2001: 16th Biennial Conference of the Estuarine Research Federation, St. Pete Beach, Fl, November 4-8, 2001.

Stumpf, R.P., M.E. Culver, E. Truby, and M. Soracco. A prototype system for monitoring and forecasting of harmful algal blooms in the Gulf of Mexico, 10th International Conference on Harmful Algae. St. Petersburg, FL. 21-25 October, 2002.

Stumpf, R.P., and M.E. Culver. Forecasting harmful algal blooms in the Gulf of Mexico, 2001, 16th Biennial Conference of the Estuarine Research Federation, St. Pete Beach, FL, 4-8 November, 2001.

Stumpf, R.P., and M.E. Culver: Forecasting of Harmful Algal Blooms in the Gulf of Mexico. Seventh International Conference on Remote Sensing for Marine and Coastal Environments, Miami, FL. 20 -22 May, 2002.

Stumpf, R.P., J. Jurado, G. Hitchcock, P. Coble, J. Boyer, M. Neely, K. Steidinger, E. Truby, B. Roberts, C. Hu, K. Carder, F. Muller-Karger, M.C. Tomlinson, B. Keller, and G. Feldman. Blackwater event in Southwest Florida in winter 2002. Seventh International Conference on Remote Sensing for Marine and Coastal Environments, Miami, FL. 20-22 May, 2002.

Stumpf, R.P., M.E. Culver, E. Truby, M. Soracco, M. Tomlinson, T.A. Villareal. Using satellite imagery to monitor harmful algal blooms in the Gulf of Mexico. Presentation at the 2003 Estuarine Research Federation Conference, 15-18 Sep 2003, Seattle, Washington.

Tester, P.A., S. Varnam, R. Swift, R.P. Stumpf, D. Eslinger, M.E. Culver, M. Black. Hurricane Floyd: NOAA, NASA and new remote sensing technologies, 16th Biennial Conference of the Estuarine Research Federation, St. Pete Beach, FL, 4-8 November, 2001.

Tester, P.A., R.P. Stumpf, V. Ransibrahmanakul, R.N. Swift, D. Eslinger, and M.E. Culver. Cumulative Effects of Three Hurricanes in One Season on Albemarle Sound and Pamlico Sound, North Carolina, American Society and Limnology and Oceanography, Victoria, BC, 10-14 June, 2002.

Tester, P.A., R.W. Litaker. Airborne detection of ecosystem responses to an extreme event. Presentation at the 2003 Estuarine Research Federation Conference, 15-18 Sep 2003, Seattle, Washington.

Tomlinson, M.C., V. Ransibrahmanakul, R.P. Stumpf, E.W. Truby, G.J. Kirkpatrick, B.A. Pederson, G.A. Vargo and C.A. Heil. Evaluation of a method for detecting *Karenia brevis* blooms in the eastern Gulf of Mexico with satellite ocean color imagery, 10th International Conference on Harmful Algae. St. Petersburg, FL. 21-25 October, 2002.

Tomlinson, M.C., V. Ransibrahmanakul, R.P. Stumpf, E. Truby, G.J. Kirkpatrick, B.A. Pederson, G.A. Vargo, and C.A. Heil. A retrospective evaluation of the use of SeaWiFS imagery to predict *Karenia brevis* blooms in the eastern Gulf of Mexico, Seventh International Conference on Remote Sensing for Marine and Coastal Environments, Miami, FL. 20-22 May, 2002.

Tomlinson, M.C., T.T. Wynne, R.P. Stumpf, E.W. Truby, G.J. Kirkpatrick, B.A. Pederson, G.A. Vargo, T.A. Villareal. Remote sensing techniques for detecting harmful algal booms in coastal waters. Presentation at the 2003 Estuarine Research Federation Conference, 15-18 Sep 2003, Seattle, Washington.

Chapter 17

Varied Waters and Hazy Skies: Validation of ocean color satellite data products in under-sampled marine areas

Ajit Subramaniam and R. Del Vecchio
University of Maryland, College Park, Maryland

Edward J. Carpenter
San Francisco State University, California

Douglas G. Capone
University of Southern California, California

17.1 INTRODUCTION

It has been hypothesized that one of the limiting micronutrients for nitrogen fixation is Iron. It has also been hypothesized that aeolian dust is the primary source of Iron for near surface open ocean waters. As a part of two National Science Foundation funded studies – "Factors affecting, and impacts of, diazotrophic microorganisms in the western equatorial Atlantic" and "Oceanic N2 fixation and global climate" – we conducted 6 field surveys in the tropical and subtropical Atlantic and Pacific Oceans between 2001 and 2003 (Table 17.1, Figures 17.1-17.6). The cruises were conducted during times of high and low aeolian dust activity in both ocean basins in order to study the impact of dust on nitrogen fixation. In addiction to dust, we also hypothesized that the Amazon River is a significant source of nutrients that stimulate nitrogen fixation, specifically Silicon and Iron that stimulate endosymbiotic diazotrophic cyanobacteria and cruises were also conducted to study the effects of the Amazon River on the phytoplankton species composition, the underwater light field and nutrient concentrations of the western Tropical Atlantic Ocean.

Our SIMBIOS activity dovetailed on the NSF funded grants and the main objectives of our SIMBIOS funded project were to obtain field measurements of Aerosol Optical Thickness (AOT), normalized water leaving radiance (nLw), absorption due to dissolved (a_{CDOM}), particulate (Ap), detrital (Ad) material, and phytoplankton pigments, under dusty skies, in the Amazon River plume, as well as in blooms of the marine diazotrophic cyanobacteria *Trichodesmium.* These measurements can then be used to validate satellite ocean color products such as those for chlorophyll concentration (chl a mg/m3), absorption due to chromophoric and detrital material (Acdm), reparameterize the algorithms for these products for specific locations such as the Amazon River plume, or to develop entirely new algorithms. In addition to the core SIMBIOS funded cruises, we also participated in six additional cruises in coastal waters where normalized water leaving radiance, aerosol optical thickness, absorption, and phytoplankton pigments were measured and data submitted to the SeaBASS archive. We also deployed a suite of optical instruments at a PIRATA mooring at 8N, 38W between April 2002 and July 2003 (Subramaniam 2002). These instruments are have just been recovered. After they have been recalibrated, the data will be analyzed to obtain a high temporal resolution time-series of normalized water leaving radiance at that site. This data will be compared to that derived from satellites as well as to study the potential enhancement of chlorophyll concentration at this site by Iron from aeolian dust.

17.2 RESULTS

Several stations on the JAN01SJ cruise were sampled under dense dust storms (Figure 17.7). The AOT matchups showed reasonable agreement between satellite derived AOTs and the field measurements except at stations where the dust was so thick that there were no satellite retrievals (Figure 8). However, the SeaWiFS normalized water leaving radiance products did not compare well with in-situ measurements and consequently the SeaWiFS chlorophyll product also performed very poorly.

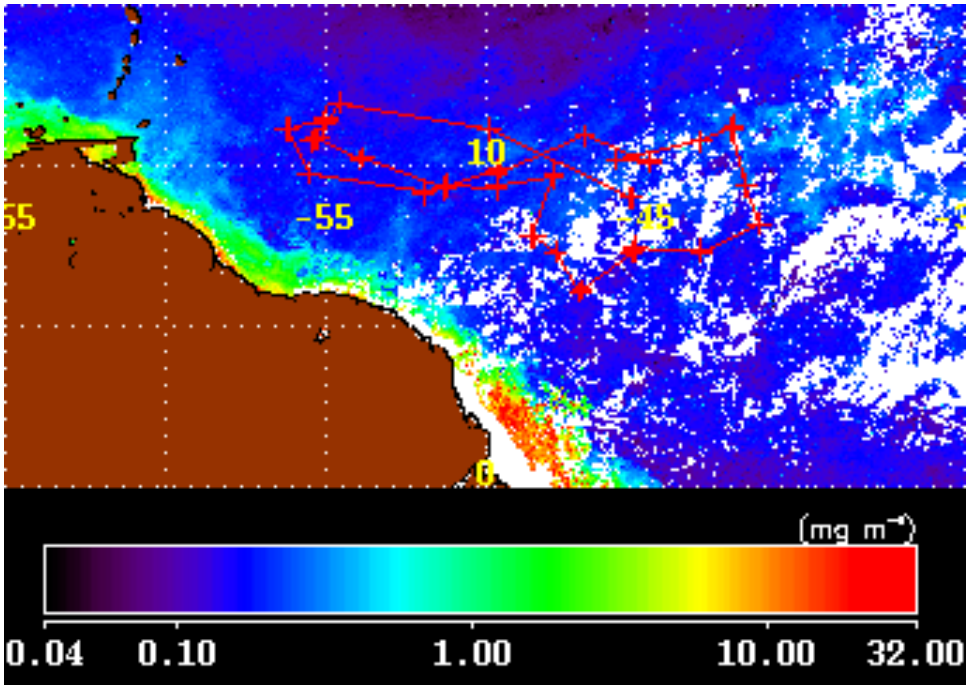

Figure 17.1: Cruise Track for JAN01SJ on monthly composite of SeaWiFS Chlorophyll map for Febuary 2001.

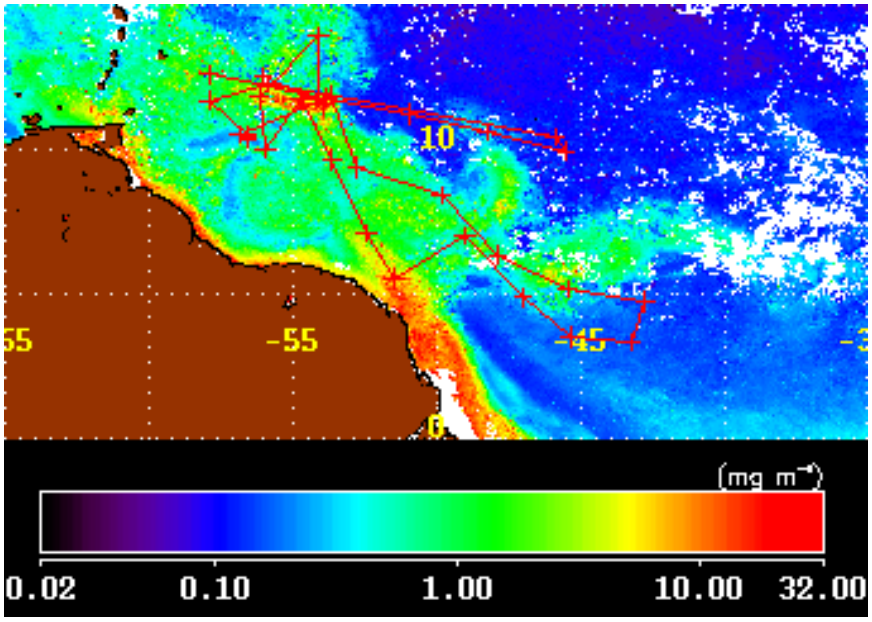

Figure 17.2: Cruise Track for JUN01KN on monthly composite SeaWiFS map for August 2001.

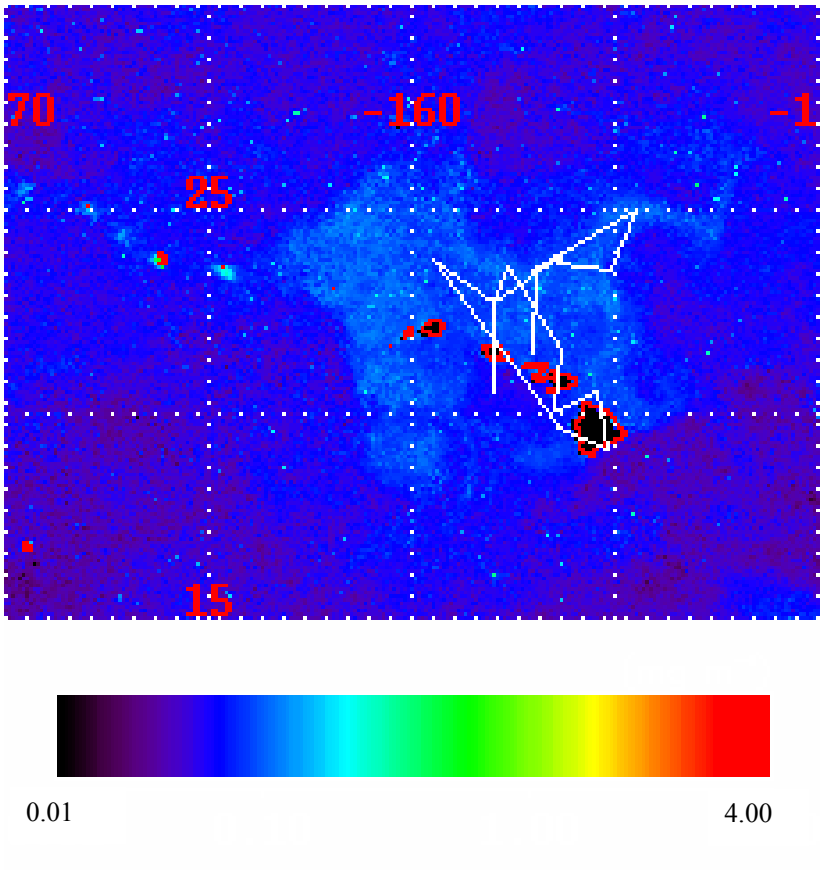

Figure 17.3: Cruise Track for SEP02PAC on monthly composite SeaWiFS map for September 2002.

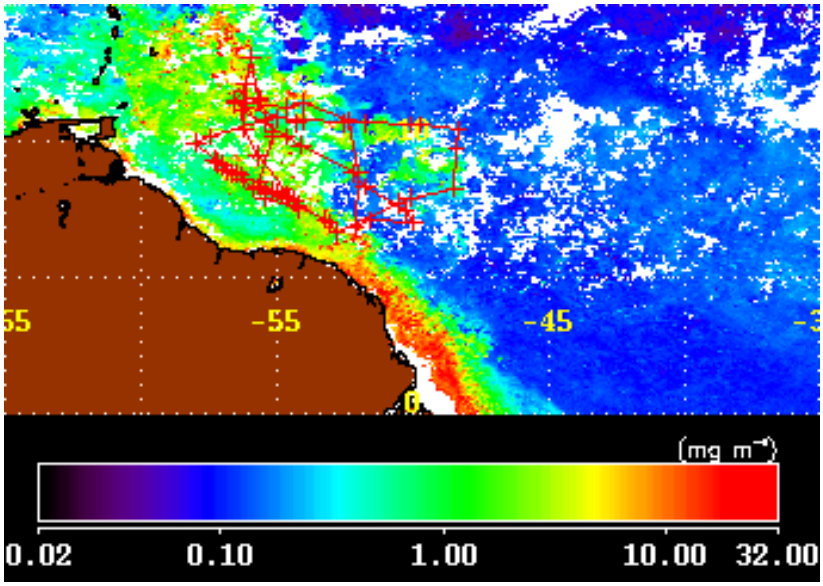

Figure 17.4: Cruise Track for APR03ATL on monthly composite SeaWiFS map for April 2003.

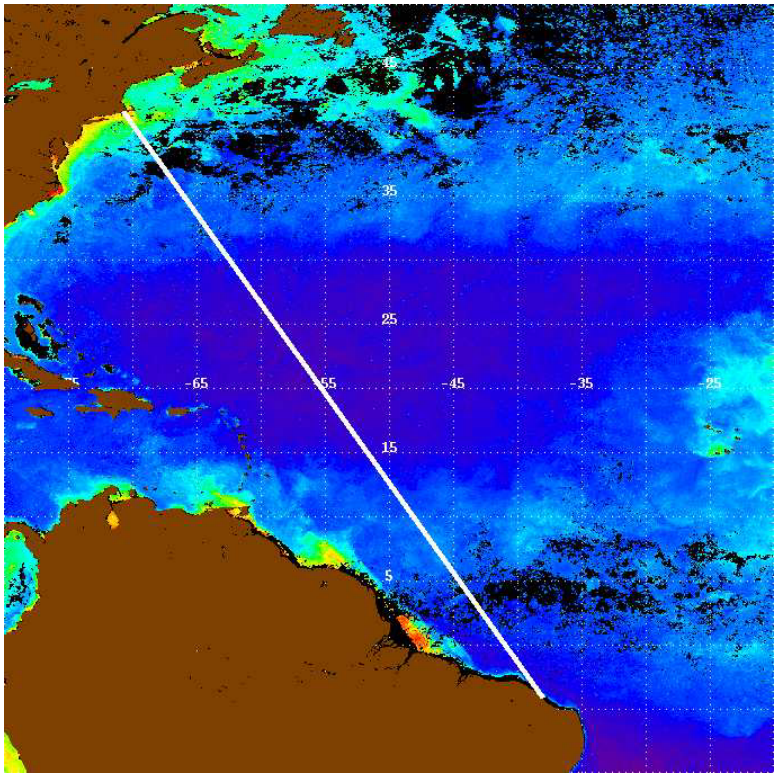

Figure 17.5: Cruise Track for JAN03ATL on monthly composite SeaWiFS map for January 2003.

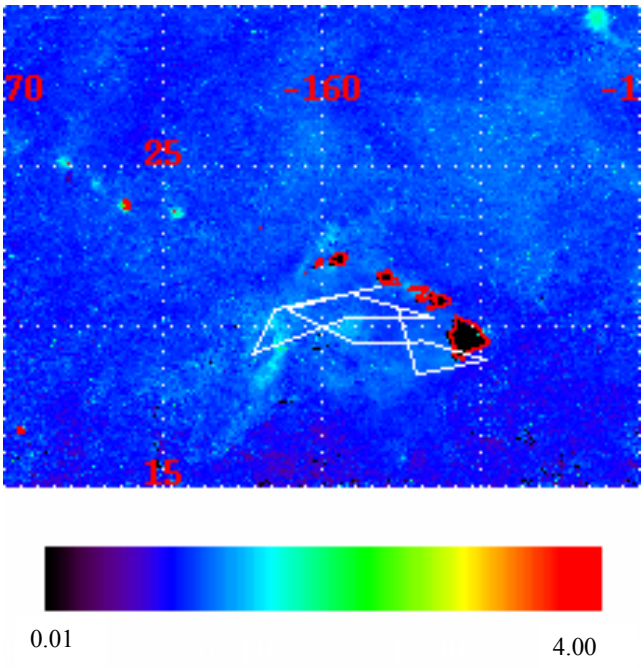

Figure 17.6: Cruise Track for JUL03PAC on monthly composite SeaWiFS map for August 2003

We provided our field measurements of AOT and nLw to the University of Miami group to test their spectral matching algorithm. Our AOT dataset was also provided to Dr. Mahowald to test her dust deposition model. We used the in-situ measurements of nLw to show that the OC4 algorithm appears to work reasonably well in these waters in absence of the Amazon River plume (Figure 17.9). For the

JUL01KN cruise, there were excellent match ups between nLw from satellites and the in-situ measurements (Figure 17.10). Our initial analyses of field measurements of pigments and absorption showed that the OC4 and the acd_gsm01 did not work in the Amazon River plume. However, as detailed below, we believe further work should allow us to develop specific algorithms for the Amazon River plume. Cloudiness, sun glint, orbital path, and tilt maneuvers did not allow for statistically meaningful comparison between satellite derived products and in-situ measurements for all our cruises. We are still analyzing the data from the last cruise that ended on the 23 of August 2003.

Our field data on the underwater light field, the absorption properties, and the phytoplankton species composition show the extraordinary magnitude of the influence of the Amazon River on the marine ecosystem of the Western Tropical Atlantic Ocean. We found that the nitrate supplied by the Amazon River is taken up very quickly and the surface nitrate concentrations (in the plume) are below detection within a short distance from the mouth of the river. The phytoplankton population in this region is composed mostly of coastal dinoflagellates and diatoms. After the nitrate is depleted, the phytoplankton population switches to one dominated by the diatom *Hemiaulus* with the endosymbiotic nitrogen fixing cyanobacteria *Richelia*. This organism appears to be dependent on the river plume for its Silicon requirements and is found at greatest numbers at salinities between 26 PSS and 34 PSS. The nitrogen fixing cyanobacteria *Trichodesmium* spp. appears at greatest concentrations at salinities greater than 34 PSS when the Silicon is depleted. We explored the relationship between absorption due to CDOM and salinity because if a constant relationship between the two could be established, it would be possible to map the salinity in this region using satellite-derived estimates of a_{CDOM} using algorithms such as acd_gsm01.

Chromophoric dissolved organic matter (CDOM) is the optically active fraction of the dissolved organic matter and is one of the primary absorbing species in aquatic environments, thus plays an important role determining the aquatic light field. CDOM absorption extends across the entire spectrum in a featureless exponential decay fashion. CDOM is also capable of emitting light as fluorescence upon excitation in the UV-visible spectral range. Thus, optical methods (absorption and fluorescence spectroscopy) have been widely used to study CDOM properties and distribution. Largest signal of CDOM is always observed in coastal regions influenced by fresh water runoff that decreases towards offshore in a seasonal-dependent linear behavior. Recently, interest in CDOM has increased because of its potential interference with remote sensing detection of chlorophyll. Additionally, a relationship between CDOM and dissolved organic carbon (DOC) has been observed in coastal regions influenced by freshwater input, thus remote sensing of ocean color (i.e. CDOM) [and thus of organic carbon] has become a growing area of interest.

The Amazon is the second longest river in the world after the Nile and it carries one sixth of the world's total river run-off, five times more than the second largest river. Once on the continental shelf, the Amazon water flows northward, first along the South American coast and then hundreds of kilometers into the Open Ocean and profoundly influences the optical properties of the Western Tropical Atlantic Ocean. Nevertheless at the best of our knowledge a detailed study that describes the optical properties of the Amazon River plume has not yet being conducted. The limited data available at today (Green and Blough, 1994) show water absorption coefficients inversely related to salinity and an extrapolated fresh water end-member (~ 4-6 m^{-1} at 355 nm) very similar to that of other large rivers and estuaries (see references in Blough and Del Vecchio, 2002).

Samples were collected using a CTD (conductivity-temperature-depth) rosette equipped with Niskin bottles onboard of the R/V Seward Johnson in January-February 2001 and April-May 2003 and on the R/V Knorr in July-August 2001. For simplicity the cruises will be referred to as the winter, spring, and summer cruises respectively. Additional samples were collected with an acid cleaned bucket during the April-May 2003 cruise to increase the sample density near the river outflow. Salinity and temperature were obtained from the CTD system. All samples were immediately filtered through pre-combusted GF/F filters (0.7 μm pore-size) before further treatment. Samples for absorption were re-filtered through 0.2 μm pore-size nylon syringe filters to remove all particles and analyzed onboard. CDOM absorption spectra were acquired with a Shimadzu 2401-PC spectrophotometer employing a 10 cm optical cell. The instrument detection limit (d.l.) was 0.002 OD. Milli-Q water was employed as the blank. Absorption spectra were recorded over the range 250-800 nm and the values at wavelengths 650-700 nm were averaged to determine the baseline. The spectral slope (S) was calculated by fitting the data to an exponential function over the range 300-700 nm: S was accepted if the residuals of the fit fell within the instrument's detection limit (0.046 m^{-1}).

During the winter cruise (February 2001), the Amazon River flow was low: surface waters in the region exhibited high salinity (> 34), low temperature (< 26 °C) and very low $a_{CDOM}(355)$ (close to our instrument detection limit, 0.046 m^{-1}). The water column was vertically mixed with physical and optical properties very similar all station and through the water column. During spring and summer, the river flow increased: surface waters closer to shore showed lower salinity (~24 in May 2003

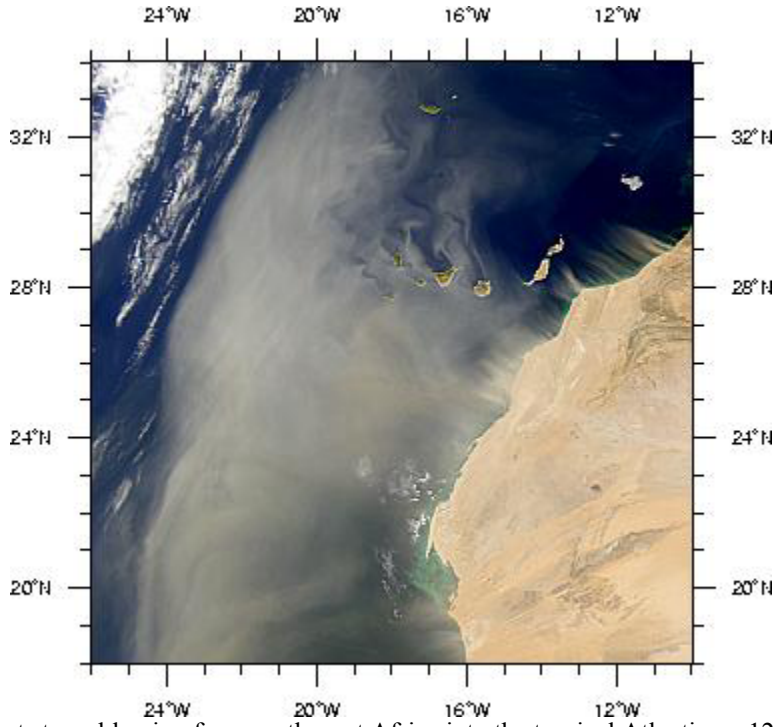

Figure 17.7: Dust storm blowing from north west Africa into the tropical Atlantic on 12 February 2001.

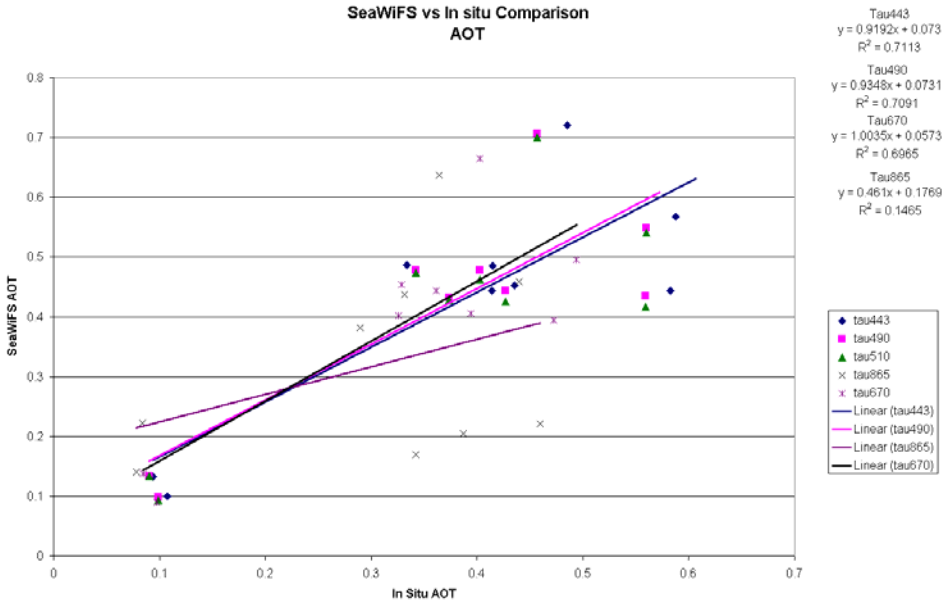

Figure 17.8: Aerosol Optical Thickness - SeaWiFS vs Field Measurements

and ~ 28 in July 2001) and higher temperature (~28 °C in May 2003 and ~ 29 °C in July 2001) compared to surface waters at offshore locales and to deeper waters. A 15-20-m-thick lens of fresh and warm water was observed during this period that moved offshore and remained constrained to the upper 20 meters where the pychnocline and the summer thermocline occurred. The water column became vertically stratified with inshore and offshore locales showing very different properties. Even the optical signal was very different at inshore and offshore locales, with higher absorption values (and lower spectral slope, S) near the surface close-to-shore that decreased with depth and distance offshore.

Early in the spring (April 2003), surface salinity was still high and $a_{CDOM}(355)$ was low in the region 9N-52W to 11N-48W (stations 4-5-8-10), thus indicating that the river waters had not yet reached far offshore. Later on the same cruise, however, surface water with lower salinity and higher $a_{CDOM}(355)$ was observed closer to shore stretching northward along the continental shelf (7N-52W to 10N-57W, stations 41 to 67). Surface waters with intermediate salinity and high $a_{CDOM}(355)$ was observed far offshore towards north-northwest (9N-54W to 13N-57W, stations 12 to 15).

Early in the summer (July 2001), surface salinity was low and $a_{CDOM}(355)$ was high even at offshore locales (~12N-54W, station 27), thus suggesting that the plume now reached > 1000 kilometers offshore. Surface "filaments" of waters moving in different directions and giving rise to surface "blobs" were seen during the summer cruise in the satellite data (Figure 17.2). One filament was found to move northward along the south American coast while another filament retroflected and moved southeastward (stations 43to 46 and 29 to 39). In addition, a North West blob (NW Blob) (~12.5N-57.5W, close to stations 13 and 22, for which no $a_{CDOM}(355)$ values are available) and a North East blob (NE Blob) (~12.5N-54W, close to station 27) detached from the main river flow and moved northward. Each of these different water masses had different nutrient and optical properties and had differing phytoplankton populations.

During both spring and summer, deeper waters (below the river plume, depth > 20 m) or surface waters outside the plume region showed high salinity and low $a_{CDOM}(355)$ typical of open ocean waters.

During the winter, $a_{CDOM}(355)$ did not show any dependence on salinity (Fig. 17.11A): surface (yellow circles) and deep (grey circles) show similar and uncorrelated high salinity and low $a_{CDOM}(355)$ values. During the spring, $a_{CDOM}(355)$ for surface waters decreases linearly with salinity (Fig. 17.11B, green circles). However, slightly different dependences were observed earlier and later during the cruise [Fig. 17.11B, compare bucket (green circles) to non-bucket (black-red circles) samples], probably associated with freshwater pulses of different intensities or to *in situ* production (see below). Most of the non-bucket samples were taken just Northwest of the core of the river plume; some of these waters were characterized by intense bloom of *Hemiaulus* and by very high chlorophyll concentrations located near the surface (< 20 m). The CDOM optical signal of these waters (Fig. 17.11B, black circles exhibited a shallower mixing line (Fig. 17.11B, black line) compared to the Amazon River mixing line (Fig. 17.11B, green line). Further, the CDOM absorption for some of these waters (Fig. 11B, stations labeled in blue) was similar in magnitude to that of phytoplankton particulate material (not shown), unusual for surface oceanic waters. Some of these locales on the other hand, did not show high chlorophyll near the surface nor CDOM absorption comparable to phytoplankton particulate material despite departing from the Amazon River linear mixing line (Fig. 17.11B, red circles). Quite interestingly, during this cruise, some stations showed very different surface properties (both physical and optical) when revisited over times while others showed very similar properties. Waters from below the plume (yellow circles) or from outside the plume (grey circles) show uncorrelated high salinity and low a_{CDOM} values (Fig. 17.11B).

During the summer, $a_{CDOM}(355)$ for surface waters decreases linearly with salinity (Fig. 17.11C, green circles). Surface waters from both filaments A and B follow the same linear dependence (Fig. 17.11C, green circles), thus suggesting simple dilution of the fresh water end-member into the salt water end-member (two end-member mixing model). Surface waters from the NE Blob on the other hand deviate from this $a_{CDOM}(355)$ to salinity linear dependence showing much lower a_{CDOM} to salinity ratio (Fig. 17.11C, blue circles). Samples collected close to the river mouth on August 6th 2001 (station 43) and further offshore on July 28th 2001 (station 29) (Fig. 17.11C) showed similar $a_{CDOM}(355)$ and salinity values; this was also the case for station 44 relative to station 27 (Fig. 11C). Station 23 (Fig. 17.11C, black circles) was occupied for three days; a large diatom bloom (*Hemiaulus*) occurred close to the surface (~ 15 m) causing a very high chlorophyll concentration of ~ 5-6 μg/L, much higher than the usual deep chlorophyll maximum (~ 100 m) of ~ 1-2 μg/L. Samples from this station did not fall on the Amazon River mixing line that was observed for the spring cruise (black circles in Fig. 17.5B). Waters just below this bloom (still within the fresh water plume) (~ 17 m) fell on the Amazon River mixing line (Fig. 17.11B, station

23:17m, green circle). Surface waters from stations 50 and 41 (Fig. 17.11C, orange circles) are characterized by a unique a_{CDOM}/salinity ratio despite being located near the NE Blob and the filament B, respectively. Deeper water samples from below the plume (yellow circles) and samples from outside the plume (grey circles) were characterized by high salinity and low a_{CDOM} values (Fig. 17.11C). We are continuing to analyze our data to better characterize and describe the relationship between a_{CDOM} and salinity to better understand the nature of local sources and sinks of CDOM.

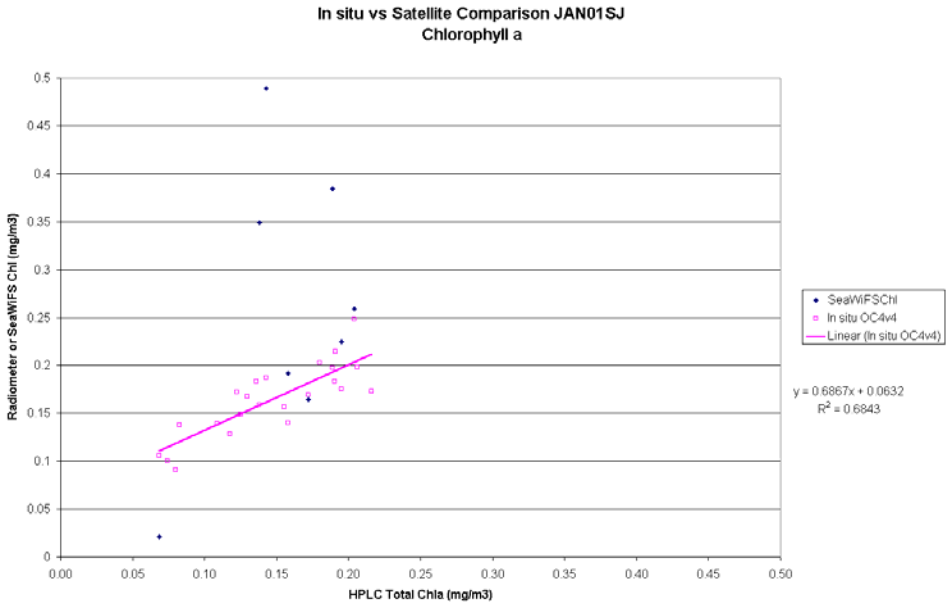

Figure 17.9: Chlorophyll Concentration - Field measurements vs SeaWiFS and in-situ OC4

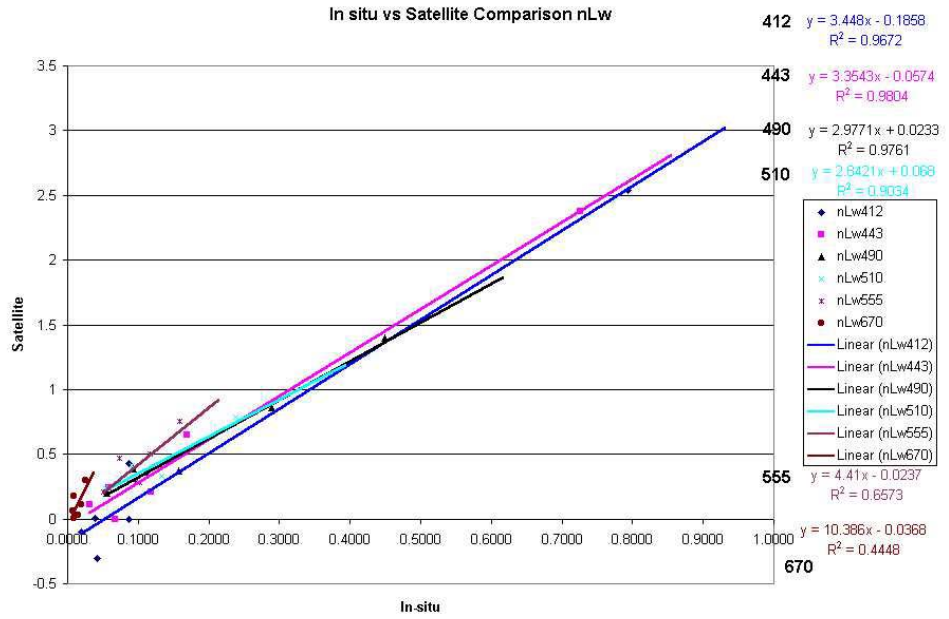

Figure 17.10: Normalized Water Leaving Radiance - Field Measurements vs SeaWiFS

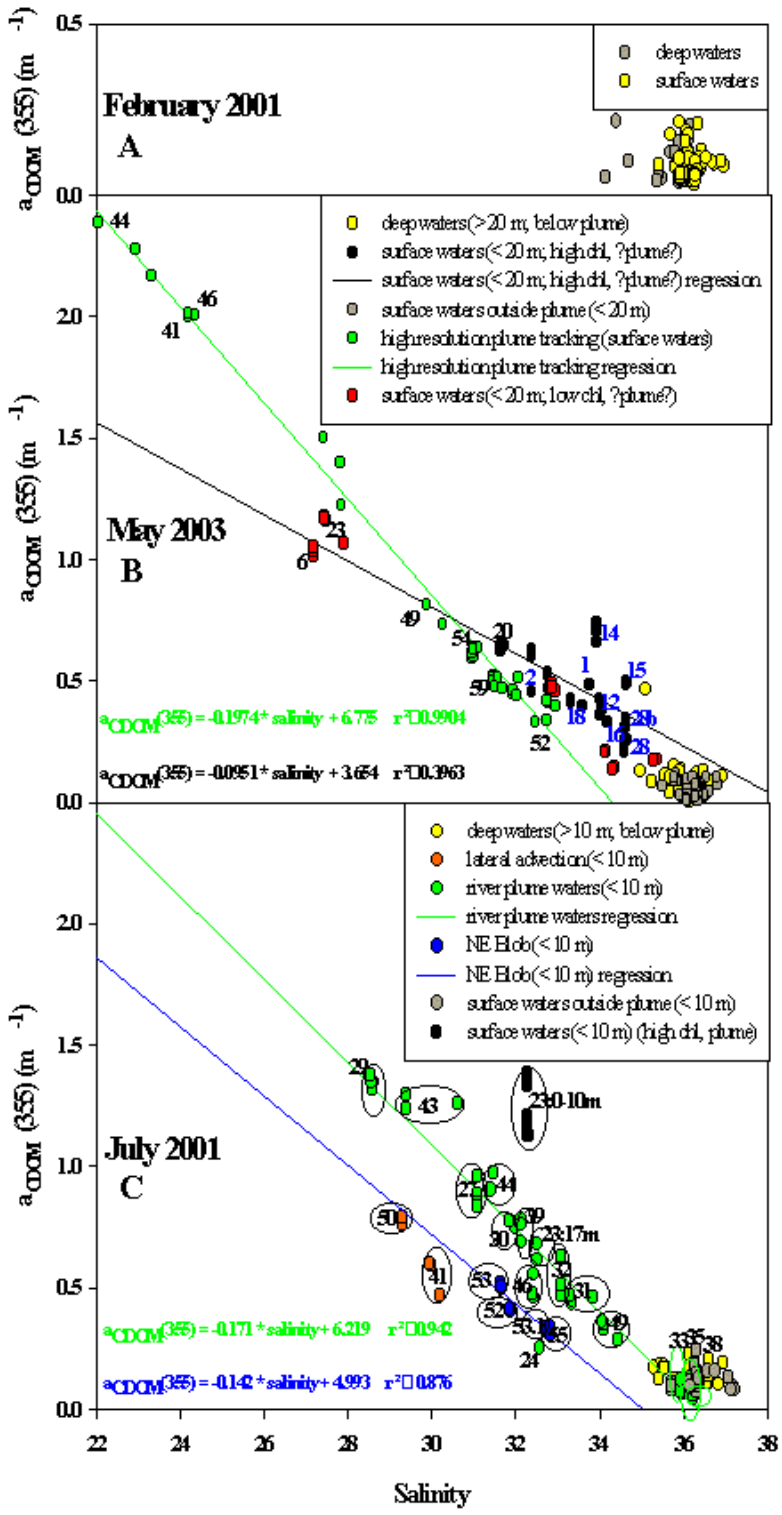

Figure 17.11: Absorption of CDOM vs Salinity from field measurements

17.3 CONCLUSIONS

Our analyzes show that great care need to be exercised while dealing with satellite ocean color data for vast areas of tropical Atlantic Ocean. Dust storms in late winter and early spring obscure the region preventing the retrieval of ocean color products or providing inaccurately high chlorophyll concentrations due to dust in the atmosphere. The Amazon River plume covers a large portion of this region between late spring and early fall – for more than 6 months of the year – and the presence of absorption due to chromophoric dissolved organic matter results in inaccurately high chlorophyll concentration retrievals in satellite imagery using standard global algorithms. Our analyzes show that while we still need further work to understand the system, it may be possible to develop crude predictive capability for salinity using CDOM absorption algorithms tuned to the region.

REFERENCES

Blough, N.V. and Del Vecchio, R., 2002: Chromophoric Dissolved Organic Matter (CDOM) in the Coastal Environment. In: D. Hansell and C. Carlson (Editors), Biogeochemistry of marine dissolved organic matter. Academic Press, San Diego, pp. 509-546.

Green, S.A. and Blough, N.V., 1994: Optical absorption and fluorescence properties of chromophoric dissolved organic matter in natural waters. *Limnol. Oceanogr.* **39**, 1903-1916.

Subramaniam, A., E.J. Carpenter, and D.G. Capone, 2002: Varied Waters and Hazy Skies: Validation of ocean color satellite data products in under-sampled marine areas: II. In SIMBIOS Project 2002 Annual Report. G.S. Fargion and C.R. McClain Eds. Pp 115-119.

Table 17.1: Cruise Details

Cruise Name	Dates	Region	Comments
JAN01SJ	7 January – 22 February 2001	Tropical Atlantic	Dust storms
JUN01KN	24 June – 18 August 2001	Tropical Atlantic	Amazon River plume
Ioffe	22 December 2001 – 9 January 2002	Drake Passage	
FEB02MB	26 – 28 February 2002	Massachusetts Bay	Coastal waters
APR02MB	4 – 6 April 2002	Massachusetts Bay	Coastal waters
APR02BR	27 March – 22 April 2002	Tropical Atlantic	Oligotrophic waters
JUL02MB	22 – 24 July 2002	Massachusetts Bay	Coastal waters
SEP02PAC	21 September – 16 October 2002	Subtropical Pacific	Diazotrophic blooms
OCT02MB	7 – 11 October 2002	Massachusetts Bay	Coastal waters
NOV02MB	18 – 19 November 2002	Massachusetts Bay	Coastal waters
JAN03ATL	4 – 18 January 2003	Tropical Atlantic	Oligotrophic waters
APR03ATL	18 April – 22 May 2003	Tropical Atlantic	Amazon River plume
JUN03MB	18 – 20 June 2003	Massachusetts Bay	Coastal waters
JUL03PAC	13 July – 22 August 2003	Subtropical Pacific	Diazotrophic blooms

Chapter 18

HPLC Pigment Measurements For Algorithm Development and Validation in Support of the SIMBIOS Science Team

Charles C. Trees and Jason R. Perl

Center for Hydro-Optics and Remote Sensing, San Diego State University, California

18.1 INTRODUCTION

Remotely sensed ocean color is determined by the absorption and scattering properties of dissolved and suspended in-water constituents. For most oceanic and coastal areas phytoplankton, with their associated suite of pigments, dominate the optical signal viewed by satellite ocean color sensors. Phytoplankton use chlorophyll *a* as their major light harvesting pigment for carbon fixation, yet there are other accessory pigment compounds (chlorophylls *b* and *c*, carotenoids, and phycobiliproteins) that play a significant role in photosynthesis. These pigments have distinct spectral signatures, and therefore, changes in the pigment-algal assemblage result in spectral shifts in absorption and scattering. Accurate measurements of phytoplankton pigments are essential in understanding global carbon cycles in oceanic and coastal areas by minimizing satellite retrieval uncertainties when mapping these properties at regional to global scales.

The focus of this 3-year program was to characterize phytoplankton pigments (excluding phycobiliproteins) in the water column during NASA's Sensor Intercomparison and Merger for Biological and Interdisciplinary Oceanic Studies (SIMBIOS) program. This research was to provide high performance liquid chromatography (HPLC) pigment analysis on samples collected by the SIMBIOS Science Team for bio-optical algorithm validation and development. The effort provided the SIMBIOS program with an internally consistent pigment database of the highest quality to evaluate ocean color products.

18.2 RESEARCH ACTIVITIES

The HPLC method (Wright et al., 1991) that was used followed the protocols set in the *Ocean Optics Protocols For Satellite Ocean Color Sensor Validation* (Bidigare *et al*., 2002) and was designed to incorporate a wide range of pigment concentrations from oceanic and coastal waters around the world. It used a reverse phase C_{18} column, with a tertiary solvent gradient. In addition, a temperature-controlled autosampler insured continuous sample injection to maintain the quota of 4000 samples per year. System calibration was routinely monitored and recorded each month to insure repeatability and consistency of data products.

The chromatographic analyses did not separate monovinyl chlorophyll *a* from divinyl chlorophyll *a*, instead these pigments were quantified using dichromatic equations at 436 nm and 450 nm (Latasa *et al*., 1996). Due to the large number of samples processed (4000 per year), the HPLC laboratory procedures were streamlined to accommodate the variety, and quantity of water samples collected by the SIMBIOS research community. By using larger HPLC solvent reservoirs, multiple sample tube racks, and running the system 24 hours a day, the laboratory could accommodate 500 samples a month, run continuously over a 3 to 4 week period.

Extraction

Pigment samples were extracted in 4.0 mL of 100% acetone, in which an internal pigment standard (canthaxanthin) was added to the acetone extract, prior to pipetting. This internal standard corrected for

any extraction volume changes during sample processing. After 24 hours of extraction in a freezer (maintained at -20°C), the samples were then sonicated for 10 seconds using an ultra-sonic microprobe tip at a 60% duty cycle. The samples were then extracted for an additional 24 hours (stored in a freezer at -20°C). Glass-fiber particulates, generated during sonication, were removed from the extract by centrifuging the samples at 5100 rpm, for 4 minutes, and subsequent filtration using 0.2 μm PTFE in-line filters.

HPLC Analysis: Equipment, Solvents, and Methods

Equipment: ThermoQuest HPLC system: Membrane Degasser, P4000 Quaternary pump; AS3000 temperature controlled autosampler; UV6000 diode array detector (scanning from 190nm to 800nm at 1nm resolution); FL3000 Fluroescence detector (Ex 404nm, Em 670nm) system controller with ChromQuest (V3.0) software.

Solvent Program: Solvent A: 80:20 methanol: 0.5M ammonium acetate (v/v); Solvent B: 90:10 acetonitrile: water (v/v); Solvent C: ethyl acetate.

Gradient Program: [Linear, 1.0 mL min^{-1} flow rate] (Minutes, % SolvA, % SolvB, % SolvC) (0.0, 100, 0, 0); (2.0, 0, 100, 0); (2.6, 0, 90, 10); (13.6, 0, 65, 35); (20.0, 0, 31, 69); (22.0, 0, 100, 0); (25.0, 100, 0, 0).

Pigments were separated on a reverse phase, Waters Spherisorb ODS-2 (5μ) C_{18} column (250mm length, 4.6mm ID), using a three solvent gradient system [Solvent A: 80:20 methanol: 0.5M ammonium acetate (v/v); Solvent B: 90:10 Acetonitrile: water (v/v); Solvent C: ethyl acetate] at a flow rate of 1.0 mL min^{-1}. A ThermoQuest P4000 pump and AS3000 Autosampler (maintained at 4° C) were used for all samples processed. Each sample extract was mixed (605μL:195μL, extract: water), and 100μL of this mix was injected onto the column.

The separation of the various pigments required 25 minutes with the pigment peaks being detected by an absorption detector; a ThermoQuest UV6000 scanning diode array detector (190 nm to 800 nm at 1 nm resolution). Pigments were monitored at 436 nm and 450 nm, with peak retention time or spectrophotometric recognition used to assign peak identification. In addition, a ThermoQuest FL3000 scanning fluorescence detector was used to detect the various chlorophyll degradation products, which occur at lower concentrations. Although the absorption peaks for monovinyl and divinyl chlorophyll *a* co-elute, each compound absorbs differently at 436 nm and 450 nm and it was therefore possible to correct for the divinyl chlorophyll *a* contribution by monitoring changes in the ratio (450 nm:436 nm) as a function of changes in the divinyl percentage (Latasa *et al*., 1996). Accuracy for each pigment compound was based on availability of pigment standards and the selection of pigment specific extinction coefficients.

The standard fluorometric method of Holm-Hansen *et al.* (1965) was used to calculate chlorophyll and phaeopigment concentrations on an aliquot (100μL) of the pigment extract. These concentrations were also corrected for extraction volume changes using the canthaxanthin internal standard. The *Ocean Optics Protocols* (Trees *et al*., 2002) for fluorometric chlorophyll *a* was followed.

Calibration

Calibration standards were purchased from Sigma Chemical Company and from DHI, Institute for Water and Environment, Denmark. System calibrations were performed to determine individual standard response factors for each compound. Each pigment response factor was determined using a multipoint calibration. Pigment standard concentrations were provided by DHI, or verified spectrophotometrically (for chlorophyll *a* and chlorophyll *b*) using published extinction coefficients.

Validation

Peak integration was performed using ChromQuest (V.3.0) software, and manually checked to insure proper integration of each peak. Retention time and spectral signatures of the standards were used to verify peak identification. Peak areas were quantified using software-aided integration. Response factors generated during the system calibration were used for final concentration calculations.

18.3 RESEARCH RESULTS

During this pigment analysis numerous pigment calibration standards were analyzed and response factors for each compound determined. A summary of the number of primary and secondary calibrations performed per year and the average response factors for those calibrations by compound are shown in Tables 18.1 and 18.2, respectively.

Table 18.1. Calibration summary during the SIMBIOS funded project.

Calibrations	**Pigments**	**2001**	**2002**	**2003**
Primary	Chls *a* & *b*	6	11	7
Secondary	Carotenoids	2	4	2

Table 18.2. Average response factors for the various pigment compounds analyzed.

Wavelength	**Pigment**	**n**	**AVERAGE**	**STD**	**CV**
PDA 436nm	MVChl *a*	25	5.5469E-04	3.2238E-05	5.81%
PDA 450nm	Chl *b*	23	4.2086E-04	1.8151E-05	4.31%
PDA 450nm	Chl *c3*	4	1.5712E-04	4.6619E-06	2.97%
PDA 450nm	Chl *c2*	4	1.3296E-04	7.8587E-06	5.91%
PDA 450nm	Perid	7	3.1793E-04	7.7302E-06	2.43%
PDA 450nm	But	8	2.4648E-04	1.1542E-05	4.68%
PDA 450nm	Fuco	8	2.4654E-04	5.9950E-06	2.43%
PDA 450nm	Hex	8	2.5317E-04	3.5938E-06	1.42%
PDA 450nm	Pras	3	2.8431E-04	1.3954E-05	4.91%
PDA 450nm	Viol	3	1.9097E-04	3.9281E-06	2.06%
PDA 450nm	Diadin	7	1.5867E-04	3.1051E-06	1.96%
PDA 450nm	Allo	4	1.6212E-04	7.9343E-06	4.89%
PDA 450nm	Diato	6	1.5968E-04	1.5684E-06	0.98%
PDA 450nm	Lut	3	1.6796E-04	2.0838E-06	1.24%
PDA 450nm	Zea	7	1.7039E-04	5.6880E-06	3.34%
PDA 436nm	DVChl *a*	3	4.0170E-04	3.6590E-05	9.11%

During this period, 15 different PI's/Projects submitted pigment samples for analysis. A list of number of samples analyzed by PI or Project is shown in Table 18.3. Included in these numbers is an estimate of the number of samples (~400) that will be submitted by three PI's (D. Siegel, G. Mitchell and N. Nelson) in November 2003.

Table 18.3. Number of samples by PI/Project received for pigment analysis at CHORS.

Principle Investigator	**2001**	**2002**	**2003**	**Total by PI**
Ajit Subramaniam	349	474	602	**1425**
Bob Arnone	130	175	142	**447**
Dave Siegel	285	806	506	**1597**
Francisco Chavez	358	631	832	**1821**
Greg Mitchell	363	818	973	**2154**
Richard Stumpf	14	118	43	**175**
Ru Morrison	44	200	0	**244**

Yves Dandonneau	21	0	0	**21**
Larry Harding	0	30	0	**30**
Norm Nelson	0	12	0	**12**
Karl Szekielda	0	30	36	**66**
Glenn Cota	0	175	0	**175**
Dariusz Stramski	0	0	131	**131**
SeaHARRE-2	---	---	53	**53**
MOBY/MOCE	255	517	192	**964**
TOTAL	**1819**	**3986**	**3510**	**9315**

18.4 CONCLUSIONS

The HPLC and fluorometric pigment analyses listed above have been processed and sent to the various PI's for validation and verification. In addition a copy was also sent to the SIMBIOS Project at Goddard Space Flight Center and was added to NASA's existing bio-optical database (SeaBASS). Plots of the SIMBIOS pigment data is shown in Figures 18.1 and 18.2, along with the entire pigment database acquired at CHORS over the past several decades. As can be seem the SIMBIOS data follows similar trends and in even some instances has reduced uncertainties. The range of pigment concentrations compared in these figures (some phytoplankton culture experiments have been included) covers over 6 orders of magnitude (<0.001 to 1000 mg m^{-3}). It seems that the log-linear relationship found by Trees *et al*. (2000) is quite ubiquitous and robust, even when monovinyl and divinyl chlorophyll a concentrations were separately quantified.

Software and Equipment Problems

Throughout the 3-year period there have been some software and hardware problems that limited or at least delayed the processing of pigment samples for the various PI's. Some of these problems by year are listed below:

Year 2001

No major software or equipment problems

Year 2002

Incompatibility between HPLC ChromQuest software and Windows NT. This required manually resetting the computer every 4 days to minimize system lockup and failures. FL3000 Fluorescence detector. Lamp failure resulting in fusing the lamp to the lamp socket. Shipped back to manufacturer for repair. UV6000 Diode Array detector. Degradation of the absorption signal caused by lamp decay, flow cell contamination and light path misalignment.

Year 2003

Pump and Autosampler were sent to manufacturer for repair. UV6000 Diode Array detector. Returned to manufacture for a lamp replacement and maintenance. Overall, lamp failure is high, due to the increased hours of usage. FL3000 Fluorescence detector. Lamp fused to the lamp socket again. Sent back to manufacturer for repair.

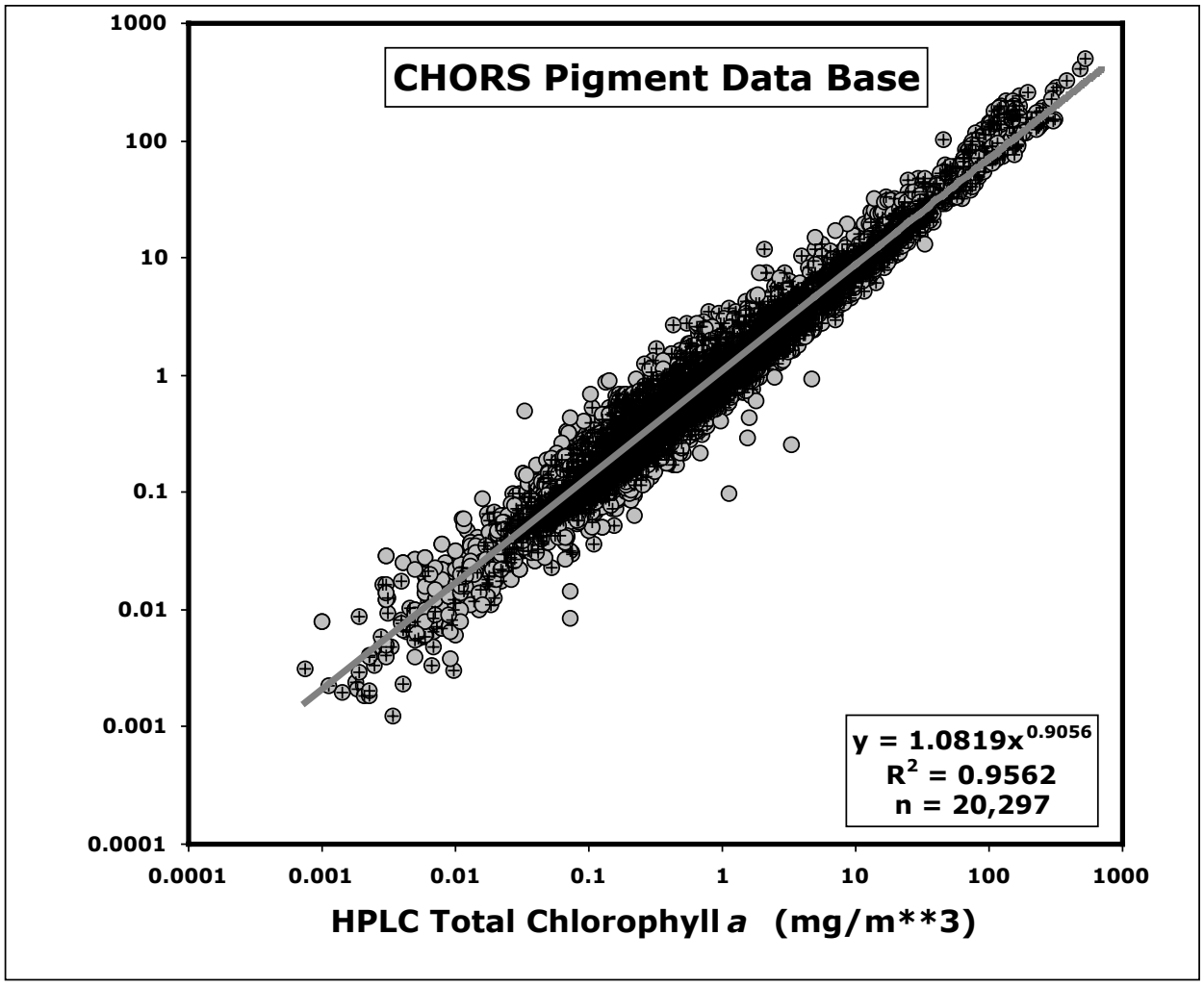

Figure 18.1: Comparison of HPLC measured total chlorophyll *a* (chlorophyllide *a*, allomer and epimer chlorophyll *a* and monovinyl and divinyl chlorophyll *a*) versus total HPLC measured accessory pigments. The plus symbols represent the 9,315 SIMBIOS processed pigment samples, where as the grey filled circles are a mixture of data from Trees *et al*. 2000, and additional pigment data from C. Trees, R. Bidigare, R. Goericke and R. Barlow.

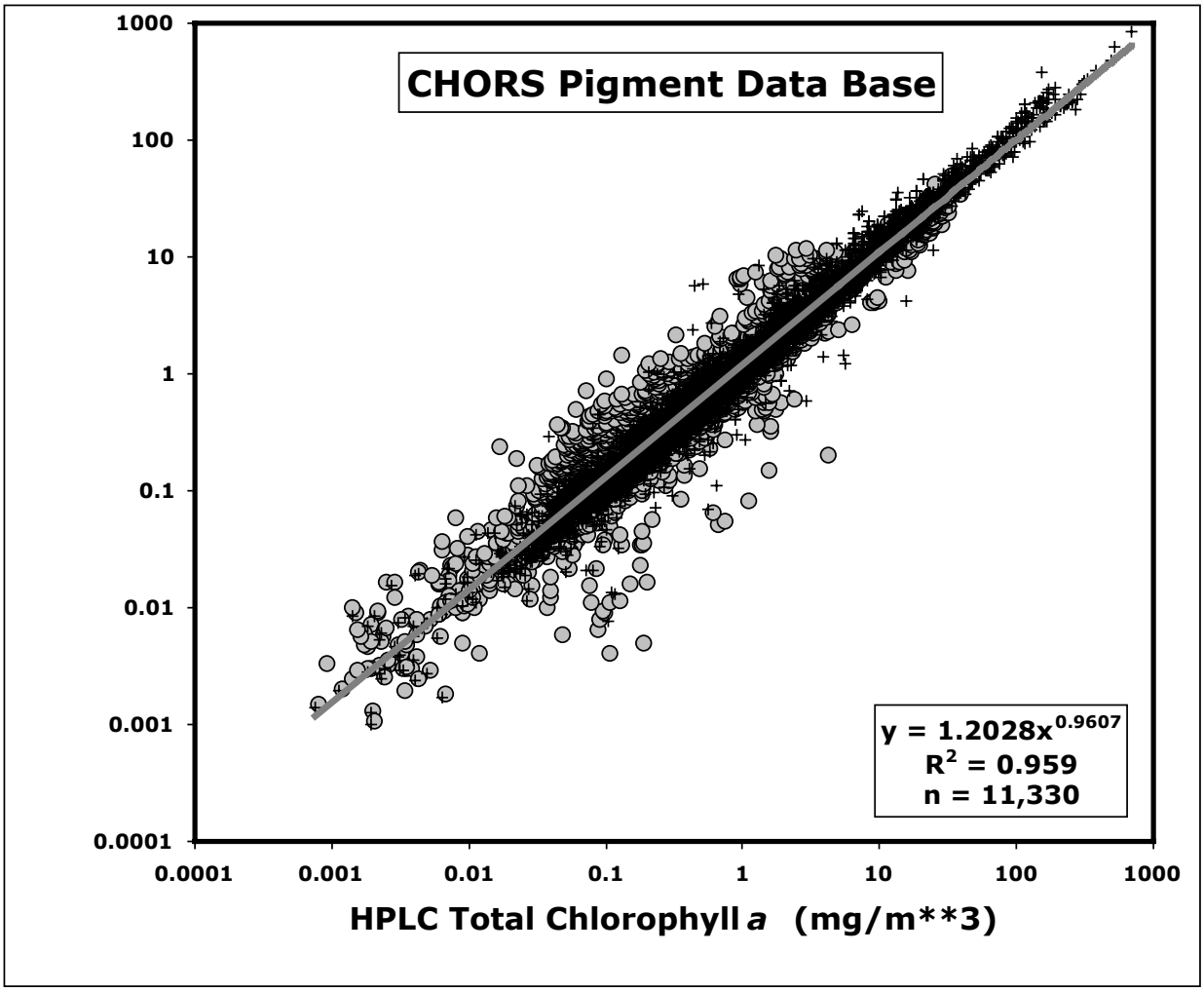

Fig.ure 18.2: Comparison of HPLC measured total chlorophyll *a* (chlorophyllide *a*, allomer and epimer chlorophyll *a* and monovinyl and divinyl chlorophylls *a*) versus fluorometrically-measured chlorophyll. The plus symbols represent the 9,015 SIMBIOS processed pigment samples, where as the grey filled circles are a mixture of data from C. Trees and R. Bidigare.

Intercalibration and Correction Efforts

Year 2001: Standard fluorometric method correction. This problem was caused by a CHORS analyst not following NASA's protocols (Trees *et al*., 2000). Problem was corrected by replacing the analyst and sending out corrected fluorometric data to the various PI's. The SeaBASS database was also updated.

Year 2002: Round Robin#1 with Dr. Larry Harding and Laurie Van Heukelem. (Horn Point Marine Laboratory). Chlorophyll *c3* response factor was off by a factor of 10. This was determined by comparing ratios of Chl *c3*: Chl *a* from previous acquired pigment data. It was then later confirmed by DHI, Denmark, who had mislabeled the concentration of that pigment batch. Corrected values were sent to PI's and updated in SeaBASS. Received a new digital Turner Designs Fluorometer from the SIMBIOS Project. Multiple calibrations were performed to document any differences between the new digital fluorometer and the older analog fluorometer.

Year 2003: Round Robin#2 with Horn Point Marine Laboratory and Dr. Norm Nelson (UCSB). SeaHARRE-2 participation. Volume extract correction (5.2% overestimation). The NASA pigment

protocols were found to have an error. An Addendum was drafted and sent to the SIMBIOS project. PI's were notified of this error, and corrected values were sent to the, as well as the SIMBIOS Project. Adjusted the percentage of acetone of the extraction solution to improve peak shape and resolution for chlorophylls *c2* & *c3*. The extraction solution was diluted from 100% to 95% acetone, based on experiments conducted at CHORS. Started to monitor samples at 664nm (in addition to 436nm and 450nm). This wavelength provides for better peak resolution for chlorophylide *a,* pheophorbide *a*, and pheophytin *a*. This wavelength is also not sensitive to the other co-eluting carotenoid pigments, making integration of the peaks easier and more accurate.

Problem with Sample Labeling and Ancillary Information

The NASA protocols recommended the proper procedure for filtering and recording samples for HPLC submission. There were a variety of trends that developed over the contract period. Below are some of the major problems that were encountered.

PI's designated their own sample labeling scheme (complicated with multiple characters), even though we recommended using a CHORS number, with the PI's initials, followed by a single number (e.g. CT0001; Charles Trees, sample# 0001).

Sample ID numbers were written on the aluminum foil **after** the filter was placed in it. Many times, the pen poked through the foil, leaving an ink mark on the filter. (This ink co-elutes with the chlorophyll c peaks in the chromatograms).

Some PI's used 47mm diameter filters instead of the recommended 25mm. CHORS extraction procedures assume that 25mm filters are used, and the method had to be modified to accommodate the larger filters. In addition, it was difficult to efficiently sonicate these large filters in the 4.0 mL of acetone extract.

Filters were not folded correctly (in half with filtered side facing in as recommended). Some were folded exposing the filtered face. Others were crammed into cryo-vials, or folded multiple times (4 times). These filters had to be thawed slightly to extract, creating possible pigment degradation.

Filters contained large amounts of frozen water, which mean too much water was left on the filter when it was placed into LN2. This additional water affects peak shape, as well as contributes to the degradation of pigments.

Filters did not contain enough pigment concentration to properly analyze on the HPLC system. The protocols recommended certain volumes to filter based on water column productivity (e.g. 4 liters for oligotrophic waters).

Ancillary logs were either incomplete or contain too much information. Files had filter numbers that did not match those delivered to CHORS. In addition, there were duplicate filter numbers that were not recorded by the PI's. It was recommend that the filters be inventoried prior to shipping to CHORS.

There were on a few occasions when dewars arrived thawed out. This was from defective a dewar or improper LN_2 charging. Samples were shipped to CHORS without prior notice.

REFERENCES

Bidigare, R.R., L.Van Heukelem, and C.C. Trees, 2002: HPLC Phytoplankton Pigments: Sampling, Laboratory Methods, and Quality Assurance Procedures, Chapter 16 in: Mueller J.L. and G.S. Fargion (Eds.) *Ocean Optics Protocols For Satellite Ocean Color Sensor Validation.* NASA/TM-2002-210004/Rev3-Vol2, NASA Goddard Space Flight Center, Greenbelt, MD. pp258-268.

Holm-Hansen, O., C.J. Lorenzen, R.W. Holmes, and J.D.H. Strickland, 1965: Fluorometric determination of chlorophyll. *J. du Cons. Intl. Pour l'Expl. de la Mer.,***30**, 3-15.

Jeffrey, S.W., R.F.C. Mantoura, and S.W. Wright (eds.), 1997: *Phytoplankton Pigments in Oceanography*, Monographs on Oceanographic Methodology, *UNESCO*, 661 pp.

Latasa, M., R. R. Bidigare, M. E. Ondrusek, and M. C. Kennicutt II, 1996: HPLC analysis of algal pigments: A comparison exercise among laboratories and recommendations for improved analytical performance. *Mar. Chem*., **51**, 315-324.

Trees, C.C., R.R. Bidigare, D.M. Karl, L. Van Heukelm, and J. Dore, 2002: Fluorometric Chlorophyll a: Sampling, Laboratory Methods, and Data Analysis Protocols, Chapter 17 in: Mueller J.L. and G.S. Fargion (Eds.) *Ocean Optics Protocols For Satellite Ocean Color Sensor Validation.* NASA/TM-2002-210004/Rev3-Vol2, NASA Goddard Space Flight Center, Greenbelt, MD. pp269-283.

Chapter 19

Assessment, Validation, and Refinement of the Atmospheric Correction Algorithm for the Ocean Color Sensors

Menghua Wang
University of Maryland, Baltimore County, Baltimore, Maryland

19.1 INTRODUCTION

The primary focus of this proposed research is for the *atmospheric correction algorithm evaluation and development* and *satellite sensor calibration and characterization*. It is well known that the atmospheric correction, which removes more than 90% of sensor-measured signals contributed from atmosphere in the visible, is the key procedure in the ocean color remote sensing (Gordon and Wang, 1994). The accuracy and effectiveness of the atmospheric correction directly affect the remotely retrieved ocean bio-optical products. On the other hand, for ocean color remote sensing, in order to obtain the required accuracy in the derived water-leaving signals from satellite measurements, an on-orbit vicarious calibration of the whole system, i.e., sensor and algorithms, is necessary. In addition, it is important to address issues of (i) cross-calibration of two or more sensors and (ii) in-orbit vicarious calibration of the sensor-atmosphere system. The goal of these researches is to develop methods for meaningful comparison and possible merging of data products from multiple ocean color missions. In the past year, much efforts have been on (a) understanding and correcting the artifacts appeared in the SeaWiFS-derived ocean and atmospheric produces; (b) developing an efficient method in generating the SeaWiFS aerosol lookup tables, (c) evaluating the effects of calibration error in the near-infrared (NIR) band to the atmospheric correction of the ocean color remote sensors, (d) comparing the aerosol correction algorithm using the single-scattering epsilon (the current SeaWiFS algorithm) vs. the multiple-scattering epsilon method, and (e) continuing on activities for the International Ocean-Color Coordinating Group (IOCCG) atmospheric correction working group. In this report, I will briefly present and discuss these and some other research activities.

19.2. RESEARCH ACTIVITIES AND RESULTS

Earth Curvature Effects Measured by SeaWiFS

This work has been described in an article by Wang (2003). It is a common fact that the Earth's atmosphere is a spherical-shell atmosphere (SSA) rather than a plane-parallel atmosphere (PPA). Thus, the light scattered by the Earth's atmosphere is governed by physics of the radiative transfer equation (RTE) with proper boundary conditions in the SSA system. In the satellite and aircraft remote sensing, however, the PPA model is usually assumed to compute the lookup tables and convert the sensor-measured signals to the desired physical and optical quantities. The PPA assumption is a simple yet very good approximation for solar and sensor zenith angles $< \sim 80°$. Note that the solar and sensor zenith angles in here are defined as a measure at the local surface. In the PPA assumption, however, the solar zenith angles $\geq 90°$ is not defined. When the solar zenith angles $\geq 90°$ in the PPA system, i.e., when the sun is below the horizon, there will be no light scattered out to the top of the atmosphere (TOA) or at the bottom of the surface. We would experience completely darkness in this situation. The ocean color satellite sensor Sea-viewing Wide Field-of-view Sensor (SeaWiFS) acquired imageries with the solar zenith angles $\geq 90°$ and provided good examples of the Earth's curvature effects on the light scattering processing in the SSA system.

On June 26, 2000, SeaWiFS has acquired imageries with significantly extended coverage, adding about another 5 minutes to the normal 40 minutes recording duty cycle. This was a test for the SeaWiFS coverage capability and to find a proper additional coverage for the SeaWiFS routine operation. For the test purpose, the SeaWiFS coverage for that specific orbit was extended significantly. A specific SeaWiFS measurement line, in which the solar zenith angles varies from ~76° to ~94°, was extracted for study and compared with both the PPA and SSA model computations (Wang, 2003). These are briefly described in here.

To understand and interpolate the SeaWiFS measurements, I have carried out the various radiative transfer simulations for the SSA model using the backward Monte-Carlo method that was developed by *Ding and Gordon* (Ding and Gordon, 1994). Figure 19.1 shows simulated results in comparing with the SeaWiFS measurements at wavelengths 443 and 670 nm for atmosphere composed of the molecules (Rayleigh scattering), molecules and aerosols, and molecules and water-clouds. In Fig. 1, the SSA simulations were carried out for the sensor located at the altitude of 705 km (SeaWiFS orbit) with the various SSA atmospheres. Detailed descriptions of the solar-sensor geometry in the SSA model can be found in *Ding and Gordon* (Ding and Gordon, 1994). For each Monte-Carlo simulation, ten million photons were used.

Figs. 19.1(a) and 19.1(b) are comparison results for atmosphere composed of molecules (Rayleigh scattering) with various physical thickness of the atmospheric layer (from 10 km to 100 km). Results from the plane-parallel atmosphere (indicated as "ppa") are also provided for comparisons. Clearly, PPA model makes significant errors (under-estimation) for the solar zenith angles > ~85°. Figs. 1(c) and 1(d) show comparison results for a two-layer SSA model with aerosols located at the bottom 2-km layer (mixed with 22% of molecules). The *Shettle and Fenn* (Shettle and Fenn, 1979) maritime aerosol model with relative humidity of 80% (M80) and aerosol optical thickness at 865 nm $\tau_a(865)$ of 0.1 were used in simulations. Figs. 19.1(e) and 19.1(f) give comparison results for a two-layer SSA model with water-clouds located at the bottom 2-km layer (mixed with 22% of molecules). These are simulations for the cloud optical thickness τ_c of 8 and an effective particle radius r_e of 8 μm with the various physical thicknesses of the SSA layer, e.g., symbol "20, 2 km" is results for a two-layer SSA atmosphere with total physical thickness of 20-km and 2-km layer at the bottom. Signals contributed from ocean waters are ignored in all these simulations. They are negligible in these cases.

As shown in Fig. 19.2, the TOA radiances at the first part (solar zenith angles from ~76° to ~85°) can be best simulated with cloud optical thickness ~8, while the next part can be well approximated with the M80 model for aerosol optical thickness of 0.1. These are comparisons in qualitatively. It is interesting to note that, however, for the very large solar zenith angles (> ~85°), the TOA radiance is very sensitive to the physical thickness of the atmospheric layer assumed in the simulation. Indeed, for the very large solar zenith angles, the TOA radiance is much more sensitive to the change of physical thickness of the layer than to the optical properties of the medium (e.g., compare results of Figs. 19.1(c) and 19.1(e)). This is because, for the SSA model with the large solar zenith angles, photons that are exiting to the TOA through scattering process are limited by the solar-sensor geometry and physical thickness of the layer. The thicker the layer is, the larger the probability that photons can be scattered into the sensor viewing direction, thereby the larger the sensor-measured radiance. At the wavelength 443 nm, the effective thickness of the SSA layer is best approximated by ~40 km, while at the band 670 nm the SSA layer can be approximated by ~20 km. The Rayleigh optical thicknesses for the wavelength at 443 nm and 670 nm are ~0.234 and ~0.045, respectively. This explains different effective physical thicknesses for the wavelengths 443 and 670 nm at which photons can interact with molecules and particles in the radiative transfer process. Photon at the wavelength 443 nm "sees" thicker of the layer than photon at 670 nm because the Rayleigh optical thickness at 443 nm is significantly larger than that of 670 nm. For the PPA model, on the other hand, the physical thickness has no effects on the TOA radiance.

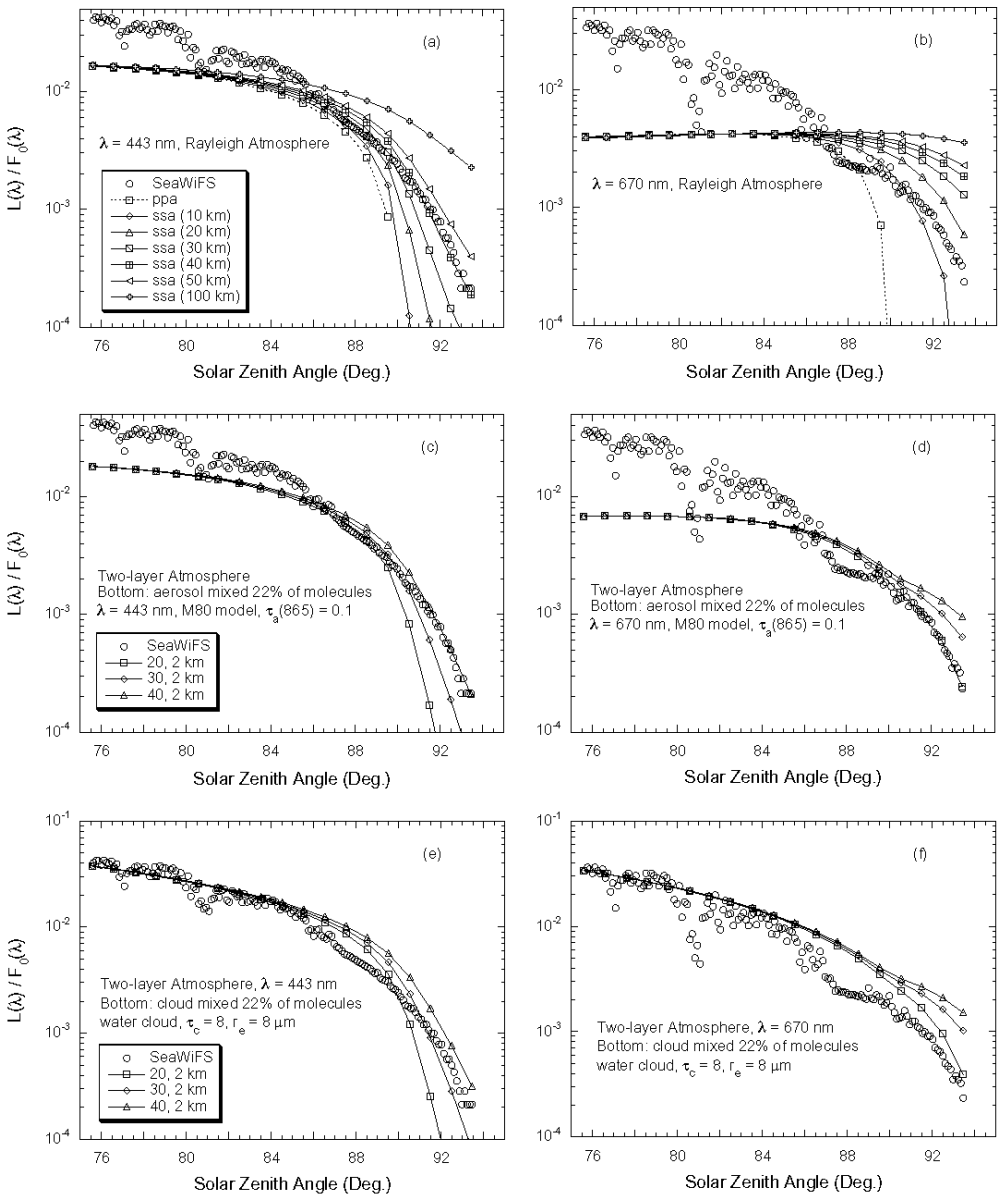

Figure 19.1: The simulated results compared with the SeaWiFS measurements for the wavelengths of 443 and 670 nm and for various cases: (a) & (b) the Rayleigh atmosphere, (c) & (d) the two-layer SSA with aerosols located at the bottom 2-km layer (mixed with 22% of molecules), and (e) & (f) the two-layer SSA with water cloud located at the bottom 2-km layer (mixed with 22% of molecules).

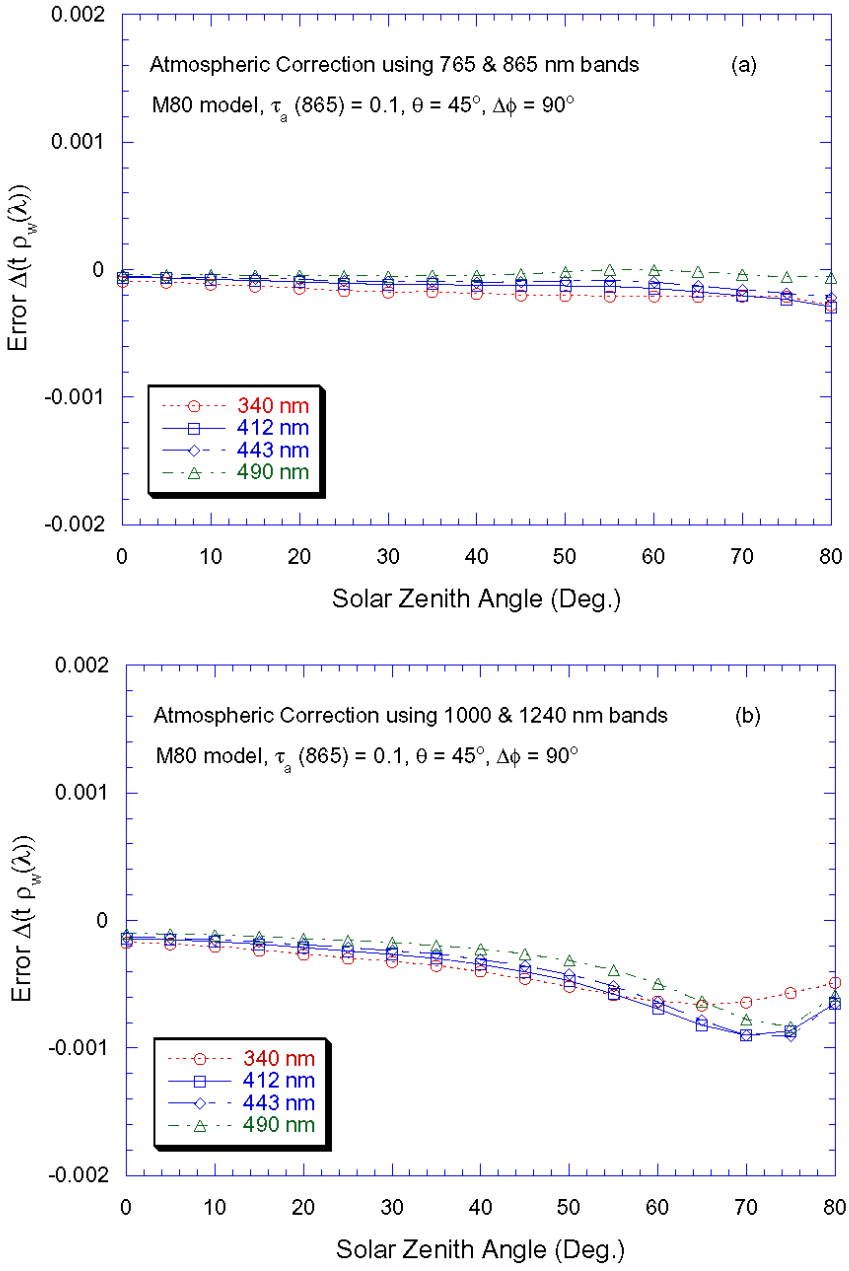

Figure 19.2: Errors in the derived water-leaving reflectance with atmospheric correction using the NIR bands of (a) 765 and 865 nm and (b) 1000 and 1240 nm.

Atmospheric Correction using the Longer NIR Bands

For the Case-2 waters, the ocean is usually not black at the near-infrared (NIR) wavelengths centered at 765 and 865 nm, which are used for the atmospheric correction for both SeaWiFS and MODIS to derive the ocean color products (Gordon and Wang, 1994). In these cases, the ocean contributions at the NIR are often mistakenly accounted as radiance scattering from atmosphere, thereby leading to over-correction of atmospheric radiance and underestimation of water-leaving radiance at the visible. Simulations have been carried out for the atmospheric correction using the longer NIR bands centered at 1000, 1240, and 1640 nm for retrievals of the ocean color product in the coastal waters. At the longer NIR bands, ocean is black even for the Case-2 waters. Thus, the Case-2 bio-optical model that has strongly regional dependence is not needed for the atmospheric correction. The atmospheric correction can be therefore operated routinely for the global coastal waters, and the water-leaving radiance spectrum from blue to the short NIR in the coastal regions can be derived. This scheme can also be applied to the cases of Case-1 waters with high chlorophyll concentrations in which the ocean contributions at the short NIR bands (765 and 865 nm) are significant. The performance of the atmospheric correction using the longer NIR bands is compared with that of the SeaWiFS and MODIS algorithm using the 765 and 865 nm bands. Figure 19.3 provides examples of comparison results with the longer NIR for the atmospheric correction. Fig. 19.3 (a) is results of error in the derived water-leaving reflectance using the NIR bands of 765 and 865 nm, while Fig. 19.3 (b) is results of atmospheric correction using the longer NIR bands of 1000 and 1240 nm. In both cases, the errors are all within ~0.001 for the derived water-leaving reflectance for wavelengths from UV to the blue.

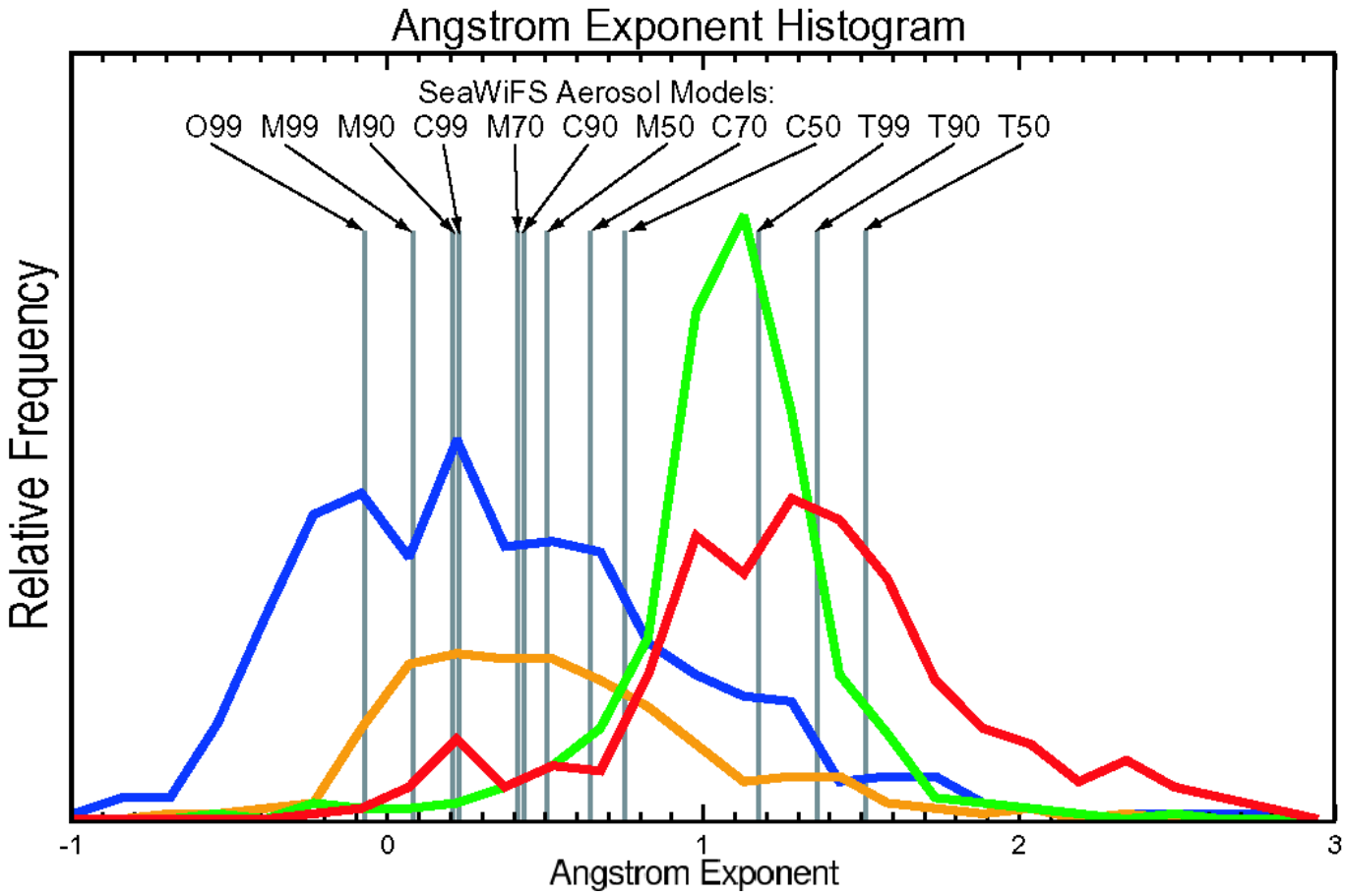

Figure 19.3: The Ångström exponents from the SeaWiFS 12 aerosol models compared with the in situ data collected bye the NASA SIMBIOS project.

Aerosol Model Validation

This is part of work reported in Knobelspiesse et al. (2003), and complete descriptions and results analyses can be found in this paper. Here is brief description of the SeaWiFS aerosol models compared with the in situ measurements.

One of the main purposes for the NASA SIMBIOS in situ aerosol data collection over oceans is to compare and validate aerosol products derived from the ocean color sensors (Wang et al., 2000), in particular, to validate the aerosol models used for the data processing in deriving the ocean color products. The primary goals of the SeaWiFS mission are routine global ocean color measurements and ocean bio-optical property data. In retrieving the ocean near-surface signals from sensor-measured radiances at the satellite, however, the atmospheric and surface effects must be removed. This is known as *atmospheric correction* (Gordon and Wang, 1994) which removes more than 90% of the sensor-observed radiance in the visible spectrum. The SeaWiFS atmospheric correction algorithm (Gordon and Wang, 1994) uses two near-infrared (NIR) bands to estimate the aerosol optical properties and extrapolate these into the visible spectrum where the ocean color products are derived. In this process, aerosol models are needed.

The SeaWiFS 12 aerosol models are the Oceanic model with the relative humidity (RH) of 99% (O99), the Maritime model with RH of 50%, 70%, 90%, and 99% (M50, M70, M90, and M99), the Coastal model with RH of 50%, 70%, 90%, and 99% (C50, C70, C90, and C99), and the Tropospheric model with RH of 50%, 90%, and 99% (T50, T90, and T99) (Wang, 2000). The Oceanic, Maritime, and Tropospheic aerosol models are from (Shettle and Fenn, 1979), while the Coastal model was introduced by (Gordon and Wang, 1994). These aerosol models are all non- and weakly absorbing. Table 19.1 summarizes optical properties for these aerosol models. In Table 19.1, the Ångström exponent is the mean value for a given aerosol model, while the single-scattering albedo is value at the wavelength 865 nm. The same atmospheric correction algorithm with similar aerosol model set is used for the retrieval of the ocean color products from the Moderate Resolution Imaging Spectroradiometer (MODIS) (Esaias et al., 1998; Salomonson et al., 1989).

The aerosol model is defined by its particle size distribution and refractive indices (real and imaginary parts). The Ångström exponent is related to the particle size distribution. Low value of the Ångström exponent indicates the large particle size, while high value of the Ångström exponent represents the small particle size of aerosols. For a given aerosol particle size distribution (aerosol model), the Ångström exponent is defined. Therefore, the Ångström exponent values obtained from the ground in situ measurements can be used to indicate if an appropriate aerosol model set in terms of the particle size distribution is used for the SeaWiFS data processing. Note that, however, this only gives part of picture, i.e., the aerosol particle size distribution. To validate the aerosol model and give a complete picture, the refractive indices are also needed. The refractive indices (or aerosol single-scattering albedo) can be derived with the sky radiance measurements (Dubovik and King, 2000; Wang and Gordon, 1993).

Figure 19.3 provides comparison results of the Ångström exponent from the SeaWiFS 12 aerosol models with those of the in situ measurements. The Ångström exponent values for the SeaWiFS 12 aerosol models are represented as vertical lines which are compared with the histograms from all in situ data collected by the NASA SIMBIOS project (Knobelspiesse *et al.*, 2003). Clearly, the in situ Ångström exponents obtained from maritime environment can be well represented with the SeaWiFS 12 aerosol models in the most of time. It appeared that, however, in the open ocean regions aerosol models with much larger particle sizes (very small Ångström exponent values) may still needed, e.g., aerosol models reported by (Porter and Clarke, 1997). On the other hand, in the coastal regions, aerosol models with low values of the single-scattering albedo (absorbing aerosols), e.g., dust aerosol models, are needed to handle these absorbing aerosol cases (Moulin et al., 2001).

The IOCCG Atmospheric Correction Working Group Activity

I have been continuing on activities for the IOCCG atmospheric correction working group. The main objective of the working group is to quantify the performance of the various exiting atmospheric correction algorithms used for the various ocean color missions. Therefore, the derived ocean color products from various ocean color missions can be meaningfully compared and possibly merged.

Table 19.1. Characteristics of the 12 aerosol models for the SeaWiFS data processing.

Aerosol Model	Relative Humidity (%)	Symbol	Ångström Exponent	Single Scattering Albedo (865 nm)
Oceanic	99	O99	-0.086	1.0
Maritime	50, 70, 90, 99	M50-M99	0.091-0.502	0.981-0.999
Coastal	50, 70, 90, 99	C50-C99	0.224-0.757	0.971-0.997
Tropospheric	50, 90, 99	T50, T90, T99	1.185-1.519	0.930-0.987

REFERENCES

Ding, K., and H.R. Gordon, 1994: Atmospheric correction of ocean-color sensors: effects of the Earth's curvature, *Appl. Opt.*, **33**: 7096-7106.

Dubovik, O., and M. King, 2000: A flexible inversion algorithm for retrieval of aerosol optical properties from Sun and sky radiance measurements, *J. of Geophys. Res.*, **105**: 20,673-20696.

Esaias, W.E., M.R. Abbott, I. Barton, O.B. Brown, J.W. Campbell, K.L. Carder, D.K. Clark, R.L. Evans, F.E. Hodge, H.R. Gordon, W.P. Balch, R. Letelier, and P.J. Minnet, 1998: An overview of MODIS capabilities for ocean science observations, *IEEE Trans. Geosci. Remote Sens.*, **36**: 1250-1265.

Gordon, H.R., and M. Wang, 1994:, Retrieval of water-leaving radiance and aerosol optical thickness over the oceans with SeaWiFS: A preliminary algorithm, *Appl. Opt.*, **33:** 443-452.

Knobelspiesse, K.D., C. Pietras, G.S. Fargion, M. Wang, R. Frouin, M.A. Miller, A. Subramaniam, and W.M. Balch, 2003: Maritime aerosol optical properties measured by handheld sun photometers, *Remote Sens. Environ.* (Submitted).

Moulin, C., H.R. Gordon, R.M. Chomko, V.F. Banzon, and R.H. Evans, 2001: Atmospheric correction of ocean color imagery through thick layers of Saharan dust, *Geophys. Res. Letters*, **28:** 5-8.

Porter, J.N., and A.D. Clarke, 1997: Aerosol size distribution models based on in situ measurements, *J. of Geophys. Res.*, **102**: 6035-6045.

Salomonson, V.V., W.L. Barnes, P.W. Maymon, H.E. Montgomery, and H. Ostrow, 1989: MODIS: advanced facility instrument for studies of the Earth as a system, *IEEE Trans. Geosci. Remote Sensing*, **27**: 145-152.

Shettle, E.P., and R.W. Fenn, 1979: Models for the Aerosols of the Lower Atmosphere and the Effects of Humidity Variations on Their Optical Properties, *AFGL-TR-79-0214*, , U.S. Air Force Geophysics Laboratory, Hanscom Air Force Base, Mass.

Wang, M., 2000: The SeaWiFS atmospheric correction algorithm updates, Vol. **9**, *NASA Tech. Memo. 2000-206892*, S.B. Hooker and E.R. Firestone, Eds., SeaWiFS Postlaunch Technical Report Series, NASA Goddard Space Flight Center, Greenbelt, Maryland.

Wang, M., 2003: Light scattering from spherical-shell atmosphere: Earth curvature effects measured by SeaWiFS, *Eos, Transactions, American Geophysical Union* (In press).

Wang, M., S. Bailey, and C.R. McClain, 2000: SeaWiFS Provides Unique Global Aerosol Optical Property Data, in *Eos, Transactions, American Geophysical Union*, pp. 197.

Wang, M., and H.R. Gordon, 1993: Retrieval of the columnar aerosol phase function and single scattering albedo from sky radiance over the ocean: simulations, *Appl. Opt.*, **32**: 4598-4609.

This Research was Supported by
the NASA Contract # 00203

Publications

Wang, M., 1999: Validation study of the SeaWiFS oxygen A-band absorption correction: Comparing the retrieved cloud optical thicknesses from SeaWiFS measurements, *Appl. Opt*., **38**, 937-944.

Wang, M., 1999: Atmospheric correction of ocean color sensors: Computing atmospheric diffuse transmittance, *Appl. Opt*. , **38**, 451-455.

Wang, M., 1999: A sensitivity study of SeaWiFS atmospheric correction algorithm: effects of spectral band variations*, Remote Sens. Environ*., **67,** 348-359.

Siegel, D. A., M. Wang, S. Maritorena, and W. Robinson, 2000: Atmospheric correction of satellite ocean color imagery: the black pixel assumption, A*ppl. Opt*., **39**, 3582-3591.

Eplee, R. E., Jr., W. D. Robinson, S. W. Bailey, D. K. Clark, P. J. Werdell, M. Wang, R. A. Barnes, and C.R. McClain, 2001: The calibration of SeaWiFS, Part 2: Vicarious techniques, *Appl. Opt.,* **40**, 6701-6718.

Wang, M. and S. W. Bailey, 2001: Correction of the sun glint contamination on the SeaWiFS ocean and atmosphere products, *Appl. Opt.,* **40**, 4790-4798.

Wang, M., B. A. Franz, R. A. Barnes, and C. R. McClain, 2001: Effects of spectral bandpass on SeaWiFS-retrieved near-surface optical properties of the ocean, *Appl. Opt*., **39**, 343-348.

Chou, M. D., P. K. Chan, and M. Wang, 2002: Aerosol radiative forcing derived from SeaWiFS-retrieved aerosol optical properties, *J. Atmos. Sci.,* **59**, 748-757.

Gregg, W. W., M. E. Conkright, J. E. O'Reilly, F. S. Patt, M. Wang, J. Yoder, and N. Casey-McCabe, 2002: NOAA-NASA Coastal Zone Color Scanner reanalysis effort, *Appl. Opt***., 41**, 1615-1628.

Wang, M. and H. R. Gordon, 2002: Calibration of ocean color scanners: How much error is acceptable in the near-infrared, *Remote Sens. Environ***., 82**, 497-504.

Wang, M., 2002: The Rayleigh lookup tables for the SeaWiFS data processing: Accounting for the effects of ocean surface roughness, *Int. J. Remote Sens.,* **23**, 2693-2702.

Wang, M., 2003: An efficient method for multiple radiative transfer computations and the lookup table generation, *J. Quant. Spectr. Rad. Trans*., **78**, 471-480.

Wang, M., 2003: Correction of artifacts in the SeaWiFS atmospheric correction: Removing the discontinuity in the derived products, *Remote Sens. Environ*., **84**, 603-611, 2003.

Tanaka, T. and M. Wang, 2003: Solution of radiative transfer in anisotropic plane-parallel atmosphere*, J. Quant. Spectr. Rad. Trans*. (In press).

Wang, M., Extrapolation of the aerosol reflectance from the near-infrared to the visible: the single-scattering epsilon vs. multiple-scattering epsilon method, *Int. J. Remote Sens*. (In press).

Wang, M., Light Scattering from Spherical-Shell Atmosphere: Earth curvature effects measured by SeaWiFS, *Eos, Transaction, American Geophysical Union*, (In press).

Other publications

Wang, M., 1998: Applying the SeaWiFS atmospheric correction algorithm to MOS: Effects of spectral band variations, Proc. the 4th Pacific Ocean Remote Sensing Conference, p88-91, Qingdao, China, July 28-31.

Wang, M., 1998: A validation of the SeaWiFS O2 A-band absorption correction, Proc. the 4th Pacific Ocean Remote Sensing Conference, p32-36, Qingdao, China, July 28-31.

Wang, M. and B. A. Franz, 1998: A vicarious intercalibration between MOS and SeaWiFS, Proc. 2nd International Workshop on MOS-IRS and Ocean Colour, p95-102, Berlin, Germany, June 10-12.

Wang, M., S. W. Bailey, C. R. McClain, C. Pietras, and T. Riley, 1999: Remote sensing of the aerosol optical thickness from SeaWiFS in comparison with the in situ measurements, Proc. Ocean color, land surface, radiation and clouds, aerosols: the contribution of new generation spaceborne sensors to global change studies, Méribel, France, WK1-O-08, p1-4, January 18-22.

Wang, M., 2000: Effects of the sea surface wind speed on the SeaWiFS derived ocean color optical property data, Proc. the ONR's Ocean Optics XV [CD-ROM], Musée Océanographique, Monaco, October 16-20.

Wang, M. and S. W. Bailey, 2000: Correction of the sun glint contamination, Proc. the 5th Pacific Ocean Remote Sensing Conference, p18-22, Goa, India, December 5-8.

Liberti, G. L, F. D'Ortenzio, R. Santoleri, G. L. Volpe, M. Wang, C. R. McClain, and V. E. Cachorro Revilla, 2001: Validation of SeaWiFS aerosol products over the Mediterranean basin," Proc. EUMETSAT Meteorological Satellite Data Users' Conference, p18-22, Antaya, Turkey, October 1-5.

Wang, M., 2002: Approaches of the aerosol correction algorithm: methods of the single-scattering vs. multiple-scattering epsilon," Proc. the ONR's Ocean Optics XVI [CD-ROM], Santa Fe, New Mexico, November 18-22.

Wang, M., 2002: Example of aerosol model effects in SeaWiFS atmospheric correction," Proc. SPIE's Third International Asia-Pacific Symposium on Remote Sensing of the Atmosphere, Ocean, Environment, and Space, Vol. 4892, p87-94, Hangzhou, China, October 23-27.

Presentations

Chou, M. D., P. K. Chan, and M. Wang, 1999: Global aerosol radiative forcing derived from SeaWiFS-inferred aerosol optical properties, The AGU Fall Meeting, San Francisco, California, December 13-17.

Wang, M. and S. W. Bailey, 2000: Correction of the sun glint contamination," The 5th Pacific Ocean Remote Sensing Conference, Goa, India, December 5-8.

Wang, M., 2000: Effects of the sea surface wind speed on the SeaWiFS derived ocean color optical property data," The Ocean Optics XV, Musée Océanographique, Monaco, October 16-20.

Wang, M., 2000: Effects of the vicarious calibration on the SeaWiFS derived aerosol optical properties, The AGU Spring Meeting, Washington, DC, May 30-June 3.

Wang, M., A. Isaacman, B. A. Franz, and C. R. McClain, 2001: A comparison study of the ocean color data derived from OCTS and POLDER, The AGU Fall Meeting, San Francisco, California, December 10-14, 2001.

Gales, J. M., B. A. Franz, and M. Wang, 2001: A three year intercomparison of oceanic optical properties from MOS and SeaWiFS, The AGU Fall Meeting, San Francisco, California, December 10-14.

Wang, M., 2002: Examples of the aerosol model effects in the SeaWiFS atmospheric correction," SPIE's Third International Asia-Pacific Symposium on Remote Sensing of the Atmosphere, Ocean, Environment, and Space, Hangzhou, China, October 23-27.

Wang, M., 2002: Approaches of the aerosol correction algorithm: Methods of the single-scattering vs. multiple-scattering epsilon," The Ocean Optics XVI, Santa Fe, New Mexico, November 18-22.